USGS
science for a changing world

Volcanic Aquifers of Hawai‘i—Contributions to Assessing Groundwater Availability on Kaua‘i, O‘ahu, and Maui

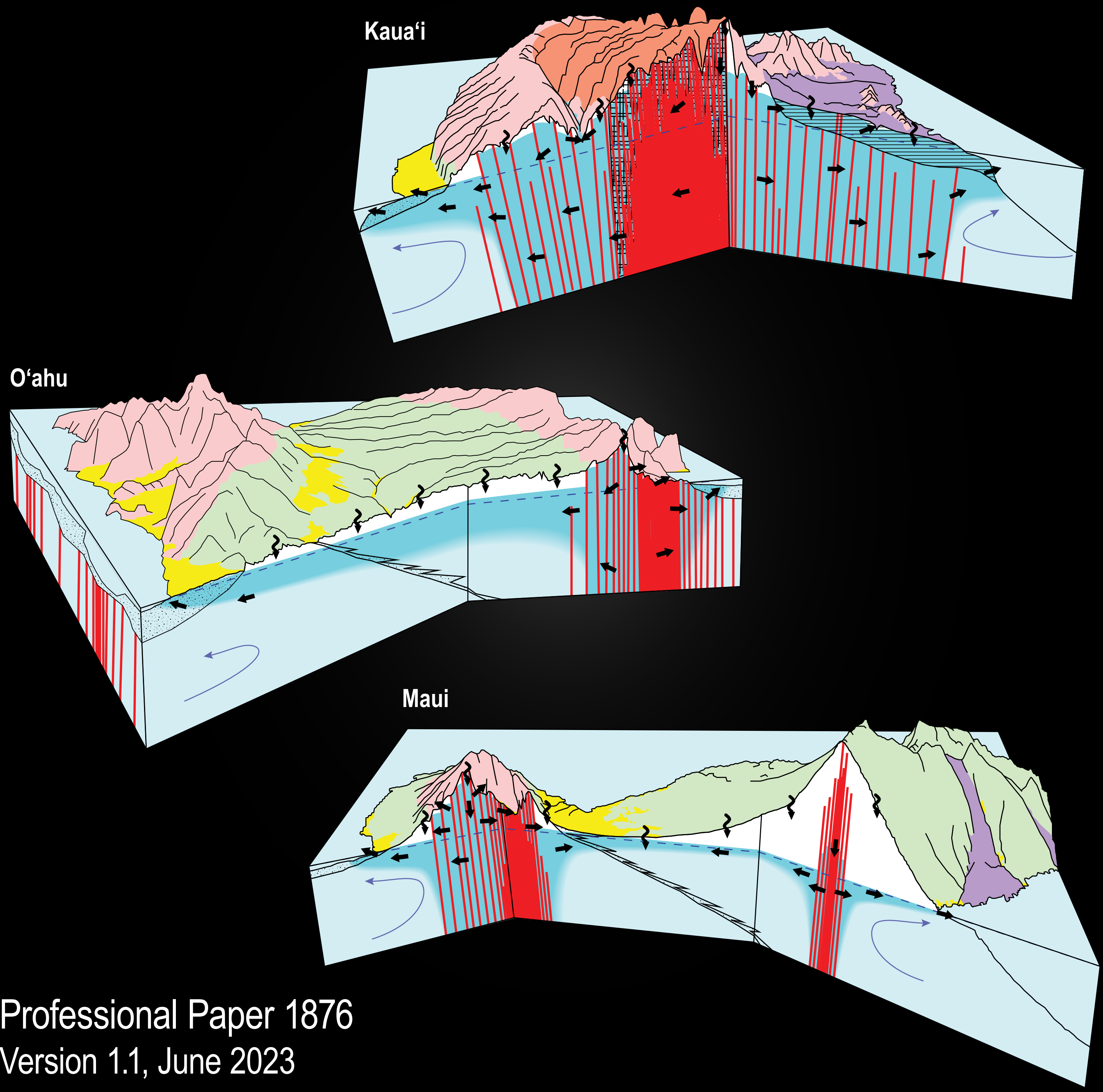

Professional Paper 1876
Version 1.1, June 2023

U.S. Department of the Interior
U.S. Geological Survey

Cover. Block diagrams showing principal aspects of groundwater occurrence and flow on Kaua‘i, O‘ahu, and Maui

Volcanic Aquifers of Hawai‘i—Contributions to Assessing Groundwater Availability on Kaua‘i, O‘ahu, and Maui

By Scot K. Izuka and Kolja Rotzoll

Professional Paper 1876
Version 1.1, June 2023

U.S. Department of the Interior
U.S. Geological Survey

U.S. Geological Survey, Reston, Virginia: 2023
First release: 2023
Revised June 2, 2023 (ver. 1.1)

Suggested citation:
Izuka, S.K., and Rotzoll, K., 2023, Volcanic aquifers of Hawai‘i—Contributions to assessing groundwater availability on Kaua‘i, O‘ahu, and Maui (ver. 1.1, June 2023): U.S. Geological Survey Professional Paper 1876, 100 p., https://doi.org/10.3133/pp1876.

Associated data for this publication:
Rotzoll, K., and Izuka, S.K., 2023, MODFLOW–2005 and SWI2 models for assessing groundwater availability scenarios in volcanic aquifers on Kauai, Oahu, and Maui, Hawaii: U.S. Geological Survey data release, https://doi.org/10.5066/P97CPK5C.

Rotzoll, K., and Johnson, A.G., 2023, Mean annual water-budget components for Oahu, Hawaii, for future-climate conditions, CMIP5 RCP8.5 2041–70 scenario rainfall and 2010 land cover: U.S. Geological Survey data release, https://doi.org/10.5066/P9L4N2ZI.

ISSN 2330-7102 (online)

Acknowledgments

This report is a product of the Hawai‘i Volcanic Aquifer Study, one of the regional groundwater-availability studies supported by the U.S. Geological Survey (USGS) Water Availability and Use Science Program. The authors are grateful to the following people for their contributions of expertise and time to this study: Lenore Ohye, Roy Hardy, Jeremy Kimura, Patrick Casey, and Robert Chenet (State of Hawai‘i Commission on Water Resource Management); Ernest Lau, Barry Usagawa, and Nancy Matsumoto (Honolulu Board of Water Supply); and Adam Johnson, Joseph Hughes, and Delwyn Oki (USGS). Devin Galloway and John Masterson (both USGS) provided helpful technical reviews.

Geographic and Geologic Names

Geographic names in this report are largely consistent with the U.S. Geological Survey (USGS) Board on Geographic Names (http://geonames.usgs.gov/), including the use of the ‘okina (‘) and kahakō (¯) diacritical marks in Hawaiian names. The diacritical marks are not used, however, in anglicized derivations from Hawaiian names (for example, the ‘okina appears in the name “Hawai‘i” but not in the derivation “Hawaiian”), or where a place name appears without the diacritical marks in an established proper noun or title in a cited reference. Names of geologic formations and features are consistent with the State geologic map by Sherrod and others (2021).

Both the entire group of Hawaiian Islands and the largest island in the group are named “Hawai‘i.” To avoid confusion in this report, the island group is referred to as “Hawai‘i” and the largest island is referred to as “Island of Hawai‘i.” The other islands, including those that are the focus of this report (O‘ahu, Maui, and Kaua‘i), are simply referred to by their names because there is no potential for confusion with other geographic entities.

Contents

Figures

Tables

Conversion Factors

U.S. customary units to International System of Units

Multiply	By	To obtain
	Length	
inch (in.)	2.54	centimeter (cm)
foot (ft)	0.3048	meter (m)
mile (mi)	1.609	kilometer (km)
	Area	
square mile (mi^2)	2.590	square kilometer (km^2)
	Flow rate	
million gallons per day (Mgal/d)	0.04381	cubic meter per second (m^3/s)
inch per year (in/yr)	25.4	millimeter per year (mm/yr)

Temperature in degrees Celsius (°C) may be converted to degrees Fahrenheit (°F) as °F = (1.8 × °C) + 32.

Temperature in degrees Fahrenheit (°F) may be converted to degrees Celsius (°C) as °C = (°F – 32) / 1.8.

Datum

Horizontal coordinate information is referenced to the North American Datum of 1983 (NAD 83).

Altitude, as used in this report, refers to distance above mean sea level.

Abbreviations

CWRM	State of Hawai‘i Commission on Water Resource Management
GCM	general circulation model
HVAS	Hawai‘i Volcanic Aquifer Study
IPCC	Intergovernmental Panel on Climate Change
K_h	horizontal hydraulic conductivity
K_v	vertical hydraulic conductivity
K zone	zone of uniform hydraulic conductivity
MODFLOW	computer code (program) for creating finite-difference numerical models of groundwater flow
RCP	representative concentration pathway
SWI2	Seawater Intrusion Package (package of MODFLOW that allows simulation of salt water and fresh water in aquifers)
USGS	U.S. Geological Survey

Volcanic Aquifers of Hawai‘i—Contributions to Assessing Groundwater Availability on Kaua‘i, O‘ahu, and Maui

By Scot K. Izuka and Kolja Rotzoll

Abstract

The volcanic aquifers of the Hawaiian Islands supply water to 1.46 million residents, diverse industries, and a large component of the U.S. military in the Pacific. Groundwater also supplies fresh water that supports ecosystems in streams and near the coast. Hawaii's aquifers are remarkably productive given their small size, but the capacity of the islands to store fresh groundwater is limited because each island is surrounded by seawater, and salt water underlies much of the fresh groundwater. The amount of fresh groundwater available for human use from Hawai‘i's volcanic aquifers is constrained by the consequences of groundwater withdrawal. Restrictions placed on these consequences can translate to limitations on groundwater availability. Changes in recharge resulting from changes in land cover or climate can alter the effect of withdrawals.

This study uses numerical models of the volcanic aquifers of the islands of Kaua‘i, O‘ahu, and Maui to quantify the consequences of historical and plausible future withdrawals and changes in recharge. The study compares the results of model simulations of multiple scenarios of historical and projected future withdrawal and recharge. Results of the simulations using the groundwater models of the islands of Kaua‘i, O‘ahu, and Maui have implications for other islands in Hawai‘i.

Since the first modern water well was drilled in Hawai‘i in 1879, total groundwater withdrawals on Kaua‘i, O‘ahu, and Maui have risen to nearly 400 million gallons per day. Model simulations indicate that these withdrawals have caused reductions in groundwater discharge to streams and springs, reductions in groundwater discharge to the ocean, changes in subsurface flow between sectors within an island, lowering of groundwater levels, and rise of the interface between fresh water and salt water in the aquifers. Future increases in withdrawals will increase the severity of the consequences. Changes in recharge can alter the effect of withdrawals—increases in recharge can offset the consequences of withdrawals, whereas decreases in recharge can exacerbate the effects of withdrawals.

This study quantifies the consequences of withdrawals for past and plausible future circumstances. The models can be used to test other circumstances. Limits placed on the consequences of withdrawals—such as restrictions to protect stream or coastal ecosystems that rely on groundwater discharge and limitations on water-level decline and rise of the freshwater-saltwater interface to protect the productivity of existing wells—can translate to limits on groundwater availability from Hawai‘i's volcanic aquifers. Setting acceptable limits to the consequences of groundwater withdrawal is also a critical part of assessing groundwater availability. Once these limits are set, numerical models can be used to quantify the amount of water that can be withdrawn within those limits and thereby inform management decisions that seek to balance the need to limit the consequences of groundwater withdrawals with the need to develop water for human use.

Introduction

Hawai‘i is a chain of islands in the tropical North Pacific Ocean (fig. 1). The islands include eight main islands, which are the tops of immense basaltic shield volcanoes that rise from the floor of the Pacific Ocean. The volcanic rocks of these islands form aquifers that supply water to 1.46 million residents (U.S. Census Bureau, 2021), diverse industries, and a large component of the U.S. military in the Pacific. Groundwater also supplies fresh water that supports traditional and customary practices, as well as ecosystems in streams and near the coast.

As a group, the volcanic aquifers of Hawai‘i[1] are identified as one of the principal aquifers in the United States (Reilly and others, 2008). The productivity of Hawai‘i's aquifers is remarkable given the small size of each island and the small total land area of the archipelago (Davis, 1963). Ultimately, however, the islands' capacity to store fresh groundwater is limited. The islands are isolated from each other by seawater, and salt water underlies much of the fresh water in the islands' aquifers (fig. 2). A transition zone of brackish water lies between the fresh water and salt water in the aquifers. The limited capacity of the islands to store fresh groundwater intensifies the effects from factors that affect groundwater resources, such as groundwater withdrawals by humans and changes in recharge linked to climate and land-cover changes.

[1]Unless otherwise noted, the name "Hawai‘i" in this report refers to the entire group of Hawaiian Islands and not the Island of Hawai‘i.

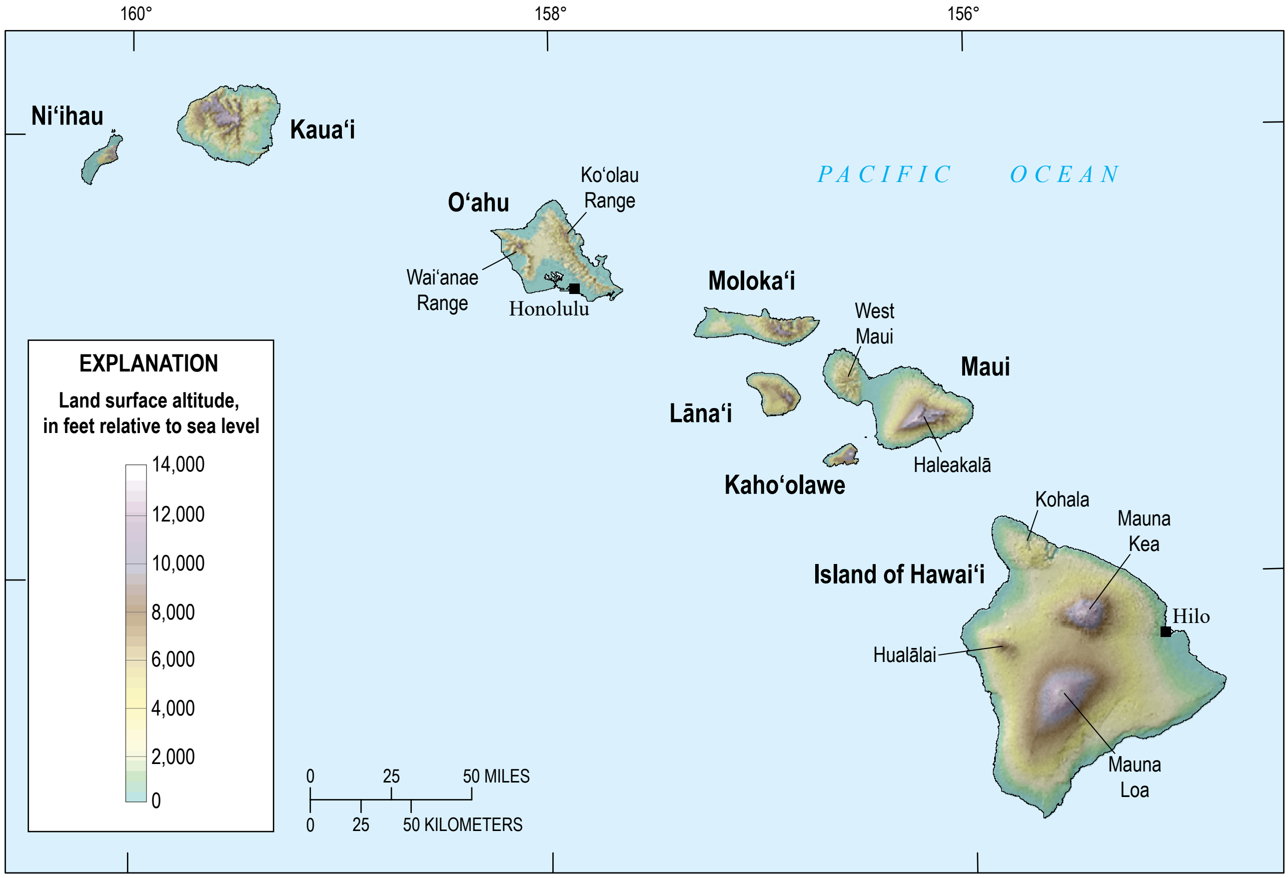

Shaded-relief map modified from U.S. Geological Survey 10-meter digital elevation model
Universal Transverse Mercator projection, zone 4 north
North American Datum of 1983

Figure 1. Shaded-relief map of the Hawaiian Islands. From Izuka and others (2018, 2021).

Figure 2. Schematic block diagram showing the occurrence and flow of fresh groundwater in a basaltic oceanic island and its relation to precipitation, evapotranspiration, runoff, and salt water. Blue arrows indicate flow of groundwater. Modified from Izuka and others (2018).

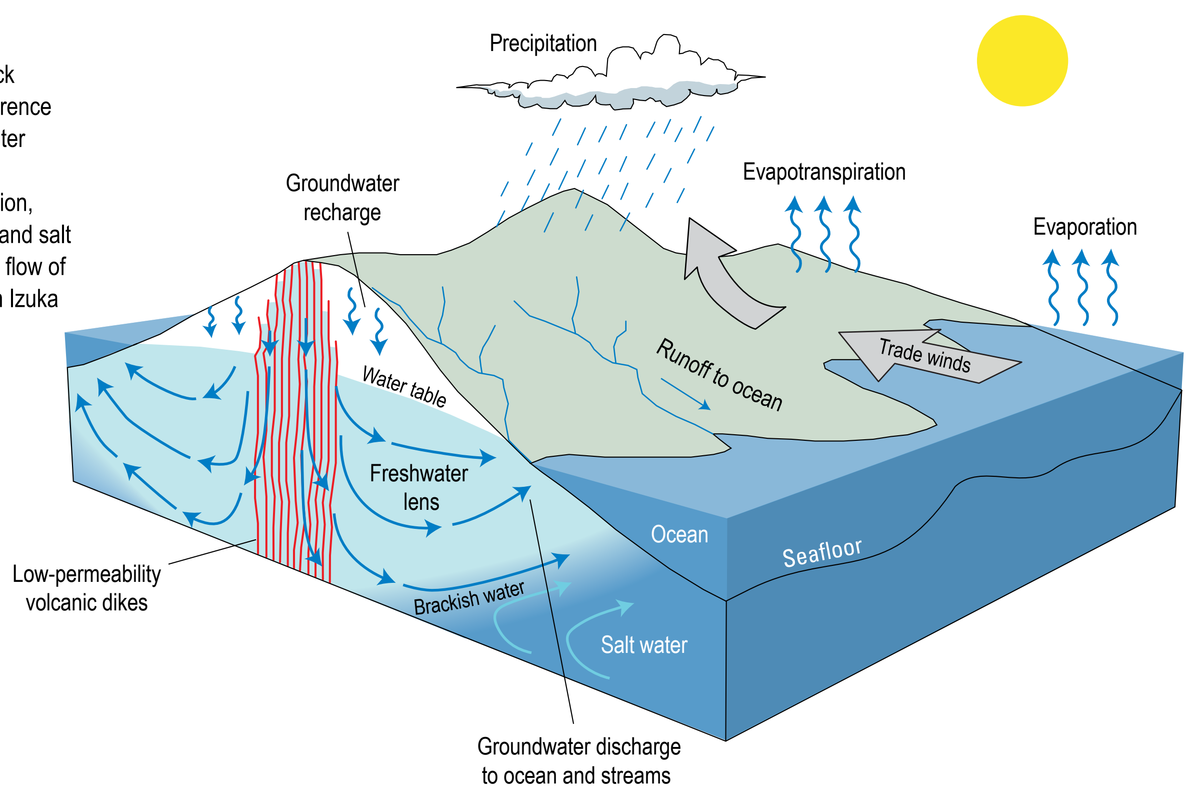

The first modern well in Hawaiʻi was drilled on Oʻahu in 1879. By the early 20th century, hundreds of wells had been drilled on Oʻahu, and a conceptual model of groundwater occurrence had been developed (Stearns and Vaksvik, 1935). This early conceptual model guided groundwater exploration and management for decades, not only on Oʻahu but also on the other islands in Hawaiʻi. As more wells were drilled, more information became available, some of which indicated that the early Oʻahu-based conceptual model did not account for all groundwater occurrences in Hawaiʻi. Also, new information from subsequent studies and data collection has advanced understanding of Hawaiʻi's climate, geology, and hydrogeology.

Recognizing the importance of groundwater development and the evolution of groundwater understanding in Hawaiʻi, the U.S. Geological Survey (USGS) has included the islands in periodic national groundwater-resource studies since the early 20th century (Meinzer, 1923; Davis, 1963; Takasaki, 1978; Nichols and others, 1996). This report is one of the products of the most recent USGS groundwater assessment for Hawaiʻi, known as the Hawaiʻi Volcanic Aquifer Study (HVAS). The HVAS is one of a number of studies under the USGS Water Availability and Use Science Program that reevaluate groundwater availability in the principal aquifers in the United States.

Groundwater Availability

Any rate of artificial groundwater withdrawal, such as pumping from wells, has consequences. The groundwater system in an island is dynamic—groundwater continuously flows from areas of inflow (recharge) to areas of outflow (natural groundwater discharge to streams and to the ocean, as well as artificial withdrawals at wells). Under natural conditions (before onset of artificial withdrawals), an aquifer is considered to be in a state of long-term average equilibrium. Although droughts and seasonal variations in groundwater recharge can cause short-term imbalances, in the long term, the average outflow rate equals the average inflow rate. On an islandwide basis, inflows to the fresh-groundwater system come solely from groundwater recharge; outflows include natural groundwater discharge to streams, wetlands, springs, and the ocean (fig. 3*A*). Introduction of artificial withdrawal, which constitutes another component of outflow, upsets the natural balance between inflows and outflows, reducing groundwater storage and natural groundwater discharge as the system transitions gradually to a new equilibrium between outflow and inflow rates (Theis, 1940). The new equilibrium is achieved when the artificial withdrawal is compensated by a commensurate reduction of groundwater discharge to streams, wetlands, springs, and the ocean. Under the new equilibrium, the volume of fresh groundwater in storage will have been reduced relative to the conditions prior to the start of withdrawal. In Hawaiʻi, the volumetric reduction is manifest as water-table decline and rise of the underlying transition zone and salt water (fig. 3*B*). The magnitude of the consequences (water-table decline, saltwater and transition-zone rise, and reduction of natural groundwater discharge) varies with the magnitude of the withdrawal—the greater the withdrawal rate, the greater the magnitude of the consequences.

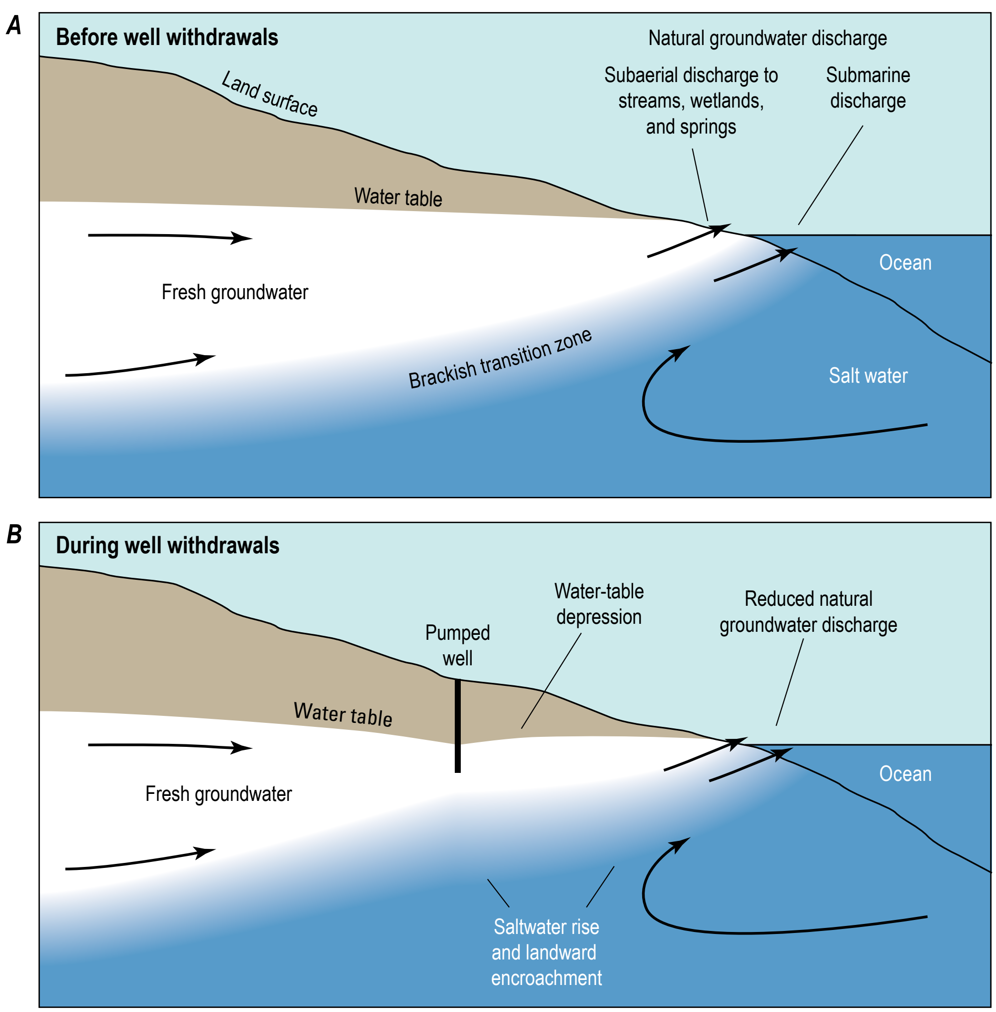

Figure 3. Diagrams showing (*A*) natural groundwater discharge from a coastal aquifer and (*B*) reduced natural groundwater discharge during well withdrawals. Black arrows show direction of groundwater flow. Modified from Izuka and others (2018).

The availability of groundwater for human use is limited by the degree to which these consequences are deemed acceptable by the community or by those to whom water-resource management has been delegated. Restrictions placed on water-table decline, saltwater rise, or reduction of natural groundwater discharge to streams, springs, wetlands, and the ocean can translate to limitations on the amount of groundwater that can be withdrawn from an aquifer for human use. Both identifying and quantifying the magnitude of the consequences for a desired withdrawal rate and well distribution are, therefore, essential for the assessment of groundwater availability.

Changes in recharge can affect groundwater availability. Recharge rates can change as a result of changes in precipitation. Changes in land use and land cover can also affect recharge because different types of vegetation and land uses have different rates of evapotranspiration. Evapotranspiration can reduce the amount of infiltration of water from the land surface and thereby the amount of groundwater recharge. Irrigation of crops, parks, and golf courses, as well as leaking water mains and seepage from septic systems, can enhance recharge, whereas urbanization that directs runoff to storm drains can decrease recharge. Changes in recharge alter the rate of inflow to the groundwater system, its balance with natural discharge, and the consequences of withdrawing water for human use.

Approach and Scope

This report is the third in a series of related publications of the HVAS. The first publication (Izuka and others, 2018) described the hydrogeology, groundwater budgets, and conceptual models of groundwater occurrence for the four largest and most populous islands in Hawai‘i: Kaua‘i, O‘ahu, Maui, and the Island of Hawai‘i. The second publication (Izuka and others, 2021) described the creation and calibration, which were based on the information in the first report, of numerical groundwater models of the volcanic aquifers of Kaua‘i, O‘ahu, and Maui—these islands have 86 percent of the population and the bulk of the groundwater demand in Hawai‘i. This report describes the use of the numerical groundwater models (described in the second report) to assess the effects of increasing groundwater withdrawals and changing recharge and their relevance to groundwater availability for human use.

Numerical modeling is the most comprehensive tool currently available to assess the consequences of groundwater withdrawals under various recharge conditions. Numerical models can account for the many diverse factors that affect how an aquifer will respond to groundwater withdrawals and can quantify resulting water-table decline, saltwater rise, and reduction of natural groundwater discharge. This study uses numerical models (developed by Izuka and others, 2021) to simulate various scenarios of historical and projected future withdrawal and recharge on Kaua‘i, O‘ahu, and Maui. Comparisons of the water-table altitude, transition-zone altitude, and the natural groundwater discharge rates from the different scenarios are used to quantify and assess the spatial distribution of the consequences of groundwater withdrawals.

Setting

The eight main islands in Hawai‘i have a total land area of 6,420 square miles (mi^2). The areas of Kauai, O‘ahu, and Maui are 552, 597, and 727 mi^2, respectively. The archipelago lies in the trade-wind belt of the tropical North Pacific Ocean. The climate for most areas of the islands is characterized by mild temperatures, moderate humidity, and prevailing northeasterly trade winds (Giambelluca and Schroeder, 1998). Precipitation distribution is influenced by the orographic effect—trade winds blow against the mountain slopes, forcing air to rise and cool and water vapor to condense (fig. 2). As a result, rainfall amounts are high over most mountain crests and on northeast-facing (windward) slopes and low in leeward areas (fig. 4). Rainfall ranges from less than 10 inches per year (in/yr) on some leeward coasts to more than 400 in/yr on some windward slopes and can vary by more than an order of magnitude within 5 horizontal miles (Giambelluca and others, 1986, 2013). Without the orographic effect, rainfall would be less than 30 in/yr, similar to that of the open ocean in this part of the Pacific Ocean (Giambelluca and Schroeder, 1998). The orographic effect is limited to an altitude of about 7,200 feet (ft) by the trade-wind temperature inversion. As a result, the peaks of the highest mountains—such as Haleakalā (10,023 ft altitude) on Maui—have low rainfall (fig. 4) (Giambelluca and others, 2013). Occasional migratory storms also can bring heavy rain to any part of an island. These storms are the primary form of precipitation in the dry, leeward areas and on mountaintops above the trade-wind inversion (Giambelluca and others, 2013). Fog interception by vegetation is another source of water for high-altitude forests in Hawai‘i (Juvik and Nullet, 1995).

Monitoring data indicate a long-term-average drying trend in Hawai‘i over the last century (Kruk and Levinson, 2008; Chu and others, 2010) and a concurrent downward trend in stream base flow that indicates decreasing groundwater in storage (Oki, 2004; Bassiouni and Oki, 2013). Downscaling of global climate models varies widely in its predictions of future rainfall for Hawai‘i but generally indicates that the drier, leeward areas of islands will become even drier in the future (see, for example, Elison Timm and others, 2015; Zhang and others, 2016).

Hawai‘i's human population is estimated to have been several hundred thousand in the 1600s to 1700s (Kirch, 1998, 2000; Ziegler, 2002), but it declined to less than 100,000 by the middle to late 19th century, primarily because of introduced diseases (Schmitt, 1998). With immigration and the stemming of disease-related deaths, the population of Hawai‘i grew to 423,000 by 1940, spiked to 859,000 during World War II, and was 622,000 in 1959 when Hawai‘i became a state (Schmitt, 1998). At the time of the 2020 census, 1,016,508 people—or about 70 percent of the state's population—lived on O‘ahu (State of Hawai‘i Department of Business, Economic Development & Tourism, 2021). O‘ahu also has the capital city of Honolulu and the large military installations, Joint Base Pearl Harbor-Hickam, Wheeler Army Airfield, Schofield Barracks, and Marine Corps Base Hawaii. At the time of the 2020 census, the populations of Kaua‘i and Maui were 73,214 and 154,100, respectively (State of Hawai‘i Department of Business, Economic Development & Tourism, 2021).

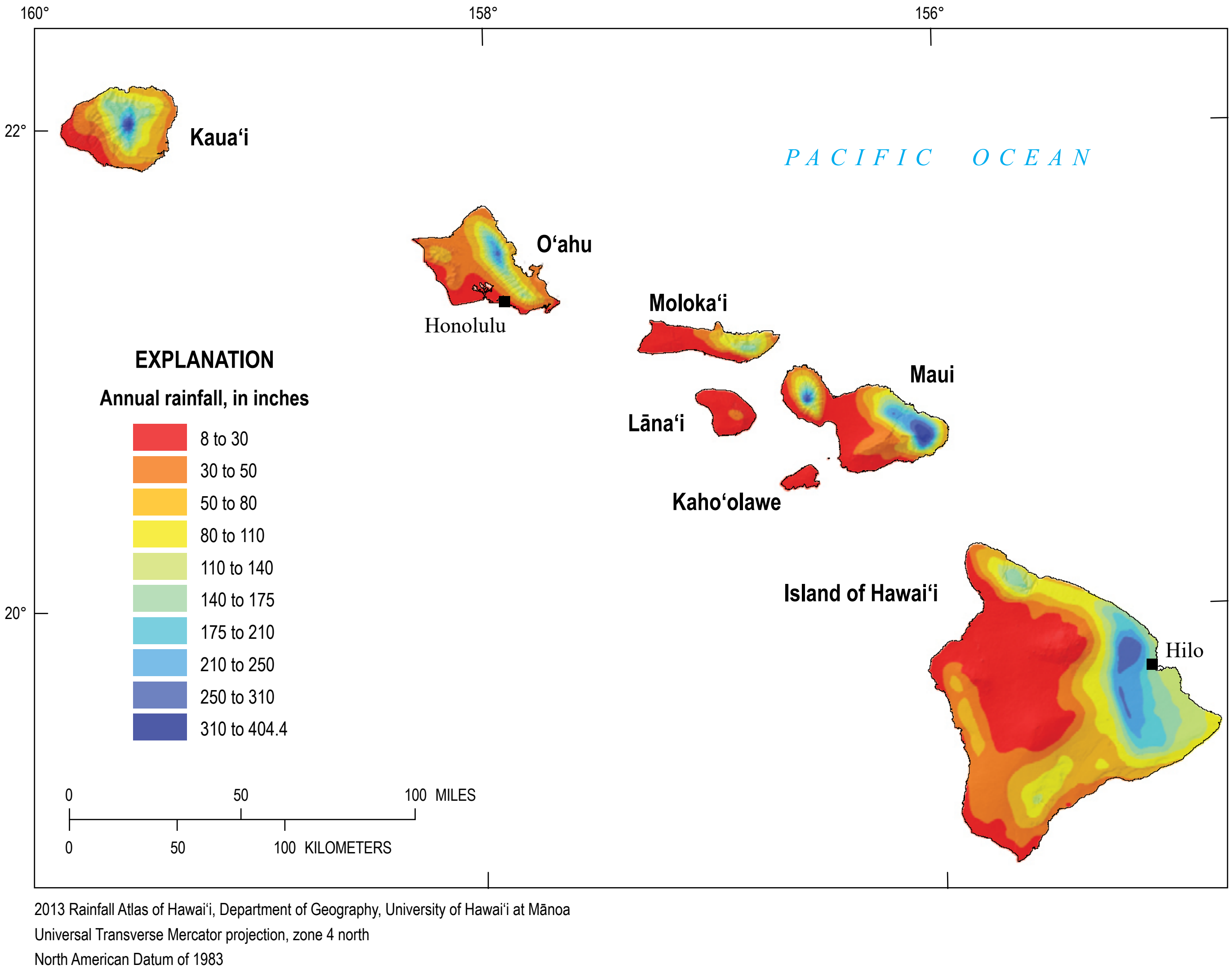

Figure 4. Map showing mean annual rainfall in Hawaiʻi during 1978–2007. Modified from Giambelluca and others (2013).

Humans have affected Hawaiʻi's groundwater resources for centuries, not only as a result of groundwater withdrawals from wells but also by affecting recharge by altering the landscape (for example, by urbanization, deforestation and reforestation, replacement of native forests by nonnative species, and agricultural irrigation). Comparison of land-cover maps (figs. 5, 6) shows how humans have transformed the landscape between 1870 and 2010. From about the mid-19th century, large sugarcane (and to a lesser extent, pineapple) plantations that dominated Hawaiʻi's agriculture and industry used hundreds of millions of gallons of water per day from streams and aquifers for irrigation and processing. The plantations began declining in the later decades of the 20th century, and the last large sugarcane plantation closed in 2016. Some former plantation fields are now used to grow other crops and some have been urbanized, but much of the former agricultural land is currently covered by grass and shrub. Other historical events and their relation to Hawaiʻi's water resources are summarized by Izuka and others (2018).

Geology

A review of the current understanding of the geology relevant to the groundwater resources of Hawaiʻi is given in the first publication of the HVAS (Izuka and others, 2018). This section is a synopsis of that review, particularly those aspects relevant to Kauaʻi, Oʻahu, and Maui.

The islands of Hawaiʻi are shield volcanoes that were built from the ocean floor by midplate hot-spot volcanism (Macdonald and others, 1983; Clague and Dalrymple, 1987). Because of the northwestward motion of the Pacific Plate over the Hawaiian Hot Spot, the islands are successively younger toward the southeast end of the chain. On Niʻihau and Kauaʻi in the northwest (fig. 1), rocks date as far back as the Miocene, whereas the Island of Hawaiʻi in the southeast is still being built by active volcanoes (Langenheim and Clague, 1987; Sherrod and others, 2021). The three islands that are the focus of this study are, from oldest to youngest, Kauaʻi, Oʻahu,

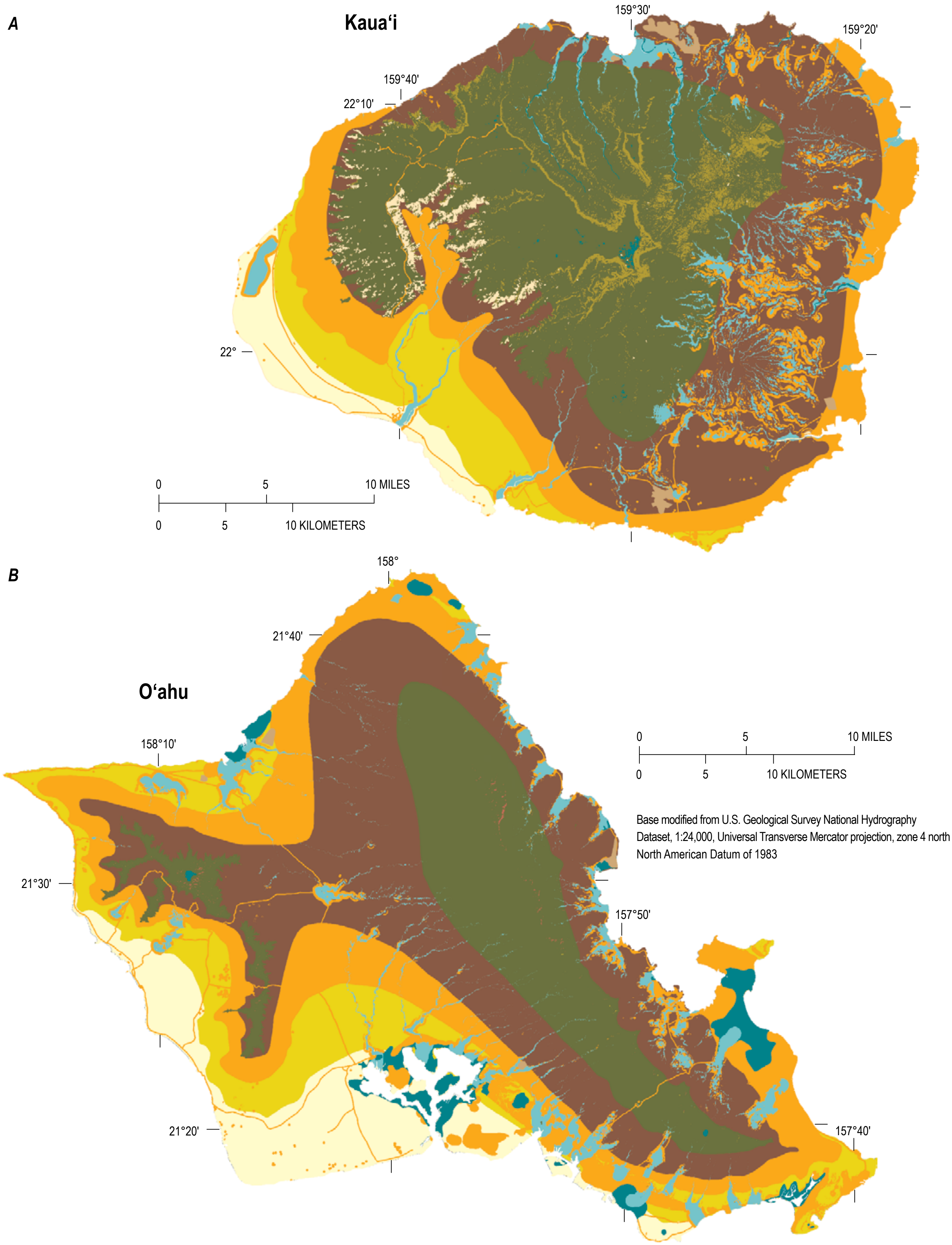

A
Kaua‘i
159°30'
159°20'
159°40'
22°10'
22°
0
5
10 MILES
0
5
10 KILOMETERS
B
158°
21°40'
O‘ahu
158°10'
0
5
10 MILES
0
5
10 KILOMETERS
Base modified from U.S. Geological Survey National Hydrography Dataset, 1:24,000, Universal Transverse Mercator projection, zone 4 north North American Datum of 1983
21°30'
157°50'
21°20'
157°40'

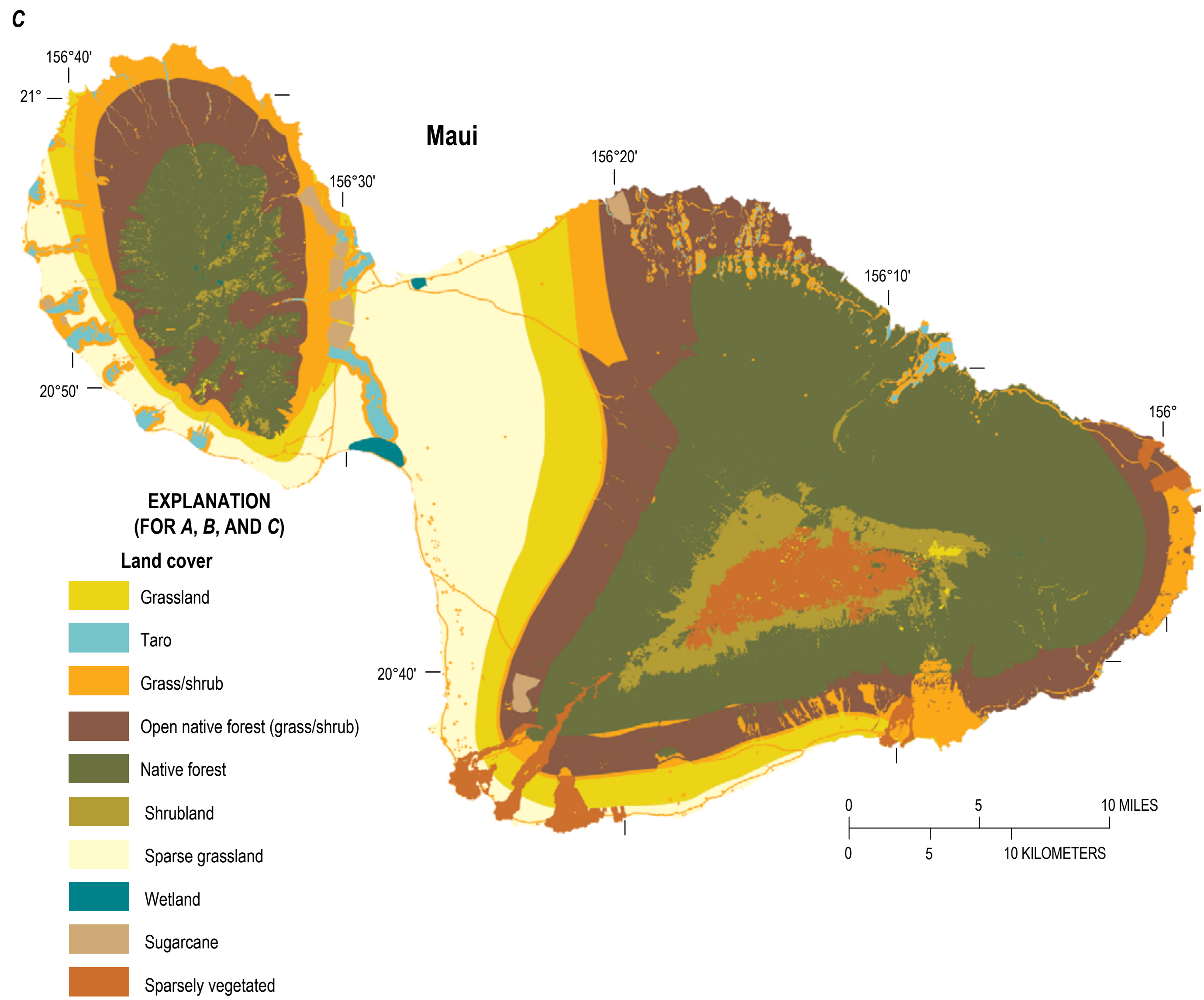

Figure 5. Maps showing 1870 land-cover distribution on (*A*) Kaua'i, (*B*) O'ahu, and (*C*) Maui, Hawai'i. This distribution was used in the computation of recharge for the Predevelopment scenario (see discussion below in the section entitled "Numerical Models"). From Izuka and others (2018).

and Maui, although ages of rocks from these islands overlap (Sherrod and others, 2021). Each island is unique, but some geologic aspects—such as eruptive stages, faulting, erosion, sedimentation, and the hydrologic properties of the rocks—can be discussed in general terms for all three islands.

Eruptive Stages

Four eruptive stages are recognized in Hawaiian volcanoes; these are, in their order of occurrence, preshield, shield, postshield, and rejuvenation (Clague and Dalrymple, 1987; Clague and Sherrod, 2014). The preshield stage is a submarine stage that becomes deeply buried beneath the latter three stages as the volcano builds to form islands. Only the latter three stages form the aquifers that contain freshwater resources presently used by humans in Hawai‘i.

The shield stage is the principal stage of growth for Hawai‘i's shield volcanoes (fig. 7*A*). Shield-stage rocks typically make up 90 percent or more of the subaerial volume of a shield volcano (Clague and Dalrymple, 1987). The shield stage is characterized by highly fluid lava erupted near a volcano's summit and rift zones (Macdonald and Katsura, 1964; Macdonald and others, 1983). Shield-stage lava deposited above sea level typically forms thin lava flows that have average thicknesses of about 15 ft (Macdonald and others, 1983), which accumulate to create the dome-shaped mountains that characterize shield volcanoes. Shield volcanoes sink as they grow; as a result, lavas flows originally deposited above sea level can subside to thousands of feet below sea level (Moore, 1987). Most shield volcanoes have a summit caldera, but a caldera can be alternately buried and reformed while the volcano is active (Wolfe and Morris, 1996).

A

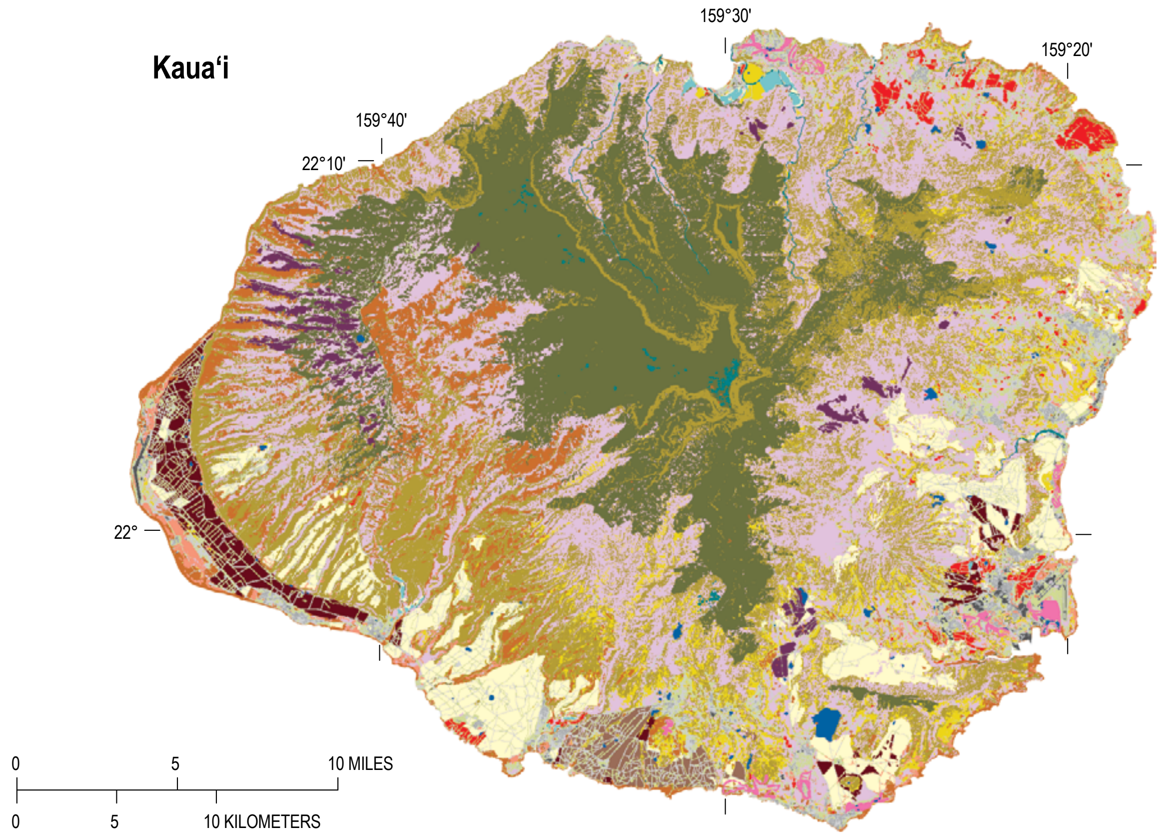
Kaua‘i
159°30'
159°20'
159°40'
22°10'
22°
0
5
10 MILES
0
5
10 KILOMETERS

B

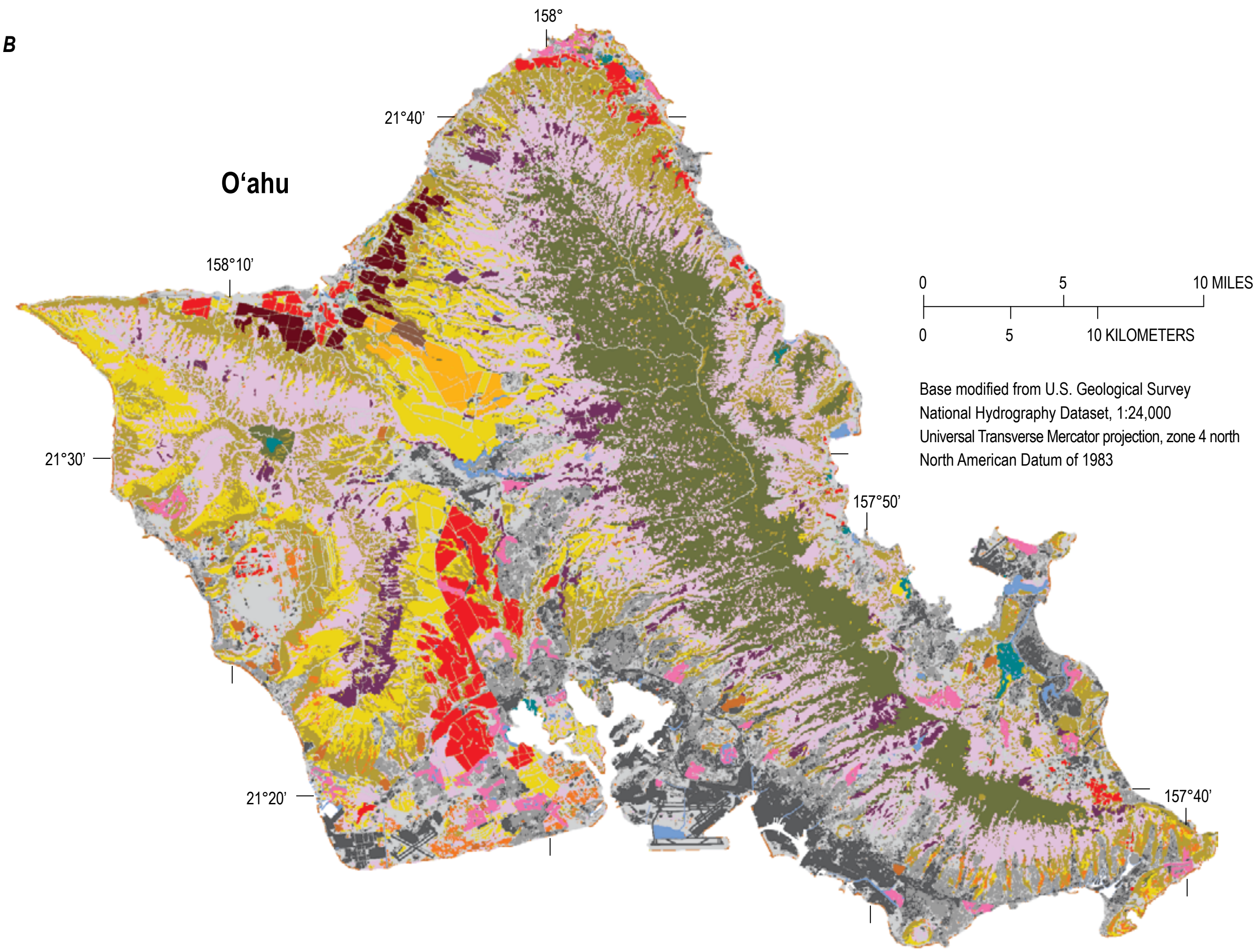
158°
21°40'
O‘ahu
158°10'
0
5
10 MILES
0
5
10 KILOMETERS
Base modified from U.S. Geological Survey
National Hydrography Dataset, 1:24,000
Universal Transverse Mercator projection, zone 4 north
North American Datum of 1983
21°30'
157°50'
21°20'
157°40'

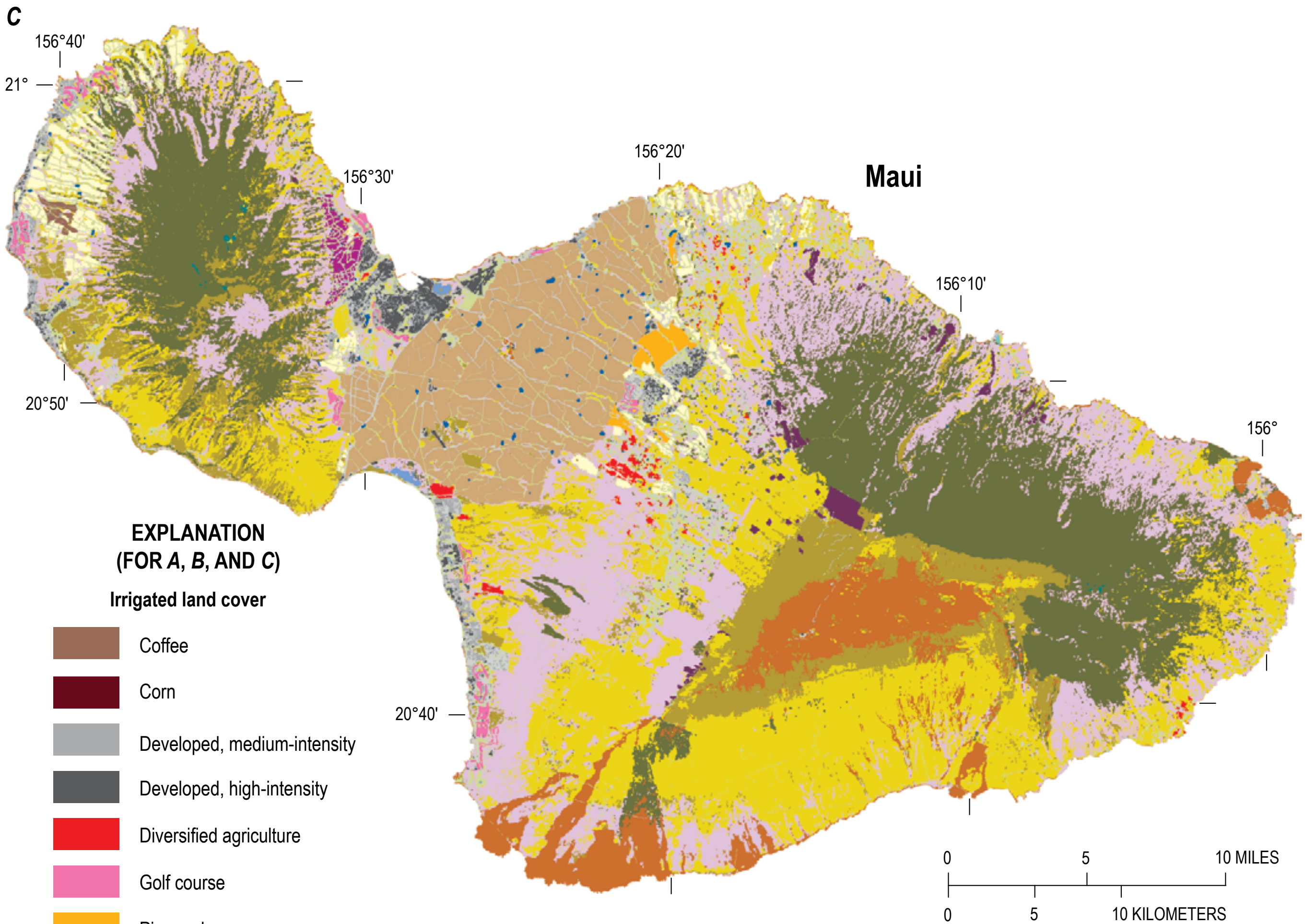

Figure 6. Maps showing 2010 land-cover distribution on (*A*) Kaua'i, (*B*) O'ahu, and (*C*) Maui, Hawai'i. This distribution was used in the computation of recharge for the Current scenario (see discussion below in the section entitled "Numerical Models"). From Izuka and others (2018).

The postshield stage is characterized by eruptions that are less frequent than in the shield stage. The lava is more viscous, lava flows are thicker and shorter, and tephra deposits are more common (Stearns, 1946, 1966; Macdonald and others, 1983). Postshield-stage rocks can be areally extensive, but they commonly form only a thin cap on Hawai‘i’s shield volcanoes (fig. 7*B*). Although postshield-stage rocks are found on all three islands in this study, they are not extensive on Kaua‘i and are much less extensive on O‘ahu than on Maui.

Not all shield volcanoes in Hawai‘i have rejuvenation-stage volcanism, but rocks from this stage are present on Kaua‘i, O‘ahu, and Maui. This stage is characterized by eruptions that are even less frequent than those of the postshield stage (Stearns, 1946, 1966; Macdonald and others, 1983). Rejuvenation-stage deposits

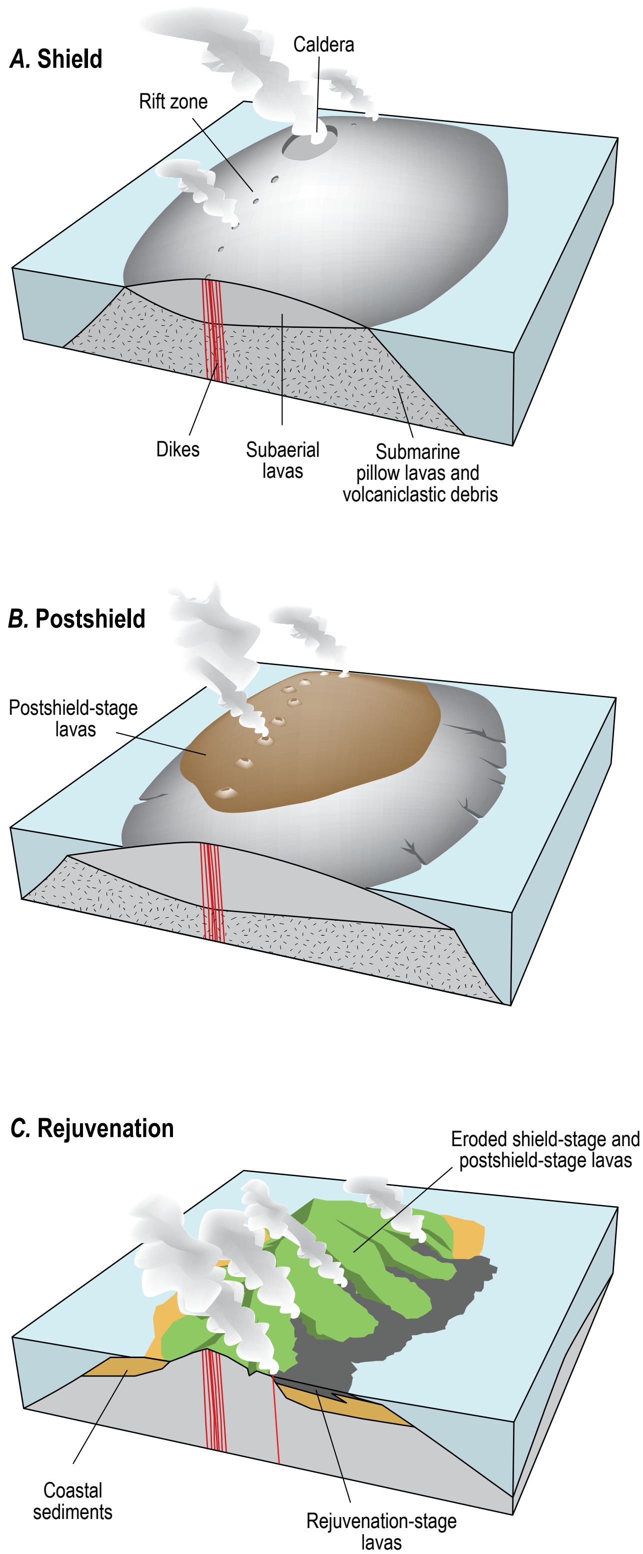

Figure 7. Schematic block diagrams showing three eruptive stages of Hawaiian shield volcanoes: (*A*) Shield stage; (*B*) Postshield stage; and (*C*) Rejuvenation stage. Modified from Izuka and others (2021).

are much less voluminous than the shield-stage deposits and vary widely in character, from ash to lava flows. Lava-flow thickness can vary depending on lava viscosity and preexisting topography. Rejuvenation-stage deposits commonly fill depressions in the eroded surface of the shield volcano (fig. 7*C*).

Faulting, Erosion, and Sedimentation

Faulting is common in and near the caldera and rift zones and on the flanks of Hawai‘i's shield volcanoes (Macdonald and others, 1983). Faults can juxtapose rocks of contrasting hydraulic properties and can form depressions that are later filled by lava flows that accumulate to form low-permeability aquifers.

Stream erosion and mass wasting create valleys in the flanks of shield volcanoes (Stearns and Vaksvik, 1935; Macdonald and others, 1983). On the older shield volcanoes of Kaua‘i, O‘ahu, and West Maui, stream erosion has incised deeply into the upper parts of the volcanic aquifers, resulting in substantial groundwater discharge to streams. Stream incision affects the location of groundwater discharge and shape of the water table, particularly where the aquifers are saturated nearly to the surface (see additional discussion below in the “Principal Groundwater Settings” section).

Sedimentation in Hawai‘i includes the deposition of marine and terrigenous sediments along the coast and in valleys and other depressions. The upper parts of stream valleys typically have little or no alluvium, but the lower parts of larger valleys have substantial deposits of alluvium and, in some cases, rejuvenation-stage volcanic rocks and marine sediments (Stearns and Vaksvik, 1935). Owing to sea-level fluctuations and island subsidence, alluvial fill extends below present sea level in some places (Palmer, 1927, 1946; Stearns, 1946; Macdonald and others, 1983). Terrigenous and marine sediments deposited along the coast—together with rocks from rejuvenation-stage volcanism—form coastal plains that partly surround some islands (fig. 7*C*) such as O‘ahu.

Rocks and Their Hydrologic Significance

Most groundwater in Hawai‘i is stored in lava-flow aquifers. Much of the permeability of lava-flow aquifers comes from zones between successive lava flows (interflow zones), especially the rubbly layers of clinker in a stack of ‘a‘ā flows. As a result, the permeability of a lava-flow aquifer is greater when the number of interflow zones is high (that is, when the aquifer is formed by many thin lava flows rather than a few thick ones). The thick accumulation of thin lava flows characteristic of Hawai‘i's shield-stage volcanoes forms highly permeable aquifers, with horizontal hydraulic-conductivity (K_h) values ranging from hundreds to tens of thousands of feet per day (Soroos, 1973; Oki, 1999; Lau and Mink, 2006; Rotzoll and El-Kadi, 2008). Values of K_h can be several orders of magnitude lower, however, where thick rejuvenation-stage lava flows formed by ponding in preexisting depressions (Izuka and Gingerich, 1998, 2003). Vertical hydraulic conductivity (K_v) values have been estimated to be one to three orders of magnitude less than K_h values (Souza and Voss, 1987), but little data exist on the hydraulic anisotropy of lava-flow aquifers in Hawai‘i.

Dikes are near-vertical, sheetlike intrusive bodies formed by magma that congeals as it rises to the surface in fractures when the volcano is active. Dikes cut across the lava flows and are usually much less porous and permeable than lava-flow aquifers of Hawai‘i (Hunt, 1996). Dikes impede groundwater flow and typically reduce the bulk permeability and storage properties of the aquifers into which they intrude. However, a few widely spaced dikes in a large area of permeable lava-flow aquifer can increase storage by impounding fresh groundwater to high altitudes (fig. 2) (Takasaki and Mink, 1985).

Weathering of basaltic rocks in Hawai‘i reduces rock porosity and permeability (Wentworth, 1928; Mink and Lau, 1980; Macdonald and others, 1983). The degree and thickness of weathering varies depending on climate, vegetation, slope, and time since the basalt was exposed to surface weathering. Low-permeability weathered volcanic rocks can impede the flow of groundwater. Weathered rock layers have been found above or buried within aquifers formed by less altered lava flows and commonly lie beneath the alluvium in stream valleys (Oki, 2005).

Valley-filling alluvium in Hawai‘i consists mostly of consolidated to unconsolidated, poorly sorted gravel with clasts ranging in size from clay particles to boulders. Alluvium typically has hydraulic conductivities that are several orders of magnitude lower than those of lava-flow aquifers (Hunt, 1996; Lau and Mink, 2006). Sedimentary rocks can substantially affect the flow and storage of water in volcanic aquifers. Coastal sediments, sometimes interlayered with some rejuvenation-stage volcanic rocks, form deposits that act as low-permeability semiconfining hydrogeologic units, locally known as caprock. Caprock partly overlies and impedes the natural discharge of groundwater from the more permeable volcanic aquifers to the ocean, causing groundwater storage in the volcanic aquifers to be greater than it would be without the caprock. Much of O‘ahu’s extensive groundwater resources is the result of the island’s well-developed caprock (Stearns and Vaksvik, 1935).

Groundwater Recharge

Flow of fresh groundwater into an oceanic island comes almost entirely through the surface from groundwater recharge (although wastewater injection contributes to groundwater in some areas). Most groundwater recharge comes from precipitation (primarily rainfall, but also fog drip). As a result, the spatial distribution of recharge (fig. 8) generally corresponds to the pattern of rainfall distribution (fig. 4). Recharge is high—as much as several hundred inches per year—on windward slopes and on mountaintops below the trade-wind inversion. The mountains of Kaua‘i, O‘ahu, and West Maui are all below the trade-wind inversion; thus, high recharge is centered at or near the summits of these mountains, consistent with orographic rainfall distribution. In contrast, highest recharge on Haleakalā on Maui is centered on the mountain’s windward-facing slopes; recharge is low on the peak of Haleakalā, which is consistent with the low-precipitation conditions above the trade-wind inversion.

In some areas, irrigation has substantially enhanced recharge over that derived from natural rainfall. For example, a large area of enhanced recharge is apparent on Haleakalā and on the isthmus of Maui; this enhancement results from the irrigation of sugarcane that was still ongoing during 2010, the period on which the recharge in figure 8 is based. Other anthropogenic sources of water entering from near the surface include septic-system leaching and leaks from water systems, sewers, and cesspools.

Principal Groundwater Settings

Izuka and others (2018, 2021) described the following four principal groundwater settings that encompass most groundwater resources in Hawai‘i: (1) the freshwater-lens setting, (2) the dike-impounded-groundwater setting, (3) the thickly saturated setting, and (4) the perched-groundwater setting (fig. 9). Each of these principal groundwater settings responds differently to groundwater withdrawals. As a result, the consequences of groundwater withdrawal that limit groundwater availability differ among the principal groundwater settings—in some settings, saltwater rise may present the primary limit to groundwater availability, whereas in other settings, reduction of groundwater discharge to streams or water-table depression may be the primary limitation. Each groundwater setting is typically associated with aquifers that have a certain type of hydrogeology, and the relation between these settings and the hydrogeologic framework in which they exist are generally well conceptualized.

Freshwater-Lens Setting

The freshwater-lens setting, which is present on all three islands in this study, is a primary source of fresh groundwater for human use in Hawai‘i. In this setting, fresh groundwater in high-permeability aquifers forms a lens-shaped body that buoyantly overlies denser salt water (fig. 10). Between the freshwater lens and salt water is a brackish transition zone. The Ghyben-Herzberg relation indicates that, owing to the buoyant relation between the freshwater lens and salt water, the thickness of the freshwater lens below sea level is 40 times the water-table altitude above sea level. Thus, most of the fresh water in the lens lies below, rather than above, sea level. The relation assumes hydrostatic conditions that do not exist in the lens, where fresh water is constantly flowing, and that the boundary between the freshwater lens and underlying salt water is sharp, rather than a diffuse transition zone. Even so, the relation yields a reasonable approximation of the thickness of some parts of the freshwater lens, such as where flow is primarily horizontal and the transition zone is thin relative to the thickness of the freshwater lens.

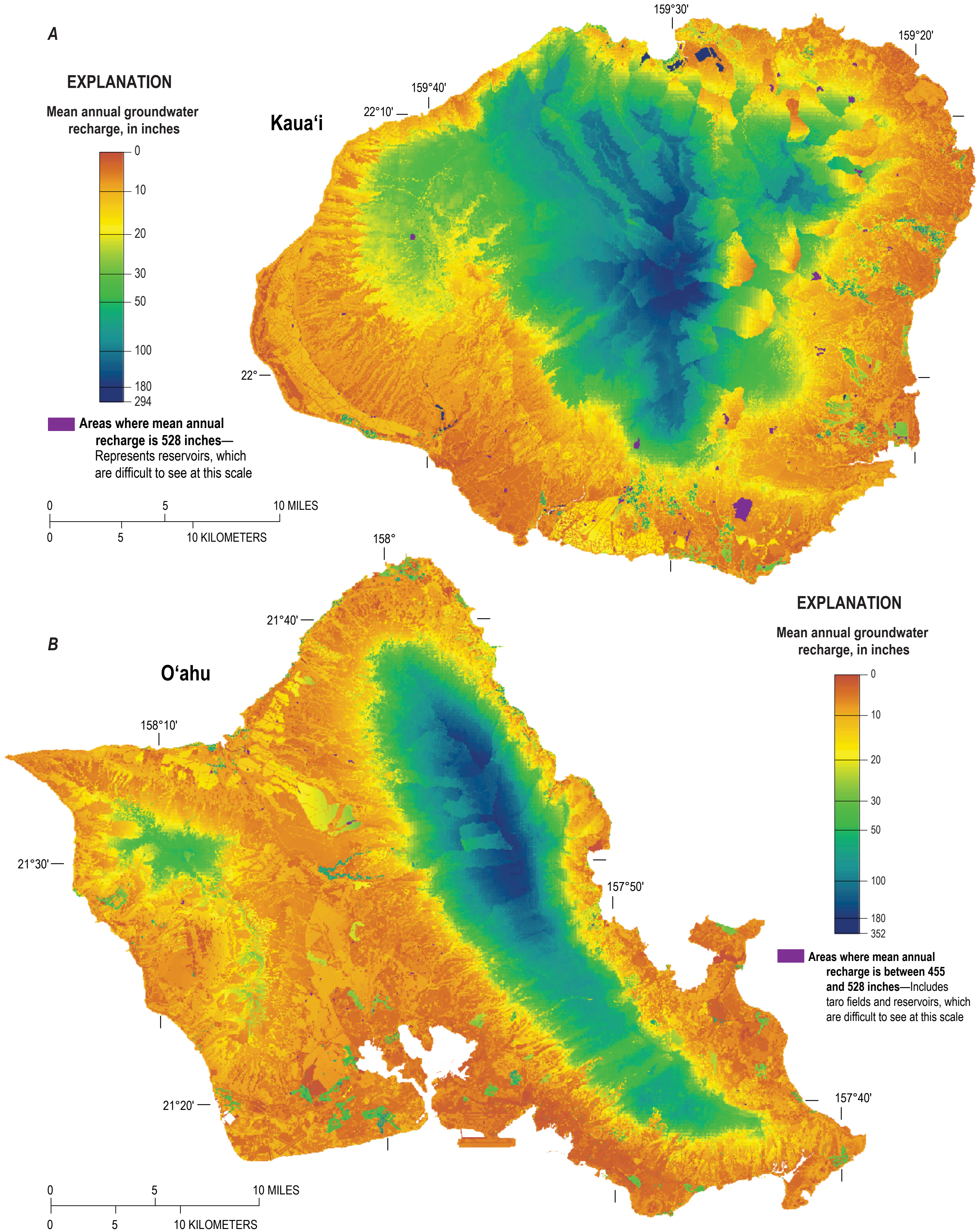
A
EXPLANATION
Mean annual groundwater recharge, in inches
0
10
20
30
50
100
180
294
Areas where mean annual recharge is 528 inches—Represents reservoirs, which are difficult to see at this scale
0 5 10 MILES
0 5 10 KILOMETERS
Kaua‘i
159°30'
159°20'
159°40'
22°10'
22°
B
O‘ahu
158°
21°40'
158°10'
21°30'
157°50'
21°20'
157°40'
EXPLANATION
Mean annual groundwater recharge, in inches
0
10
20
30
50
100
180
352
Areas where mean annual recharge is between 455 and 528 inches—Includes taro fields and reservoirs, which are difficult to see at this scale
0 5 10 MILES
0 5 10 KILOMETERS

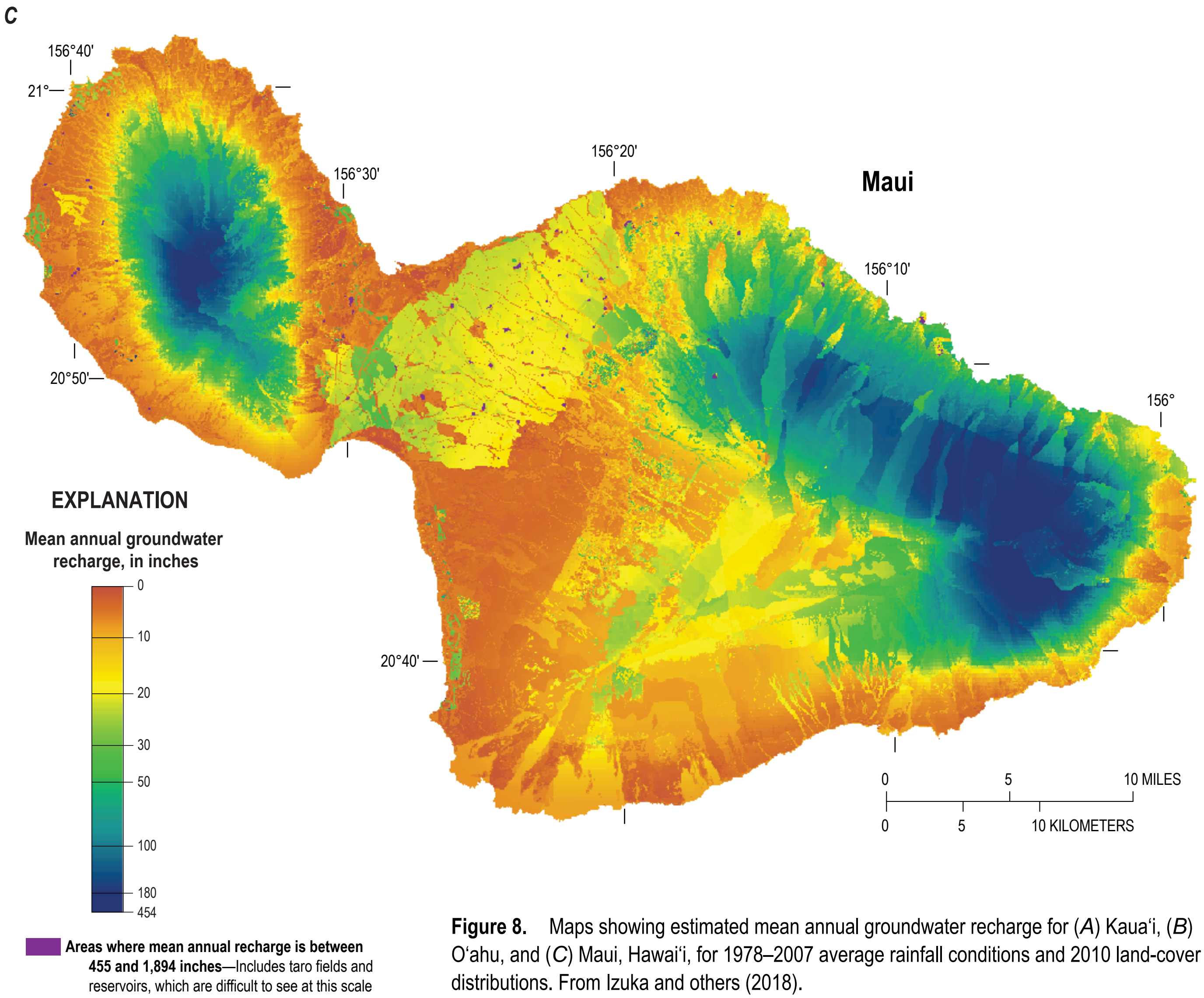

Figure 8. Maps showing estimated mean annual groundwater recharge for (*A*) Kaua'i, (*B*) O'ahu, and (*C*) Maui, Hawai'i, for 1978–2007 average rainfall conditions and 2010 land-cover distributions. From Izuka and others (2018).

The upper surface of the freshwater lens forms a water table that is typically no higher than a few tens of feet above sea level and slopes gently toward the coast. Inflow to the freshwater lens comes from groundwater recharge through the land surface and from subsurface flow from adjacent groundwater bodies such as dike-impounded or perched groundwater. Water in the freshwater-lens setting generally flows from inland areas toward discharge areas at or near the coast (fig. 10). Water in the transition zone also flows toward discharge zones near the coast. The entrainment of salt water into the flowing transition zone also sets up flow in the part of the aquifer occupied by salt water (Cooper, 1964).

In Hawai‘i, the most extensive high-permeability aquifers are formed by a thick accumulation of thin lava flows that were erupted during the shield stage, although rocks from other eruptive stages can also form high-permeability aquifers. Where little or no caprock exists, resistance to groundwater flow is less, the freshwater lens is thin, and most groundwater discharge near the coast happens below sea level (fig. 10*A*). Where substantial caprock resists coastal discharge, the freshwater lens in the high-permeability aquifer is thicker; some groundwater discharges to the surface where the caprock pinches out above sea level, and some groundwater flows through the caprock and discharges above or below sea level (fig. 10*C*).

Effects of withdrawing groundwater.—Groundwater can be developed from the freshwater lens by conventional vertical wells or by horizontal galleries connected to the surface by shafts (fig. 10*B, D*). Shaft-and-gallery systems skim water from near the surface of a freshwater lens and are the largest individual producers of fresh groundwater from Hawai‘i’s volcanic aquifers. In this report, conventional vertical wells and shaft-and-gallery systems are both referred to as “wells.”

Withdrawing water from the freshwater-lens setting causes water-table depression (drawdown), saltwater rise, and reduction

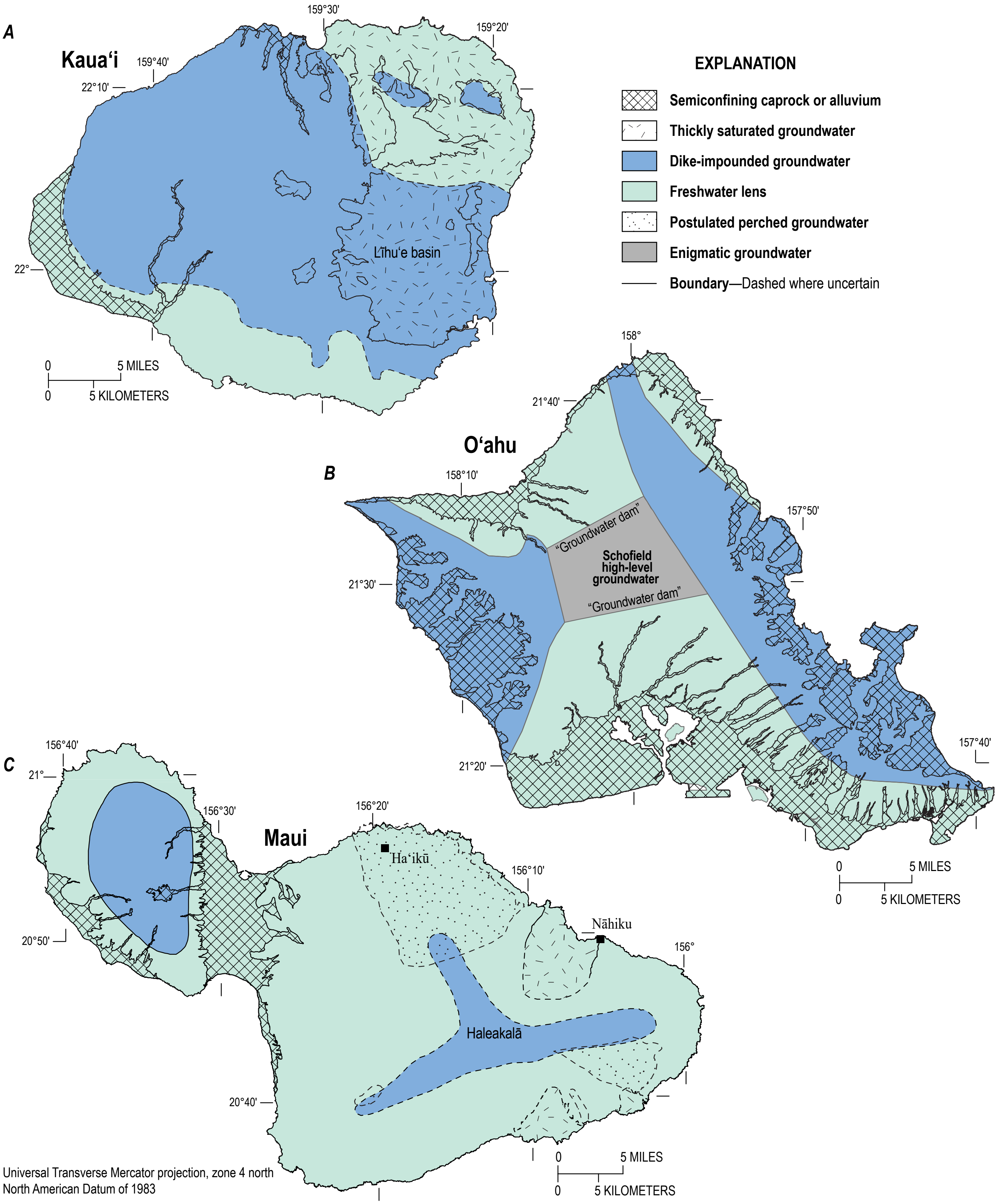

Figure 9. Maps showing distribution of principal groundwater settings on (*A*) Kauaʻi, (*B*) Oʻahu, and (*C*) Maui, Hawaiʻi. Modified from Izuka and others (2018).

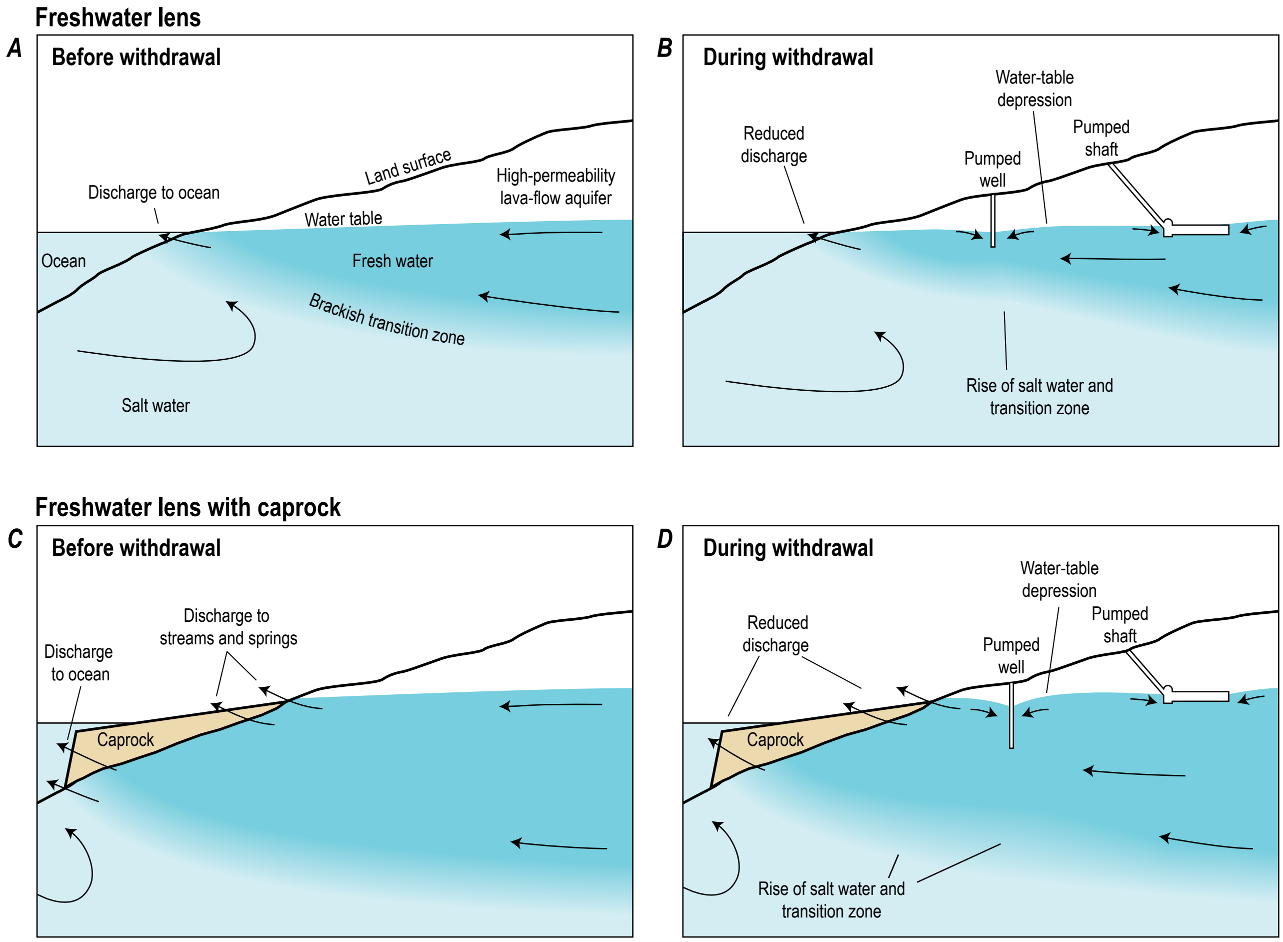

Figure 10. Conceptual diagrams showing the freshwater-lens setting, both with and without caprock: (*A*, *C*) Before withdrawal; (*B*, *D*) During withdrawal. Black arrows show direction of groundwater flow.

of natural groundwater discharge to the ocean and to streams, springs, and wetlands on the caprock (fig. 10*A, D*). However, owing to the high permeability that typifies aquifers in this setting, water-table depression is not as great as it can be in lower permeability settings and thus presents a lesser limitation on groundwater availability. On the other hand, saltwater rise and its effects on water quality may limit groundwater availability where the lens is thin (for example, where caprock is absent) or where wells penetrate to near the transition zone or are excessively pumped. Reduction of natural groundwater discharge to the ocean and to streams, springs, and wetlands on the caprock may limit groundwater availability if such reductions are a concern (for example, where the discharge supports vulnerable ecosystems).

Dike-Impounded-Groundwater Setting

In some areas of a shield volcano, particularly beneath its summit and rift zones, dikes that intrude the shield volcano's lava flows form near-vertical, low-permeability structures that impede groundwater flow. The hydrology of dike-intruded areas can be conceptualized as a system of compartments—groundwater is stored in compartments of high-permeability lava flows between the low-permeability dikes. Because of the impounding effect of the dikes, groundwater can accumulate to high altitudes in the dike zone, which increases the volume of stored fresh groundwater (fig. 11). In this report, the system of groundwater stored in high-permeability rock between low-permeability dikes is referred to as the dike-impounded-groundwater setting.

Groundwater can flow from one compartment to another and from the dike-impounded-groundwater setting to adjacent downgradient groundwater bodies such as freshwater lenses (fig. 11). Where erosion has exposed the dikes, dike-impounded groundwater commonly discharges to the surface and feeds streams and springs or the ocean (fig. 11*C, D*). In some shield volcanoes, such as the Koʻolau volcano on Oʻahu, dikes are aligned in linear trends that result in preferential groundwater flow parallel to the orientation of the dikes (Hirashima, 1962).

The ability of the dike-impounded-groundwater setting to store groundwater diminishes where dikes are so densely clustered that the volume of high-permeability lava flows between the dikes is small (Takasaki and Mink, 1985). Dikes are more densely clustered at the center of rift zones and diminish in

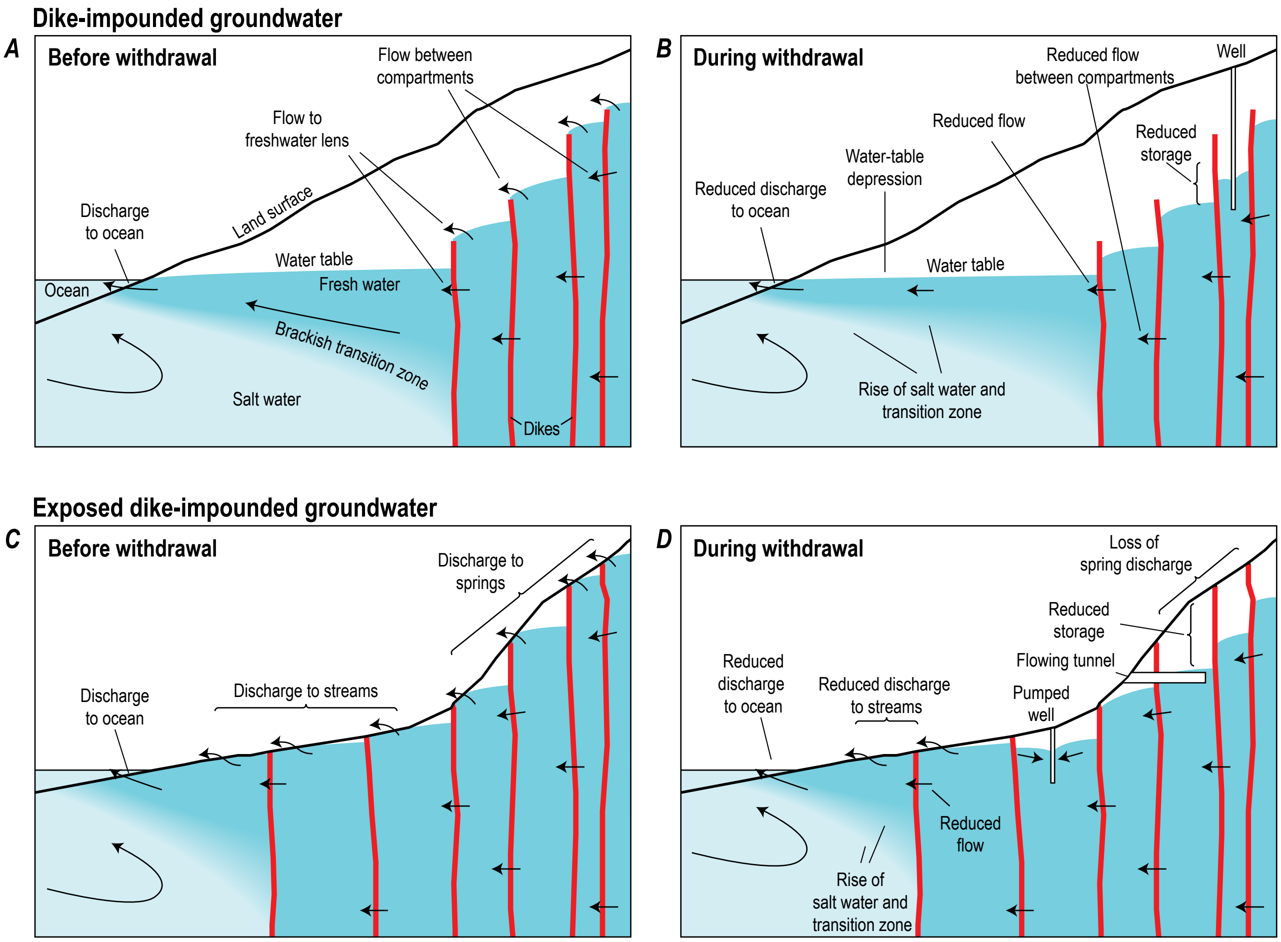

Figure 11. Conceptual diagrams showing the dike-impounded-groundwater setting, both unexposed and exposed: (*A*, *C*) Before withdrawal; (*B*, *D*) During withdrawal. Black arrows show direction of groundwater flow.

abundance toward the margins (Macdonald and others, 1983; Walker, 1987). Dike abundance also increases with depth, and at some depth, the effective porosity and permeability of the aquifer probably approaches zero (Takasaki and Mink, 1985; Kauahikaua, 1993; Moore and Trusdell, 1993). In most dike compartments, fresh water probably extends through the entire depth in which groundwater is significantly mobile.

Effects of withdrawing groundwater.—Groundwater is developed from the dike-impounded-groundwater setting by conventional vertical wells or by tunnels driven nearly horizontally into the dike compartments (fig. 11*D*). Many tunnels in the dike-impounded-groundwater setting are free flowing, but in some tunnels, a bulkhead is installed to regulate flow. Withdrawing water from the dike-impounded-groundwater setting causes water-table depression, which can be substantial in the relatively small volumes of dike compartments. Withdrawal from the dike-impounded-groundwater setting can also cause reductions in freshwater discharge to streams and springs, flows to adjacent groundwater bodies (such as freshwater lenses), and discharge to the ocean. Saltwater rise is not likely to be a major limiting factor of groundwater availability in this setting, except near the coast. However, because subsurface flow from the dike-impounded-groundwater setting can constitute a substantial part of the total groundwater flow through an adjacent freshwater lens, withdrawal from some dike-impounded-groundwater settings can reduce the flow and contribute to saltwater rise in the freshwater lens. These effects can limit the availability of groundwater from the dike-impounded-groundwater setting.

Thickly Saturated Setting

The thickly saturated setting occurs in low-permeability aquifers that are not intruded by dikes. In this setting, low permeability is characteristic of the aquifer as a whole, not just of intrusive structures such as dikes. The aquifer becomes thickly saturated as the low-permeability aquifer resists the flow of groundwater (fig. 12). An example of a thickly saturated setting in a low-permeability aquifer is in eastern Kaua‘i (fig. 9), where the low-permeability aquifer probably results from thick lava flows, which formed by ponding in preexisting depressions on the eroded shield volcano, interbedded with low-permeability sediment (Izuka

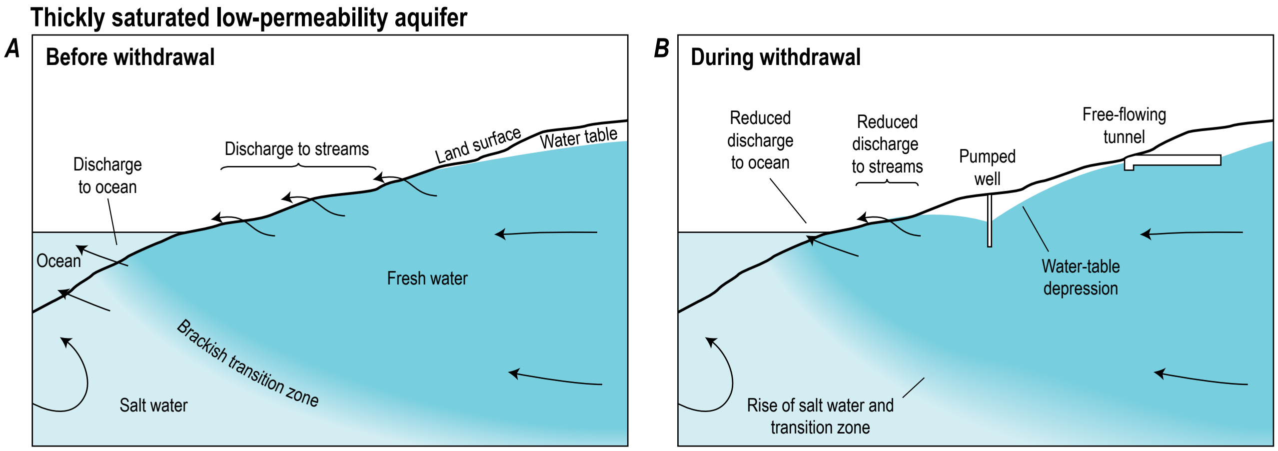

Figure 12. Conceptual diagrams showing the thickly saturated setting: (*A*) Before withdrawal; (*B*) During withdrawal. Black arrows show direction of groundwater flow.

and Gingerich, 1998, 2003). The combination of high rainfall and low aquifer permeability causes groundwater to saturate the aquifer to hundreds of feet above sea level. The water table is kept just below most of the land surface by streams that drain some of the groundwater. As a result, most natural groundwater discharge in this setting occurs above sea level at streams; less groundwater discharges directly to the ocean through submarine seeps. Head gradients in both the horizontal and vertical directions are steep. Salt water and a transition zone probably underlie the fresh-groundwater body near the coast, but whether the salt water and transition zone exist farther inland is not known. Another occurrence of the thickly saturated setting is the area near Nāhiku on the northeast coast of Haleakalā volcano on Maui (Gingerich, 1999b; Meyer, 2000; Scholl and others, 2002).

Effects of withdrawing groundwater.—Groundwater is developed from the thickly saturated setting by conventional vertical wells, but withdrawals tend to cause substantial water-table depression because drawdowns are high in wells in low-permeability aquifers. Horizontal tunnels are also used to develop groundwater because the water table is near the surface (fig. 12*B*). Withdrawal from wells and tunnels can cause substantial reductions in freshwater discharge, especially to streams and springs where most groundwater naturally discharges. These effects can limit the availability of groundwater from the thickly saturated setting. The depth of the transition zone, if it exists, is not known for most occurrences of this setting, but because the aquifers are thickly saturated in most areas, saltwater rise is not likely to be a major limiting factor in this setting, except near the coast.

Perched-Groundwater Setting

In the perched-groundwater setting, groundwater saturates the aquifer above a low-permeability layer (perching member) embedded within a body of higher permeability rock (fig. 13). Beneath the perching member is a zone of unsaturated aquifer, and below the unsaturated zone the aquifer is again saturated by water

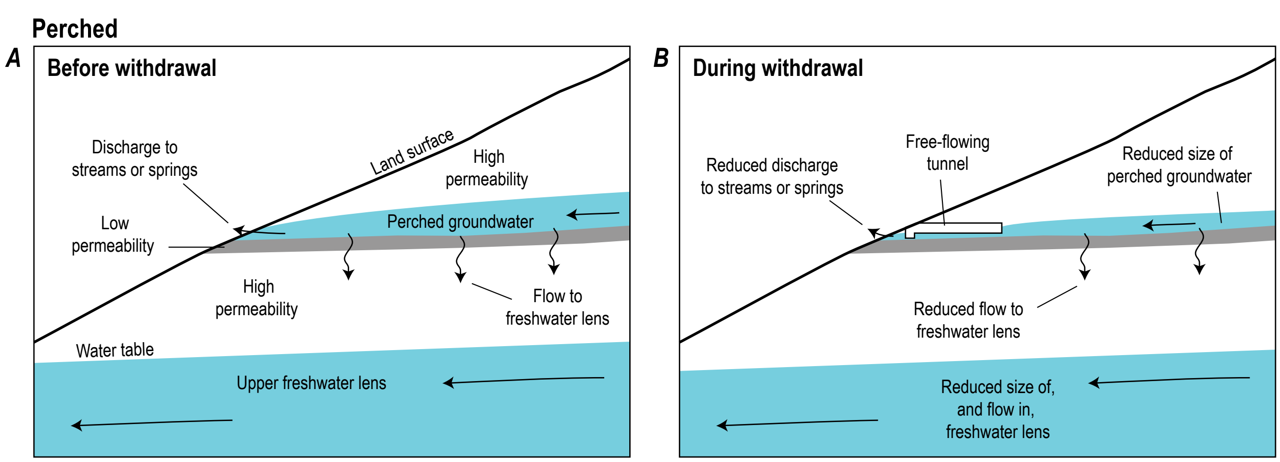

Figure 13. Conceptual diagrams showing the perched-groundwater setting: (*A*) Before withdrawal; (*B*) During withdrawal. Black arrows show direction of groundwater flow.

that is commonly part of a freshwater-lens setting. Groundwater temporarily stored in the perched-groundwater setting eventually continues downward to the freshwater lens or discharges to streams and springs. Withdrawing groundwater from the perched-groundwater setting can result in reductions in discharge to streams and springs or in the availability of water from underlying freshwater-lens settings.

The models in this study do not simulate perched groundwater. Groundwater bodies identified as perched on O‘ahu and Kaua‘i are small and considered insignificant at the whole-island scale of the models in this study, but Gingerich (1999a) postulated the existence of a large perched groundwater body near Ha‘ikū, Maui (fig. 9). Gingerich (1999a) suggested that more than 90 percent of the recharge in the general area moves downward to the freshwater lens rather than to streams.

Schofield High-Level Groundwater

The Schofield high-level groundwater in central O‘ahu (fig. 9*B*) is an area of enigmatically high water levels (about 270–290 ft above sea level) that does not fit into any of the four principal groundwater settings described above. Data from wells indicate that groundwater in this area exists in a high-permeability, dike-free lava-flow aquifer, but the high water levels are not consistent with such aquifer characteristics. Data from deep wells also indicate that the groundwater is not perched (Stearns, 1940; Oki, 1998). Some conceptualizations invoke low-permeability “groundwater dams” along the north and south boundaries, but the geologic nature of the structures and their location are not known precisely.

Effects of withdrawing groundwater.—Groundwater is developed from the Schofield high-level groundwater by conventional vertical wells and shaft-and-gallery systems. Withdrawing groundwater from the Schofield high-level groundwater lowers the water table, but owing to the high permeability of the aquifer, water-table depression is not as great as it can be in lower permeability settings. Saltwater rise and reduction of natural groundwater discharge to the ocean are not likely to be major limiting factors on groundwater availability because the Schofield high-level groundwater is landlocked, and data indicate that fresh groundwater likely extends far below sea level in this area. Reduction of natural groundwater discharge to streams and springs is also not likely to be a limiting factor on groundwater availability because no streams drain the high-level water body.

Withdrawal from the Schofield high-level groundwater can, however, result in reductions in subsurface flow to adjacent groundwater settings, particularly the freshwater-lens settings that are important sources of water on O‘ahu. This effect can limit the availability of groundwater from the Schofield high-level groundwater.

Conceptual Models

Although Kaua‘i, O‘ahu, and Maui share many general hydrogeologic characteristics, each island is unique in terms of age, size, shape, number of shield volcanoes, eruptive stages present, degrees of erosion and sedimentation, geometry of rift zones, and relation to winds and the orographic effect. The following descriptions of conceptual models of groundwater occurrence and flow for Kaua‘i, O‘ahu, and Maui are largely based on descriptions by Izuka and others (2018), whose descriptions are more detailed and include extensive literature and data citations that support the conceptualizations. The summary given here has been substantially abridged.

Kaua‘i

The prevailing view is that most of the subaerial part of Kaua‘i was built by a single shield volcano. The original form of the shield has been carved by erosion and collapse, resulting in a large depression known as the Līhu‘e basin and stream valleys that radiate from the central highland (fig. 14). These depressions have been partly filled by sediments and rejuvenation-stage volcanic rocks.

The bulk of Kaua‘i is formed by stacks of thin lava flows erupted during the island’s shield stage. These lava flows form some of the most permeable aquifers on Kaua‘i. In much of the interior of Kaua‘i, however, the lava flows are intruded by low-permeability dikes that reduce the overall permeability of the aquifers (fig. 15). Near the center of the island is an accumulation of thick caldera-filling lava flows; the unit has low permeability as a result of dike intrusion and thicker lava flows.

In eastern Kaua‘i, dike-intruded lava flows are overlain by rejuvenation-stage lava flows that form low-permeability aquifers (purple area in fig. 15). The low permeability probably results from thick lava flows that formed by ponding in preexisting depressions and interbedded low-permeability sediments.

Dike-free lava flows form high-permeability aquifers along the south coast of Kaua‘i (fig. 15). In southwestern Kaua‘i, the high-permeability aquifers are partly overlain by caprock formed by the sediments in the coastal plain. Dike-free lava flows likely form high-permeability aquifers in much of the Kaua‘i massif below sea level. The dike-free lava-flow aquifer probably emerges on the seafloor where younger units pinch out.

Groundwater flow.—The flow of fresh groundwater on Kaua‘i is governed by the hydraulic properties of the rocks and geologic structures of the island, the distribution of recharge, and the location of groundwater discharge. Recharge on Kaua‘i is high in the high-altitude center of the island where rainfall is highest. The high recharge occurs over predominantly low-permeability rocks, including dike-intruded lava flows and caldera fill. The high water table in the interior of the island is consistent with the high recharge and low bulk permeability of these rocks (fig. 15).

In the area of the low-permeability caldera fill, groundwater saturates nearly to the surface and emerges as a high-altitude wetland (fig. 15). The shape of the water table is largely controlled by streams that incise the aquifer and drain some groundwater. Groundwater that does not discharge to streams or to the high-altitude wetland flows through the subsurface to the surrounding area of dike-intruded lava flows where groundwater exists in the dike-impounded-groundwater setting.

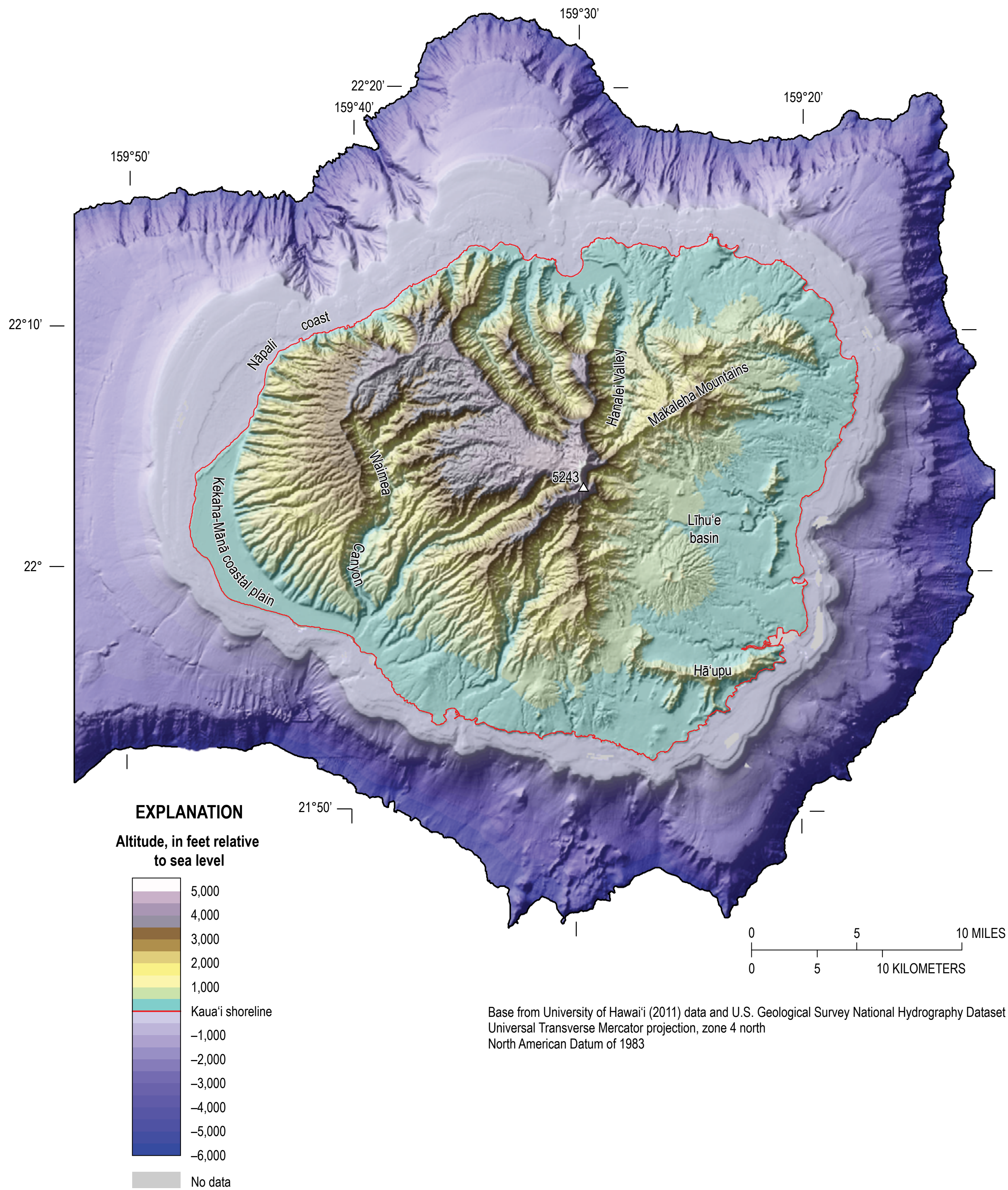

Figure 14. Shaded-relief map of Kaua'i, Hawai'i, and surrounding seafloor. Map is cropped at −6,000 ft, approximate base of the Kaua'i groundwater model. From Izuka and others (2018).

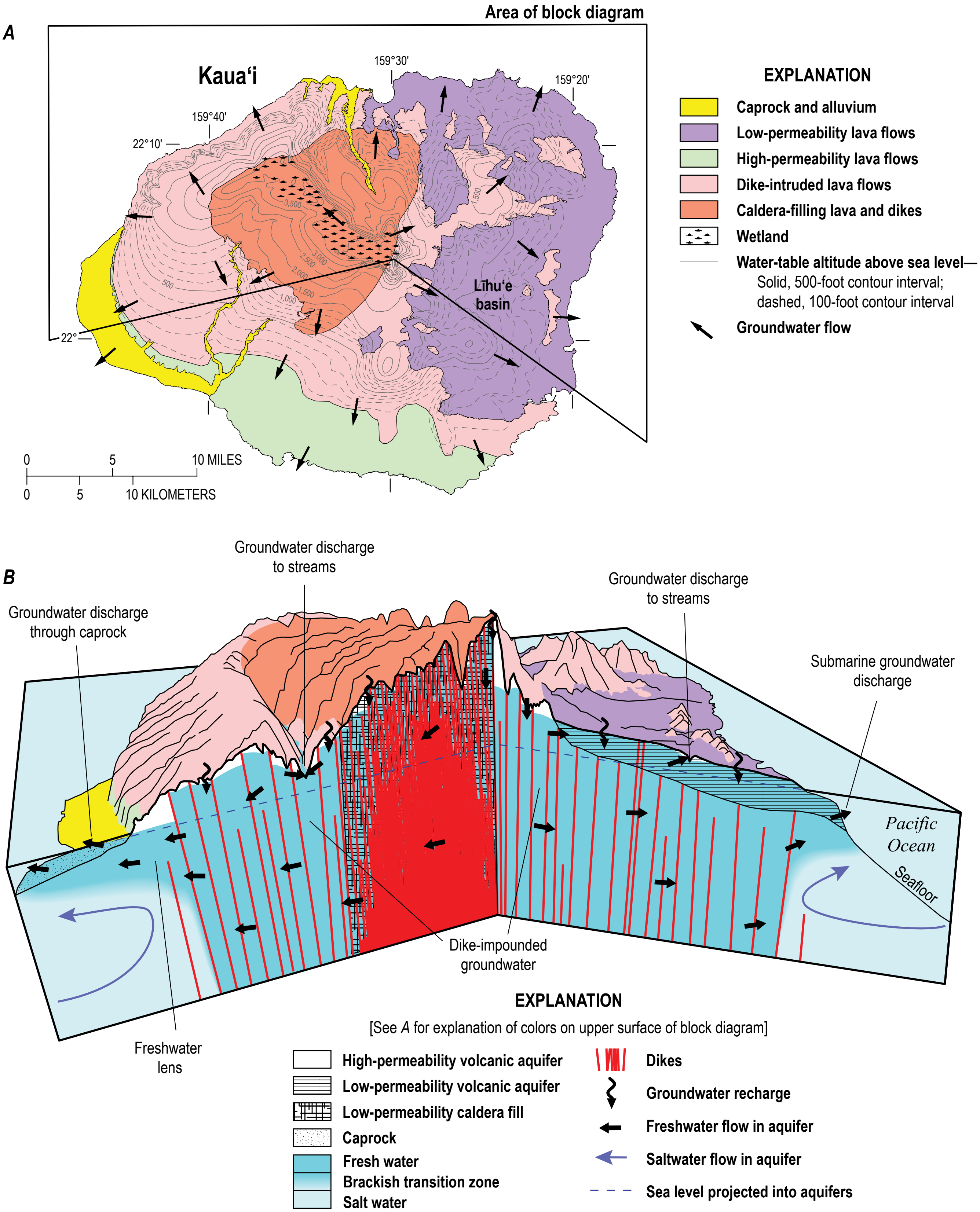

Figure 15. (*A*) Map and (*B*) block diagram showing principal aspects of the conceptual model of groundwater occurrence and flow on Kauaʻi, Hawaiʻi. Map modified from Izuka and others (2021).

Most dike compartments on Kaua‘i have been breached by erosion (fig. 15*B*), so most of the groundwater flowing through the dike-impounded-groundwater setting discharges to streams and springs. Some groundwater is withdrawn by wells and tunnels. Groundwater that is not withdrawn by wells and tunnels or does not discharge to streams and springs flows through the subsurface toward the coast.

In eastern Kaua‘i, some subsurface flow from the dike-impounded-groundwater setting enters the low-permeability lava flows that have accumulated in depressions such as the Līhu‘e basin (fig. 15). The low-permeability lava-flow aquifer also receives inflow from recharge through the surface. The low-permeability lava flows resist groundwater flow, which causes formation of the thickly saturated setting. In some places, the water table rises hundreds of feet above sea level to near the land surface, where groundwater drains into streams. Streams are the primary means by which groundwater discharges naturally from the thickly saturated setting in eastern Kaua‘i.

Near the south coast of Kaua‘i, groundwater from the dike-intruded lava-flow aquifer flows into high-permeability dike-free lava flows (fig. 15). Groundwater in the high-permeability dike-free aquifer exists in the freshwater-lens setting. In the western part of the island, the high-permeability lava-flow aquifer is overlain by caprock that forms a semiconfining hydrogeologic unit. The caprock impedes groundwater discharge from the volcanic aquifers to the ocean and causes the freshwater lens to be thicker than it would be without the caprock. Some groundwater seeps through the caprock and emerges above sea level to form springs and seeps on the coastal plain, and some of it discharges through the caprock below sea level.

O‘ahu

O‘ahu has two prominent mountain ranges, the Wai‘anae and Ko‘olau Ranges (fig. 16). The mountain ranges are the remnants of two basaltic shield volcanoes that have been modified by erosion and faulting (fig. 17). The Ko‘olau volcano is the younger of the two and partly overlaps the eroded flank of the Wai‘anae volcano. The elevated saddle between the two mountain ranges is known as the Schofield plateau. A coastal plain, which is mostly composed of sediments but also includes rocks from the rejuvenation stage of volcanism, surrounds much of O‘ahu.

The bulk of O‘ahu is formed by thin, shield-stage lava flows of the Wai‘anae and Ko‘olau volcanoes (fig. 17). Thick accumulations of these thin lava flows form highly permeable aquifers. Coastal-plain deposits form an extensive semiconfining caprock unit that impedes groundwater discharge from the high-permeability lava-flow aquifers. The caprock allows large volumes of groundwater to accumulate in the underlying highly permeable lava-flow aquifers to greater thicknesses than would be possible without the caprock. The freshwater lenses that form in the high-permeability lava-flow aquifers of O‘ahu are among the most productive in Hawai‘i.

Stream-eroded valleys that cut into the lava flows are partly filled with alluvium and rejuvenation-stage volcanic rocks. These valley-filling deposits, along with weathering of the underlying basalt, form low-permeability barriers to groundwater flow in the otherwise high-permeability lava-flow aquifers. Sediments and weathered basalt also form a low-permeability barrier that separates the lava flows of the Ko‘olau volcano from those of the Wai‘anae volcano (fig. 17*B*).

The lava flows on O‘ahu are intruded by dikes in areas that roughly correspond with parts of the Ko‘olau and Wai‘anae Ranges that have been interpreted as rift zones and calderas (fig. 17*B*). Most dikes on O‘ahu are oriented subparallel within the trends of the rift zones.

Groundwater flow.—Groundwater generally flows from the areas of high water levels in the dike-impounded-groundwater settings of the Ko‘olau and Wai‘anae Ranges through the subsurface to adjacent groundwater bodies such as the Schofield high-level groundwater and the freshwater-lens settings (fig. 17*B*). Groundwater also discharges from the dike-impounded-groundwater setting to streams and springs at the surface. Discharge from the dike-impounded-groundwater setting to streams and springs occurs where dike compartments have been breached by erosion, especially on the northeast flank of the Ko‘olau Range. Discharge from the dike-impounded-groundwater setting to the ocean occurs where the setting extends offshore. In other areas, groundwater from the dike-impounded-groundwater setting flows into adjacent downgradient high-permeability dike-free lava-flow aquifers.

Groundwater in most of the high-permeability dike-free lava-flow aquifers (except for the enigmatic Schofield high-level groundwater) exists in the freshwater-lens setting (fig. 17*B*). The freshwater lenses receive additional groundwater recharge through the land surface. The water tables of the freshwater lenses slope gently from a few tens of feet above sea level in inland areas to near sea level at the coast. Water in the lenses flows toward discharge areas at or near the coast. O‘ahu has extensive semiconfining caprock that impedes discharge from the freshwater lenses near the coasts; as a result, the freshwater lenses are thicker than if the caprock were absent. Because of its extensive caprock, O‘ahu has substantial fresh-groundwater resources that are more readily accessible to humans than do the other islands in Hawai‘i. Some groundwater from O‘ahu’s freshwater-lens settings discharges subaerially to streams and springs at the inland margin of the caprock where it pinches out (fig. 10*C, D*); some of the remaining groundwater flows through the caprock and discharges above and below sea level, and some may discharge directly from the volcanic aquifer where caprock pinches out below sea level.

The Schofield high-level groundwater receives subsurface flow from the dike-impounded-groundwater settings in the Wai‘anae and Ko‘olau Ranges as well as recharge through the land surface. The only means of natural outflow from the Schofield high-level groundwater is through the subsurface to adjacent freshwater lenses in high-permeability lava-flow aquifers to the north and south (fig. 17*A*).

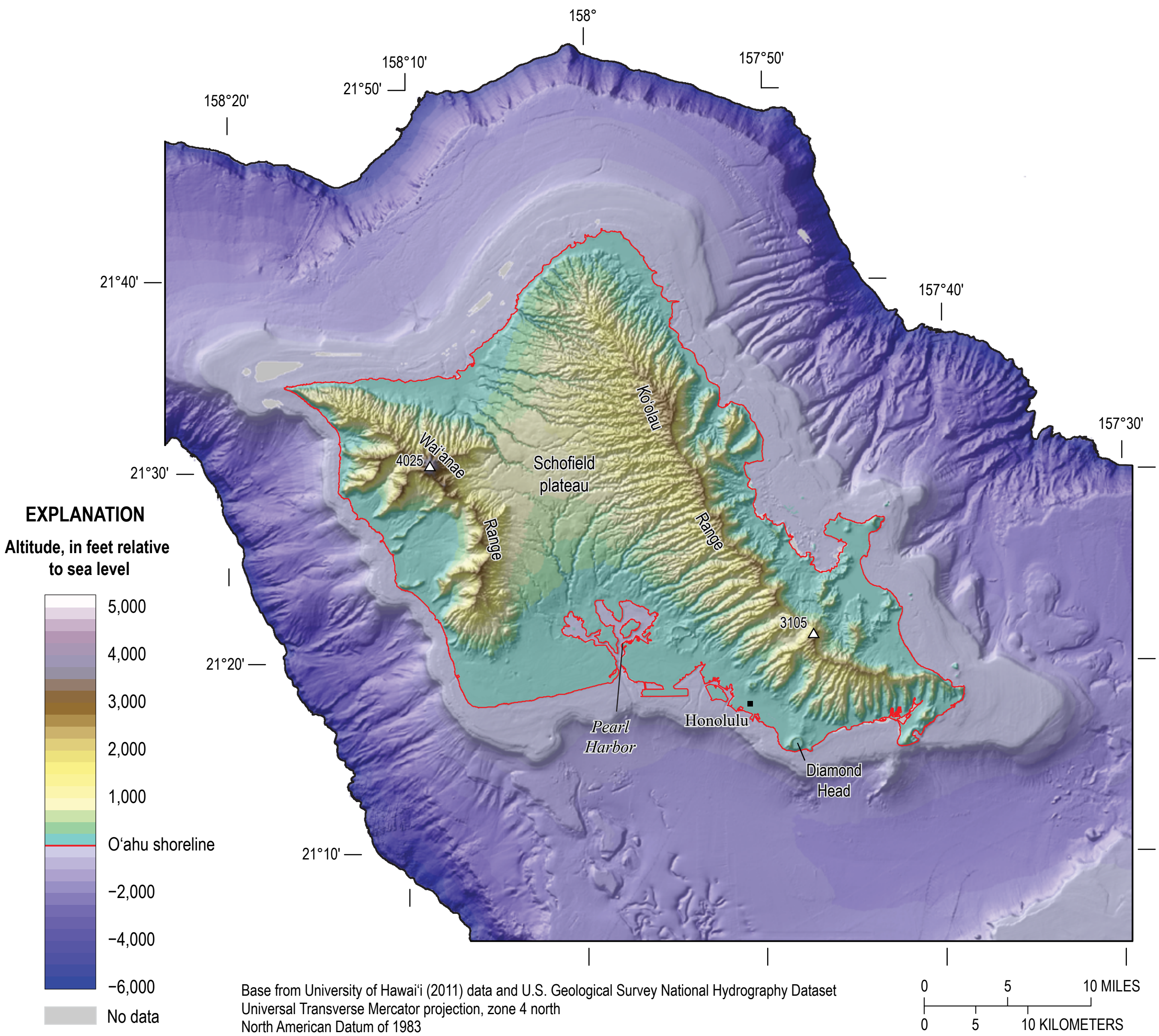

Figure 16. Shaded-relief map of O‘ahu, Hawai‘i, and surrounding seafloor. Map is cropped at −6,000 ft, approximate base of the O‘ahu groundwater model. From Izuka and others (2018).

Maui

Maui is formed by two large shield volcanoes that are connected by a lowland isthmus of sedimentary deposits (fig. 18). The older of the two volcanoes is known as West Maui; to the east lies the younger, larger volcano known as Haleakalā. Haleakalā reaches an altitude of 10,023 ft, making it the tallest shield volcano in the three islands of this study.

Most of the volume of the West Maui volcano is formed by high-permeability lava flows (fig. 19). Dikes intrude the lava flows in a large ovate area near the center of the volcano. Streams have carved deep valleys into the West Maui volcano (fig. 18). Alluvium partly fills the valleys and forms the coastal plain along part of the volcano’s base.

Most of the volume of Haleakalā is formed by high-permeability lava flows (fig. 19). Low-permeability lava flows partly fill large valleys such as Ke‘anae Valley, Kīpahulu Valley, and Kaupō Gap. Three rift zones have been delineated on Haleakalā on the basis of postshield-stage eruptive vents. The distribution of these vents suggests that rift-zone dikes of Haleakalā, similar to those of the Ko‘olau volcano on O‘ahu, are concentrated in narrow, elongate complexes.

The rocks of the West Maui volcano and Haleakalā come together beneath a low-lying area known as the isthmus (fig. 19).

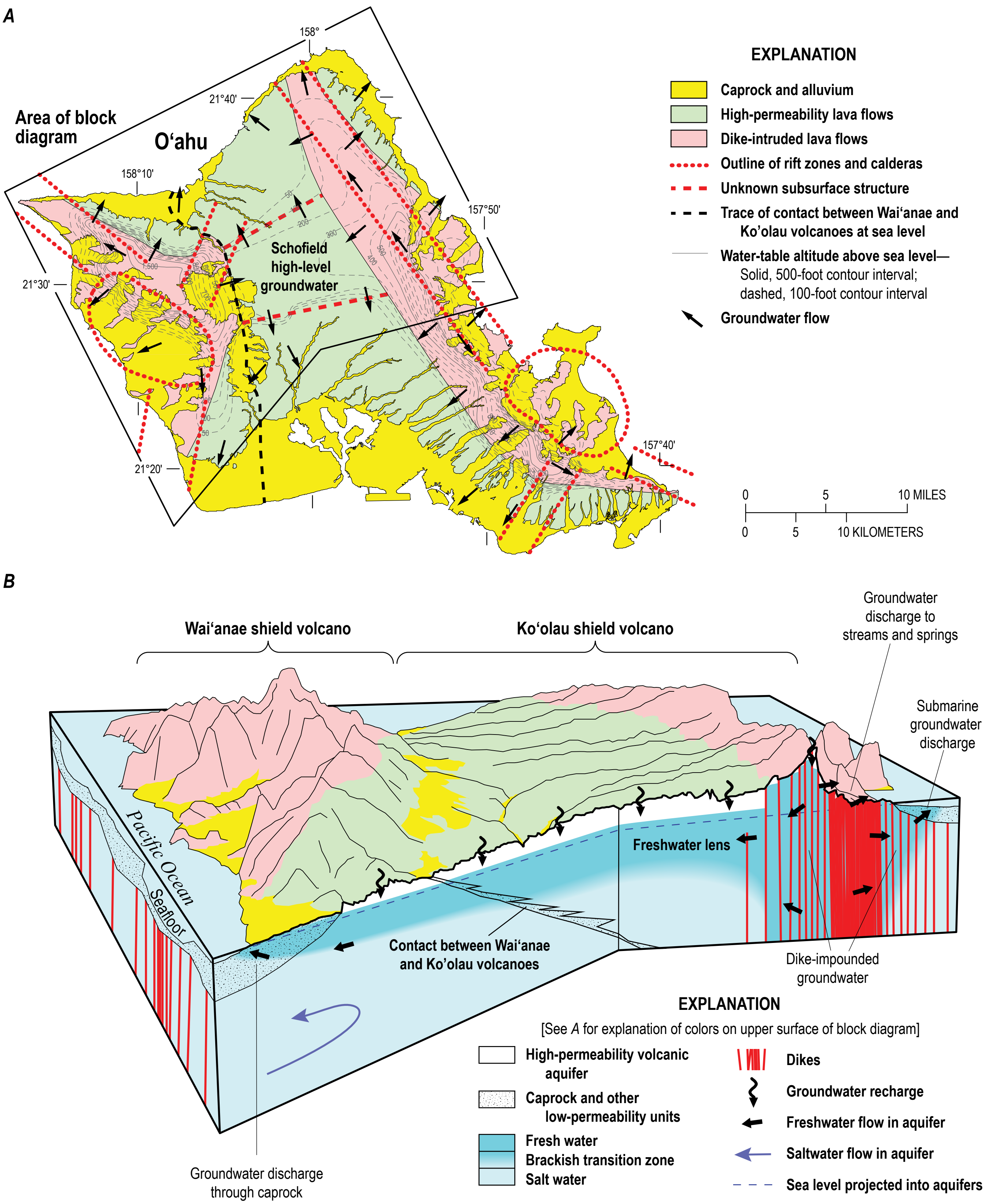

Figure 17. (*A*) Map and (*B*) block diagram showing principal aspects of the conceptual model of groundwater occurrence and flow on O'ahu, Hawai'i. Map modified from Izuka and others (2021).

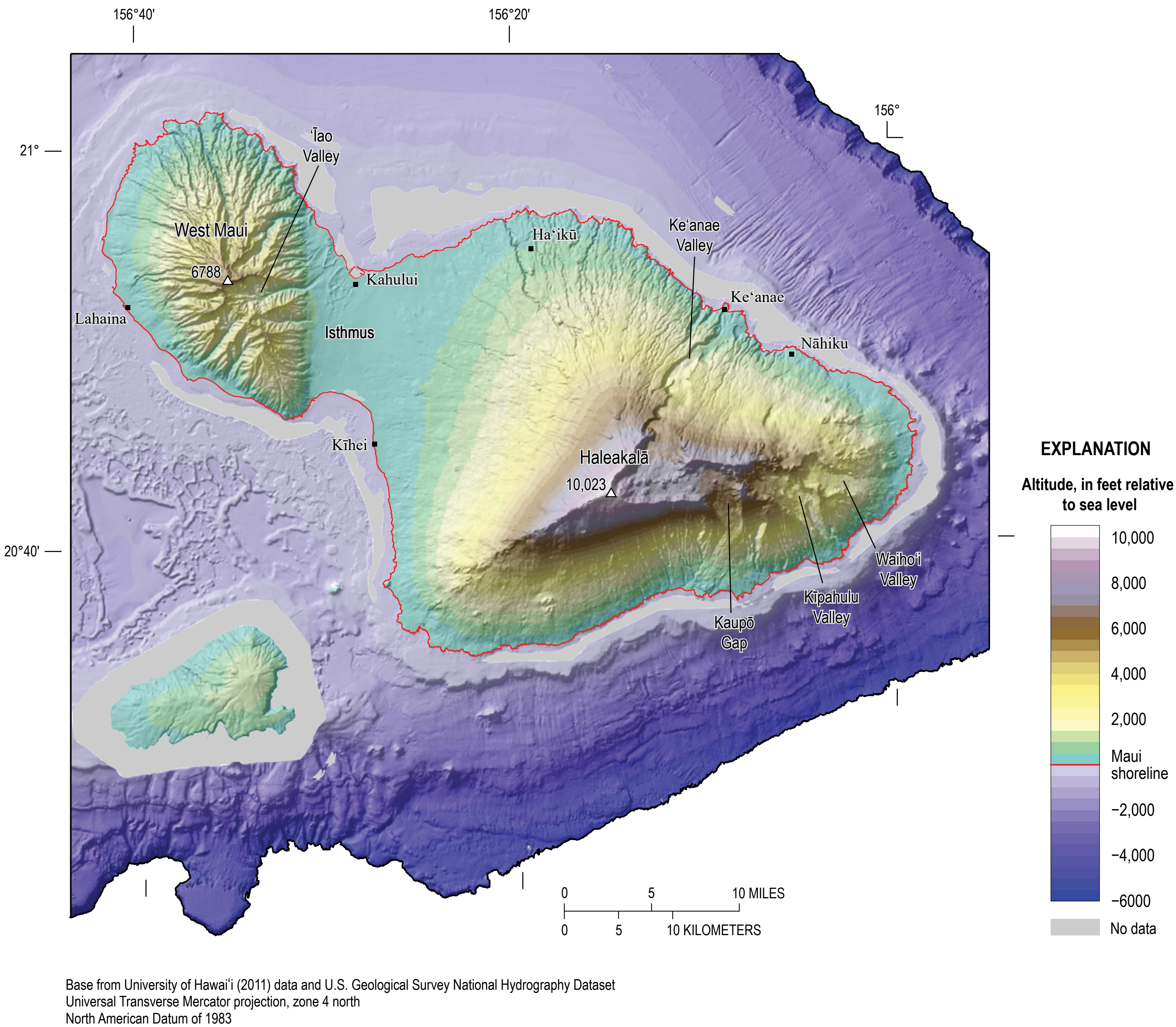

Figure 18. Shaded-relief map of Maui (red outline) and Kahoʻolawe, Hawaiʻi, and surrounding seafloor. Map is cropped at −6,000 ft, approximate base of the Maui groundwater model. From Izuka and others (2018).

The east flank of the West Maui volcano extends beneath lavas from Haleakalā; the west end of Haleakalā extends under the sediments of the isthmus. Sediments and weathered rock also separate the lavas of the West Maui volcano from those of Haleakalā.

Groundwater flow.—In West Maui, groundwater flows from high water levels in the central dike-impounded-groundwater setting toward high-permeability lava-flow aquifers along the coast (fig. 19). Some groundwater naturally discharges from the dike compartments and feeds streams and springs. Streams have eroded into the dike compartments, drain the upper part of the dike-impounded-groundwater setting, and largely control the shape of the water table in the central part of the West Maui volcano (fig. 19*B*).

Groundwater from the central dike-intruded region on West Maui flows into the freshwater-lens setting in the high-permeability lava-flow aquifers along the coast (fig. 19). The water table of the freshwater lens is mostly less than 25 ft above sea level and slopes gently toward the coast. On the southwest side of West Maui, groundwater flows through the freshwater lens and discharges through semiconfining caprock that covers part

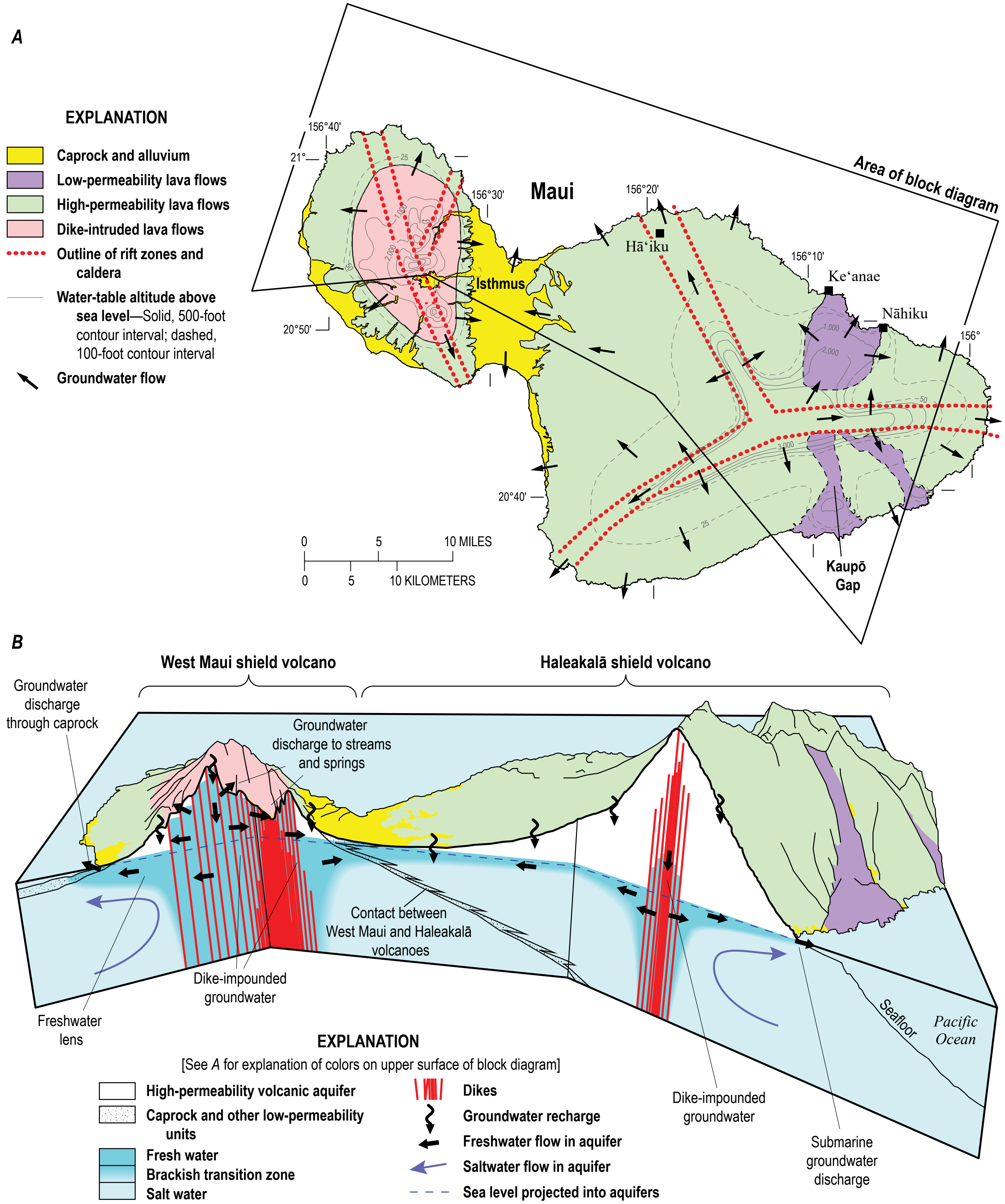

Figure 19. (*A*) Map and (*B*) block diagram showing principal aspects of the conceptual model of groundwater occurrence and flow on Maui, Hawaiʻi. Map modified from Izuka and others (2021).

of the volcanic aquifer near the coast. Compared to O‘ahu, the caprock of West Maui is thinner and less effective in impeding groundwater flow, but the freshwater lens is thicker than it would be without the caprock. Caprock is less extensive along the north coast of West Maui.

Some groundwater from West Maui flows eastward beneath the sediments of the isthmus, where it converges with groundwater flow from Haleakalā (fig. 19). Fresh groundwater in the isthmus exists in the freshwater-lens setting. Groundwater from the lens discharges through caprock along the north and south coasts. The sediments and weathered rock that separate the rocks of West Maui and Haleakalā impede groundwater flow between the two volcanoes.

Conceptualization of groundwater flow in Haleakalā is constrained by the paucity of water-level data from wells. The wells that do exist indicate that the water table is less than 25 ft above sea level throughout much of Haleakalā (fig. 19), which is consistent with a thin freshwater lens in aquifers formed by high-permeability, dike-free lava flows. Except near the isthmus, Haleakalā has no substantial caprock. Some groundwater from Haleakalā flows westward beneath the caprock of the isthmus where it joins groundwater flowing eastward from West Maui and diverts to discharge through caprock to the ocean along the north and south coasts of the isthmus.

Groundwater-level information is lacking for most of Haleakalā's uplands, including the summit and rift zones. Analogy with other shield volcanoes suggests that dike-impounded groundwater probably exists beneath Haleakalā's rift zones, but the dikes have not been extensively breached by erosion as they have been on Kaua‘i, O‘ahu, and West Maui. Groundwater probably flows from the dike-impounded-groundwater setting to the freshwater-lens setting in adjacent high-permeability lava-flow aquifers (fig. 19).

Groundwater in the low-permeability lava flows of the area near Ke‘anae and Nāhiku (fig. 19) exists in the thickly saturated setting (Meyer, 2000). The water table lies nearly at the ground surface, and groundwater discharges to streams that incise the upper saturated aquifer. Much of the groundwater that flows through this area discharges to streams, but some groundwater flows to adjacent freshwater-lens settings or discharges to the ocean below sea level.

Numerical Models

Construction and calibration of the steady-state numerical groundwater-flow models of the volcanic aquifers of Kaua‘i, O‘ahu, and Maui used in this study were described in detail by Izuka and others (2021). This section summarizes parts of their descriptions that are relevant to the numerical models' ability to quantify the consequences of groundwater withdrawals and changes in groundwater recharge that can place limits on groundwater availability.

The numerical models were created using MODFLOW-2005 with the Seawater Intrusion (SWI2) Package (Bakker and others, 2013), which allows simulation of fresh water and salt water in aquifers. The boundary between the saltwater and freshwater bodies is simulated as a sharp interface rather than a transition zone (fig. 20). The sharp interface is an approximation of the part of the transition zone where the brackish water is a mixture of 50 percent fresh water and 50 percent seawater (Izuka and others, 2021).

The active domains of the numerical models include offshore areas; the boundaries of the active domains are set far enough beyond the islands' coasts that the boundaries do not limit fresh-groundwater flow in the models (fig. 21). The altitude of the top of each cell in the upper layer of the model represents the altitude of the surface of the volcanic aquifer within the model cell. Caprock and streambed sediment are not simulated as aquifer units in the models; instead, their effects on groundwater flow in the volcanic aquifers are simulated using head-dependent boundaries. The bottoms of all models are at an altitude of –5,906 ft. The active domains of the models are horizontally divided (discretized) into 500- by 500-ft cells; the number of cells in each model depends on the model size and number of layers (table 1). The number of layers varies among the models depending on whether the conceptual model indicates a need to account for layering of hydraulic properties: O‘ahu and Maui are single-layer models; Kaua‘i is a two-layer model.

The Recharge Package in MODFLOW-2005 (Harbaugh, 2005) is used to simulate water entering the model through the upper surface as groundwater recharge (table 1, fig. 22). Recharge is applied only to model cells whose tops were above sea level. No recharge is applied, however, to cells covered by caprock; these areas are assumed to be zones of discharge. Recharge

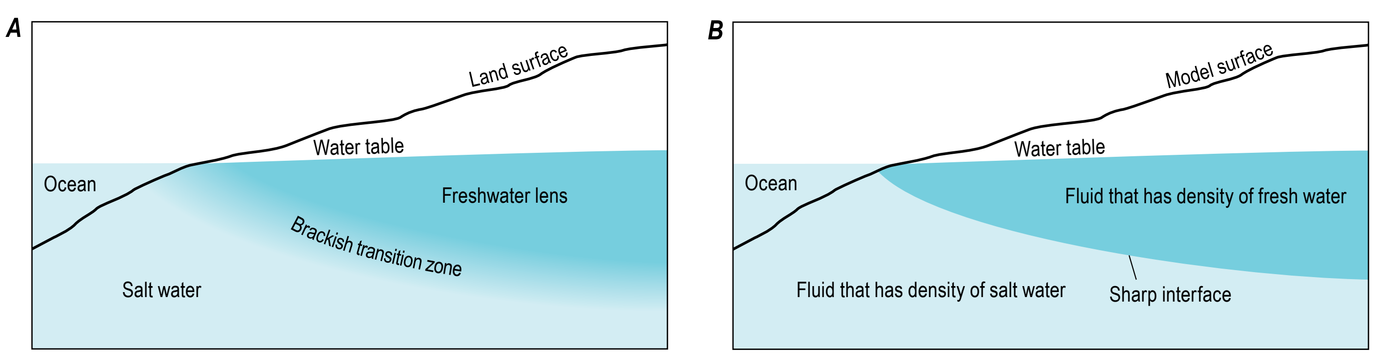

Figure 20. Diagrams showing the boundary between fresh water and salt water in an aquifer. (*A*) An actual freshwater-saltwater boundary is a zone that transitions gradually from fresh water above to salt water below. (*B*) In the numerical groundwater models in this study, the boundary is simulated as a sharp interface (that is, a surface) between immiscible fluids that have different densities (fresh water is less dense than salt water).

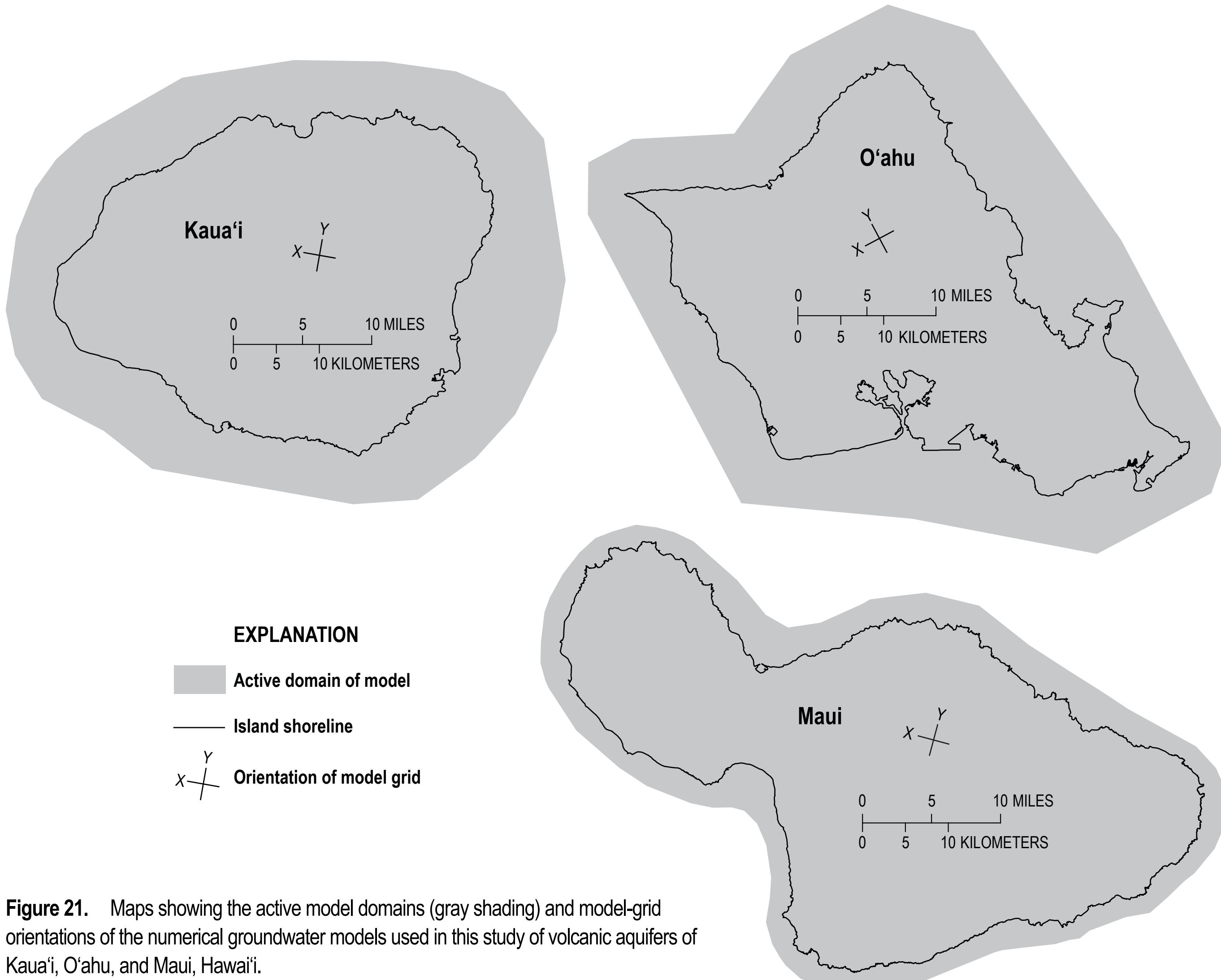

Figure 21. Maps showing the active model domains (gray shading) and model-grid orientations of the numerical groundwater models used in this study of volcanic aquifers of Kaua‘i, O‘ahu, and Maui, Hawai‘i.

Table 1. Selected aspects of calibrated numerical groundwater models of the volcanic aquifers of Kaua‘i, O‘ahu, and Maui, Hawai‘i, used in this study.

[Data from Izuka and others (2021). no., number; *K* zone, hydraulic-conductivity zone; Mgal/d, million gallons per day]

Model	No. of layers	Active cells	*K* zones	Total recharge (Mgal/d)	Withdrawal (Mgal/d)		Groundwater discharge (Mgal/d)	
					Pumped wells	Tunnels	Streams and springs	Ocean
Kaua‘i	2	191,399	12	871.2	49.1	0.6	701.2	120.4
O‘ahu	1	130,429	37	597.6	188.0	33.2	127.7	248.6
Maui	1	107,399	20	1,166.7	97.5	11.4	156.6	901.2

applied to most areas of the models was extracted from the datasets of average recharge for 2001–2010 computed by Izuka and others (2018); this period corresponds with the 2001–2010 period for withdrawal and observation data used for calibration. Recharge applied to areas of the models that represent zones of dike intrusion was extracted from datasets of average recharge for 1978–2007 computed by Izuka and others (2018). The average recharge from the earlier and longer 1978–2007 period is a better representation of the source of the water that was flowing slowly through the dike-intruded setting during the 2001–2010 calibration period (Izuka and others, 2021).

In MODFLOW-2005, the Well Package is used to simulate groundwater withdrawn by wells, and the Drain Package is used to simulate groundwater discharge to streams and springs, flow from free-flowing tunnels, and discharge to the ocean through inland parts of the caprock where the top of the caprock is above sea level. The General-Head Boundary Package is used to simulate exchange of water between the aquifers and the ocean where the top of the caprock lies below sea level.

Active cells in each model are grouped into zones having uniform hydraulic properties (fig. 23). All cells within a zone of uniform hydraulic conductivity (*K* zone) were calibrated to the

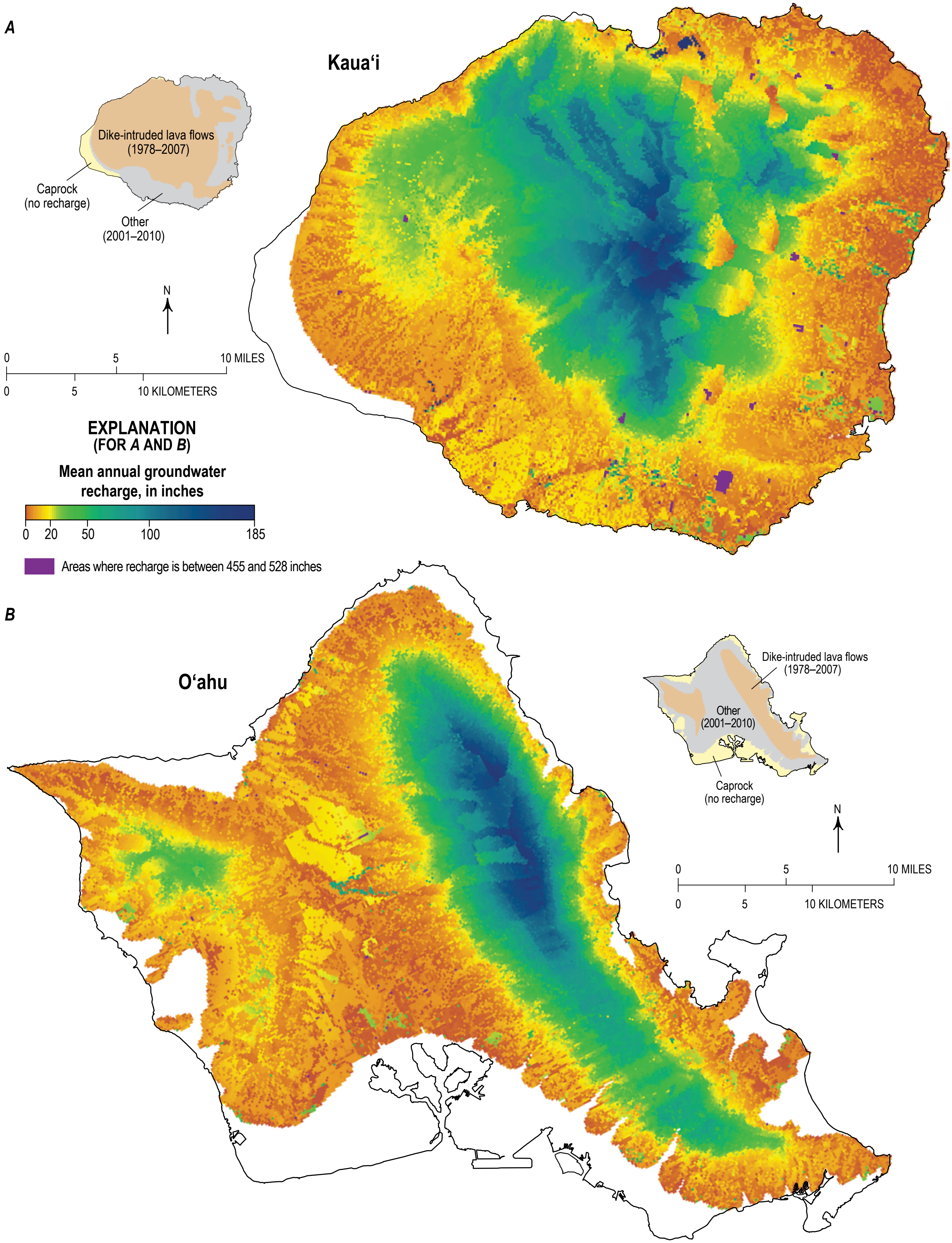
A
Kauaʻi
Dike-intruded lava flows (1978–2007)
Caprock (no recharge)
Other (2001–2010)
N
0 5 10 MILES
0 5 10 KILOMETERS
EXPLANATION (FOR A AND B)
Mean annual groundwater recharge, in inches
0 20 50 100 185
Areas where recharge is between 455 and 528 inches
B
Oʻahu
Dike-intruded lava flows (1978–2007)
Other (2001–2010)
Caprock (no recharge)
N
0 5 10 MILES
0 5 10 KILOMETERS

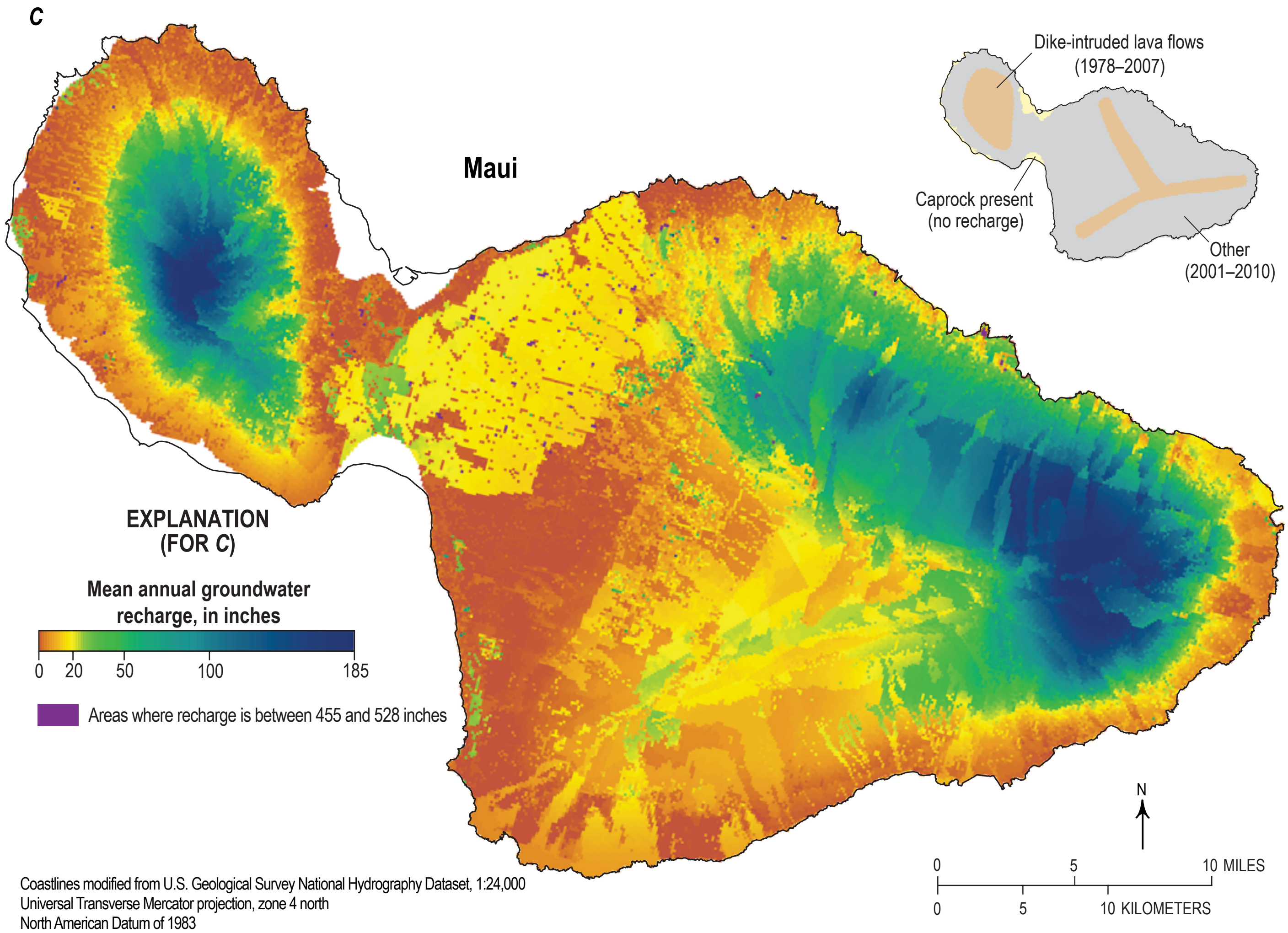

Figure 22. Maps showing the distribution of groundwater recharge in the numerical groundwater models of (*A*) Kaua'i, (*B*) O'ahu, and (*C*) Maui, Hawai'i. Recharge is based on averages computed by Izuka and others (2018) for time periods shown on inset maps. From Izuka and others (2021).

same horizontal hydraulic conductivity (and vertical hydraulic conductivity for the two-layer Kaua'i model). The number of *K* zones varies among the models (table 1) but generally corresponds with the hydrogeology described by Izuka and others (2018), with some adjustments to account for local hydrogeologic details. The *K* zones also are generally consistent with the spatial distribution of the principal groundwater settings (fig. 9) and conceptual models (figs. 15, 17, 19), although some differences result from limitations inherent in model discretization. For example, dikes were not simulated as individual hydrogeologic units, but *K* zones representing dike-intruded areas were assigned an overall hydraulic conductivity representing a combination of low-permeability dikes and higher permeability lava flows.

The models were calibrated in the steady-state mode for conditions representing 2001–2010 (Izuka and others, 2021). In the steady-state mode, groundwater inflow (from recharge) is balanced by the total of all outflow (groundwater withdrawals by humans and groundwater discharge to the ocean, streams, and springs). Steady-state models indicate the water-table altitude, altitude of the freshwater-saltwater interface, and rates of groundwater discharge to streams and the ocean that would ultimately exist if recharge and withdrawal rates remained constant indefinitely (figs. 24, 25, 26, 27). Also, changes in stresses such as groundwater withdrawals or recharge will be balanced by equivalent changes in simulated groundwater discharge to streams or the ocean. For models created with the SWI2 Package of MODFLOW, steady state is achieved by running in the transient mode until the altitude of the freshwater-saltwater interface stops changing from one time step to the next. However, in some model cells at boundaries between two *K* zones that have sharply contrasting hydraulic properties (for example, between dike-intruded aquifers and dike-free lava-flow aquifers), the interface altitude oscillated about an average value as the model approached steady state, leading to an inability to achieve steady state and imbalances between changes in stresses and changes in groundwater discharge. To mitigate the effect of the oscillation,

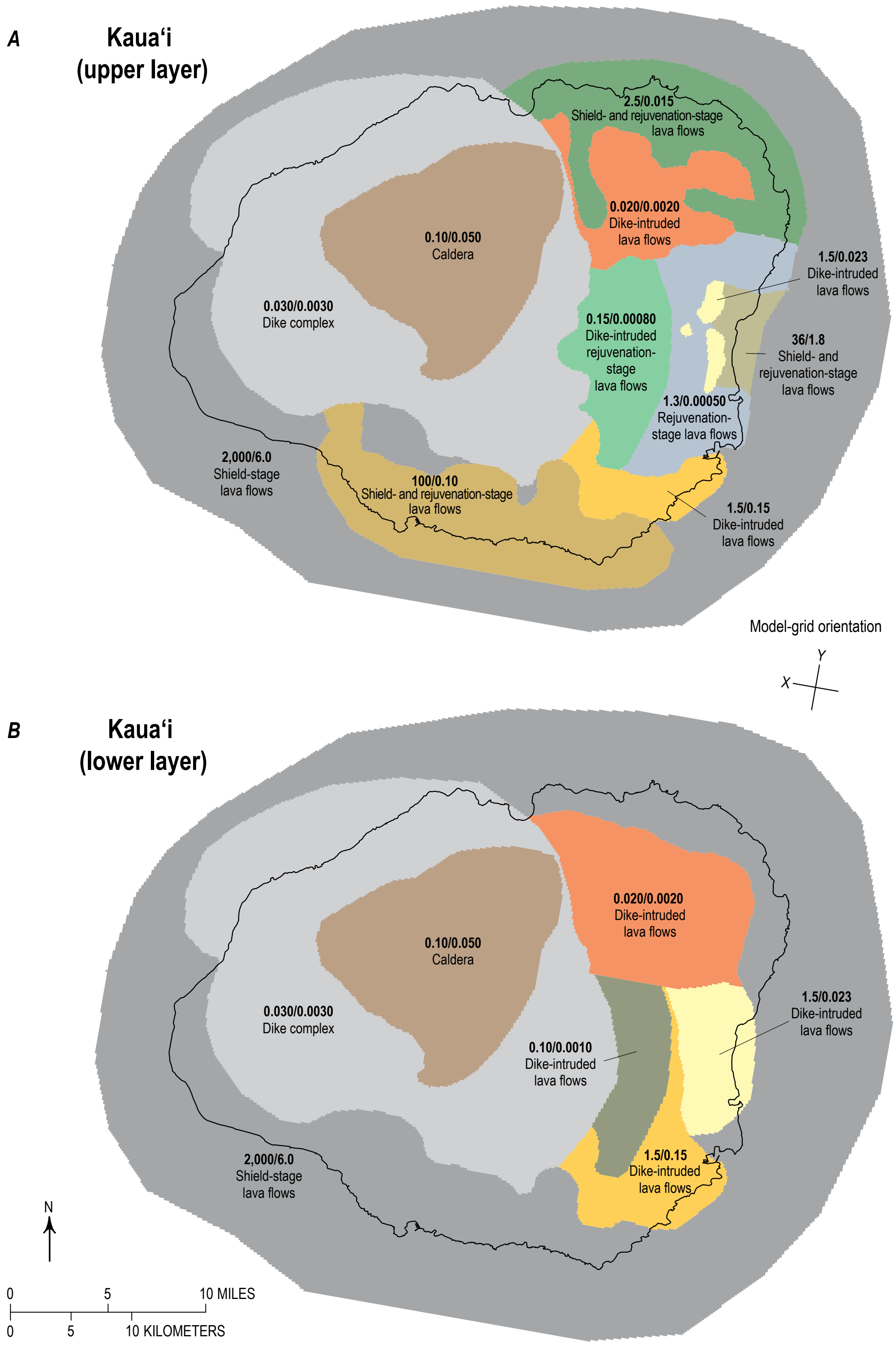

Figure 23. Maps showing the hydraulic-conductivity zones (*K* zones) and values in the numerical groundwater models of (*A*) Kaua‘i (upper layer), (*B*) Kaua‘i (lower layer), (*C*) O‘ahu, and (*D*) Maui, Hawai‘i. Numbers show hydraulic conductivity, in feet per day. For the two layers of the Kaua‘i model (*A*, *B*), values to the left of the slash are horizontal hydraulic conductivity in both the X and Y directions of the model grid; values to the right are vertical hydraulic conductivity. For the O‘ahu (*C*) model, values to the left of the slash indicate horizontal hydraulic conductivity in the X direction; values to the right indicate horizontal hydraulic conductivity in the Y direction. For the O‘ahu (*C*) and Maui (*D*) models, values without slashes indicate horizontal hydraulic conductivity in both the X and Y directions. Modified from Izuka and others (2021).

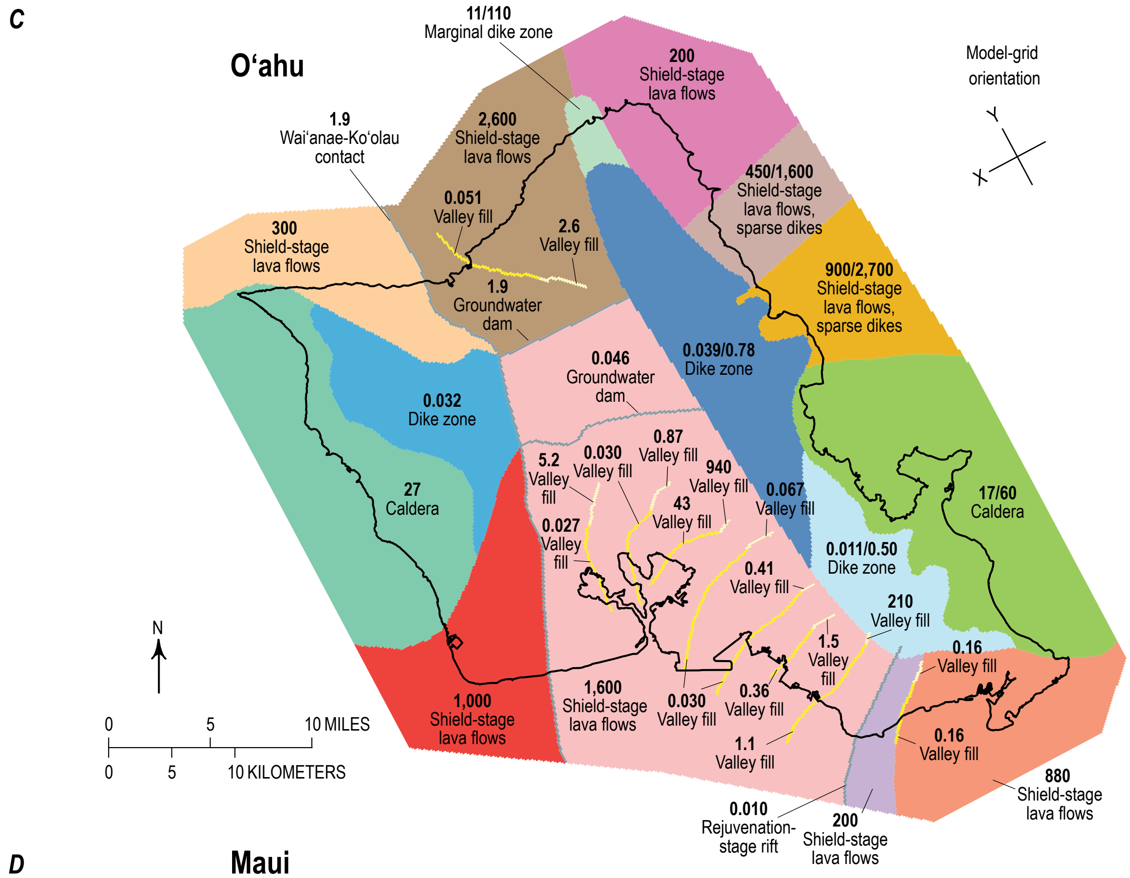

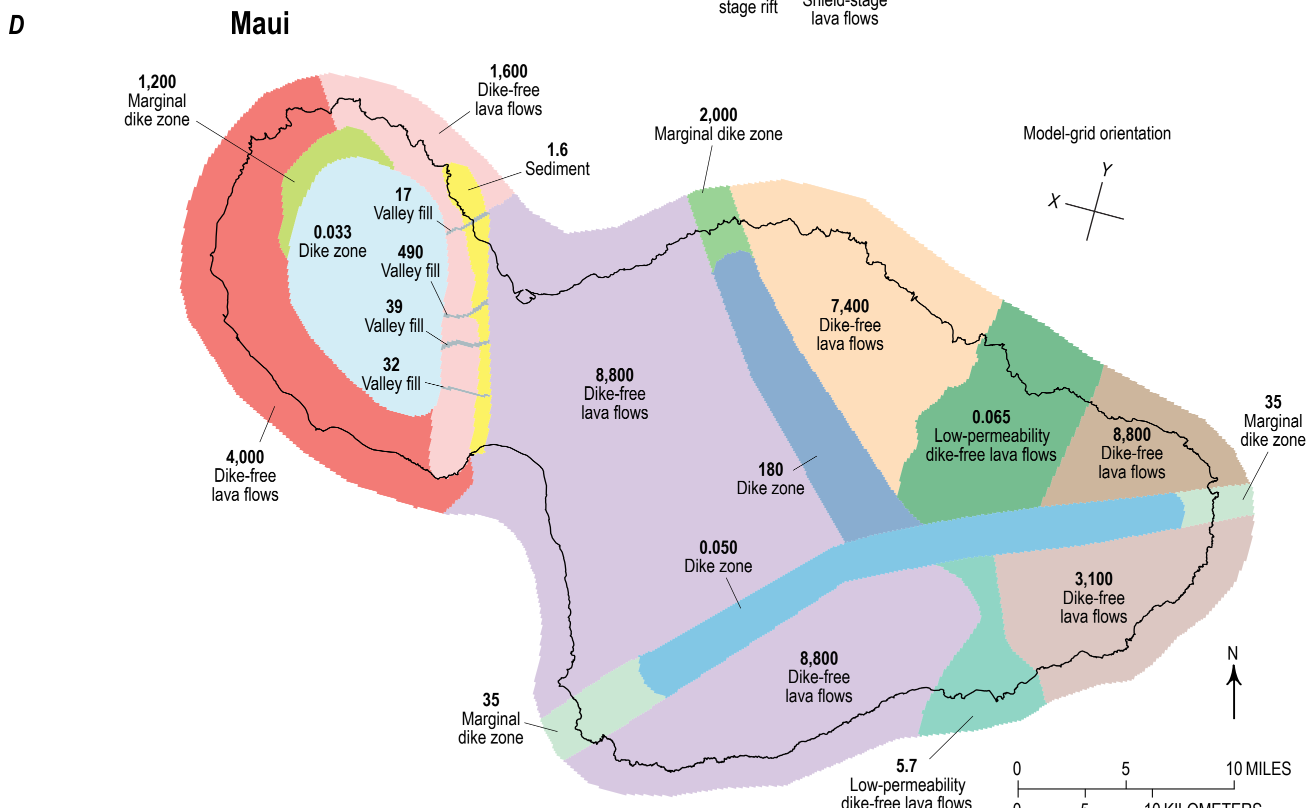

Coastlines modified from U.S. Geological Survey National Hydrography Dataset

Figure 23.—Continued

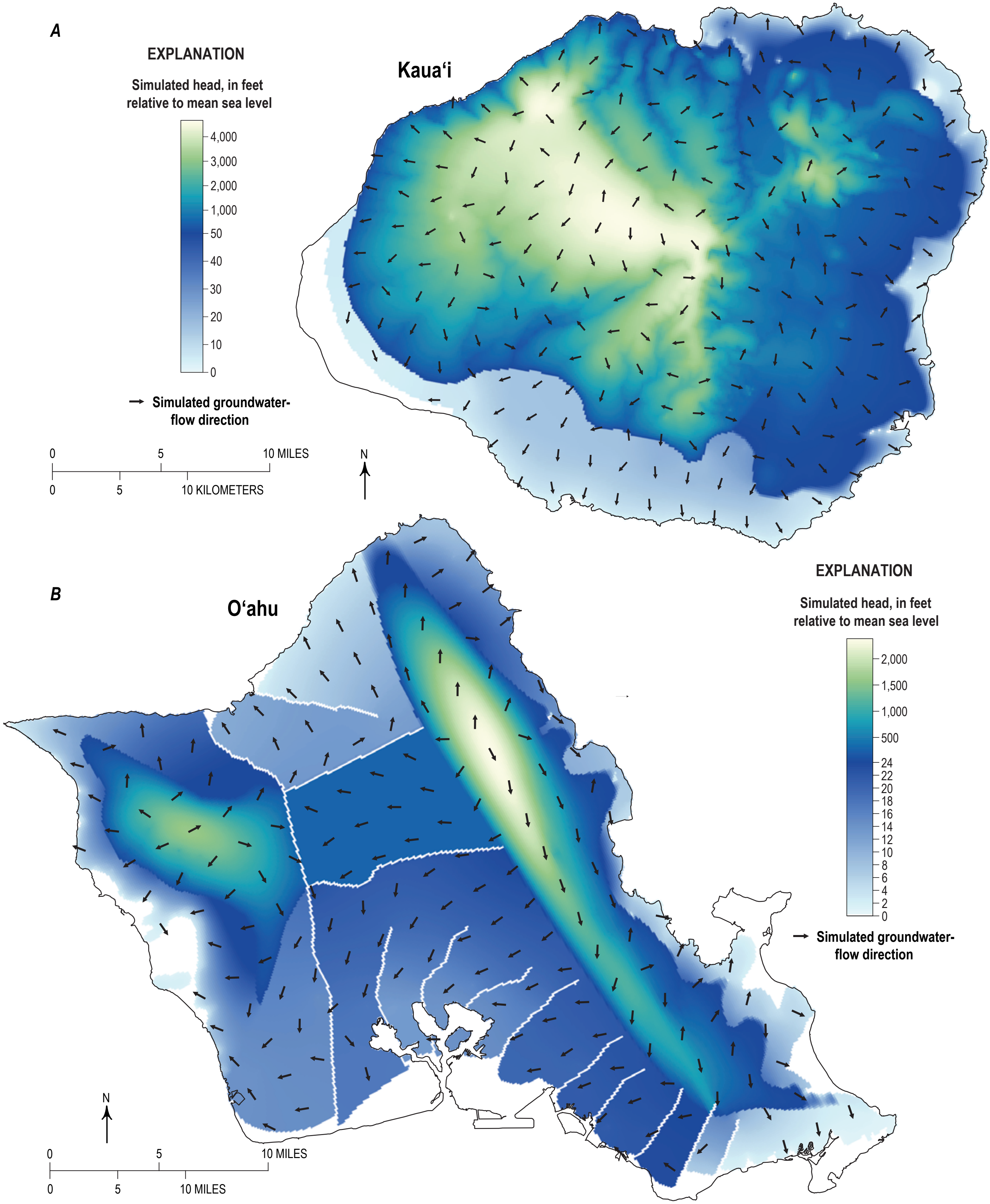
A
EXPLANATION
Simulated head, in feet relative to mean sea level
4,000
3,000
2,000
1,000
50
40
30
20
10
0
Simulated groundwater-flow direction
0
5
10 MILES
0
5
10 KILOMETERS
N
Kauaʻi
B
Oʻahu
EXPLANATION
Simulated head, in feet relative to mean sea level
2,000
1,500
1,000
500
24
22
20
18
16
14
12
10
8
6
4
2
0
Simulated groundwater-flow direction
N
0
5
10 MILES
0
5
10 MILES

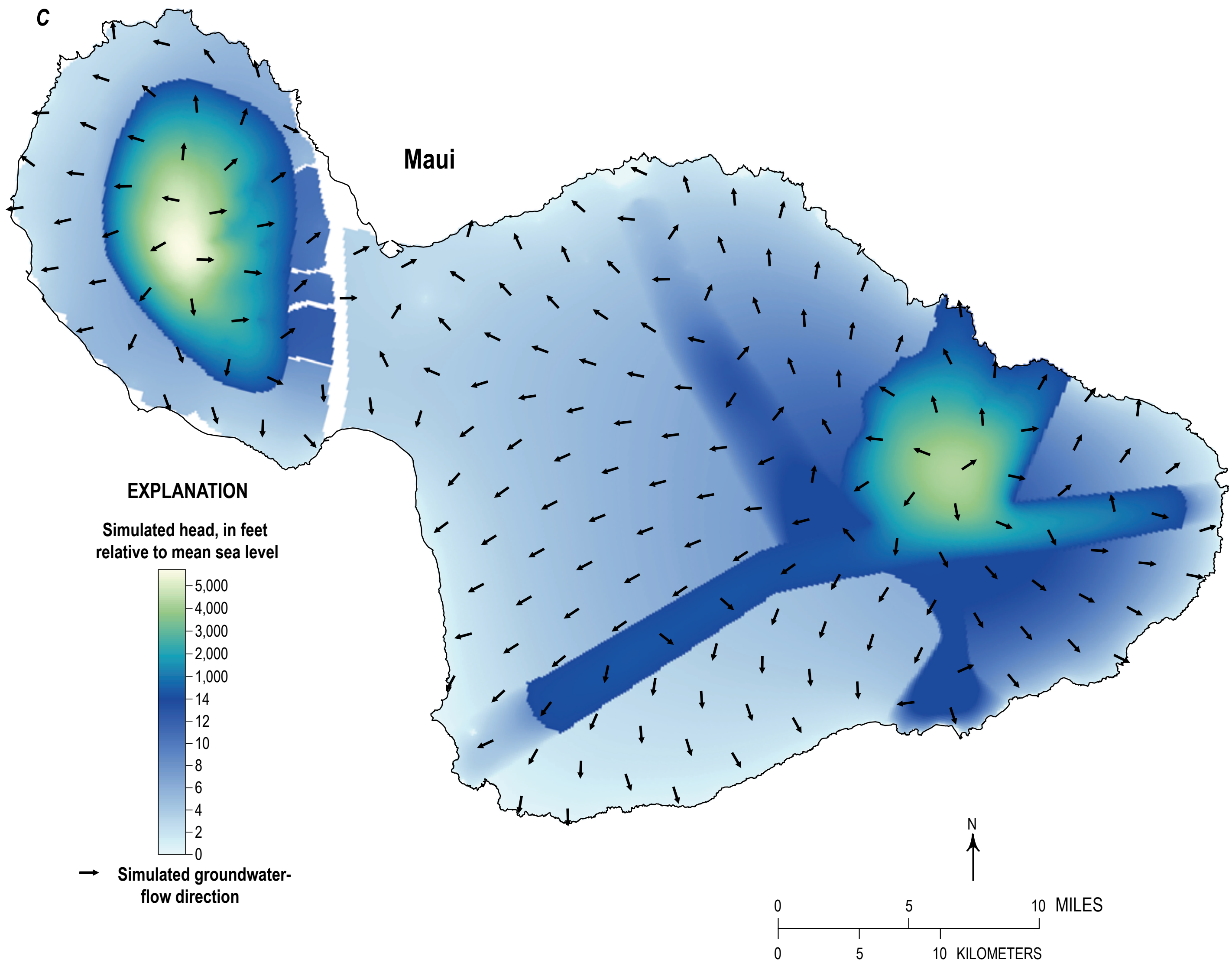

Figure 24. Maps showing the simulated head and groundwater flow in the calibrated numerical groundwater models of (*A*) Kaua‘i (upper layer), (*B*) O‘ahu, and (*C*) Maui, Hawai‘i. Modified from Izuka and others (2021).

model results from the last two time steps of the final runs for each model were averaged and the averages were used for the purposes of calibration and simulation results discussed in this report. Some imbalances persisted, but they were rare and small.

In this study, the simulated heads in the upper layer of each model represent the altitude of the water table of that island. The simulated heads and flows in the calibrated models of Kaua‘i, O‘ahu, and Maui (fig. 24) are generally consistent with the respective conceptual models (figs. 15, 17, 19). In this study, simulated heads in the upper layer of each model are considered to represent water levels in the volcanic aquifers. Simulated heads are highest in the high-altitude areas of each island, which generally correspond to the interior of the shield volcanoes where the dike-impounded-groundwater setting predominates. Draining by incised streams controls heads in most areas of the dike-impounded-groundwater setting, except on Haleakalā, where stream incision is less advanced. Groundwater in the dike-impounded-groundwater setting that does not discharge to streams and springs flows through the subsurface to downgradient aquifers—such as the high-permeability aquifers of the freshwater-lens setting, the low-permeability aquifers of the thickly saturated setting (eastern Kaua‘i), or the Schofield high-level groundwater (O‘ahu)—or discharges directly from the dike-impounded-groundwater setting to the ocean.

The simulated altitudes of the freshwater-saltwater interface in the calibrated models (figs. 25, 26) are also consistent with the

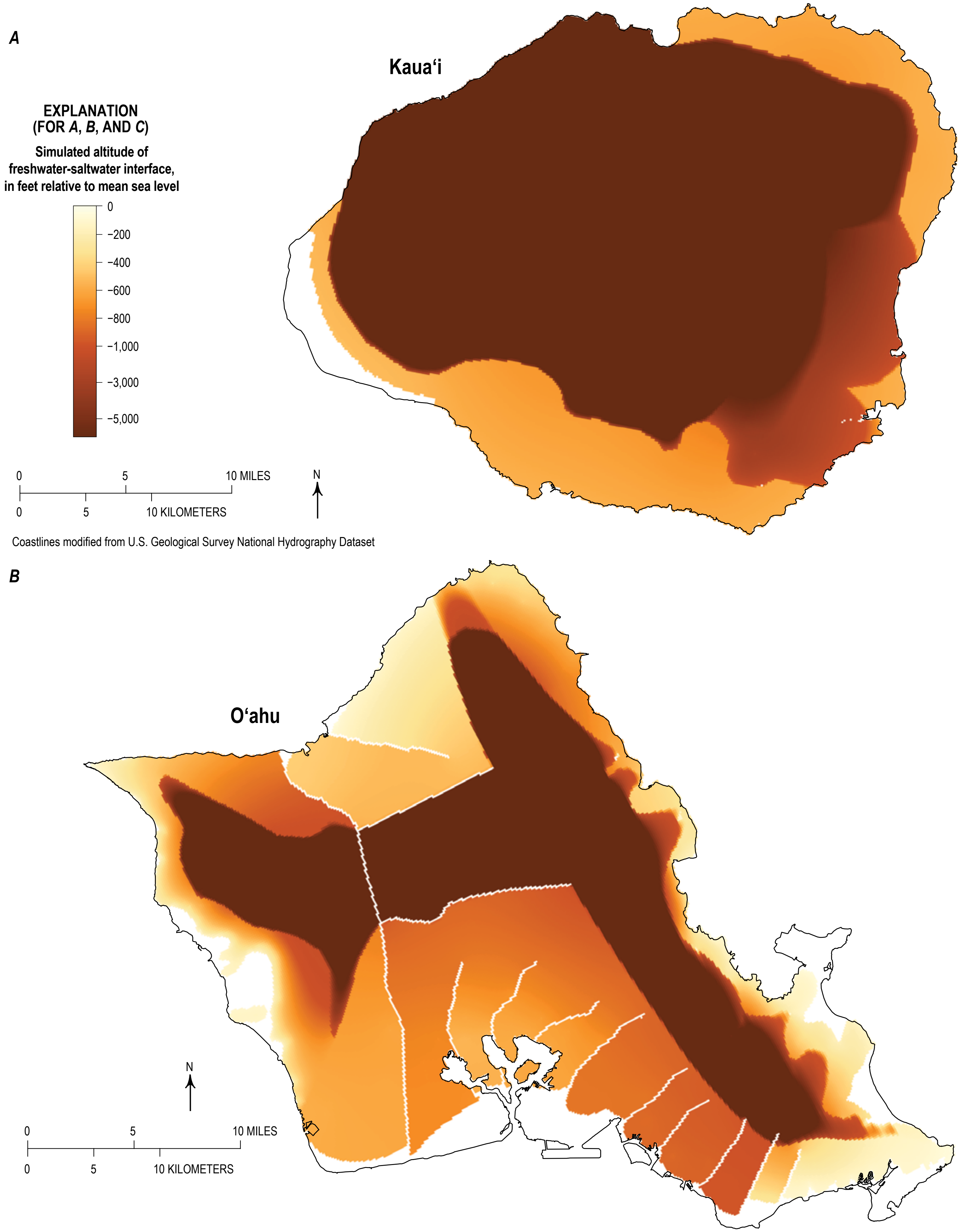
A
Kaua‘i
EXPLANATION
(FOR A, B, AND C)
Simulated altitude of
freshwater-saltwater interface,
in feet relative to mean sea level
0
−200
−400
−600
−800
−1,000
−3,000
−5,000
0
5
10 MILES
0
5
10 KILOMETERS
N
Coastlines modified from U.S. Geological Survey National Hydrography Dataset
B
O‘ahu
N
0
5
10 MILES
0
5
10 KILOMETERS

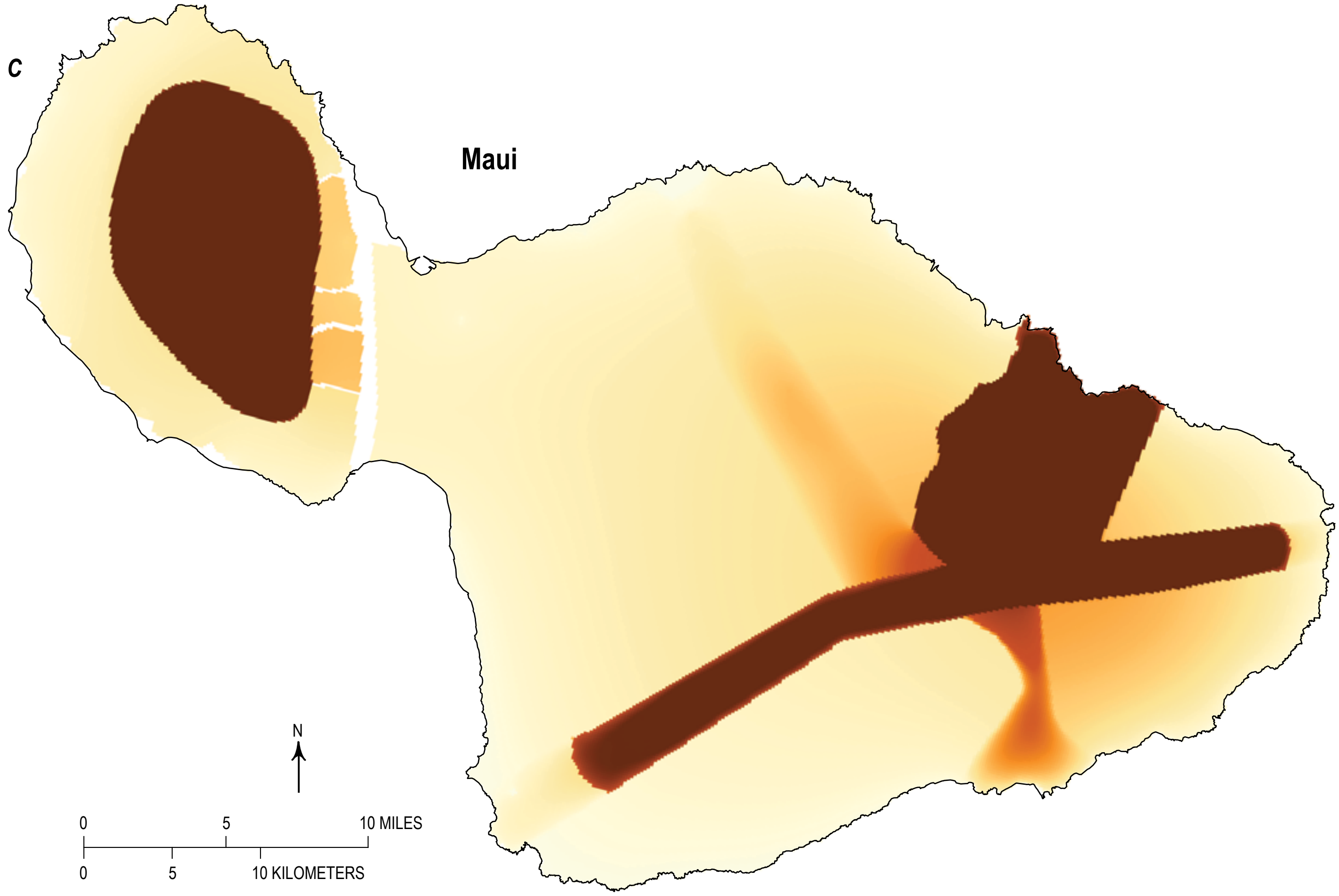

Figure 25. Maps showing the simulated altitude of the freshwater-saltwater interface in the calibrated numerical groundwater models of (*A*) Kauaʻi, (*B*) Oʻahu, and (*C*) Maui, Hawaiʻi. Modified from Izuka and others (2021).

conceptual models. The interface is shallowest in the freshwater-lens setting and deeper in the thickly saturated setting. Fresh groundwater extends down to the bottom of the model in the dike-impounded-groundwater setting and the Schofield high-level groundwater.

The calibrated steady-state models of Kauaʻi, Oʻahu, and Maui show substantial differences in the relative distribution of discharge among the outflow components (Izuka and others, 2021) (fig. 28). These differences reflect the different principal groundwater settings that are predominant on each island and differences in groundwater-withdrawal rates. Withdrawals as a percentage of the total fresh-groundwater discharge are highest in the Oʻahu model, which is commensurate with the large population of that island. Discharge to streams and springs as a percentage of total freshwater discharge is highest in the Kauaʻi model, which is consistent with the large areas of the island where streams cut into and drain the dike-impounded-groundwater and thickly saturated settings (figs. 9 and 15). Groundwater discharge directly to the ocean as a percentage of total freshwater discharge is highest in the Maui model, which is consistent with the island's extensive freshwater-lens settings. These results indicate that consequences that potentially limit the availability of fresh groundwater for human use are likely to differ among the three islands.

Numerical-Model Simulations to Assess Groundwater Availability

Five scenarios representing current conditions and various historical and projected future groundwater-withdrawal and recharge conditions (table 2) were simulated using the numerical models (Rotzoll and Izuka, 2023). The Current scenario represents conditions in 2010, which were used to calibrate the Kauaʻi, Oʻahu, and Maui models (Izuka and others, 2021). This scenario is the baseline to which all other scenarios are compared. Two historical scenarios—No Withdrawal and Predevelopment—represent selected aspects of conditions that existed in 1870, before the first modern well was drilled in 1879; these scenarios were simulated using all three models in this study. Two future

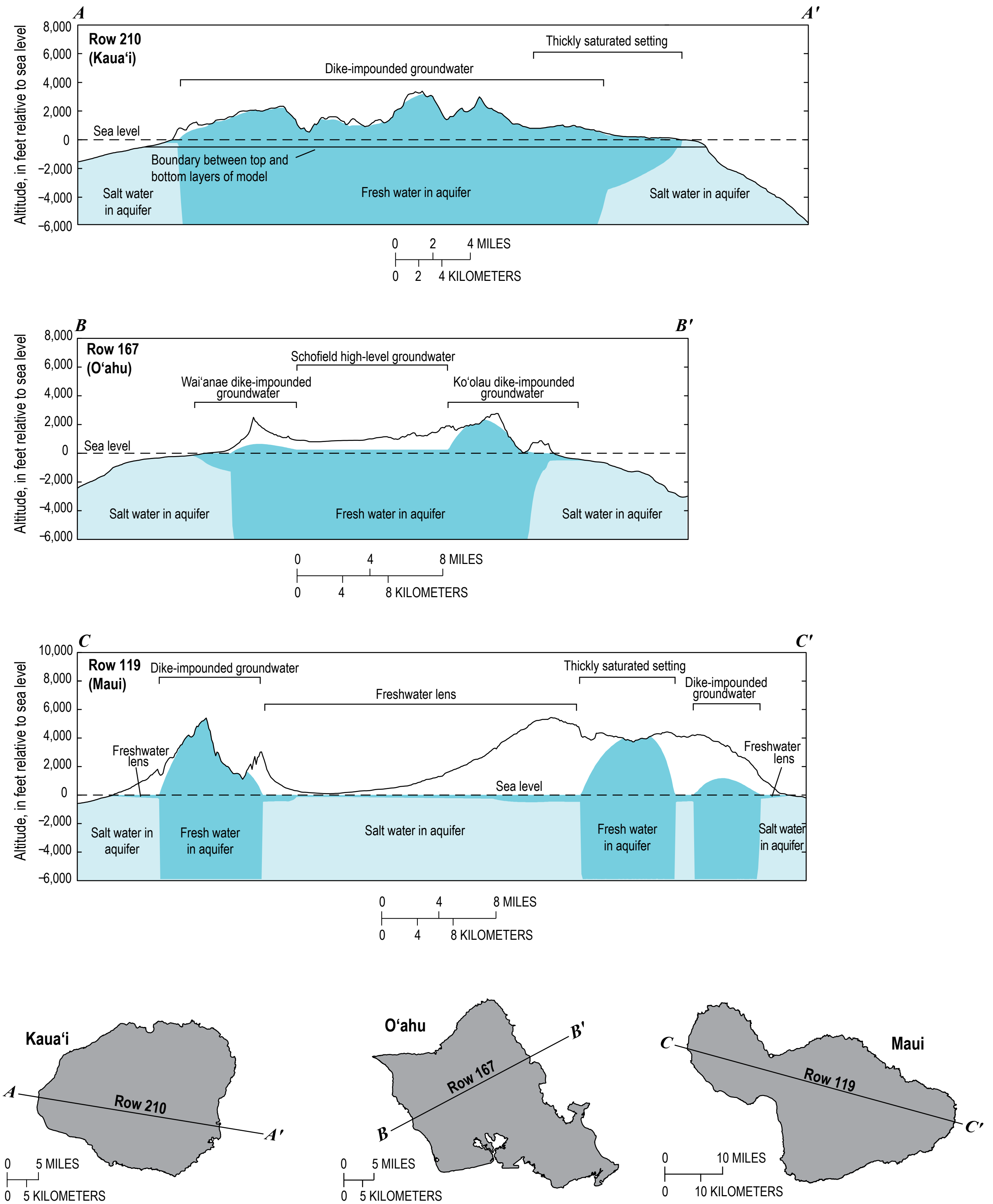

Figure 26. Cross sections showing the simulated freshwater and saltwater extents in the calibrated numerical groundwater models of (*A*) Kauaʻi (*A—A′*), (*B*) Oʻahu (*B—B′*), and (*C*) Maui (*C—C′*), Hawaiʻi. Approximate vertical exaggeration varies from 4 to 5 times. Inset maps show locations of cross-section lines on each island. Modified from Izuka and others (2021).

scenarios—Future Rainfall and Increased Withdrawal—represent projections of future conditions and were simulated using the O‘ahu model only.

Approach to Assessing Groundwater Availability

The scenario results were compared to assess the consequences that can limit groundwater availability. The No Withdrawal and Predevelopment historical scenarios were compared to the Current scenario to assess the effects of historical changes in groundwater withdrawals and recharge. The Increased Withdrawal and Future Rainfall scenarios were compared to the Current scenario to assess the possible effects of increases in groundwater withdrawals and climate change that may occur in the future. To facilitate discussion in this report, each of the four assessments is identified by a unique Roman numeral (I, II, III, IV; table 3).

Table 2. Scenarios simulated using numerical groundwater models of the volcanic aquifers of Kaua‘i, O‘ahu, and Maui, Hawai‘i.

Scenario name	Recharge based on		Withdrawal from wells	Yields from tunnels	Represents	Model(s)
	Rainfall	Land cover				
Current	2001–2010 average applied to most areas; 1978–2007 average applied to dike zones	2010	2001–2010 average	2001–2010 average	Baseline condition, to which all other scenarios will be compared	Kaua‘i, O‘ahu, Maui
Historical scenarios						
No Withdrawal	2001–2010 average applied to most areas; 1978–2007 average applied to dike zones	2010	None	None	Withdrawal conditions in 1870	Kaua‘i, O‘ahu, Maui
Predevelopment	1978–2007 average	1870	None	None	Withdrawal and recharge conditions in 1870	Kaua‘i, O‘ahu, Maui
Future scenarios						
Increased Withdrawal	2001–2010 average applied to most areas; 1978–2007 average applied to dike zones	2010	Higher of (1) rate on water-use permits[1] or (2) 2001–2010 average rate	Variable[2]	Withdrawal at permitted rate under current recharge conditions	O‘ahu
Future Rainfall	Statistically downscaled projection for 2041–2070 for RCP[3] 8.5	2010	2001–2010 average	Variable[2]	Withdrawal at current rate under possible future climate/recharge[4] conditions	O‘ahu

[1]Permits issued by the State of Hawai‘i Commission on Water Resource Management.

[2]Yield can change if other scenario factors cause model-simulated heads in the aquifers to change.

[3]Representative concentration pathway (RCP) (as defined by Intergovernmental Panel on Climate Change, 2013).

[4]“Climate/recharge” indicates that changes in climate can cause changes in recharge.

Table 3. Assessments that compare the five scenarios simulated using numerical groundwater models of the volcanic aquifers of Kaua‘i, O‘ahu, and Maui, Hawai‘i.

[Scenario comparisons are computed by subtracting results of one scenario from those of another]

Assessment	Scenario comparison	Objective	Model(s)
Historical			
I	Current minus No Withdrawal	Study effect of withdrawal changes between 1870 and 2010, independent of recharge changes	Kaua‘i, O‘ahu, Maui
II	Current minus Predevelopment	Study combined effect of withdrawal and recharge changes between 1870 and 2010	Kaua‘i, O‘ahu, Maui
Future			
III	Increased Withdrawal minus Current	Study effect of increased pumping, independent of rainfall change	O‘ahu
IV	Future Rainfall minus Current	Study effect of potential changes in future rainfall, independent from effects of increased withdrawals	O‘ahu

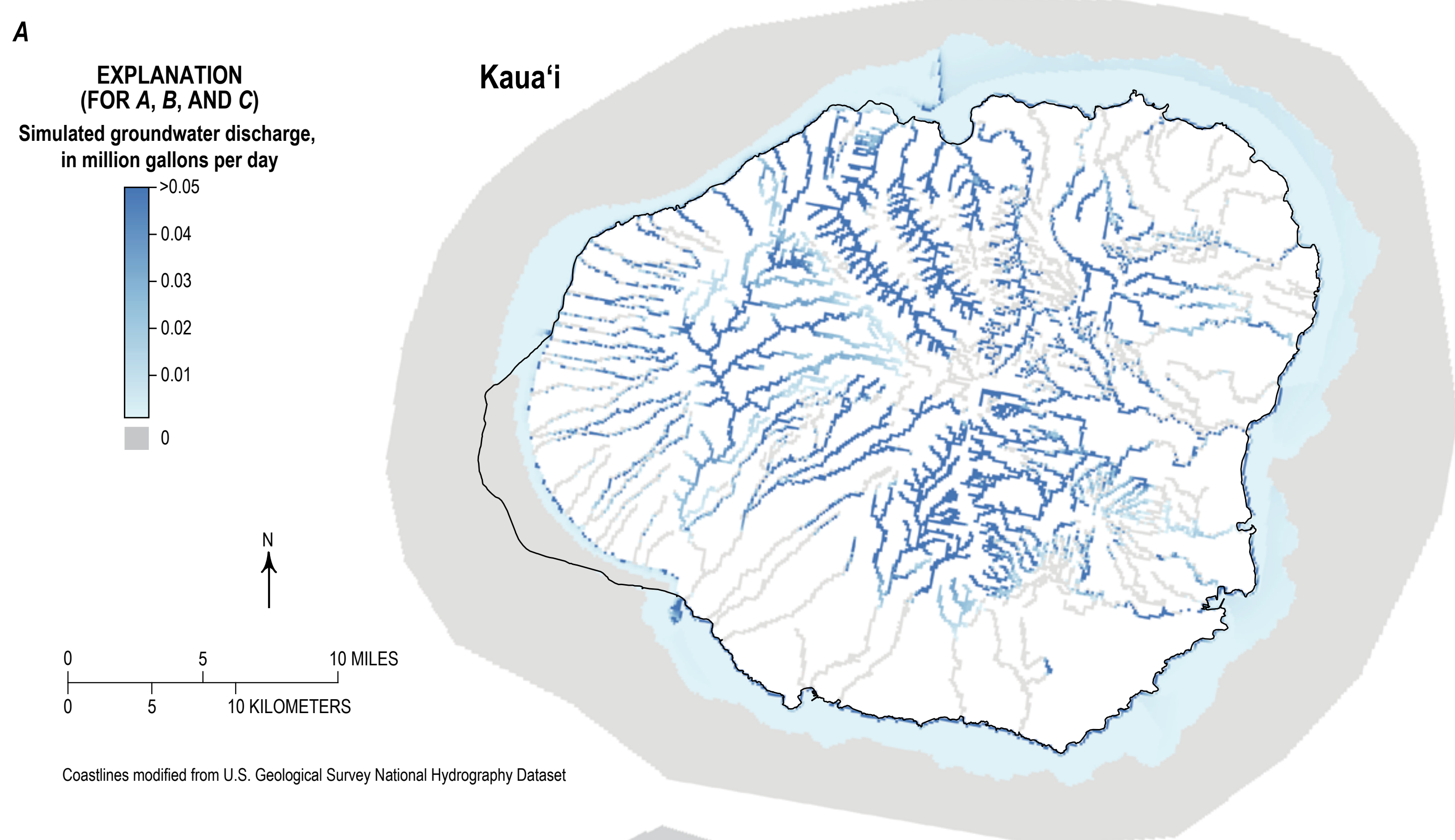

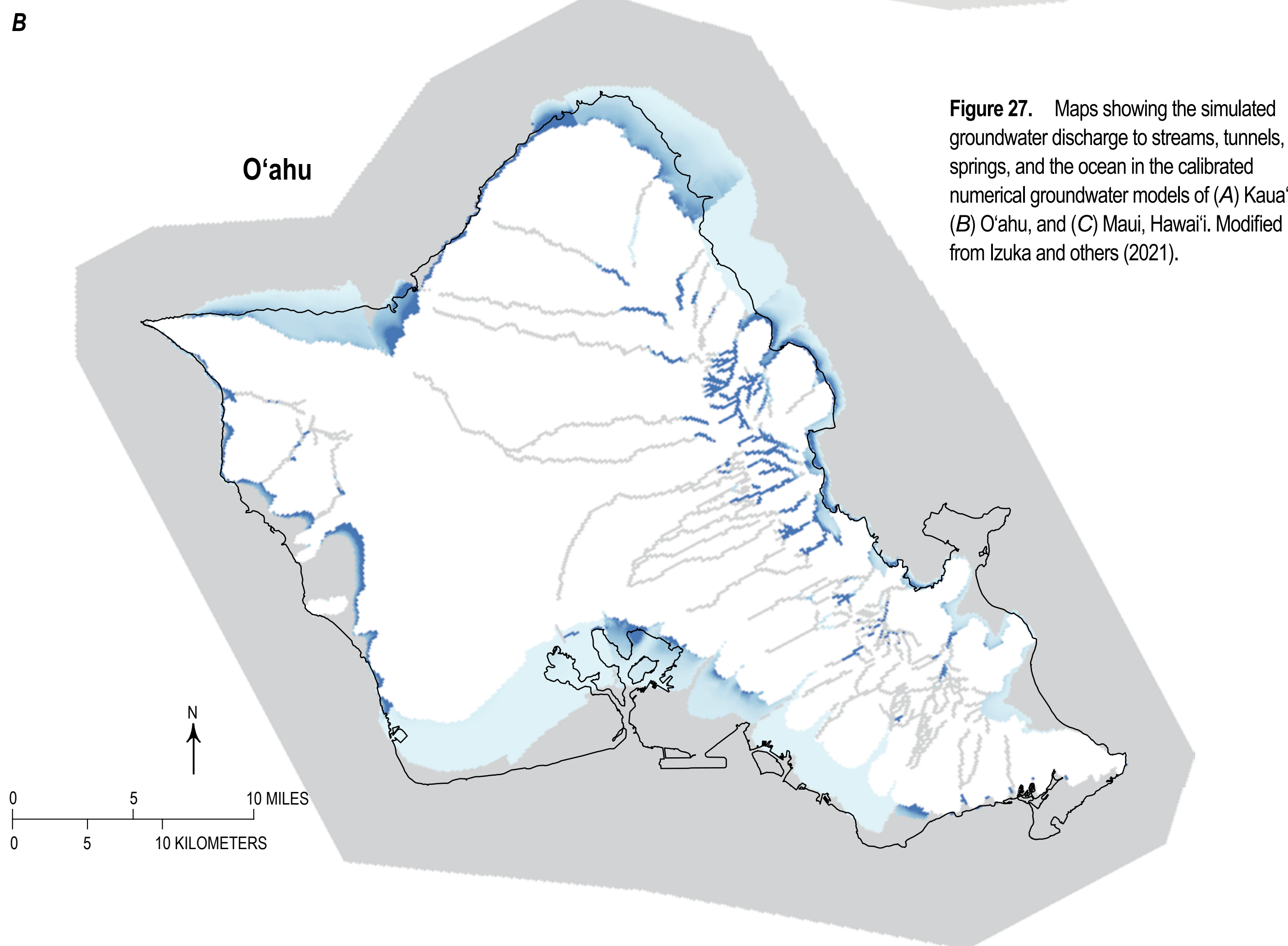

Figure 27. Maps showing the simulated groundwater discharge to streams, tunnels, springs, and the ocean in the calibrated numerical groundwater models of (*A*) Kauaʻi, (*B*) Oʻahu, and (*C*) Maui, Hawaiʻi. Modified from Izuka and others (2021).

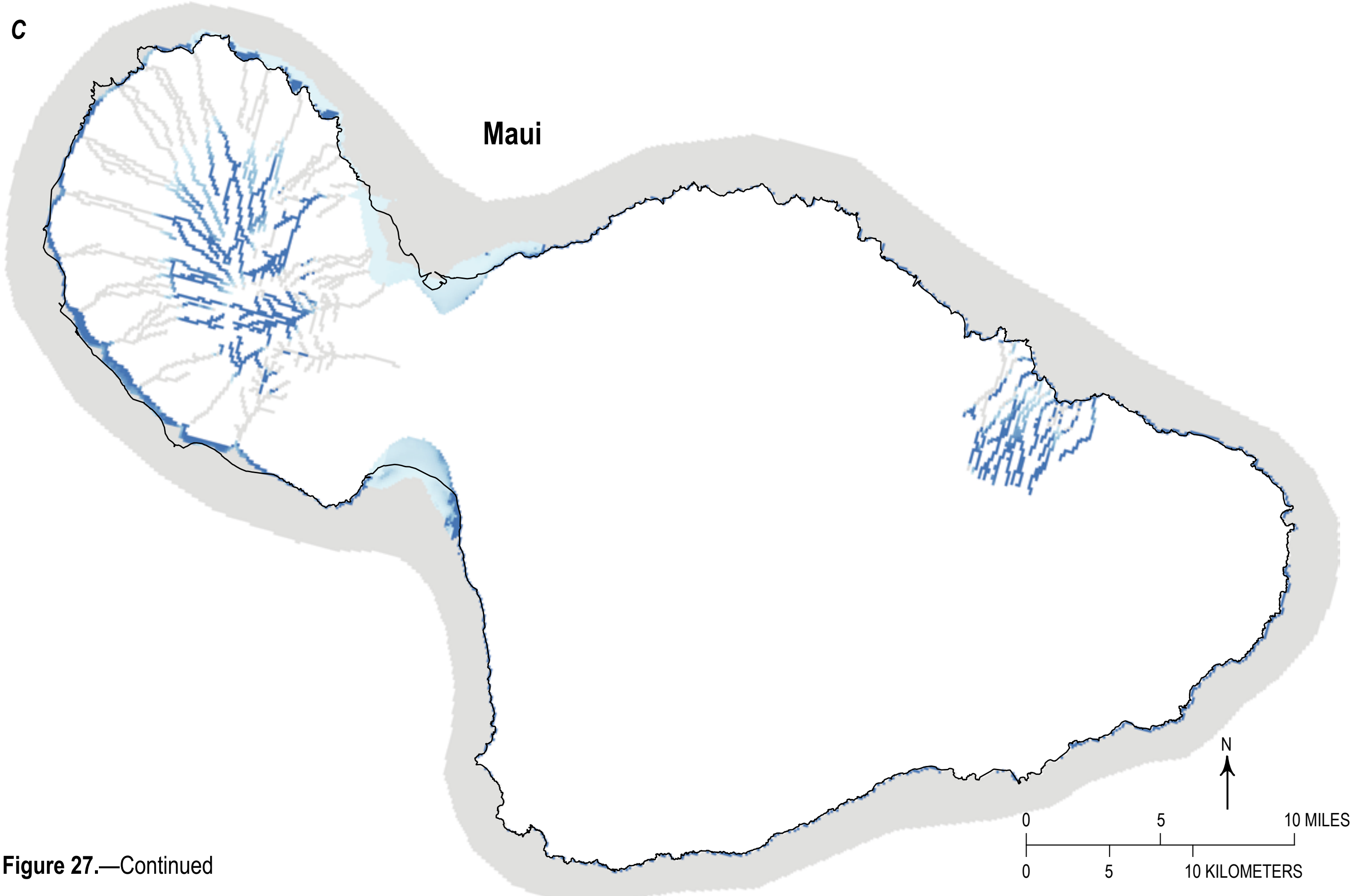

Figure 27.—Continued

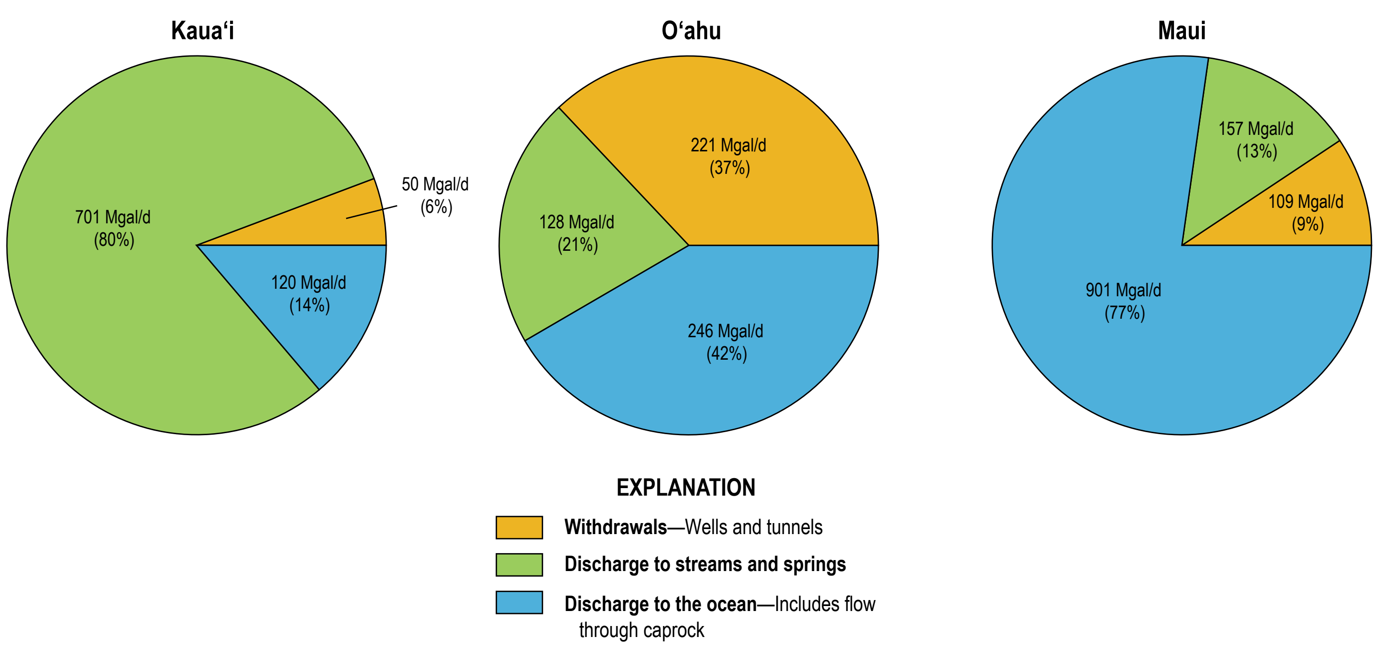

Figure 28. Pie diagrams showing the distribution of simulated discharge of fresh groundwater, in million gallons per day (Mgal/d) and as a percentage (%) of the island's total, for the calibrated groundwater models of Kauaʻi, Oʻahu, and Maui, Hawaiʻi. Percentages may not add to 100 because of rounding. From Izuka and others (2021).

Each assessment for each model examines differences in recharge, groundwater withdrawal from wells and tunnels, water level, freshwater-saltwater interface altitude, thickness of fresh groundwater (that is, distance between simulated interface and simulated head [in areas without caprock] or top of the volcanic aquifer [in areas with caprock]), and flows to streams, springs, and the ocean between the Current scenario and one of the other scenarios. The differences were computed by subtracting simulated values of the historically earlier scenario from those of the historically later scenario so that the differences indicate a directional change over time. For example, in Assessment I (table 3), the simulated values from the No Withdrawal scenario (which represents the absence of modern wells in 1870 [table 2]) were subtracted from the Current scenario (which represents 2010); a negative difference in groundwater discharge to streams and springs indicates that the discharge decreased between 1870 and 2010 as a result of introduction of withdrawal rates simulated in the Current scenario. In Assessments III and IV, values from the Current scenario were subtracted from scenarios that represent potential future conditions of withdrawal and rainfall.

Differences in flows were summed on an islandwide basis for individual models. Because all scenario simulations in this study are steady state, the differences in islandwide total inflows (recharge) balance differences in outflows (groundwater withdrawals from wells and tunnels and discharge to streams, springs, and the ocean) from the model. Stated alternatively, reductions in the rate of recharge or increases in the rate of groundwater withdrawn from wells and tunnels are compensated by an equivalent reduction in discharge to streams, springs, and the ocean. The relative amounts compensated by streams, springs, and the ocean depend, in part, on how close the withdrawals are to each of these types of groundwater-discharge sites.

This study also evaluates differences in the way the principal groundwater settings within each island respond to hydrologic stresses such as changes in groundwater withdrawals and recharge. To facilitate this evaluation, each model is divided into sectors that encompass a single type of principal groundwater setting (fig. 29, table 4). In the model, regions that have the same type of principal groundwater setting but are not connected are placed in separate sectors. For example, the dike-impounded-groundwater settings in the O‘ahu model are assigned to two sectors, Ko‘olau and Wai‘anae. The Central Kaua‘i sector includes dike-impounded-groundwater areas that appear to be separate at the surface but are connected in the lower layer of the model.

Water budgets were computed for each sector. In addition to the inflow and outflow components in islandwide water budgets, sector water budgets include subsurface flow (groundwater flow) between adjacent sectors. For a given sector, subsurface flow can be an inflow or outflow component, depending on the head in the sector relative to the head in adjacent sectors. If a sector has multiple sectors adjacent to it, groundwater may flow in from one of the adjacent sectors and out to another. Stresses such as increased withdrawals or reduced recharge in one sector can cause increases in subsurface inflow from, or decreases in subsurface outflow to, adjacent sectors. Sector water budgets of the various scenarios were compared in the assessments described in table 3.

Effects of Historical Changes in Groundwater Withdrawal and Recharge

Since the first modern well was drilled in Hawai‘i in 1879, total groundwater withdrawals on Kaua‘i, O‘ahu, and Maui have increased to nearly 400 million gallons per day (Mgal/d) (table 1). In addition, land-cover changes since 1870 have altered groundwater-recharge rates. Prior to 1870, the extent of Hawai‘i’s native forests had been reduced by human activities such as clearing for agriculture, harvesting of trees, and introduction of nonnative ungulates (Newman, 1972; Kirch, 1982; Cuddihy and Stone, 1990; Ziegler, 2002). Efforts in reforestation, mostly using nonnative trees, were made in the early 1900s (Woodcock, 2003). From about the mid-19th century to the end of the 20th century, large-scale agriculture, particularly the cultivation of sugarcane, withdrew hundreds of millions of gallons per day from Hawai‘i’s aquifers and diverted hundreds of millions of gallons more per day from streams for irrigation and for transport and processing of the harvest. Sugarcane cultivation declined in the late 20th and early 21st centuries, and by 2010 (the land-cover period used in the Current scenario [table 2]), only one large sugarcane plantation (on Maui) remained in Hawai‘i (see Izuka and others [2018] for additional discussion of historical factors that affected groundwater resources in Hawai‘i).

The net effect of crop irrigation on groundwater availability depends on the source of the irrigation water. Irrigation that uses water diverted from streams that would normally have run off to the ocean can have a positive net effect on groundwater availability (although the effect on streamflow is negative). However, irrigation that uses groundwater withdrawn from the aquifers has a net negative effect on groundwater availability because it exposes groundwater to evapotranspiration and runoff losses; as a result, the amount of irrigation water that returns to groundwater is less than the amount withdrawn.

In this study, numerical-model simulations were used to assess how differences in withdrawals and recharge between 1870 and 2010 have affected groundwater resources. Scenario simulations were run on the Kaua‘i, O‘ahu, and Maui models to assess (1) the effect of historical groundwater-withdrawal rates independent of changes in recharge, and (2) the combined effect of historical withdrawal rates and changes in recharge.

Assessment I—Effects of Current-Scenario Withdrawal Rates

The objective of Assessment I is to evaluate the effects that current (which represents conditions in 2010) groundwater-withdrawal rates have had on the resource (table 3). The No Withdrawal scenario, which represents withdrawal conditions that are presumed to have existed in 1870 prior to the drilling of Hawai‘i’s first modern well (table 2), was simulated using the Kaua‘i, O‘ahu, and Maui numerical models and compared to the Current scenario. Differences between the two scenarios for each model provide information on the effect that Current-scenario withdrawal

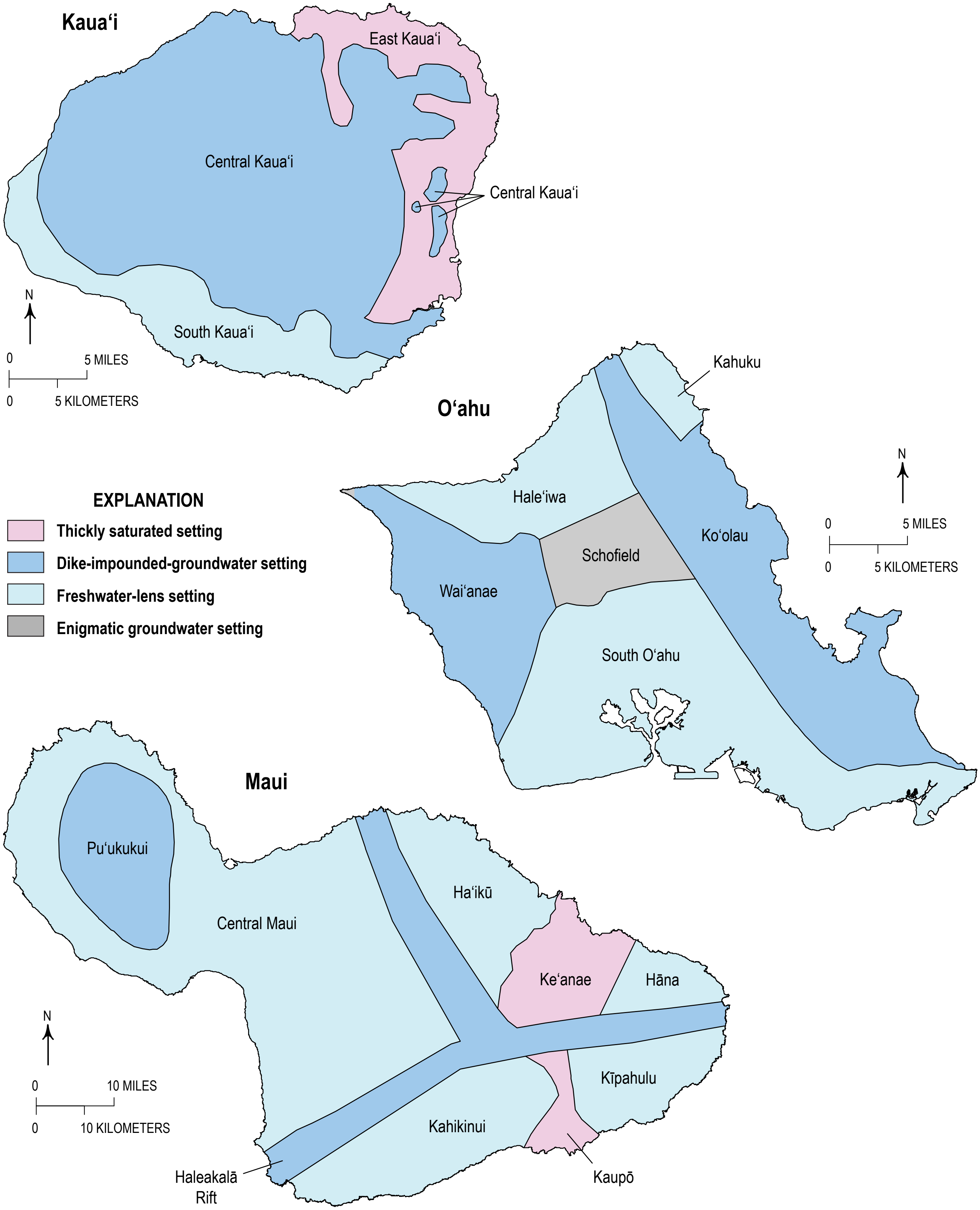

Figure 29. Maps showing sectors that encompass principal groundwater settings in models of the volcanic aquifers of Kaua‘i, O‘ahu, and Maui, Hawai‘i.

Table 4. Sectors, principal groundwater settings, and Current-scenario rates for selected water-budget components of numerical groundwater models of the volcanic aquifers of Kaua‘i, O‘ahu, and Maui, Hawai‘i.

[Totals may not be equal to sum of values in columns, owing to rounding. Mgal/d, million gallons per day]

Sector	Principal groundwater setting	Current-scenario rates (Mgal/d)		
		Recharge	Withdrawal from wells	Tunnel yield
	Kaua‘i model			
Central Kaua‘i[1]	Dike-impounded groundwater	770.7	5.9	0.2
East Kaua‘i	Thickly saturated	56.3	7.0	0.4
South Kaua‘i	Freshwater lens	44.3	36.2	0.0
	Total	871.2	49.1	0.6
	O‘ahu model			
Ko‘olau	Dike-impounded groundwater	359.1	13.7	32.0
Wai‘anae	Dike-impounded groundwater	53.2	3.3	1.2
South O‘ahu	Freshwater lens	102.2	149.7	0.0
Hale‘iwa	Freshwater lens	31.2	3.7	0.0
Kahuku	Freshwater lens	4.7	8.7	0.0
Schofield	Enigmatic[2]	47.2	9.0	0.0
	Total	597.6	188.0	33.2
	Maui model			
Pu‘ukukui	Dike-impounded groundwater	215.1	0.8	11.4
Haleakalā Rift	Dike-impounded groundwater	200.5	3.5	0.0
Ke‘anae	Thickly saturated	189.4	0.1	0.0
Kaupō	Thickly saturated	16.0	0.0	0.0
Central Maui	Freshwater lens	160.8	92.3	0.0
Ha‘ikū	Freshwater lens	132.0	0.4	0.0
Hāna	Freshwater lens	76.4	0.2	0.0
Kīpahulu	Freshwater lens	129.0	0.2	0.0
Kahikinui	Freshwater lens	47.5	0.0	0.0
	Total	1,166.7	97.5	11.4

[1]Sector encompasses areas that appear to be separate at surface but are connected in lower layer of the model.

[2]Enigmatic groundwater occurrences do not fit into one of the four principal groundwater settings discussed in this report, and their relation to the geologic framework of volcanic aquifers is not fully understood (see Izuka and others, 2018, 2021).

rates have had on groundwater levels, freshwater-saltwater interface altitudes, freshwater thicknesses, and groundwater discharge to streams, springs, and the ocean.

No Withdrawal Scenario

In the No Withdrawal scenario, groundwater withdrawals are halted by setting withdrawal rates in the Well Package of MODFLOW and conductance values for tunnels in the Drain Package to zero. Other conditions represented by the No Withdrawal and Current scenarios are the same; thus, Assessment I evaluates the effect of groundwater withdrawals independently from changes in recharge.

Results

Model-simulated Current-scenario total (wells and tunnels) groundwater-withdrawal rates for Kaua‘i, O‘ahu, and Maui are 49.7, 221.2, and 108.9 Mgal/d, respectively (table 5, fig. 30). Simulations for Assessment I indicate the extent to which these withdrawal rates have caused reductions in groundwater discharge to streams and springs (figs. 30, 31), reductions in groundwater discharge to the ocean (fig. 32), declines in groundwater levels (fig. 33), upward movement of the freshwater-saltwater interface (fig. 34), and reductions in fresh-groundwater thickness (fig. 35) relative to conditions that existed prior to 1870.

The islandwide groundwater budgets (fig. 30) indicate that the consequences of groundwater withdrawals differ among the three islands. In the Kaua‘i model, the largest effect of the simulated groundwater withdrawals is reduction of groundwater discharge to the ocean, which is consistent with the location of the largest withdrawals on the island's south coast (fig. 36). The largest effect of the simulated withdrawals in the islandwide groundwater budget for O‘ahu is reduced groundwater discharge to streams and springs, much of which occurs at springs associated with the caprock near Pearl Harbor and streams in the Ko‘olau sector (fig. 31). In the Maui model, the effects of the simulated withdrawals are consistent with the location of large withdrawals from aquifers that naturally discharge groundwater to the ocean.

Differences in effects of withdrawals among the three models, and how the differences are related to the principal

Table 5. Comparison of islandwide groundwater budgets for the Current and No Withdrawal scenarios (Assessment I) simulated using numerical groundwater models of the volcanic aquifers of Kaua‘i, O‘ahu, and Maui, Hawai‘i.

[Differences between scenarios represent Current minus No Withdrawal scenarios; differences between scenarios may not be equal to differences between values in columns, owing to rounding. Mgal/d, million gallons per day]

Model	Scenario	Recharge (Mgal/d)	Withdrawal (Mgal/d)			Groundwater discharge (Mgal/d)	
			Wells	Tunnels	Total	To streams and springs	To ocean
Kaua‘i	No Withdrawal	871.2	0.0	0.0	0.0	705.7	165.6
	Current	871.2	49.1	0.6	49.7	701.2	120.4
	Difference between scenarios	0.0	49.1	0.6	49.7	−4.5	−45.1
O‘ahu	No Withdrawal	597.6	0.0	0.0	0.0	262.7	334.8
	Current	597.6	188.0	33.2	221.2	127.7	248.6
	Difference between scenarios	0.0	188.0	33.2	221.2	−135.0	−86.2
Maui	No Withdrawal	1,166.7	0.0	0.0	0.0	166.1	1,000.6
	Current	1,166.7	97.5	11.4	108.9	156.6	901.2
	Difference between scenarios	0.0	97.5	11.4	108.9	−9.5	−99.4

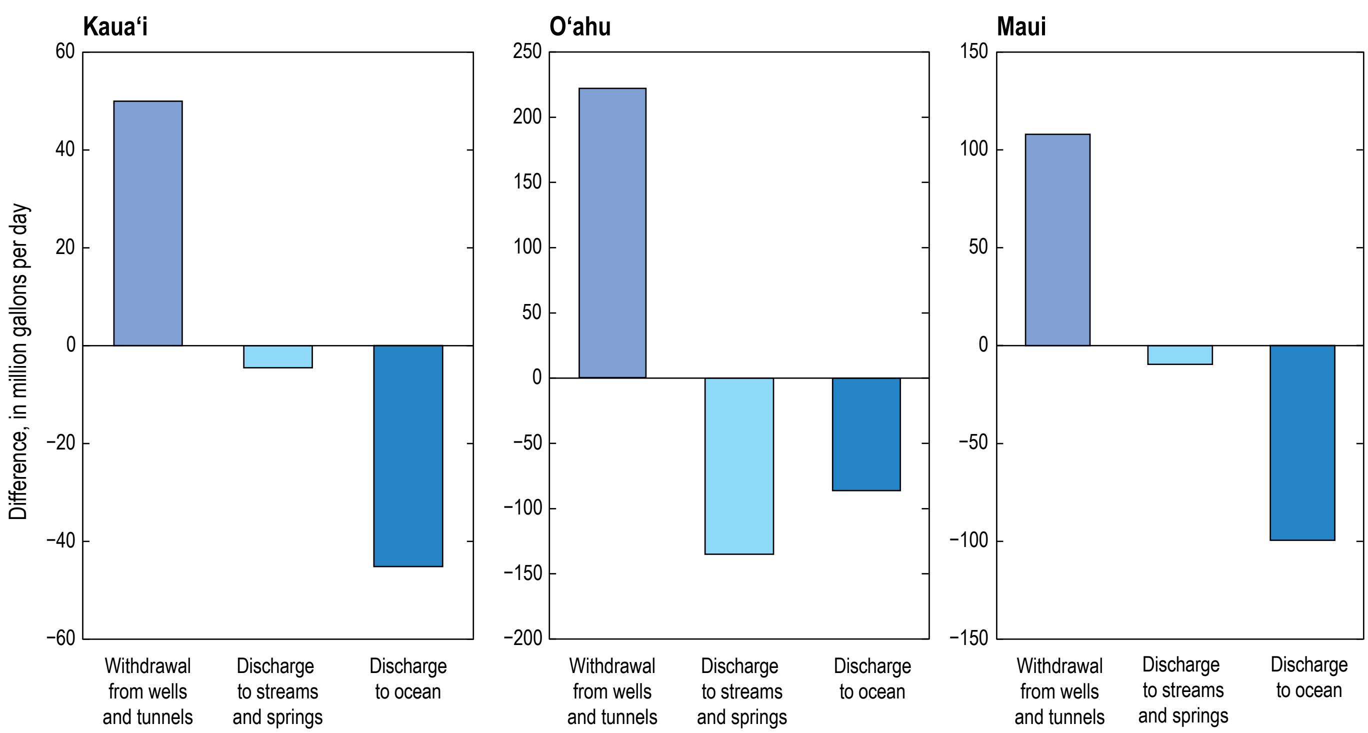

Figure 30. Bar graphs showing differences in islandwide groundwater budgets from Assessment I, computed by subtracting results of the No Withdrawal scenario from those of the Current scenario simulated using models of the volcanic aquifers of Kaua‘i, O‘ahu, and Maui, Hawai‘i. Differences indicate changes caused by withdrawing groundwater at rates represented by the Current scenario. Note that vertical axes of bar graphs are at different scales to show wide range of values.

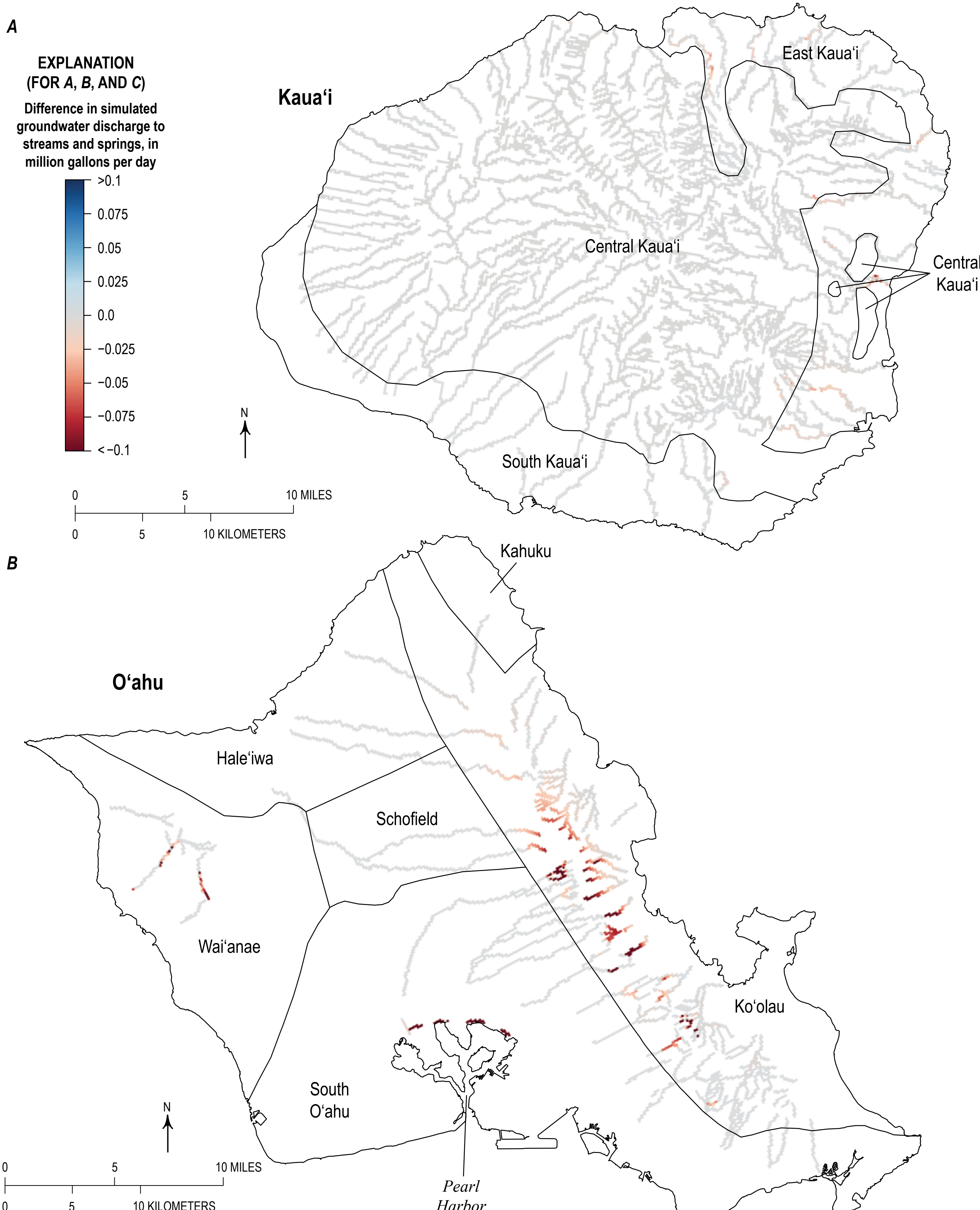
A
EXPLANATION
(FOR A, B, AND C)
Difference in simulated groundwater discharge to streams and springs, in million gallons per day
>0.1
0.075
0.05
0.025
0.0
−0.025
−0.05
−0.075
< −0.1
Kaua‘i
East Kaua‘i
Central Kaua‘i
Central Kaua‘i
South Kaua‘i
N
0 5 10 MILES
0 5 10 KILOMETERS
B
Kahuku
O‘ahu
Hale‘iwa
Schofield
Wai‘anae
Ko‘olau
South O‘ahu
N
0 5 10 MILES
0 5 10 KILOMETERS
Pearl Harbor

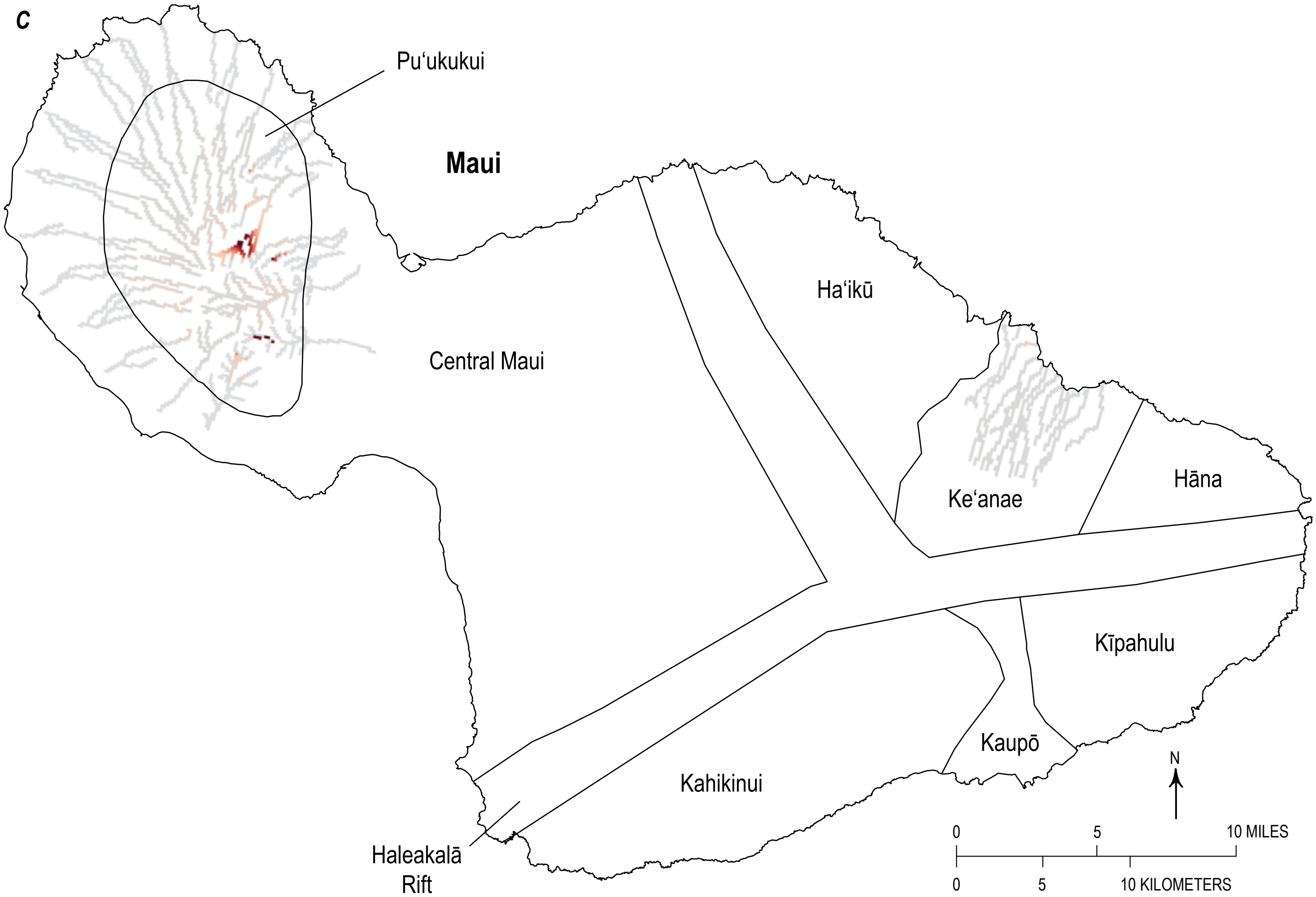

Figure 31. Maps showing differences in groundwater discharge to streams and springs from Assessment I, computed by subtracting results of the No Withdrawal scenario from those of the Current scenario simulated using models of the volcanic aquifers of (*A*) Kaua‘i, (*B*) O‘ahu, and (*C*) Maui, Hawai‘i. Differences indicate changes caused by withdrawing groundwater at rates represented by the Current scenario. Gray areas represent 0.0 values.

hydrogeologic settings, are evident in the water budgets for sectors within the models. Simulated groundwater withdrawals affect the water balances of sectors within the models, as shown in table 6 and figure 37. Positive values on the graphs in figure 37 indicate increased outflow from, or decreased inflow to, the sector; these positive values include withdrawals within the sector (olive-green bars) and in some cases, effects from withdrawals from adjacent sectors, such as induced subsurface outflows or reduced subsurface inflows (yellow bars). Negative values on the graphs in figure 37 indicate decreased outflow from the sector, such as decreases in groundwater discharge to streams and springs (turquoise bars), decreased groundwater discharge to the ocean (navy-blue bars), or decreased outflow to or increased inflow from adjacent aquifers (yellow bars). These decreases compensate for the positive values resulting from withdrawals from within the sector, decreased subsurface inflows from other sectors, or increased subsurface outflows to other sectors. The black arrows in figure 37 indicate changes in flow across specific sector boundaries.

The specific effects of groundwater withdrawals in a given sector depend on (1) the sector’s hydrogeologic setting, (2) the magnitude and proximity of withdrawals relative to sites of groundwater discharge to streams, springs, and the ocean, and (3) the magnitude and proximity of withdrawals relative to sector boundaries. Because withdrawals from upgradient sectors can affect water balances in downgradient sectors, the following discussion starts with sectors formed by the dike-impounded-groundwater setting, which are typically upgradient of other sectors. The discussion progresses to the next-downgradient sectors, which include the Schofield sector (O‘ahu) and those sectors formed by the thickly saturated settings (Kaua‘i and Maui), and then to the sectors formed by the freshwater-lens setting, which are typically the sectors that are farthest downgradient.

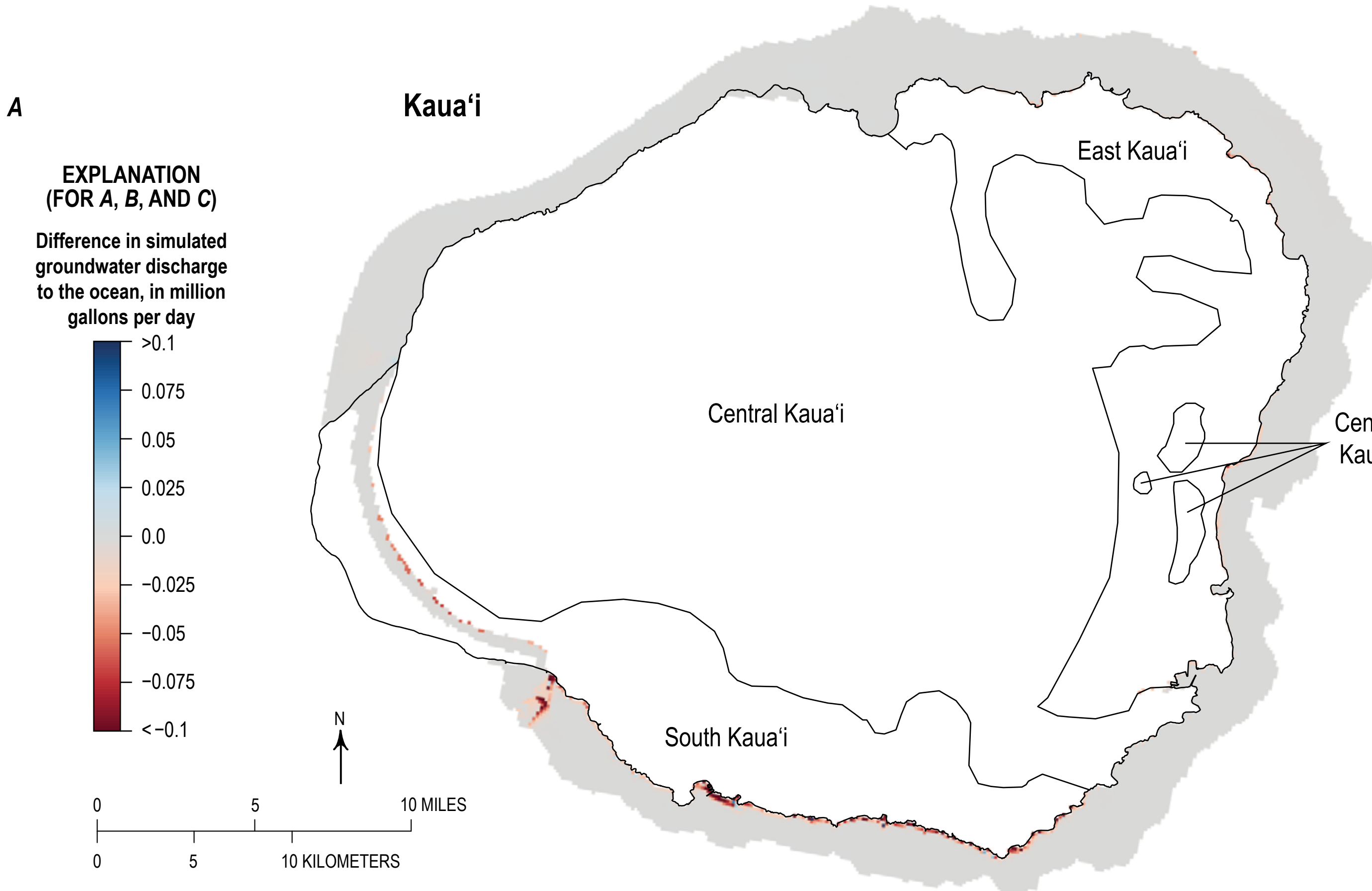
A
Kaua‘i
EXPLANATION
(FOR A, B, AND C)
Difference in simulated groundwater discharge to the ocean, in million gallons per day
>0.1
0.075
0.05
0.025
0.0
−0.025
−0.05
−0.075
<−0.1
East Kaua‘i
Central Kaua‘i
Central Kaua‘i
South Kaua‘i
N
0
5
10 MILES
0
5
10 KILOMETERS

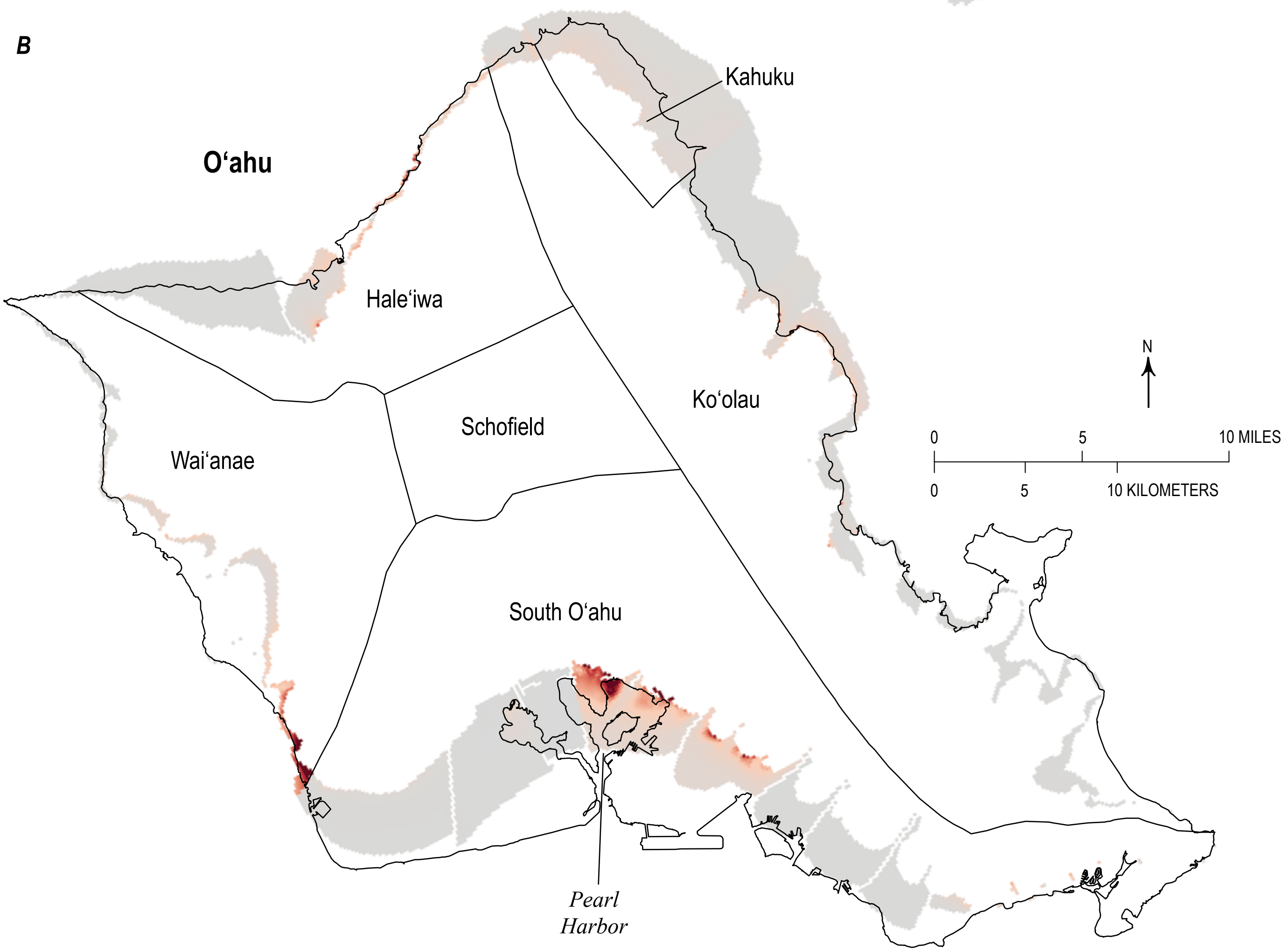
B
O‘ahu
Kahuku
Hale‘iwa
Ko‘olau
Schofield
Wai‘anae
South O‘ahu
Pearl Harbor
N
0
5
10 MILES
0
5
10 KILOMETERS

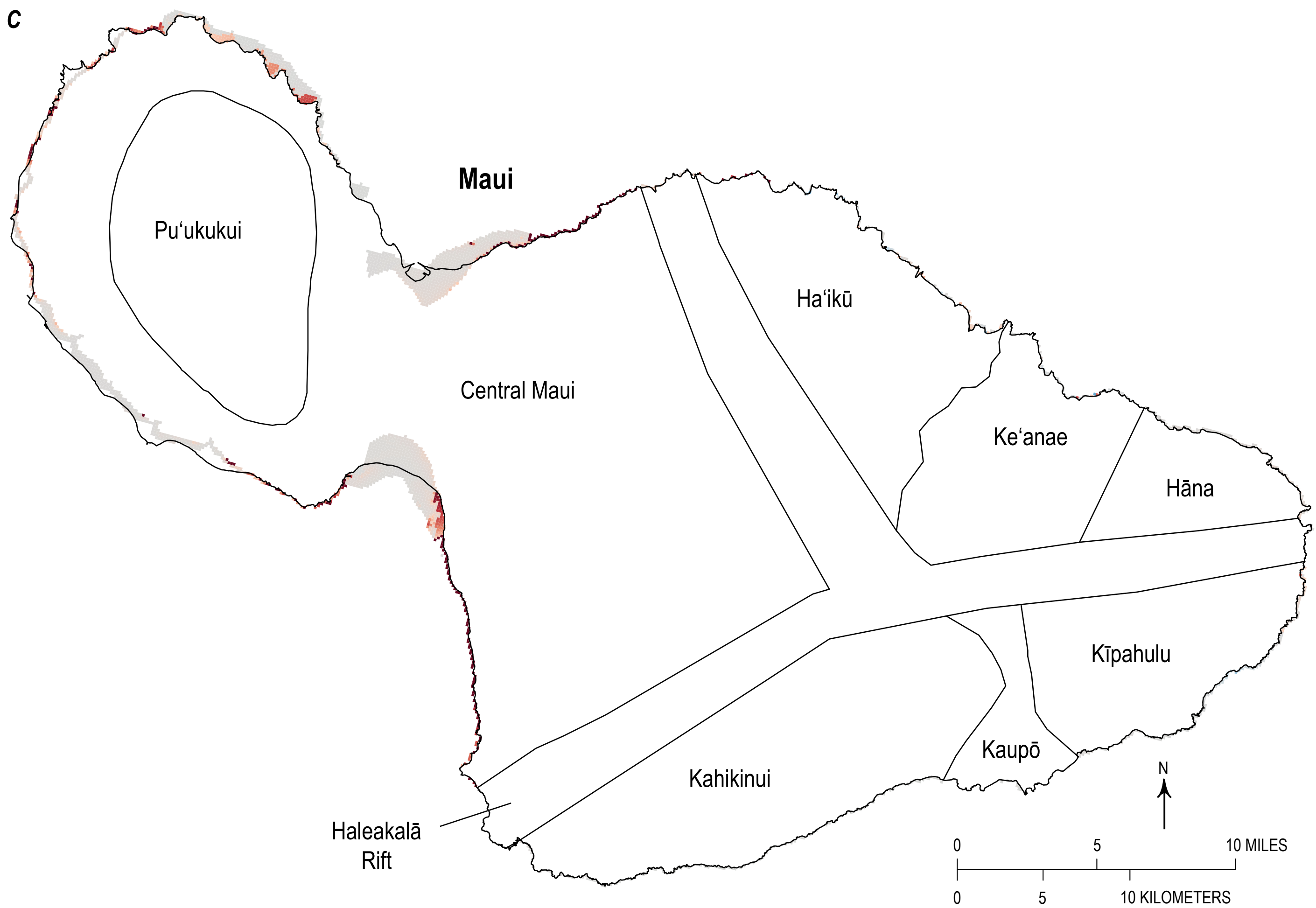

Figure 32. Maps showing differences in groundwater discharge to the ocean from Assessment I, computed by subtracting results of the No Withdrawal scenario from those of the Current scenario simulated using models of the volcanic aquifers of (*A*) Kaua‘i, (*B*) O‘ahu, and (*C*) Maui, Hawai‘i. Differences indicate changes caused by withdrawing groundwater at rates represented by the Current scenario. Gray areas represent 0.0 values.

Sectors that encompass dike-impounded-groundwater settings.—Five sectors of the models in this study encompass dike-impounded-groundwater settings (table 4, fig. 29). Prior to the onset of groundwater withdrawals, water levels in these sectors are typically higher than in other sectors, and groundwater flows in the subsurface from these sectors to adjacent sectors that have lower water levels. The model simulations for Assessment I indicate that Current-scenario withdrawals from sectors that encompass the dike-impounded-groundwater settings are compensated by reductions in groundwater discharge to streams and springs, groundwater discharge to the ocean, and subsurface flow to adjacent sectors (figs. 31, 32, 37). In the Ko‘olau sector on O‘ahu and the Pu‘ukukui sector on Maui, reductions in groundwater discharge to streams and springs compensate for most of the withdrawals (fig. 37*B*, *C*). The remainder of the withdrawal from the Ko‘olau sector is compensated by reduction in groundwater discharge to the ocean and reductions in subsurface flow to adjacent sectors. The remainder of the withdrawals from the Pu‘ukukui sector is compensated only by reductions in subsurface flow to adjacent sectors; the Pu‘ukukui sector has no ocean discharge component because the sector is landlocked.

Model simulations indicate that in the Haleakalā Rift sector, decreases in subsurface flow to adjacent sectors compensate for more of the groundwater withdrawal than do decreases in groundwater discharge to streams and springs or decreases in groundwater discharge to the ocean (fig. 37*C*). This sector lacks connections to stream discharge and has limited connections to ocean discharge. Simulated decreases in subsurface flow to adjacent sectors is also the largest component compensating for withdrawal from the Central Kaua‘i sector (fig. 37*A*) because most of the withdrawal comes from wells that are near the border with the South Kaua‘i sector (fig. 36). However, reductions in groundwater discharge to streams and springs and, to a lesser

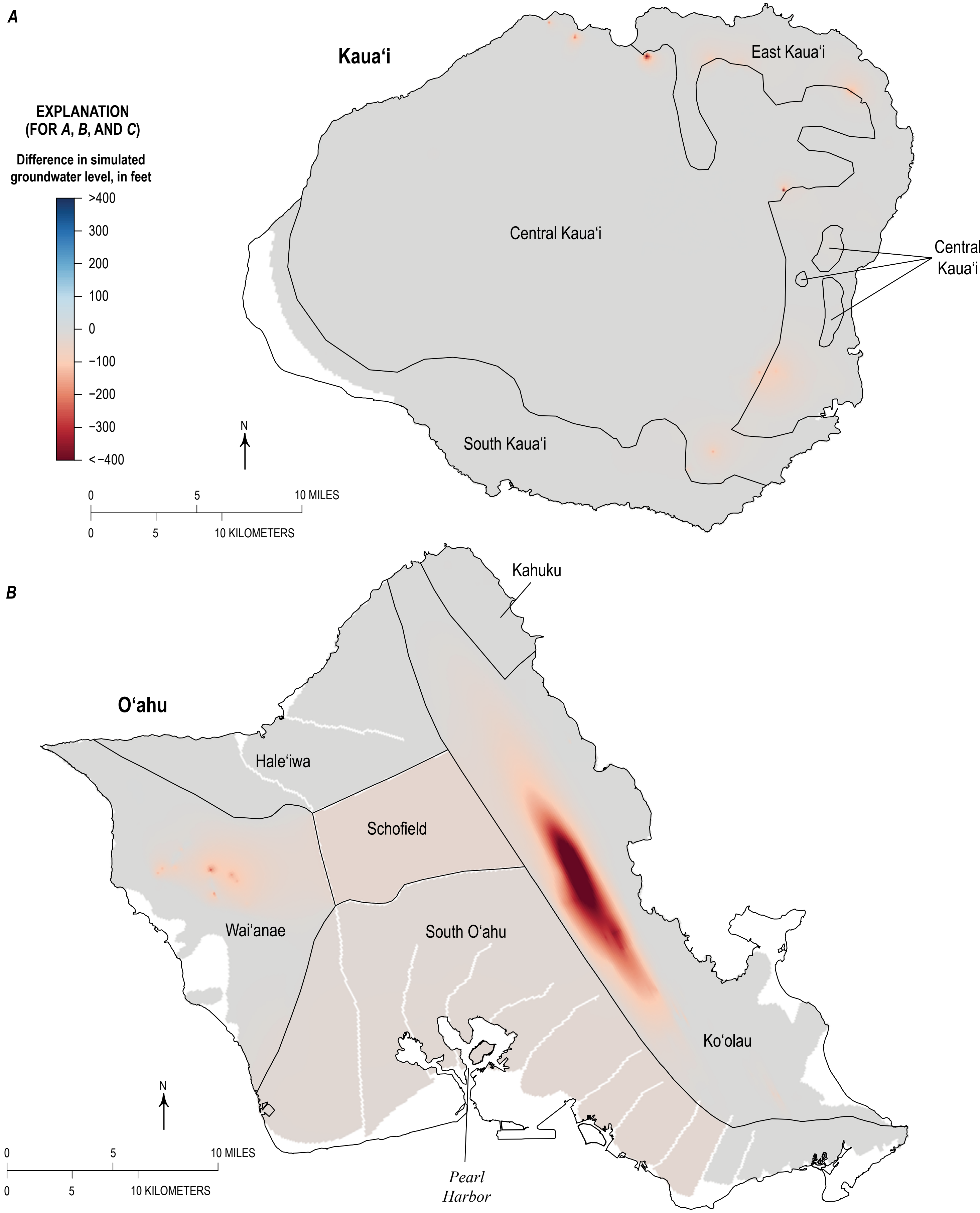
A
Kaua‘i
East Kaua‘i
Central Kaua‘i
Central Kaua‘i
South Kaua‘i
EXPLANATION (FOR A, B, AND C)
Difference in simulated groundwater level, in feet
>400
300
200
100
0
−100
−200
−300
< −400
N
0 5 10 MILES
0 5 10 KILOMETERS
B
O‘ahu
Kahuku
Hale‘iwa
Schofield
Wai‘anae
South O‘ahu
Ko‘olau
N
0 5 10 MILES
0 5 10 KILOMETERS
Pearl Harbor

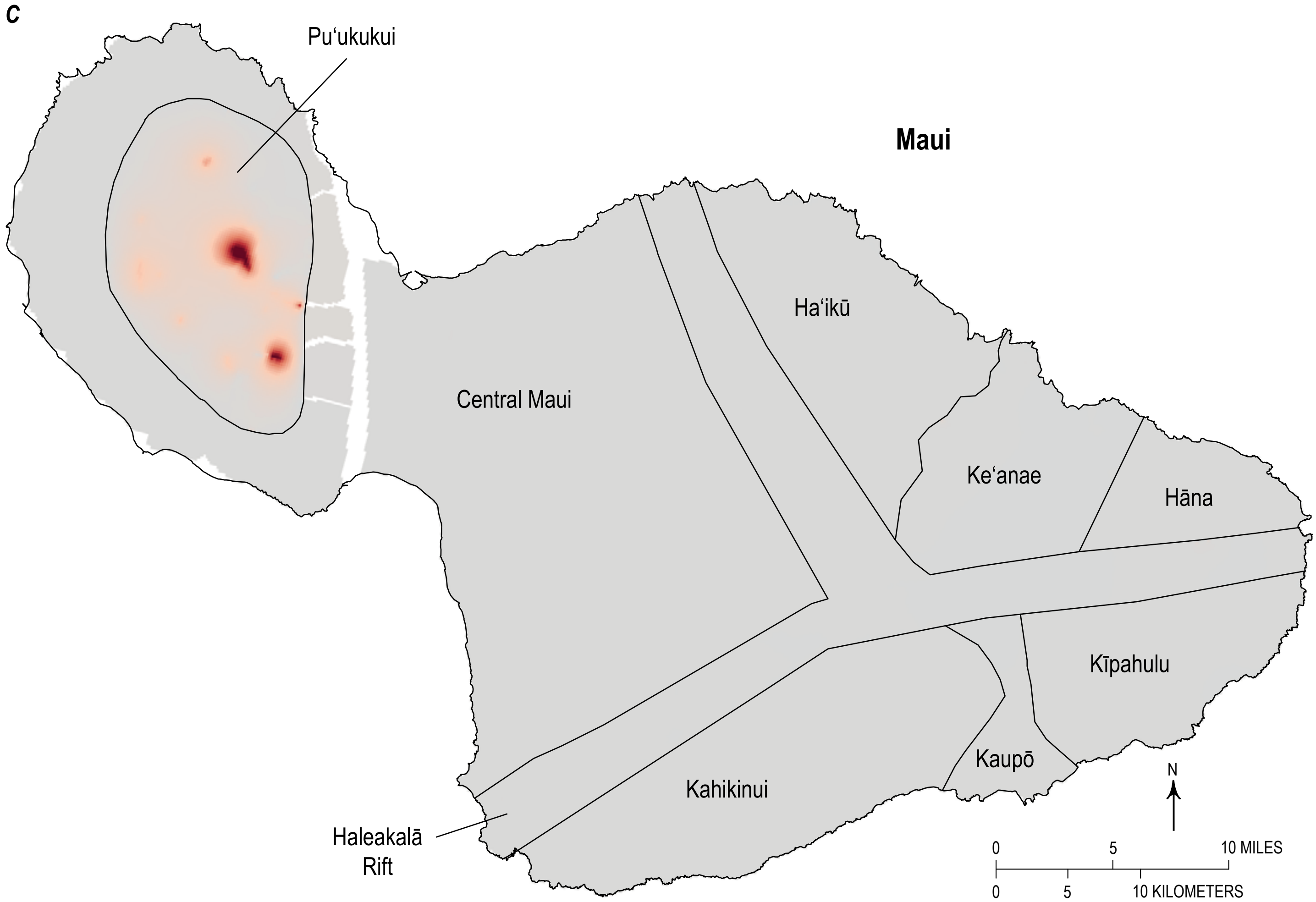

Figure 33. Maps showing differences in groundwater levels from Assessment I, computed by subtracting results of the No Withdrawal scenario from those of the Current scenario simulated using models of the volcanic aquifers of (*A*) Kaua‘i, (*B*) O‘ahu, and (*C*) Maui, Hawai‘i. Differences indicate changes caused by withdrawing groundwater at rates represented by the Current scenario. Gray areas represent 0.0 values.

extent, discharge to the ocean do compensate for some of the withdrawal from the Central Kaua‘i sector (fig. 37).

The Wai‘anae sector on O‘ahu is unique among the sectors formed by the dike-impounded-groundwater setting. In the No Withdrawal scenario, groundwater flows from the South O‘ahu sector to the Wai‘anae sector, but in the Current scenario, groundwater flow reverses direction as a result of groundwater withdrawals from the South O‘ahu sector that are much larger than those from the Wai‘anae sector. The net difference is a decrease of 11.1 Mgal/d in subsurface flow from the South O‘ahu to Wai‘anae sector (fig. 37*B*). This decrease dominates the subsurface-flow component shown in the bar graphs of the water balance in the Wai‘anae sector. The combined effects of reduced subsurface inflow and withdrawals from wells and tunnels in the Wai‘anae sector are compensated mostly by reductions in discharge to the ocean; a lesser amount of the combined effects is compensated by reductions in groundwater discharge to streams.

Model simulations for Assessment I indicate that Current-scenario groundwater withdrawals have caused substantial localized water-level declines in parts of sectors that encompass dike-impounded-groundwater settings (fig. 33), especially in the Ko‘olau sector of O‘ahu and the Pu‘ukukui sector on Maui. This result is consistent with the low bulk aquifer permeability that is characteristic of these settings. The most notable simulated declines in the dike-impounded-groundwater settings are focused in areas where withdrawals are high. Rise of the freshwater-saltwater interface in the Ko‘olau and Wai‘anae sectors is localized (fig. 34), although in areas slightly seaward of the areas of declining water levels. Interface rise is not apparent in the dike-impounded-groundwater setting of the Pu‘ukukui sector, where fresh groundwater extends down to the bottom of the model even under the Current-scenario withdrawal conditions. In the Central Kaua‘i sector, withdrawals near the southeast coast (fig. 36*A*) have caused the interface to rise substantially over a fairly large area, including

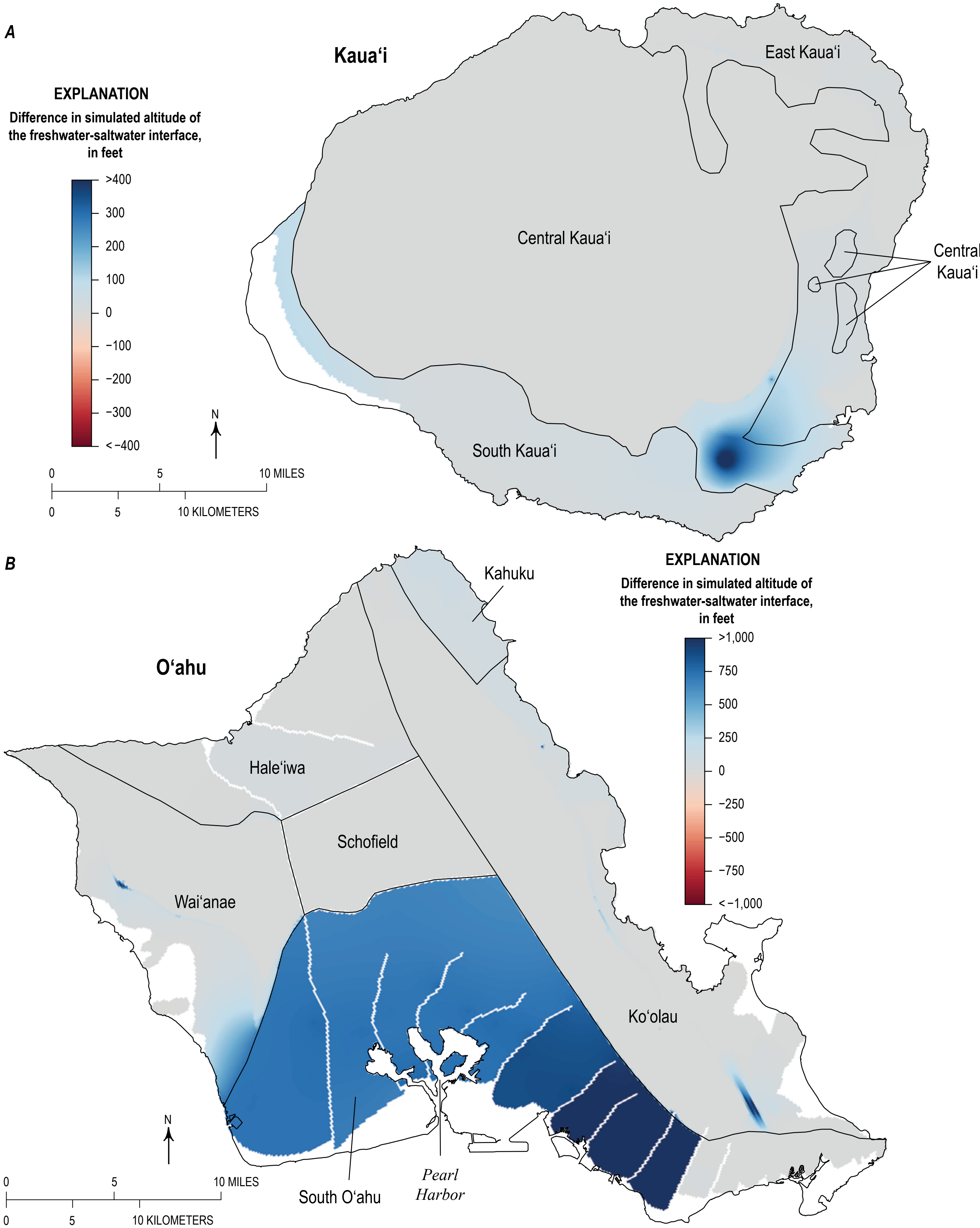
A
Kaua‘i
EXPLANATION
Difference in simulated altitude of the freshwater-saltwater interface, in feet
>400
300
200
100
0
−100
−200
−300
< −400
N
0
5
10 MILES
0
5
10 KILOMETERS
East Kaua‘i
Central Kaua‘i
Central Kaua‘i
South Kaua‘i
B
O‘ahu
Kahuku
EXPLANATION
Difference in simulated altitude of the freshwater-saltwater interface, in feet
>1,000
750
500
250
0
−250
−500
−750
< −1,000
Hale‘iwa
Schofield
Wai‘anae
Ko‘olau
N
0
5
10 MILES
0
5
10 KILOMETERS
South O‘ahu
Pearl Harbor

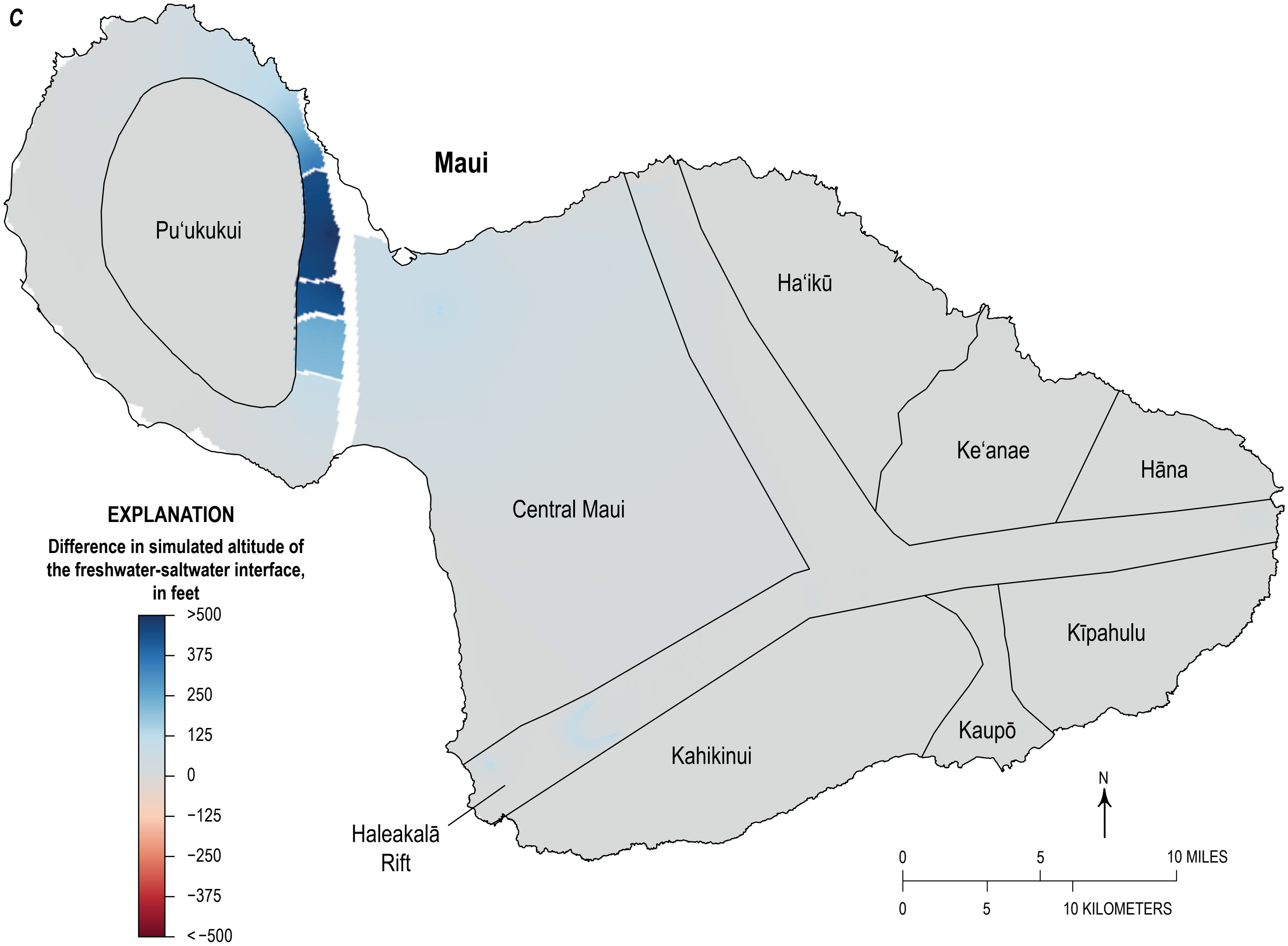

Figure 34. Maps showing differences in altitude of the freshwater-saltwater interface from Assessment I, computed by subtracting results of the No Withdrawal scenario from those of the Current scenario simulated using models of the volcanic aquifers of (*A*) Kaua‘i, (*B*) O‘ahu, and (*C*) Maui, Hawai‘i. Differences indicate changes caused by withdrawing groundwater at rates represented by the Current scenario. Gray areas represent 0.0 values.

parts of the adjacent East Kaua‘i sector (fig. 34*A*). The water-level decline and interface rise result in reduction of fresh-groundwater thicknesses in parts of sectors that encompass dike-impounded-groundwater settings (fig. 35).

Schofield sector.—In the O‘ahu model, the Schofield sector receives subsurface inflow from the dike-impounded-groundwater settings of the Ko‘olau and Wai‘anae sectors (fig. 37*B*). Simulated subsurface outflow from the Schofield sector contributes groundwater to the freshwater-lens settings in the Hale‘iwa and South O‘ahu sectors. Model simulations for Assessment I indicate that the Current-scenario groundwater withdrawals of 9.0 Mgal/d (table 6) from the Schofield sector are compensated entirely by simulated changes in subsurface flow to or from adjacent sectors. Because the sector is landlocked and has no streams or springs that receive groundwater discharge, model-simulated changes in groundwater discharge to the ocean and to streams and springs cannot compensate for the withdrawals. The model simulations indicate that withdrawals from the Schofield sector cause substantial reductions in subsurface outflow to the Hale‘iwa and South O‘ahu sectors and induce small increases in subsurface flow from the Ko‘olau and Wai‘anae sectors.

The model simulations for Assessment I indicate that Current-scenario groundwater withdrawals from the Schofield sector cause water-level decline, but the decline is lower in magnitude and less focused than in sectors that encompass dike-impounded-groundwater settings (fig. 33*B*). The smaller but more dispersed water-table decline is consistent with the high-permeability aquifer that forms the Schofield sector. The model-simulated freshwater-saltwater interface in the Schofield sector did not rise in response to withdrawals (fig. 34*B*) because

A

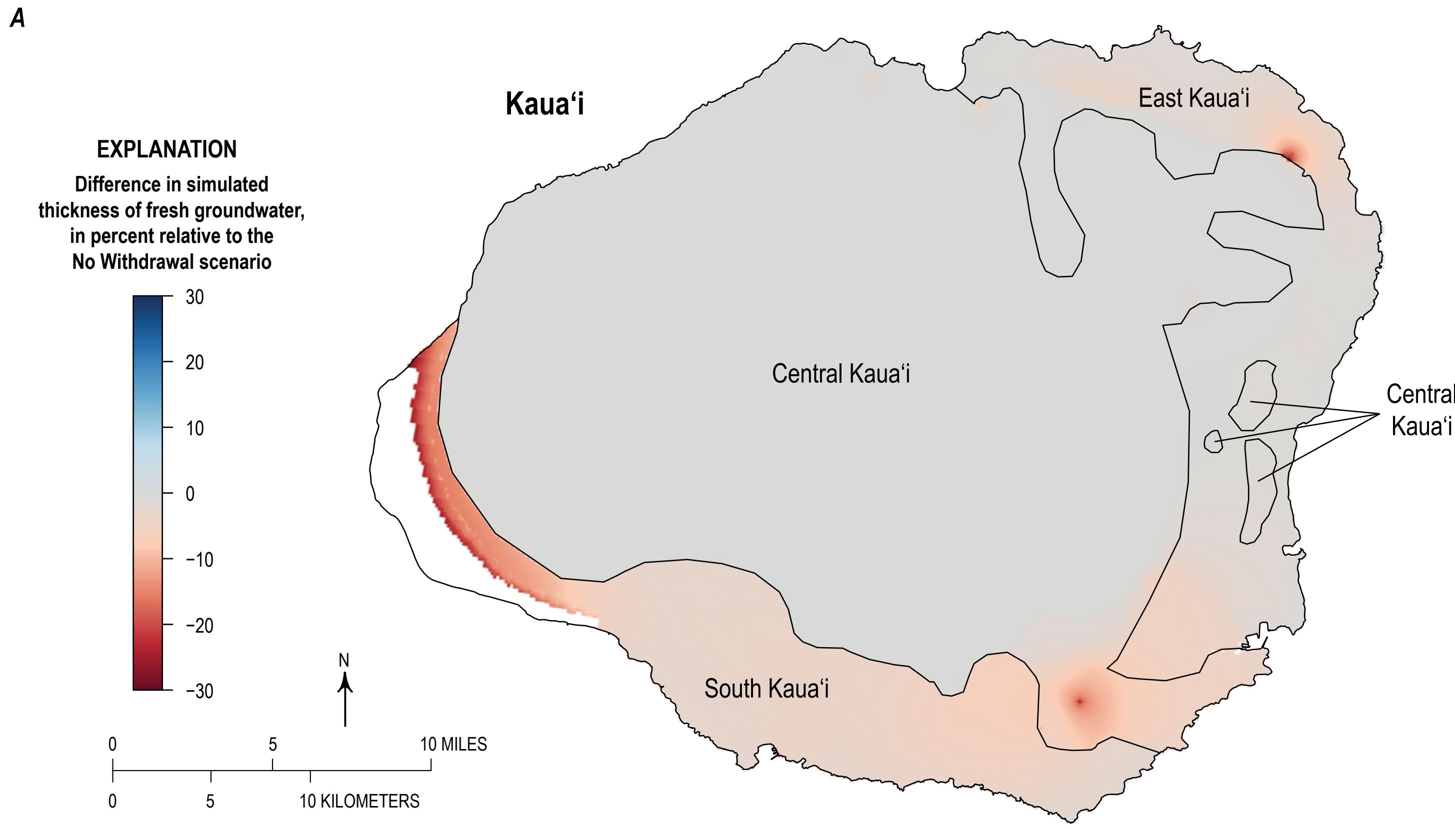
Kaua‘i
EXPLANATION
Difference in simulated thickness of fresh groundwater, in percent relative to the No Withdrawal scenario
30
20
10
0
−10
−20
−30
East Kaua‘i
Central Kaua‘i
Central Kaua‘i
South Kaua‘i
N
0 5 10 MILES
0 5 10 KILOMETERS

B

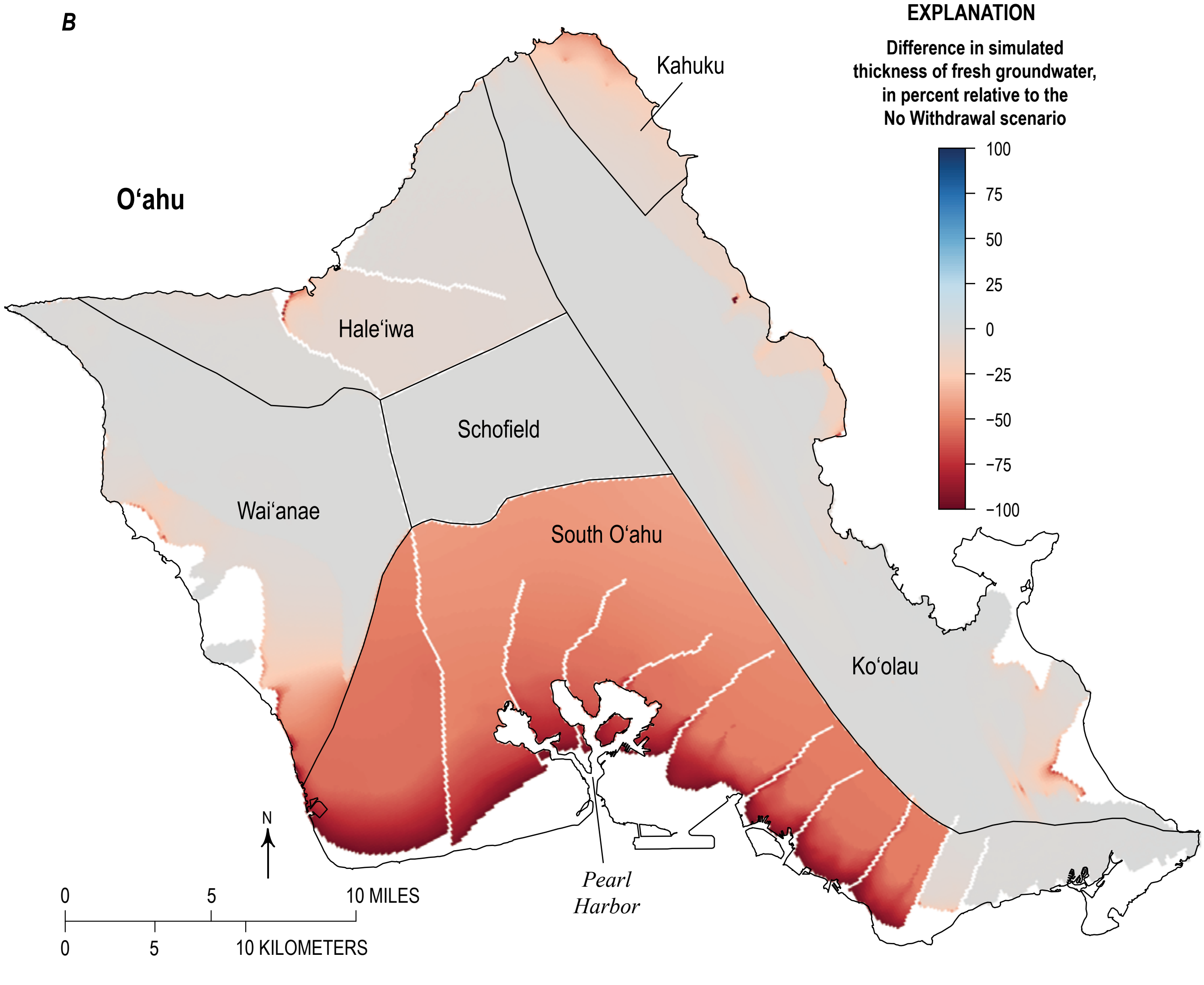
O‘ahu
Kahuku
EXPLANATION
Difference in simulated thickness of fresh groundwater, in percent relative to the No Withdrawal scenario
100
75
50
25
0
−25
−50
−75
−100
Hale‘iwa
Schofield
Wai‘anae
South O‘ahu
Ko‘olau
Pearl Harbor
N
0 5 10 MILES
0 5 10 KILOMETERS

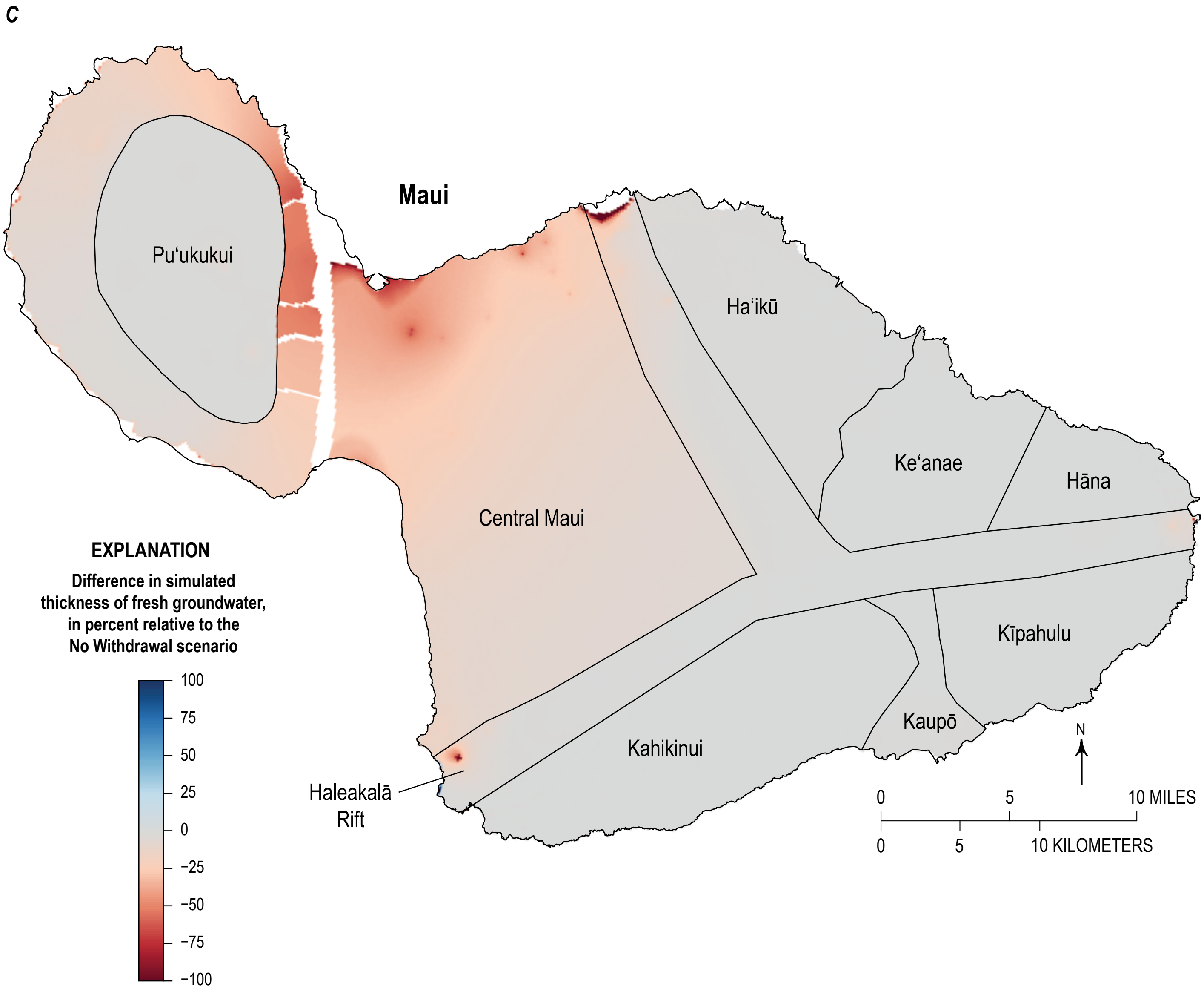

Figure 35. Maps showing percentage differences in thickness of fresh groundwater from Assessment I, computed by subtracting results of the No Withdrawal scenario from those of the Current scenario simulated using models of the volcanic aquifers of (*A*) Kaua'i, (*B*) O'ahu, and (*C*) Maui, Hawai'i. Differences indicate changes caused by withdrawing groundwater at rates represented by the Current scenario. Gray areas represent 0.0 values.

fresh groundwater extends down to the bottom of the O'ahu model, and thinning of the fresh-groundwater body is negligible (fig. 35*B*).

Sectors that encompass thickly saturated settings.—Three sectors of the models in this study encompass thickly saturated settings (table 4, fig. 29). The Kaupō sector (on Maui) and the East Kaua'i sector receive simulated subsurface inflow from the dike-impounded-groundwater settings, whereas the Ke'anae sector (on Maui) does not receive any subsurface groundwater (fig. 37*A*, *C*). All three sectors contribute subsurface flow to adjacent sectors and discharge groundwater to the ocean, and two (East Kaua'i and Ke'anae) also discharge water to streams and springs.

Model-simulation results for Assessment I indicate that Current-scenario groundwater withdrawals affect simulated subsurface flow to and from sectors that encompass the thickly saturated setting. In the thickly saturated setting of the East Kaua'i sector, simulated subsurface inflow from the Central Kaua'i sector decreases slightly as a result of withdrawals from the upgradient dike-impounded-groundwater settings (fig. 37*A*). The combined effect of withdrawals and decreased inflow to the East Kaua'i sector is compensated by substantial reductions in groundwater discharge to the ocean and to streams and springs (figs. 31*A*, 32*A*, 37*A*).

Current-scenario groundwater-withdrawal rates from the thickly saturated settings of the Ke'anae and Kaupō sectors on Maui are small (table 6, fig. 37*C*). The model simulations indicate that withdrawals from the Ke'anae sector are largely compensated by simulated reductions in groundwater discharge to the ocean

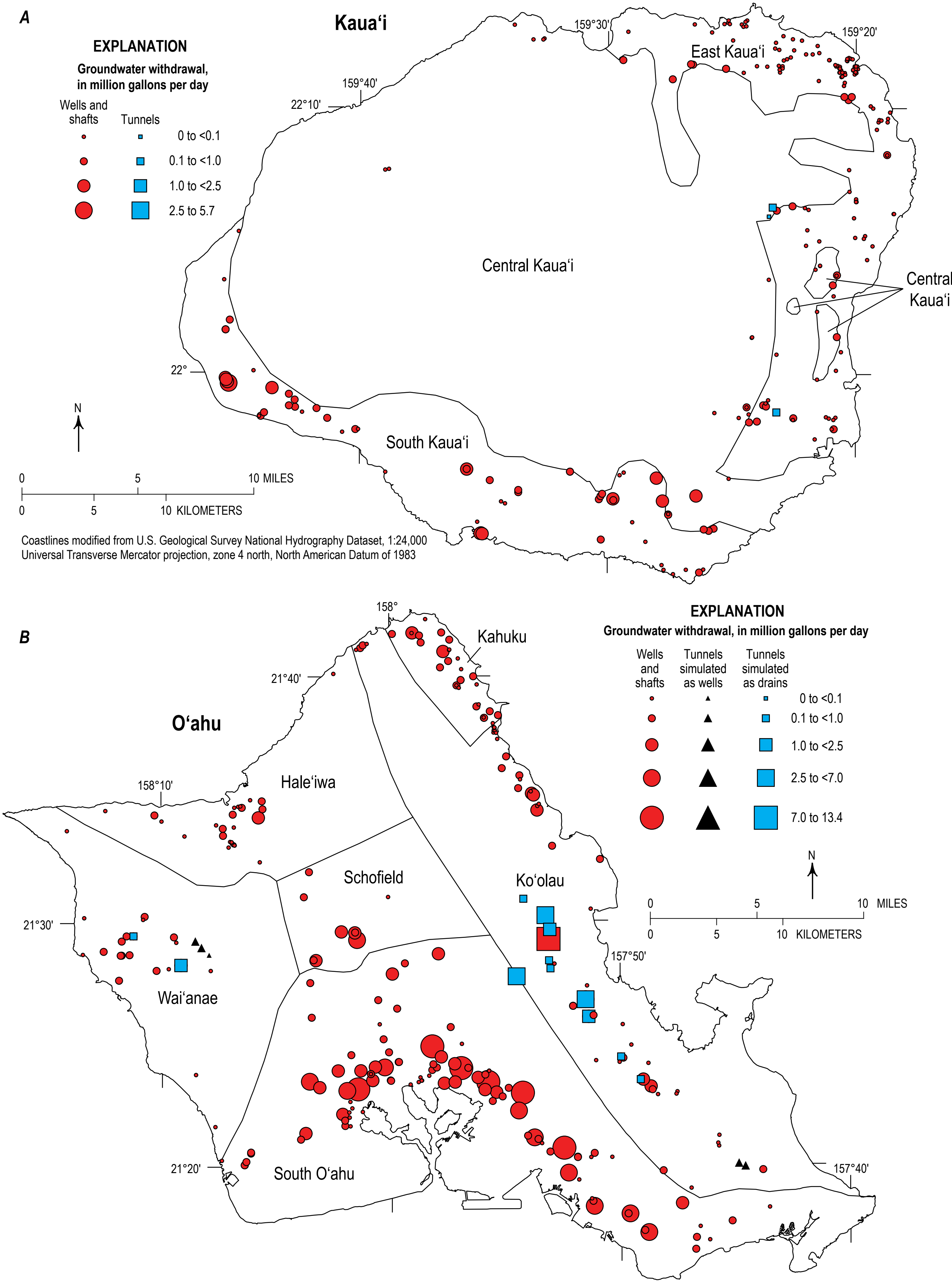
A
Kaua‘i
EXPLANATION
Groundwater withdrawal, in million gallons per day
Wells and shafts
Tunnels
0 to <0.1
0.1 to <1.0
1.0 to <2.5
2.5 to 5.7
159°40'
159°30'
159°20'
22°10'
22°
East Kaua‘i
Central Kaua‘i
Central Kaua‘i
South Kaua‘i
N
0 5 10 MILES
0 5 10 KILOMETERS
Coastlines modified from U.S. Geological Survey National Hydrography Dataset, 1:24,000
Universal Transverse Mercator projection, zone 4 north, North American Datum of 1983
B
O‘ahu
158°
158°10'
157°50'
157°40'
21°40'
21°30'
21°20'
Kahuku
Hale‘iwa
Schofield
Ko‘olau
Wai‘anae
South O‘ahu
EXPLANATION
Groundwater withdrawal, in million gallons per day
Wells and shafts
Tunnels simulated as wells
Tunnels simulated as drains
0 to <0.1
0.1 to <1.0
1.0 to <2.5
2.5 to <7.0
7.0 to 13.4
N
0 5 10 MILES
0 5 10 KILOMETERS

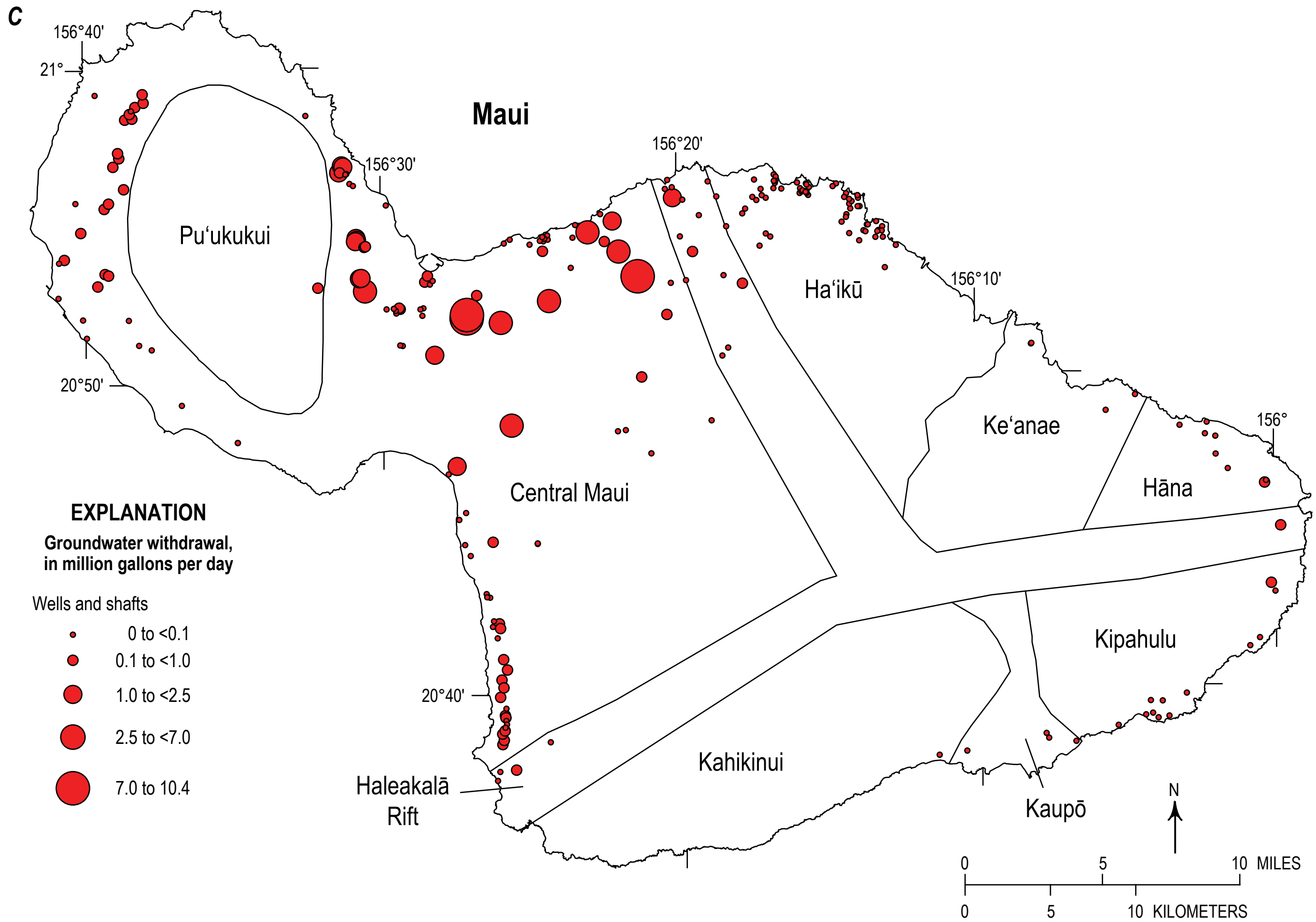

Figure 36. Maps showing distribution of groundwater withdrawal simulated in models of the volcanic aquifers of (*A*) Kaua‘i, (*B*) O‘ahu, and (*C*) Maui, Hawai‘i. Modified from Izuka and others (2021).

and only a small reduction in groundwater discharge to streams and springs, a result that is consistent with the locations of wells near the coast (fig. 36*C*). Withdrawals from the Kaupō sector are compensated by simulated reductions in subsurface flows to adjacent sectors and decreased groundwater discharge to the ocean, which is consistent with the locations of wells near the coast and near the boundaries of the sector.

Model simulations for Assessment I indicate that Current-scenario groundwater withdrawals have caused water-level declines, rise of the freshwater-saltwater interface, and reduction in the thickness of fresh groundwater in the thickly saturated setting of the East Kaua‘i sector (figs. 33*A*, 34*A*, 35*A*), but the effects are small because withdrawal is distributed among many low-producing wells (fig. 36*A*). The largest change in interface altitude and freshwater thickness in the East Kaua‘i sector appears to result not from withdrawals within the sector but from the large withdrawals in the adjacent Central Kaua‘i sector. Withdrawals from the thickly saturated setting of the Ke‘anae and Kaupō sectors on Maui (fig. 36*C*) are even less than withdrawals from East Kaua‘i and result in small simulated water-level declines, interface rise, and thinning of fresh groundwater (figs. 33*C*, 34*C*, 35*C*).

Sectors that encompass the freshwater-lens setting.—Nine sectors of the models in this study encompass freshwater-lens settings (table 4, fig. 29). Because freshwater-lens settings are typically downgradient from other settings, a substantial part of the inflow to a sector that has the freshwater-lens setting is subsurface inflow from adjacent settings (fig. 37). Groundwater withdrawals from adjacent settings can cause reductions in subsurface flows to a freshwater lens. These reductions, along with any withdrawals from the freshwater lens itself, are compensated by decreases in groundwater discharge to streams, springs, and the ocean. On the other hand, withdrawals from a freshwater lens can induce additional subsurface flow from an adjacent setting; the induced additional inflow compensates for part of the withdrawals from these sectors.

Model results for Assessment I indicate that, in all sectors that encompass the freshwater-lens setting except South O‘ahu, groundwater withdrawals from within the sector or reductions in subsurface inflow caused by withdrawals from adjacent sectors

Table 6. Differences in sector groundwater budgets from Assessment I (Current scenario minus No Withdrawal scenario), determined from simulations using numerical groundwater models of the volcanic aquifers of Kauaʻi, Oʻahu, and Maui, Hawaiʻi.

[Actual model totals may not be equal to sum of values in columns, owing to rounding. Mgal/d, million gallons per day]

Sector	Principal groundwater setting	Differences (Mgal/d)					
		Recharge	Withdrawal from wells	Tunnel yield	Discharge to streams and springs	Discharge to ocean	Subsurface flow to or from other sectors[1]
Kauaʻi model							
Central Kauaʻi	Dike-impounded groundwater	0.0	5.9	0.2	−1.1	−0.3	−4.8
South Kauaʻi	Freshwater lens	0.0	36.2	0.0	0.0	−39.8	3.5
East Kauaʻi	Thickly saturated	0.0	7.0	0.4	−3.4	−5.1	1.2
	Total	0.0	49.1	0.6	−4.5	−45.1	0.0
Oʻahu model							
South Oʻahu	Freshwater lens	0.0	149.7	0.0	−101.9	−46.7	−1.1
Haleʻiwa	Freshwater lens	0.0	3.7	0.0	0.0	−7.7	3.9
Kahuku	Freshwater lens	0.0	8.7	0.0	0.0	−8.3	−0.3
Koʻolau	Dike-impounded groundwater	0.0	13.7	32.0	−31.0	−10.3	−4.5
Waiʻanae	Dike-impounded groundwater	0.0	3.3	1.2	−2.1	−13.3	11.0
Schofield	Enigmatic[2]	0.0	9.0	0.0	0.0	0.0	−9.0
	Total	0.0	188.0	33.2	−135.0	−86.2	0.0
Maui model							
Puʻukukui	Dike-impounded groundwater	0.0	0.8	11.4	−9.5	0.0	−2.8
Central Maui	Freshwater lens	0.0	92.3	0.0	0.0	−95.0	2.7
Haʻikū	Freshwater lens	0.0	0.4	0.0	0.0	−2.5	2.1
Keʻanae	Thickly saturated	0.0	0.1	0.0	0.0	−0.1	0.0
Hāna	Freshwater lens	0.0	0.2	0.0	0.0	−0.3	0.1
Kīpahulu	Freshwater lens	0.0	0.2	0.0	0.0	−0.2	0.1
Kaupō	Thickly saturated	0.0	0.0	0.0	0.0	0.0	0.0
Kahikinui	Freshwater lens	0.0	0.0	0.0	0.0	−0.1	0.1
Haleakalā Rift	Dike-impounded groundwater	0.0	3.5	0.0	0.0	−1.2	−2.2
	Total	0.0	97.5	11.4	−9.5	−99.4	0.0

[1]Positive values indicate increased outflow or decreased inflow; negative values indicate decreased outflow or increased inflow.

[2]Enigmatic groundwater occurrences do not fit into one of the four principal groundwater settings discussed in this report, and their relation to the geologic framework of volcanic aquifers is not fully understood (see Izuka and others, 2018, 2021).

are compensated entirely by simulated reductions in groundwater discharge to the ocean or changes in subsurface flows to adjacent sectors (table 6). No simulated streams or springs drain the freshwater lens in these sectors of the models, so groundwater withdrawals cannot be compensated by reductions in groundwater discharge to these water bodies. In the South Kauaʻi, Haleʻiwa, Central Maui, Haʻikū, Hāna, Kīpahulu, and Kahikinui sectors, net subsurface inflow from adjacent aquifers decreases (fig. 37) as a result of withdrawals from adjacent sectors. These net reductions in subsurface inflow, along with withdrawals from within these sectors, are compensated by simulated reductions in groundwater discharge to the ocean. Groundwater withdrawals from the Kahuku sector induced additional simulated subsurface inflow from adjacent sectors; the induced additional inflow together with reductions in groundwater discharge to the ocean compensate for withdrawals from the Kahuku sector.

The South Oʻahu sector is the only sector, among those that encompass the freshwater-lens setting, in which simulated reductions in streamflow and springflow compensate for most of the groundwater withdrawals from the sector (fig. 37*B*). The reductions occur near Pearl Harbor, where groundwater discharges from springs that issue from where the caprock overlying the volcanic aquifer pinches out (figs. 10*C, D*; 31*B*). The model simulations also indicate that reductions in groundwater discharge to the ocean through the caprock compensate for a substantial fraction of the withdrawals from the South Oʻahu sector (figs. 32*B*, 37*B*). Large withdrawals from the South Oʻahu sector induce simulated net subsurface inflow, even though simulated inflows from some sectors decrease.

Model simulations for Assessment I indicate that Current-scenario groundwater withdrawals cause water-level declines in these sectors. Compared to declines in the dike-impounded-groundwater setting, declines in the freshwater-lens setting are generally of lower magnitude and unfocused (fig. 33), even though withdrawals are high (fig. 37). The smaller but more widespread water-level decline is typical of high-permeability aquifers such as those in which the freshwater-lens setting exists. In contrast, withdrawals result in substantial model-simulated rise of the freshwater-saltwater interface in sectors that encompass the freshwater-lens settings (fig. 34), particularly in South Oʻahu and Central Maui where withdrawals are large (fig. 36*B, C*) and water-level declines and rise of the freshwater-saltwater interface result in substantial reduction in the thickness of fresh groundwater (fig. 35*B, C*).

Assessment II—Combined Effects of Changing Withdrawal and Recharge Rates

Assessment II evaluates the combined effects of Current-scenario groundwater-withdrawal rates and recharge differences related to land-cover changes between 1870 and 2010 (table 3). The Predevelopment scenario, which represents recharge conditions and absence of groundwater withdrawal that existed in 1870 (table 2), is simulated using the Kauaʻi, Oʻahu, and Maui numerical models and compared to the Current scenario. Differences between the Current and Predevelopment scenarios provide information on the combined effect that Current-scenario withdrawal rates and land-cover changes between 1870 and 2010 have had on groundwater availability.

Predevelopment Scenario

The Predevelopment scenario represents a period before groundwater development; however, the scenario does not represent a period devoid of all human impacts. As discussed above, humans had affected recharge through agriculture and deforestation, even before the first modern well was drilled. The Predevelopment scenario uses recharge distributions computed by Izuka and others (2018) for 1870 land cover. Comparison of land-cover maps for 1870 (fig. 5) and 2010 (the land-cover period represented by the recharge in the Current scenario) (fig. 6) show substantial differences in the extents of native and alien (nonnative) forests, developed land, areas of agriculture or former agriculture (fallow/grassland), and agricultural infrastructure such as reservoirs. The 1870 recharge computation used average rainfall from 1978 to 2007 because it is a better representation of the probable long-term average. In general, average rainfall amounts indicate that the 1978-to-2007 period was slightly wetter than the 2001-to-2010 period represented by the Current scenario, although some areas within an island were drier.

For the Predevelopment scenario, the 1870 recharge computed by Izuka and others (2018) was discretized into the Kauaʻi, Oʻahu, and Maui models using the methods described by Izuka and others (2021). Groundwater-withdrawal rates for wells and tunnels are set to zero, as described above for the No Withdrawal scenario.

Results

Recharge over some areas in the lower altitudes of the three models is greater in the Current scenario than in the Predevelopment scenario (fig. 38), owing to the emergence of sources from human activity between 1870 and 2010 such as irrigation in agricultural areas and irrigation and leakage from water mains and cesspools in developed areas (compare figures 5 and 6). Recharge is substantially less in areas near streams where flood-irrigated taro land cover in 1870 no longer existed in 2010. Recharge at some midaltitude areas is lower in the Current scenario than in the Predevelopment scenario, owing, in part, to replacement of native forest with nonnative forest since 1870. Local differences in the rainfall periods used in the two scenarios also contribute to local differences in recharge.

In the Oʻahu model, recharge in the Current scenario and Predevelopment scenarios differ by only 1.9 Mgal/d (table 7, fig. 39), which is less than one percent of the island's Predevelopment-scenario recharge rate. On an islandwide basis, the combined effects of increased groundwater withdrawal and changes in recharge indicated in Assessment II are similar to the effect of increased groundwater withdrawal alone indicated in Assessment I—reduction of groundwater discharge to streams and springs compensates for most of the combined effect of simulated withdrawals and changes in recharge (compare figures 30 and 39).

Table 7. Comparison of islandwide groundwater budgets for the Current and Predevelopment scenarios (Assessment II) simulated using numerical groundwater models of the volcanic aquifers of Kauaʻi, Oahu, and Maui, Hawaiʻi.

[Differences between scenarios represent Current minus Predevelopment scenarios; differences between scenarios may not be equal to differences between values in columns, owing to rounding. Mgal/d, million gallons per day]

Model	Scenario	Recharge (Mgal/d)	Withdrawal (Mgal/d)			Groundwater discharge (Mgal/d)	
			Wells	Tunnels	Total	To streams and springs	To ocean
Kauaʻi	Predevelopment	866.2	0.0	0.0	0.0	740.4	125.8
	Current	871.2	49.1	0.6	49.7	701.2	120.4
	Difference between scenarios	5.0	49.1	0.6	49.7	−39.2	−5.4
Oʻahu	Predevelopment	599.5	0.0	0.0	0.0	271.2	328.2
	Current	597.6	188.0	33.2	221.2	127.7	248.6
	Difference between scenarios	−1.9	188.0	33.2	221.2	−143.5	−79.7
Maui	Predevelopment	1,275.6	0.0	0.0	0.0	185.7	1,089.9
	Current	1,166.7	97.5	11.4	108.9	156.6	901.2
	Difference between scenarios	−109.0	97.5	11.4	108.9	−29.2	−188.8

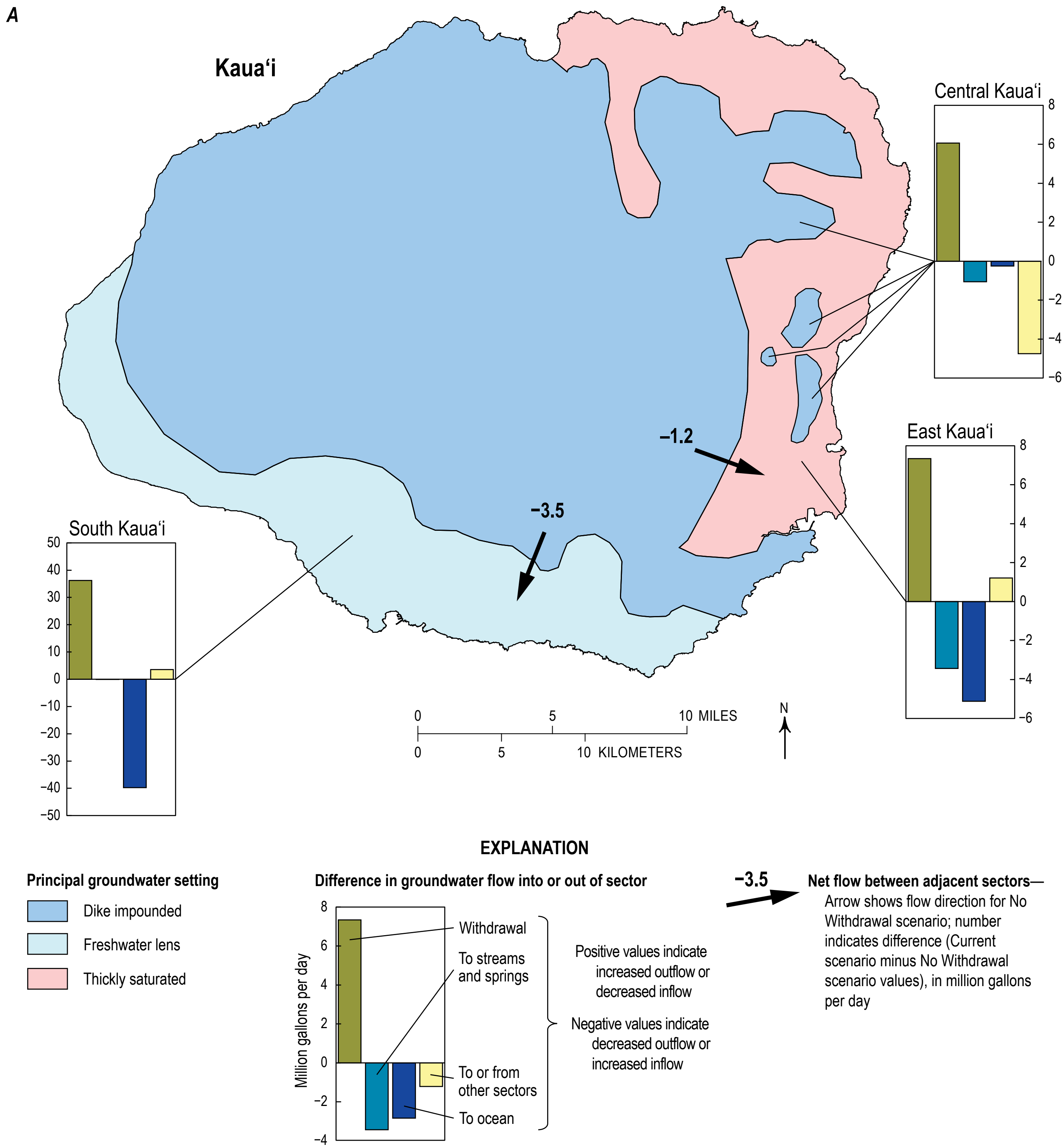

Figure 37. Maps and bar graphs showing differences in sector groundwater budgets from Assessment I, computed by subtracting results of the No Withdrawal scenario from those of the Current scenario simulated using models of the volcanic aquifers of (*A*) Kaua‘i, (*B*) O‘ahu, and (*C*) Maui, Hawai‘i. Differences indicate changes caused by withdrawing groundwater at rates represented by the Current scenario. Note that vertical axes of bar graphs are at different scales to show wide range of values. Values that indicate flow between sectors may not agree exactly with totals shown in table 6, owing to rounding.

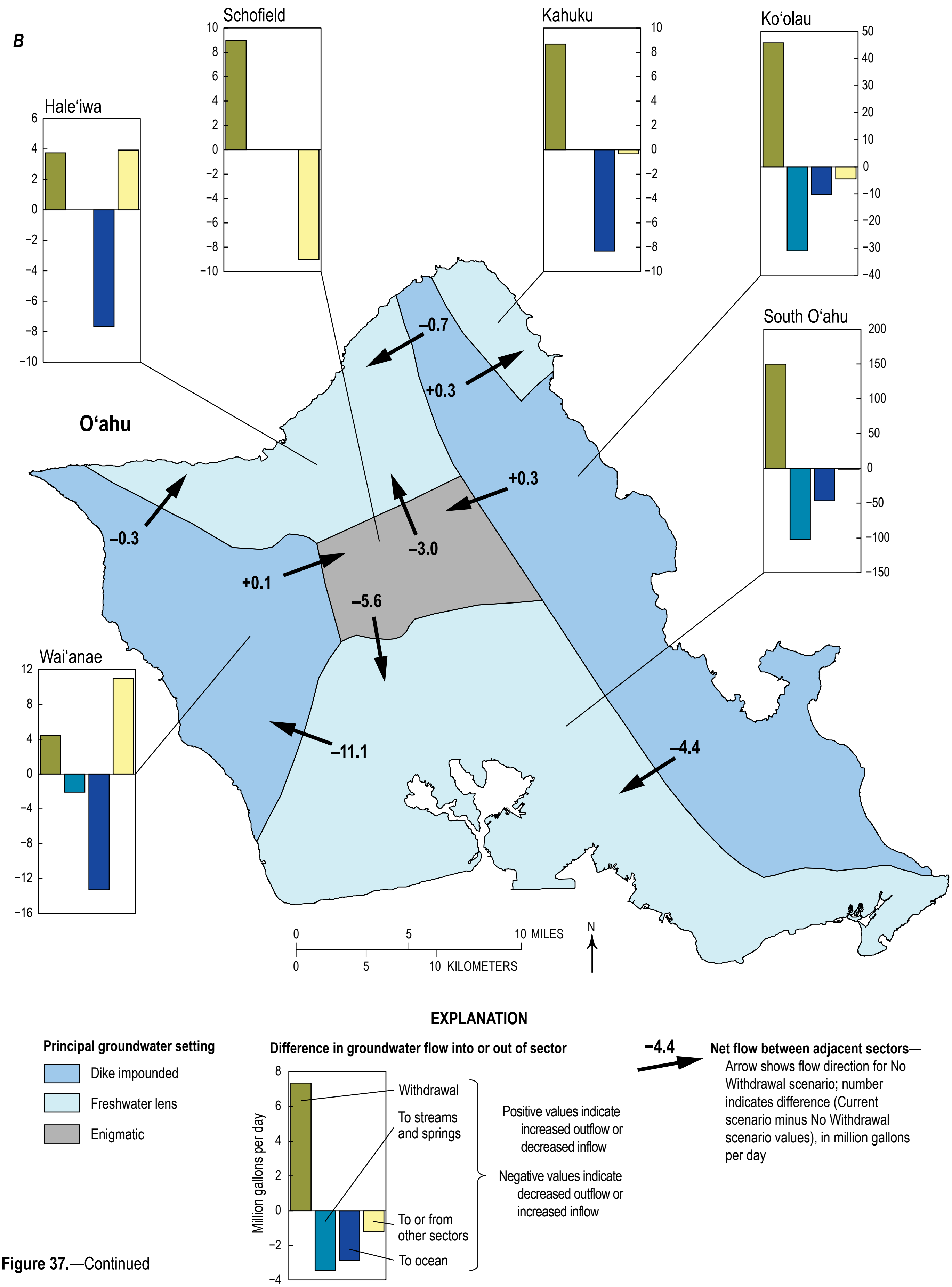

Figure 37.—Continued

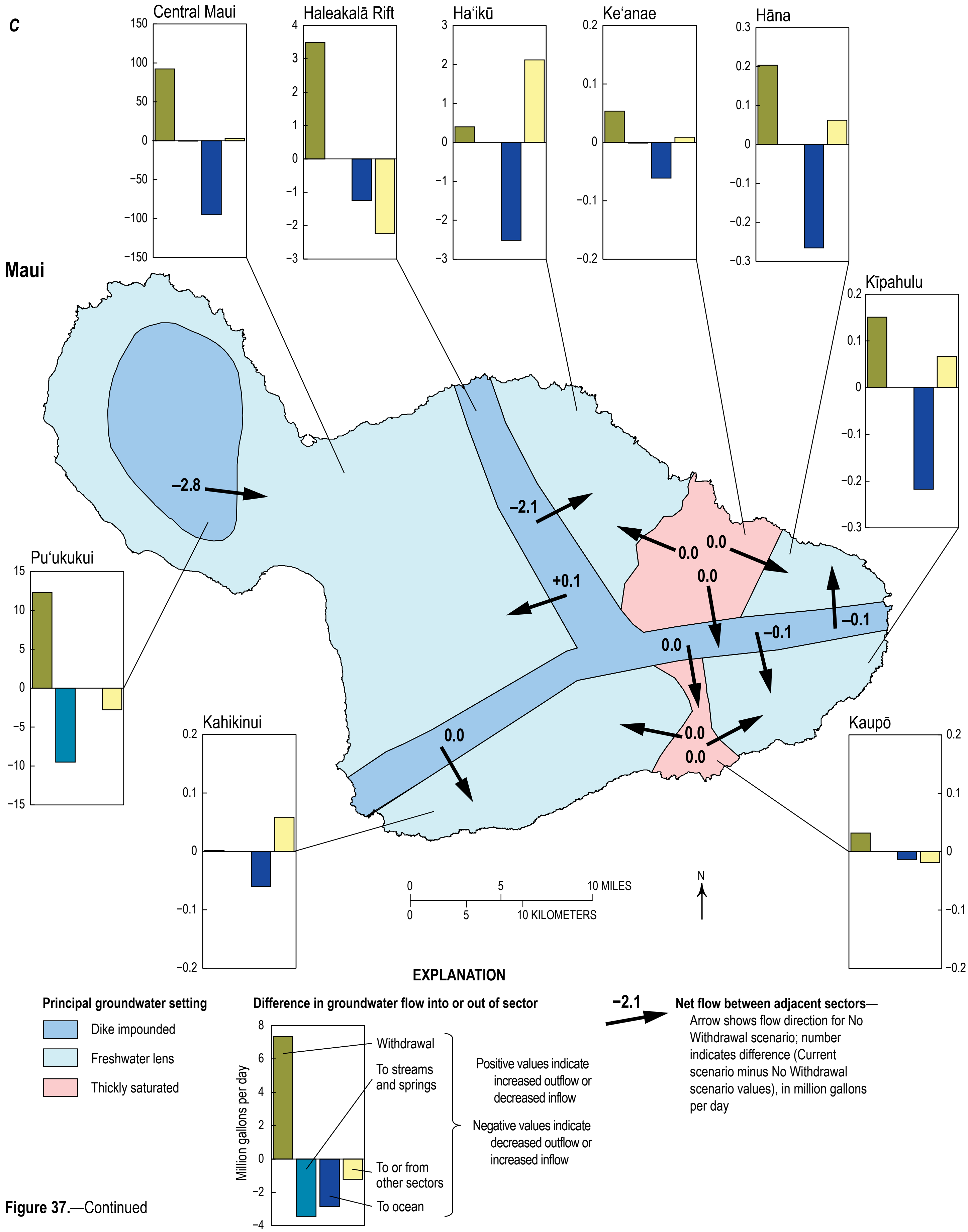

Figure 37.—Continued

In the Kauaʻi model, islandwide recharge in the Current scenario is 5.0 Mgal/d higher than in the Predevelopment scenario (table 7, fig. 39). Despite this small increase (less than 1 percent) in islandwide recharge, reduction in groundwater discharge to streams is much greater in Assessment II, when the combined effects of groundwater withdrawals and differences in recharge are considered, than in Assessment I, when only the effect of withdrawal is considered (compare figures 30 and 39). This result indicates that even though islandwide recharge is higher in the Current scenario than in the Predevelopment scenario, recharge near streams that receive groundwater discharge decreased.

In the Maui model, islandwide recharge in the Current scenario is 109.0 Mgal/d, or about 9 percent less than in the Predevelopment scenario (table 7, fig. 39). As a result of the combination of widespread reductions in islandwide recharge and addition of groundwater withdrawals in the Current scenario, reduction in groundwater discharge to streams, springs, and the ocean is greater in Assessment II than in Assessment I (compare figures 30 and 39).

Sectors that encompass dike-impounded-groundwater settings.—In the dike-impounded-groundwater settings of the Central Kauaʻi, Koʻolau, and Haleakalā Rift sectors, recharge rates in the Current scenario are less than they are in the Predevelopment scenario (table 8, fig. 40). In these sectors, the combination of lower recharge and higher groundwater withdrawals in the Current scenario result in greater differences in groundwater discharge to streams, springs, and the ocean, and subsurface flows to adjacent aquifers in Assessment II than is indicated in Assessment I (compare figures 37 and 40, 31 and 41, and 32 and 42). The effects vary depending on the spatial distribution of recharge differences.

In the Central Kauaʻi sector, recharge in the Predevelopment scenario is 8.3 Mgal/d greater than it is in the Current and No Withdrawal scenarios (table 8, fig. 40*A*). Most of the recharge reduction is in the interior of the sector (fig. 38*A*), far from ocean discharge and boundaries with other sectors. As a result, reduction of groundwater discharge to streams and springs is greater in Assessment II (in which the effects of differences in both recharge

Table 8. Differences in sector groundwater budgets from Assessment II (Current scenario minus Predevelopment scenario), determined from simulations using numerical groundwater models of the volcanic aquifers of Kauaʻi, Oʻahu, and Maui, Hawaiʻi.

[Totals may not be equal to sum of values in columns, owing to rounding. Mgal/d, million gallons per day]

Sector	Principal groundwater setting	Differences (Mgal/d)					
		Recharge	Withdrawal from wells	Tunnel yield	Discharge to streams and springs	Discharge to ocean	Subsurface flow to or from other sectors[1]
Kauaʻi model							
Central Kauaʻi	Dike-impounded groundwater	−8.3	5.9	0.2	−26.2	0.4	11.4
South Kauaʻi	Freshwater lens	23.2	36.2	0.0	0.0	−2.0	−11.0
East Kauaʻi	Thickly saturated	−9.9	7.0	0.4	−13.0	−3.8	−0.5
	Total	5.0	49.1	0.6	−39.2	−5.4	0.0
Oʻahu model							
South Oʻahu	Freshwater lens	−10.1	149.7	0.0	−106.5	−51.5	−1.8
Haleʻiwa	Freshwater lens	7.1	3.7	0.0	0.0	3.2	0.3
Kahuku	Freshwater lens	0.5	8.7	0.0	0.0	−7.3	−0.9
Koʻolau	Dike-impounded groundwater	−4.5	13.7	32.0	−34.9	−11.6	−3.8
Waiʻanae	Dike-impounded groundwater	2.3	3.3	1.2	−2.1	−12.5	12.5
Schofield	Enigmatic[2]	2.7	9.0	0.0	0.0	0.0	−6.3
	Total	−1.9	188.0	33.2	−143.5	−79.7	0.0
Maui model							
Puʻukukui	Dike-impounded groundwater	2.2	0.8	11.4	−9.2	0.0	−0.9
Central Maui	Freshwater lens	51.9	92.3	0.0	0.0	−49.4	9.0
Haʻikū	Freshwater lens	−44.7	0.4	0.0	0.0	−55.0	9.9
Keʻanae	Thickly saturated	−41.9	0.1	0.0	−19.9	−2.4	−19.6
Hāna	Freshwater lens	−20.6	0.2	0.0	0.0	−30.4	9.6
Kīpahulu	Freshwater lens	−27.0	0.2	0.0	0.0	−32.5	5.3
Kaupō	Thickly saturated	−3.5	0.0	0.0	0.0	0.1	−3.6
Kahikinui	Freshwater lens	−14.2	0.0	0.0	0.0	−18.5	4.3
Haleakalā Rift	Dike-impounded groundwater	−11.0	3.5	0.0	0.0	−0.6	−13.9
	Total	−109.0	97.5	11.4	−29.2	−188.8	0.0

[1]Positive values indicate increased outflow or decreased inflow; negative values indicate decreased outflow or increased inflow.

[2]Enigmatic groundwater occurrences do not fit into one of the four principal groundwater settings discussed in this report, and their relation to the geologic framework of volcanic aquifers is not fully understood (see Izuka and others, 2018, 2021).

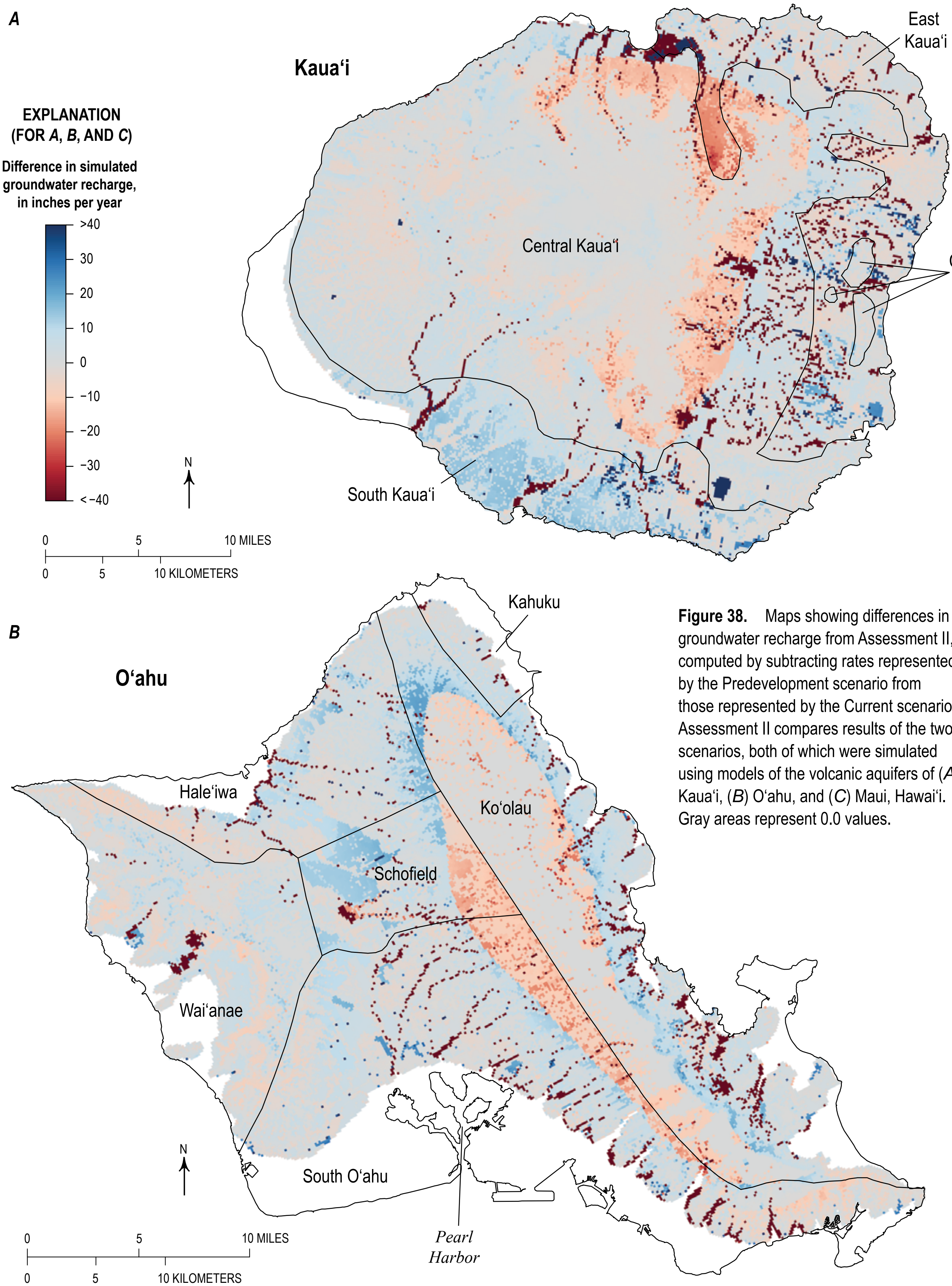

Figure 38. Maps showing differences in groundwater recharge from Assessment II, computed by subtracting rates represented by the Predevelopment scenario from those represented by the Current scenario. Assessment II compares results of the two scenarios, both of which were simulated using models of the volcanic aquifers of (*A*) Kauaʻi, (*B*) Oʻahu, and (*C*) Maui, Hawaiʻi. Gray areas represent 0.0 values.

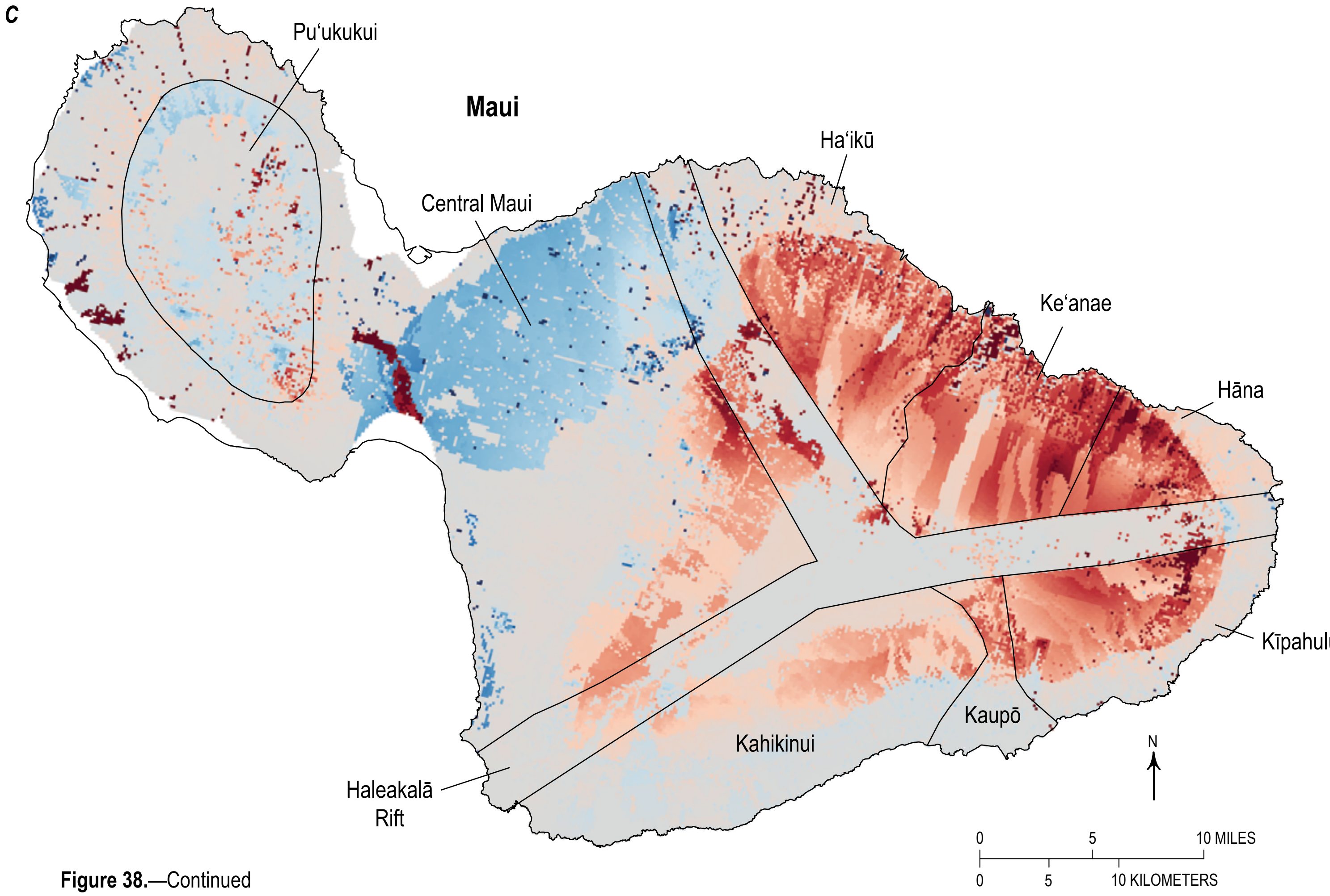

Figure 38.—Continued

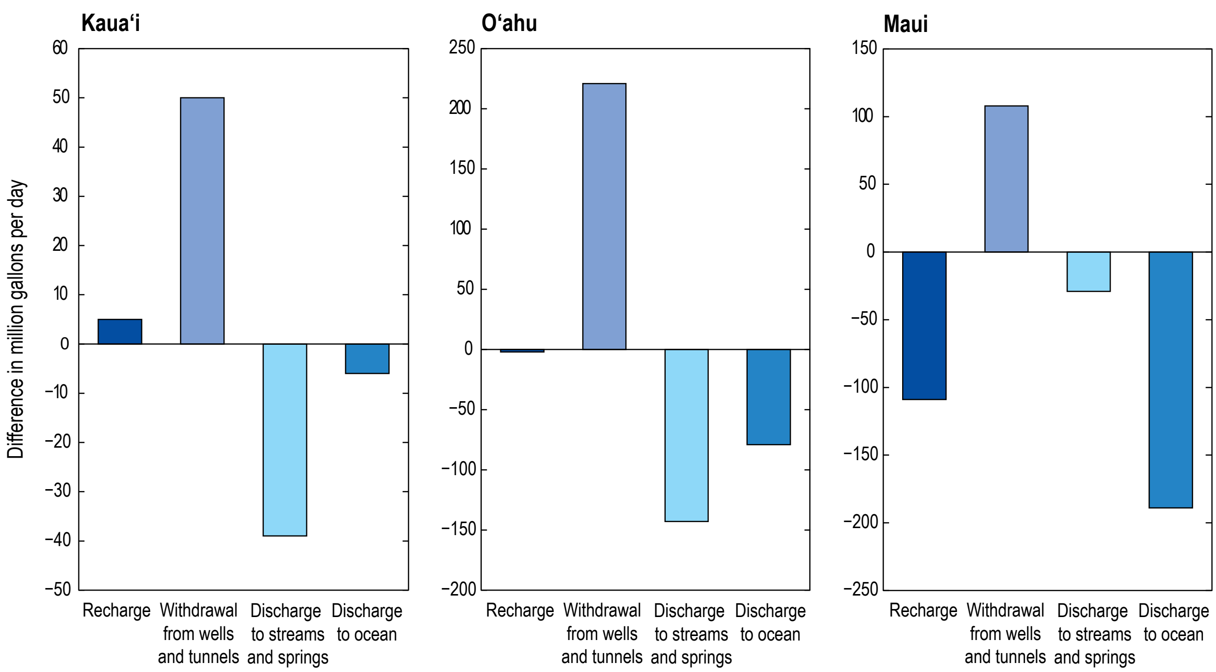

Figure 39. Bar graphs showing differences in islandwide groundwater budgets from Assessment II, computed by subtracting results of the Predevelopment scenario from those of the Current scenario simulated using models of the volcanic aquifers of Kauaʻi, Oʻahu, and Maui, Hawaiʻi. Differences indicate changes caused by increasing groundwater withdrawal and changing recharge from rates represented by the Predevelopment scenario to those represented by the Current scenario. Note that vertical axes of bar graphs are at different scales to show wide range of values.

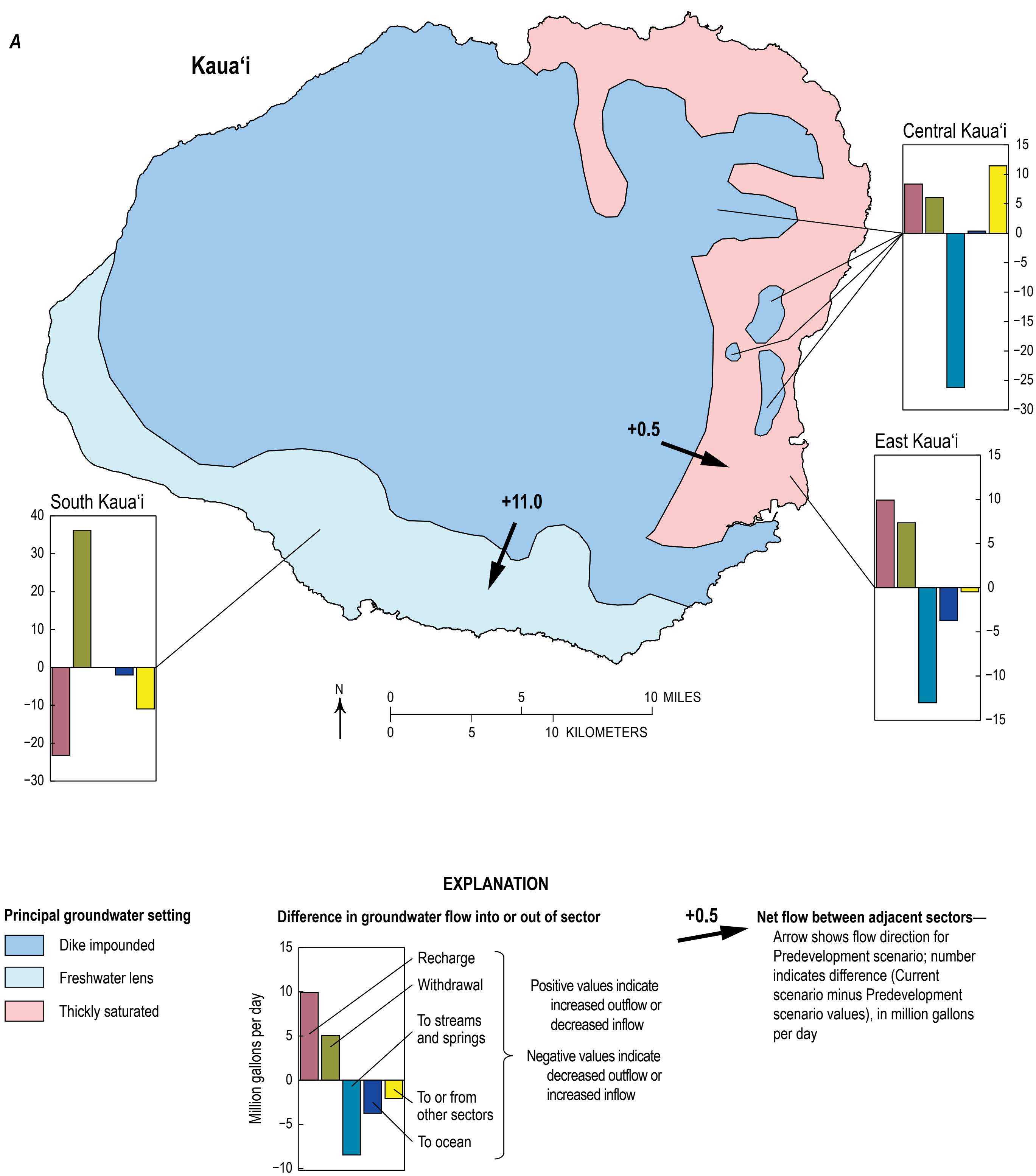

Figure 40. Maps and bar graphs showing differences in sector groundwater budgets from Assessment II, computed by subtracting results of the Predevelopment scenario from those of the Current scenario simulated using models of the volcanic aquifers of (*A*) Kaua‘i, (*B*) O‘ahu, and (*C*) Maui, Hawai‘i. Differences indicate changes caused by increasing groundwater withdrawal and changing recharge from rates represented by the Predevelopment scenario to those represented by the Current scenario. Note that vertical axes of bar graphs are at different scales to show wide range of values. Values that indicate flow between sectors may not agree exactly with totals shown in table 8, owing to rounding.

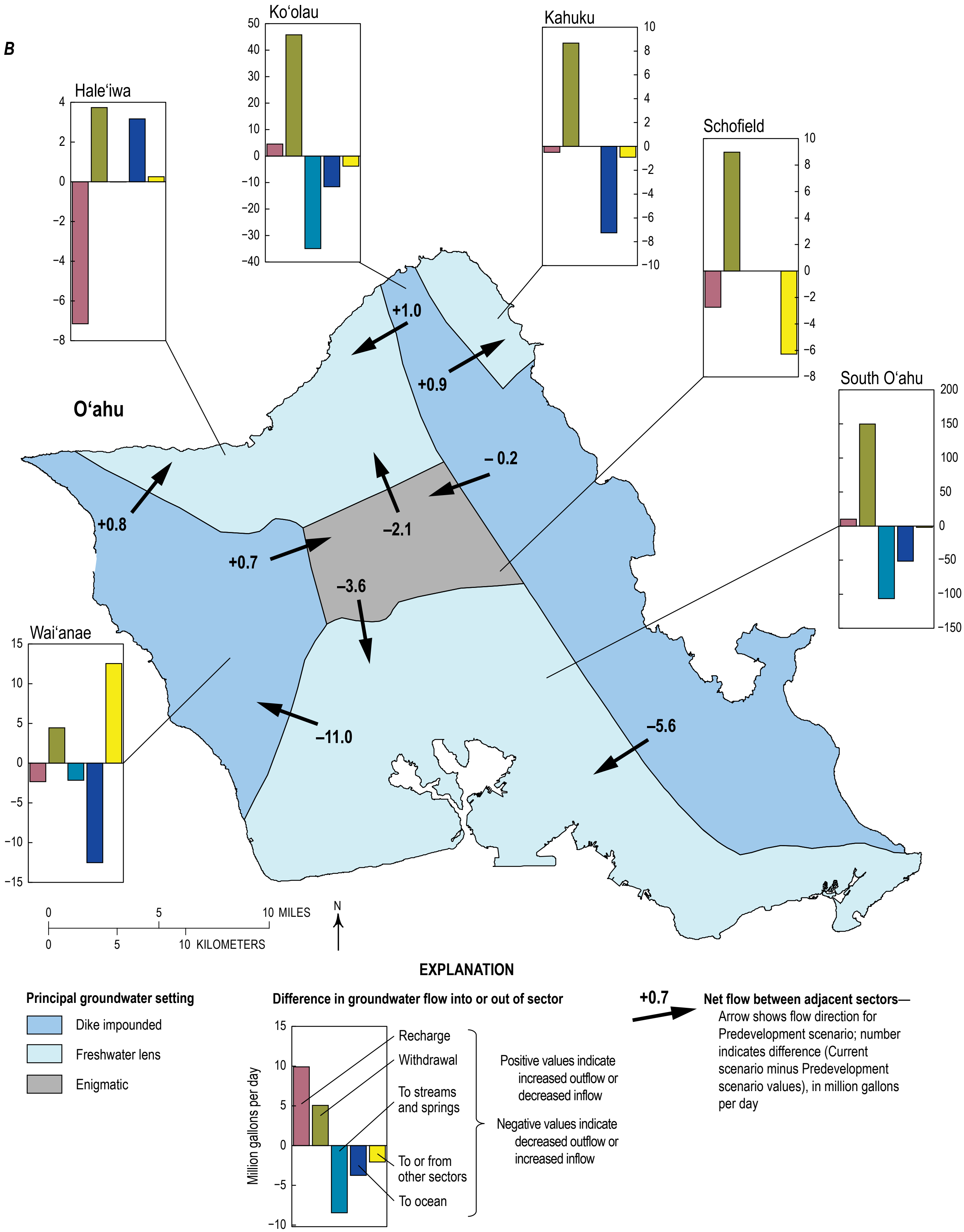

Figure 40.—Continued

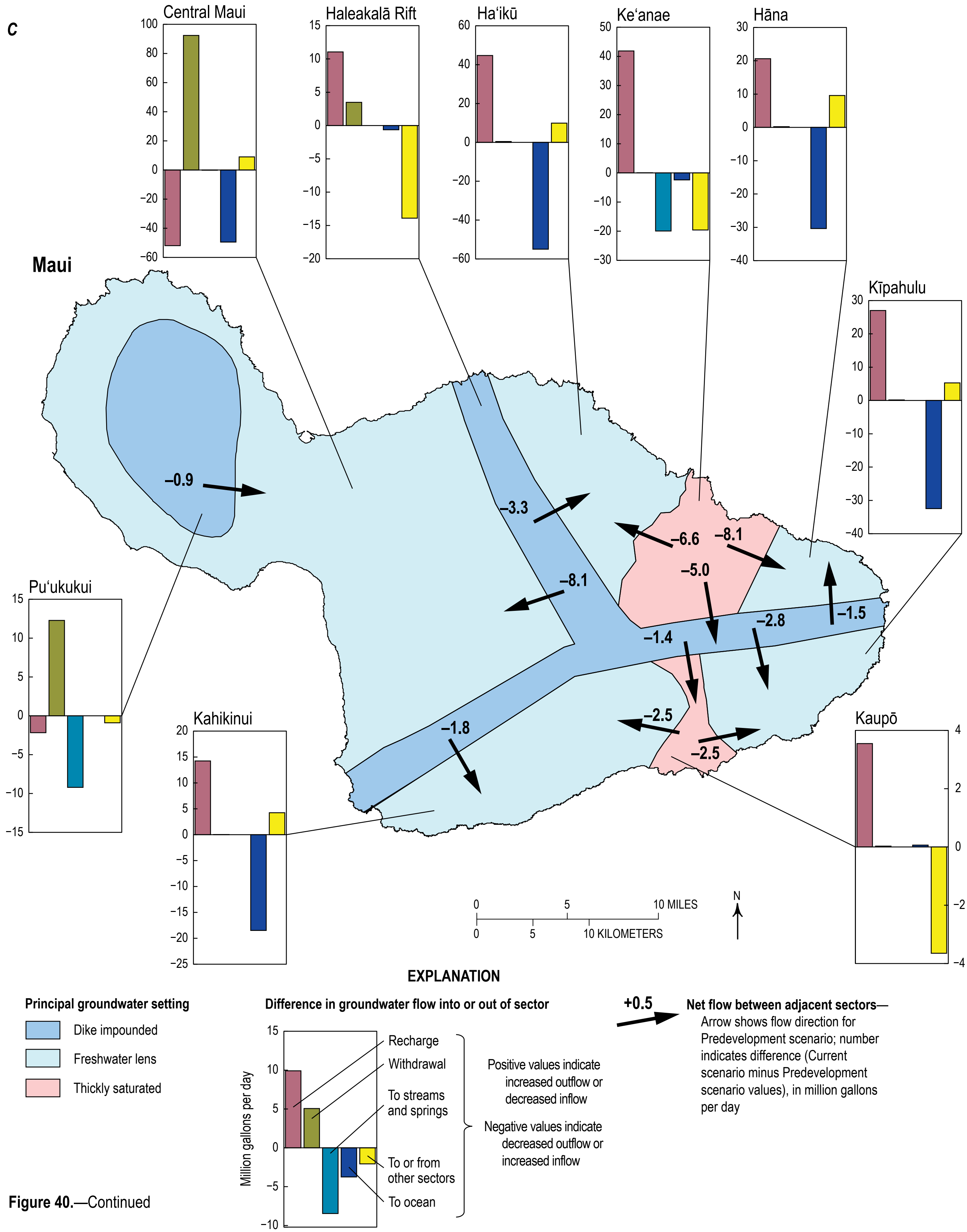

Figure 40.—Continued

and withdrawal are considered) than in Assessment I (in which only the effects of differences in withdrawal are considered) (compare figures 37*A* and 40*A*). On the other hand, subsurface flow to adjacent sectors to the south and southeast are greater in Assessment II than in Assessment I, owing to large, localized increases in recharge that result from leaks from surface-water reservoirs used for storing water for agriculture in the Current scenario, particularly in the southeastern part of the sector.

In the Koʻolau sector (on Oʻahu), recharge in the Current scenario is 4.5 Mgal/d less than it is in the Predevelopment scenario (table 8, fig. 40*B*), and reduction of groundwater discharge to streams, springs, and the ocean, and reduction in net subsurface outflow to adjacent sectors, is greater in Assessment II (figs. 40*B*, 41*B*, 42*B*) than in Assessment I (figs. 37*B*, 31*B*, 32*B* [listed in the order of comparison with figures 40*B*, 41*B*, and 42*B*, respectively]). In the Haleakalā Rift sector (on Maui), recharge in the Current scenario is 11.0 Mgal/d less than it is in the Predevelopment scenario (table 8, fig. 40*C*). This reduction in recharge is about three times more than the total Current-scenario withdrawal rate from this sector. The combined effect of groundwater withdrawal and lower recharge in the Current scenario is mostly compensated by reduced subsurface flow to adjacent aquifers, but it is also partly compensated by reduced flow to the ocean. Because the recharge reduction is mostly in the interior parts of the sector (fig. 38*C*), the reduction of subsurface flow is much greater in Assessment II than it is in Assessment I.

In the Waiʻanae (on Oʻahu) and Puʻukukui (on Maui) sectors, recharge rates in the Current scenario are higher than they are in the Predevelopment scenario (table 8, fig. 40*B, C*). The greater recharge compensates for some of the Current-scenario groundwater withdrawals. As a result, the effect of withdrawals on discharge to streams, springs, and the ocean in Assessment II (figs. 40*B, C*; 41*B, C*; 42*B, C*) differs from that indicated by Assessment I (figs. 37*B, C*; 31*B, C*; 32 *B, C* [listed in the order of comparison with figures 40, 41, and 42, respectively]). The effects on discharge to streams, springs, and the ocean depend on how close the areas that have recharge differences are relative to streams and coasts within a given sector. In the Waiʻanae sector, reduction in groundwater discharge to streams and springs in Assessments I and II are the same, whereas reduction in groundwater discharge to the ocean is less in Assessment II than in Assessment I (compare tables 6 and 8). In the Puʻukukui sector, reduction in flow to streams and springs is less in Assessment II than in Assessment I. Assessments I and II also differ in the effect of withdrawals on subsurface flow to adjacent aquifers—in the Waiʻanae sector, increase in outflow is greater in Assessment II than it is in Assessment I, whereas in the Puʻukukui sector, decrease in outflow is less in Assessment II than it is in Assessment I (compare tables 6 and 8).

Model simulations for Assessment II indicate that in sectors that encompass dike-impounded-groundwater settings, differences in groundwater withdrawals and recharge between the Current and Predevelopment scenarios result in differences in water levels (fig. 43). As in Assessment I, simulated water-level declines in Assessment II are focused in areas where withdrawals are high, but in Assessment II, effects of recharge differences are superimposed on the withdrawal effects. Effects of recharge differences are more apparent in areas where they are not obscured by the effects of withdrawal—water-level increases occur beneath areas of increased recharge, and water-level decreases occur beneath areas of decreased recharge. For example, in the Central Kauaʻi sector, water-level increases shown in figure 43*A* are prominent beneath areas occupied by the high-recharge reservoir land cover in the Current scenario, whereas water-level decreases are prominent beneath areas where high-recharge taro land cover that exist in the Predevelopment scenario no longer exist in the Current scenario (compare figures 5*A*, 6*A*, and 38*A* with figure 43*A*). In areas where withdrawals are substantial, the effects of changes in recharge combine with effects of withdrawal. For example, as a result of decreased recharge in the upper altitudes of the Koʻolau sector (fig. 38*B*), water-level decline that corresponds to withdrawals from tunnels is slightly larger in Assessment II (fig. 43*B*) than indicated in Assessment I (fig. 33*B*).

Model simulations for Assessment II indicate that within sectors that encompass dike-impounded-groundwater settings, differences in groundwater withdrawals and recharge between the Current and Predevelopment scenarios result in differences in the altitude of the freshwater-saltwater interface (fig. 44). In some areas, increased recharge has mitigated the effects of withdrawals. For example, a prominent lowering of the interface altitude in the southeastern part of the Central Kauaʻi sector results from enhanced recharge from water leaking from beneath a large irrigation reservoir (figs. 6*A*, 38*A*, 44*A*). This lowering of the interface indicated in Assessment II offsets the rise in the same location caused by withdrawals indicated in Assessment I.

In contrast, a prominent rise in interface altitude is apparent at the periphery of a low-permeability *K* zone in the Haleakalā Rift sector (on Maui), where upgradient decreases in recharge cause the interface to encroach landward (fig. 44*C*). In the Koʻolau and Waiʻanae sectors (on Oʻahu), changes in the interface altitude are apparent in seaward areas of the sectors (fig. 44*B*). The combination of water-level decline and interface rise result in changes in fresh-groundwater thickness (fig. 45), although as a percentage of the Predevelopment-scenario thickness, the changes in thickness are small in some areas of the dike-impounded-groundwater setting.

Schofield sector.—In the Schofield sector (on Oʻahu), the total recharge rate is 2.7 Mgal/d greater in the Current scenario than it is in the Predevelopment scenario (table 8, fig. 40*B*). The increase in recharge offsets some of the effects of groundwater withdrawal. As a result, reductions in outflows to the Haleʻiwa and South Oʻahu sectors and induced inflow from the Koʻolau sector are less in Assessment II than they are in Assessment I (compare figures 37*B* and 40*B*).

As a result of the offsetting effect of the increases in recharge, the broad water-level declines in the Schofield sector are even less in magnitude in Assessment II (fig. 43*B*) than they are in Assessment I (fig. 33*B*). Similar to Assessment I, the

A

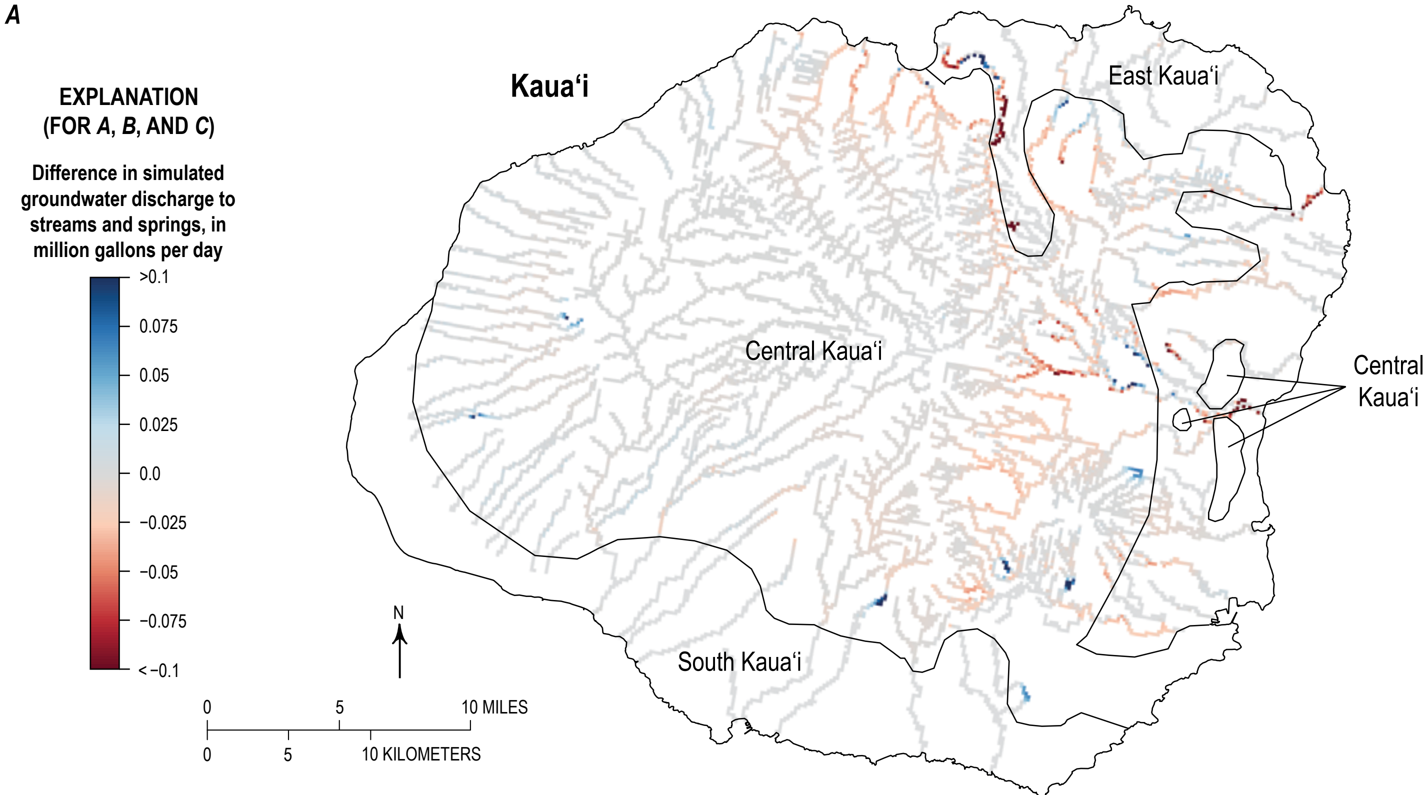
EXPLANATION
(FOR A, B, AND C)
Difference in simulated groundwater discharge to streams and springs, in million gallons per day
>0.1
0.075
0.05
0.025
0.0
−0.025
−0.05
−0.075
< −0.1
Kaua‘i
East Kaua‘i
Central Kaua‘i
Central Kaua‘i
South Kaua‘i
N
0
5
10 MILES
0
5
10 KILOMETERS

B

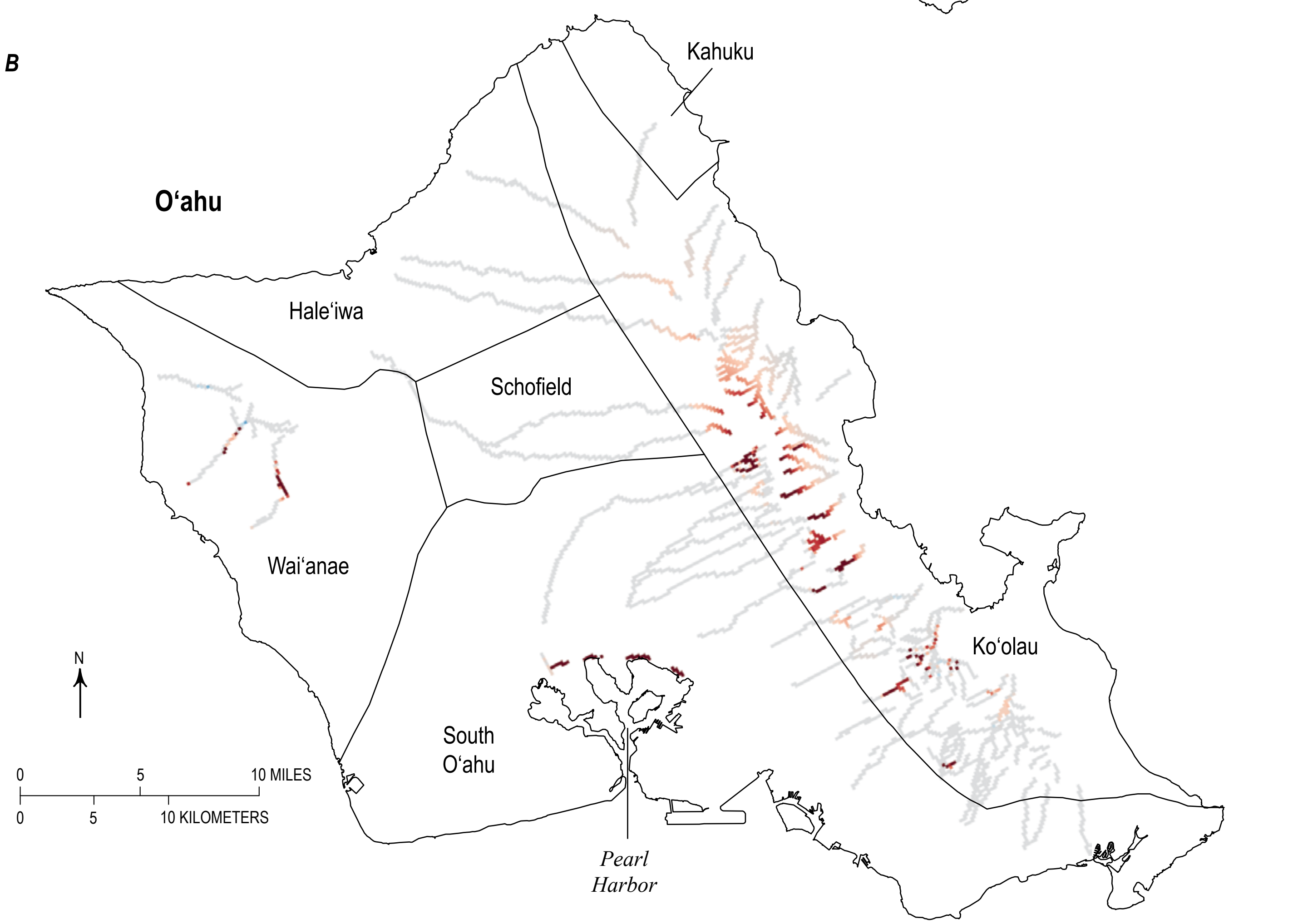
O‘ahu
Kahuku
Hale‘iwa
Schofield
Wai‘anae
Ko‘olau
South O‘ahu
Pearl Harbor
N
0
5
10 MILES
0
5
10 KILOMETERS

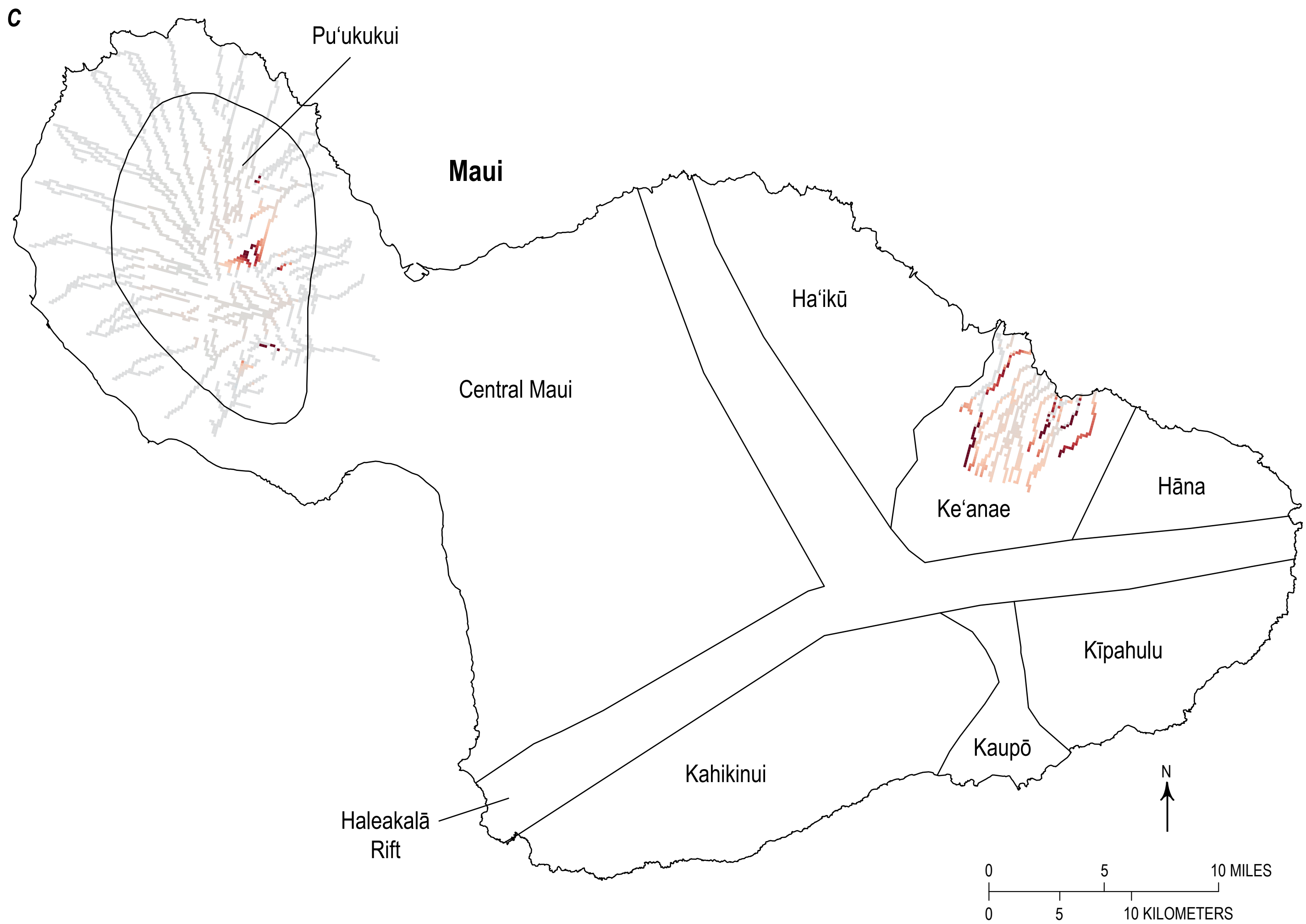

Figure 41. Maps showing differences in groundwater discharge from volcanic aquifers to streams and springs from Assessment II, computed by subtracting results of the Predevelopment scenario from those of the Current scenario simulated using models of the volcanic aquifers of (*A*) Kaua‘i, (*B*) O‘ahu, and (*C*) Maui, Hawai‘i. Differences indicate changes caused by increasing groundwater withdrawal and changing recharge from rates represented by the Predevelopment scenario to those represented by the Current scenario. Gray areas represent 0.0 values.

model-simulated freshwater-saltwater interface in the Schofield sector in Assessment II did not rise (fig. 44*B*) because fresh groundwater extends down the bottom of the O‘ahu model and thinning of the fresh-groundwater body is negligible as a percentage of the total thickness of fresh groundwater (fig. 45*B*).

Sectors that encompass the thickly saturated setting.—Recharge to all sectors that encompass the thickly saturated setting is lower in the Current scenario than it is in the Predevelopment scenario. Current-scenario recharge in the East Kaua‘i sector is 9.9 Mgal/d less than it is in the Predevelopment scenario (table 8, fig. 40*A*). Model simulations for Assessment II indicate that the combined effects of lower recharge and the Current-scenario groundwater withdrawals in this sector are compensated by decreases in groundwater discharge to streams, springs, and the ocean, as well as by induced inflow from the Central Kaua‘i sector. The reduction in groundwater discharge to streams in the East Kaua‘i sector is notably greater in Assessment II than it is in Assessment I (compare figures 37*A* and 40*A*; 31*A* and 41*A*).

Current-scenario recharge in the Ke‘anae sector (on Maui) is 41.9 Mgal/d less than in the Predevelopment scenario (table 8, fig. 40*C*), which is several orders of magnitude greater than the Current-scenario groundwater-withdrawal rate. The lower recharge rate is largely compensated by decreases in groundwater discharge to streams and springs, and in subsurface outflows to adjacent aquifers; these decreases are much greater in Assessment II than they are in Assessment I (compare figures 37*C* and 40*C*).

In the Kaupō sector (on Maui), Current-scenario recharge is 3.5 Mgal/d less than it is in the Predevelopment scenario (table 8, fig. 40*C*), whereas the Current-scenario groundwater-withdrawal rate is less than 0.1 Mgal/d. The lower recharge rate is largely compensated by decreases in subsurface outflows to adjacent aquifers, the sum of which is much greater in Assessment II than it is in Assessment I (compare figures 37*C* and 40*C*).

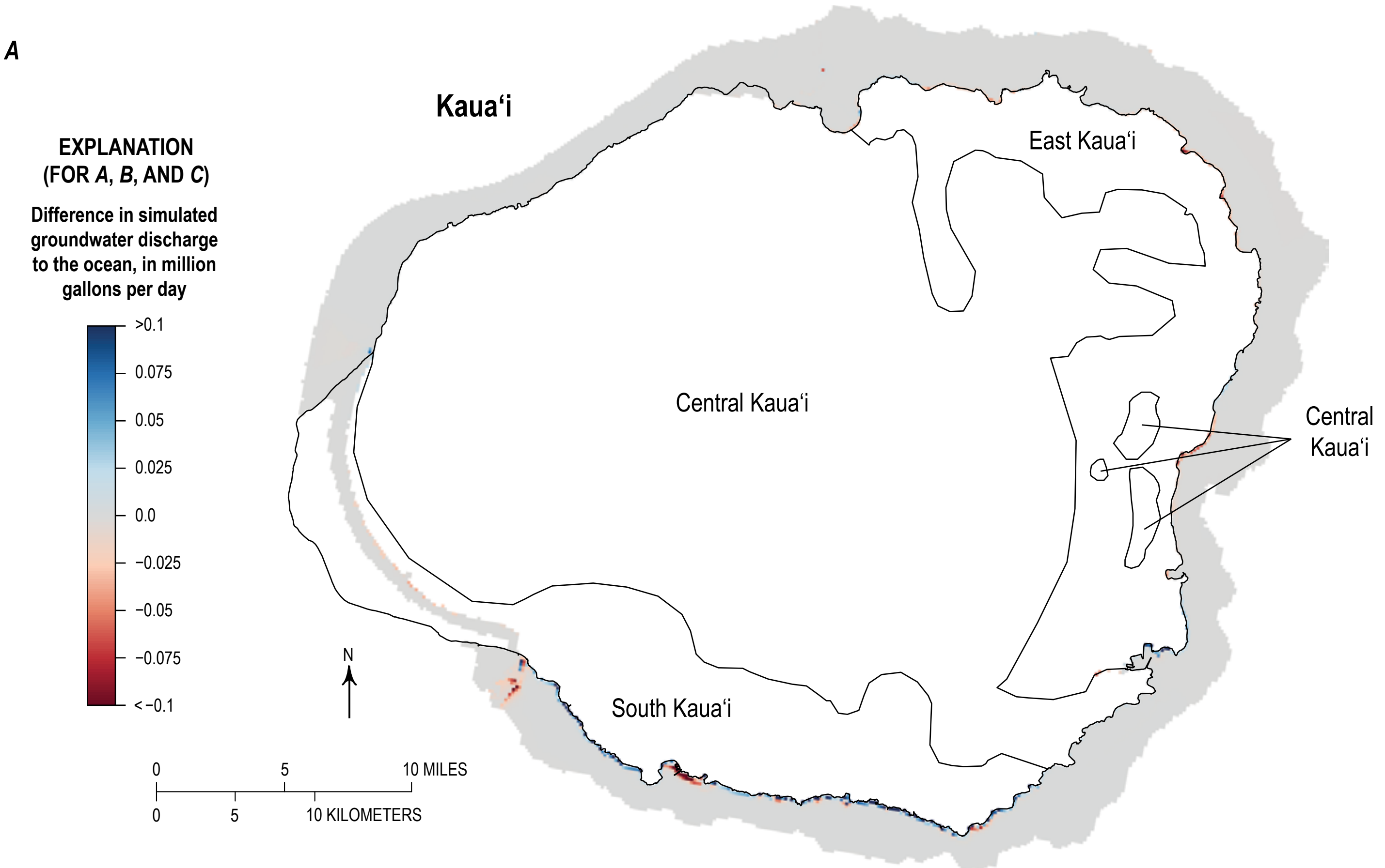
A
Kaua‘i
EXPLANATION
(FOR A, B, AND C)
Difference in simulated groundwater discharge to the ocean, in million gallons per day
>0.1
0.075
0.05
0.025
0.0
−0.025
−0.05
−0.075
< −0.1
East Kaua‘i
Central Kaua‘i
Central Kaua‘i
South Kaua‘i
N
0
5
10 MILES
0
5
10 KILOMETERS

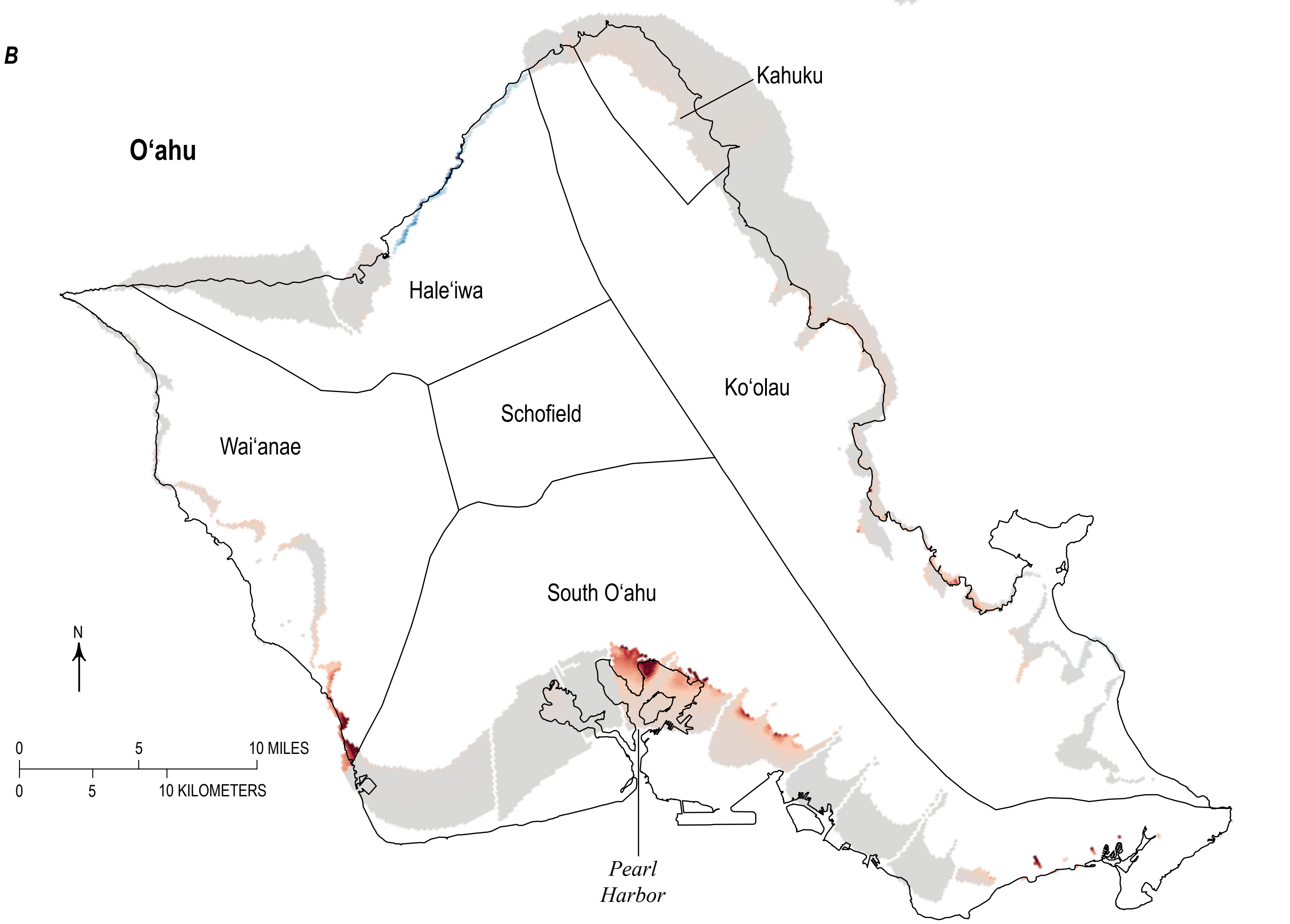
B
O‘ahu
Kahuku
Hale‘iwa
Schofield
Ko‘olau
Wai‘anae
South O‘ahu
N
0
5
10 MILES
0
5
10 KILOMETERS
Pearl Harbor

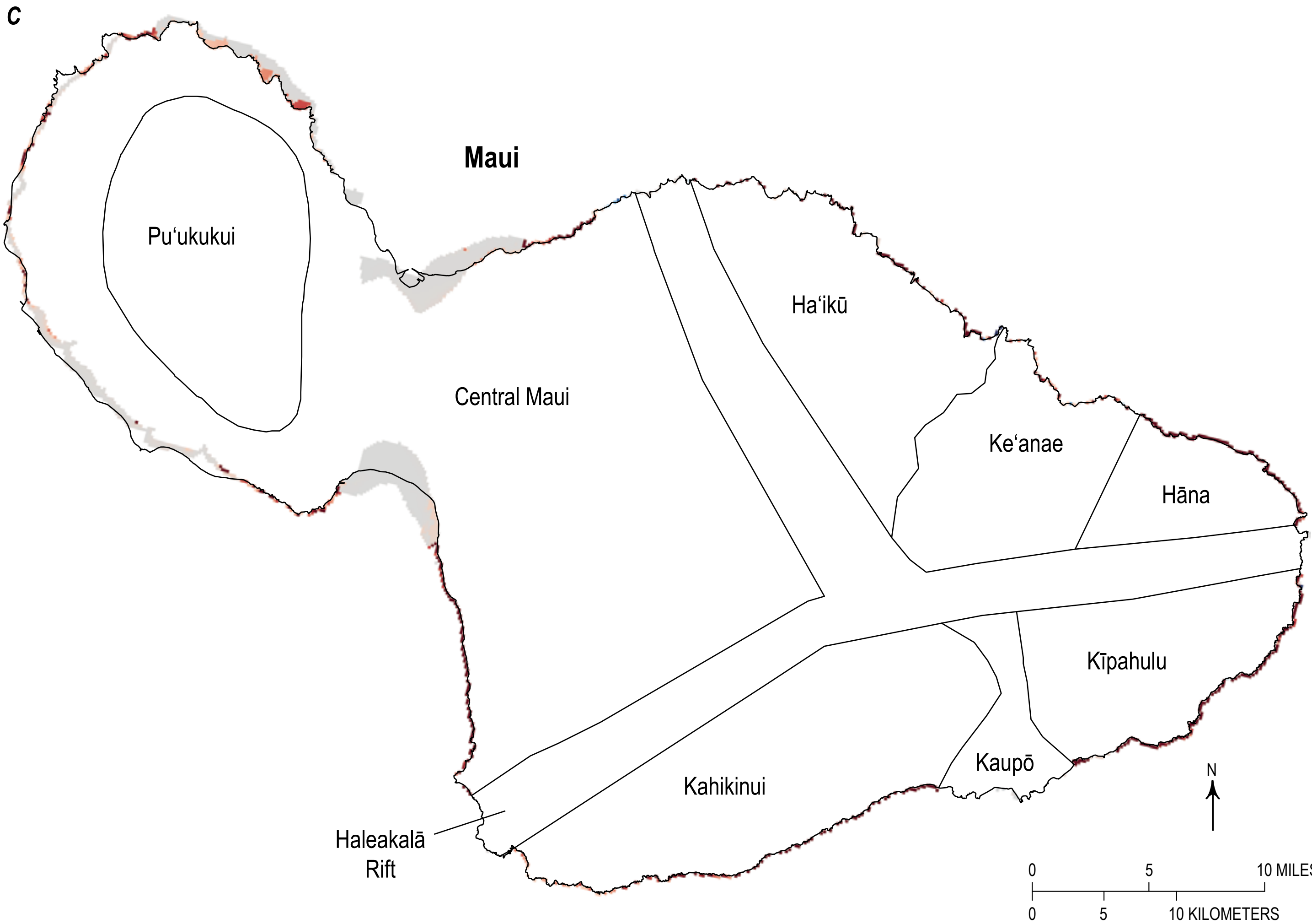

Figure 42. Maps showing differences in groundwater discharge from volcanic aquifers to the ocean from Assessment II, computed by subtracting results of the Predevelopment scenario from those of the Current scenario simulated using models of the volcanic aquifers of (*A*) Kaua‘i, (*B*) O‘ahu, and (*C*) Maui, Hawai‘i. Differences indicate changes caused by increasing groundwater withdrawal and changing recharge from rates represented by the Predevelopment scenario to those represented by the Current scenario. Gray areas represent 0.0 values.

In the thickly saturated setting of the East Kaua‘i sector, changes in water levels, altitude of the freshwater-saltwater interface, and thickness of fresh groundwater in Assessment II (figs. 43*A*, 44*A*, 45*A*) are similar to those in Assessment I—widespread small changes caused by groundwater withdrawals distributed among many small wells. In contrast, water-level declines and rise of the freshwater-saltwater interface in the Ke‘anae sector are greater in Assessment II (figs. 43*C*, 44*C*, 45*C*) than they are in Assessment I (figs. 33*C*, 34*C*, 35*C*). Also, interface rise in the Kaupō sector is greater in Assessment II (fig. 44*C*) than it is in Assessment I (34*C*). These changes in the Ke‘anae and Kaupō sectors can be attributed largely to differences in recharge between the Current and Predevelopment scenarios, which are orders of magnitude greater than differences in withdrawals from these sectors.

Sectors that encompass the freshwater-lens setting.—Among the sectors that encompass the freshwater-lens setting, Current-scenario recharge is greater than Predevelopment-scenario recharge in the Hale‘iwa and Kahuku (on O‘ahu), South Kaua‘i, and Central Maui sectors (table 8, fig. 40). In the Central Maui sector, recharge increases by 51.9 Mgal/d. Comparison of the maps that show recharge differences (fig. 38*C*) and Current-scenario land cover (fig. 6*C*) indicates that the increase is largely the result of irrigation of sugarcane fields. The results of Assessment II indicate that the substantial increase in recharge offsets the effect of groundwater withdrawals in the Central Maui sector—reductions in groundwater discharge to the ocean are less in Assessment II than they are in Assessment I (compare table 6 and 8, figures 37*C* and 40*C*, and figures 32*C* and 42*C*).

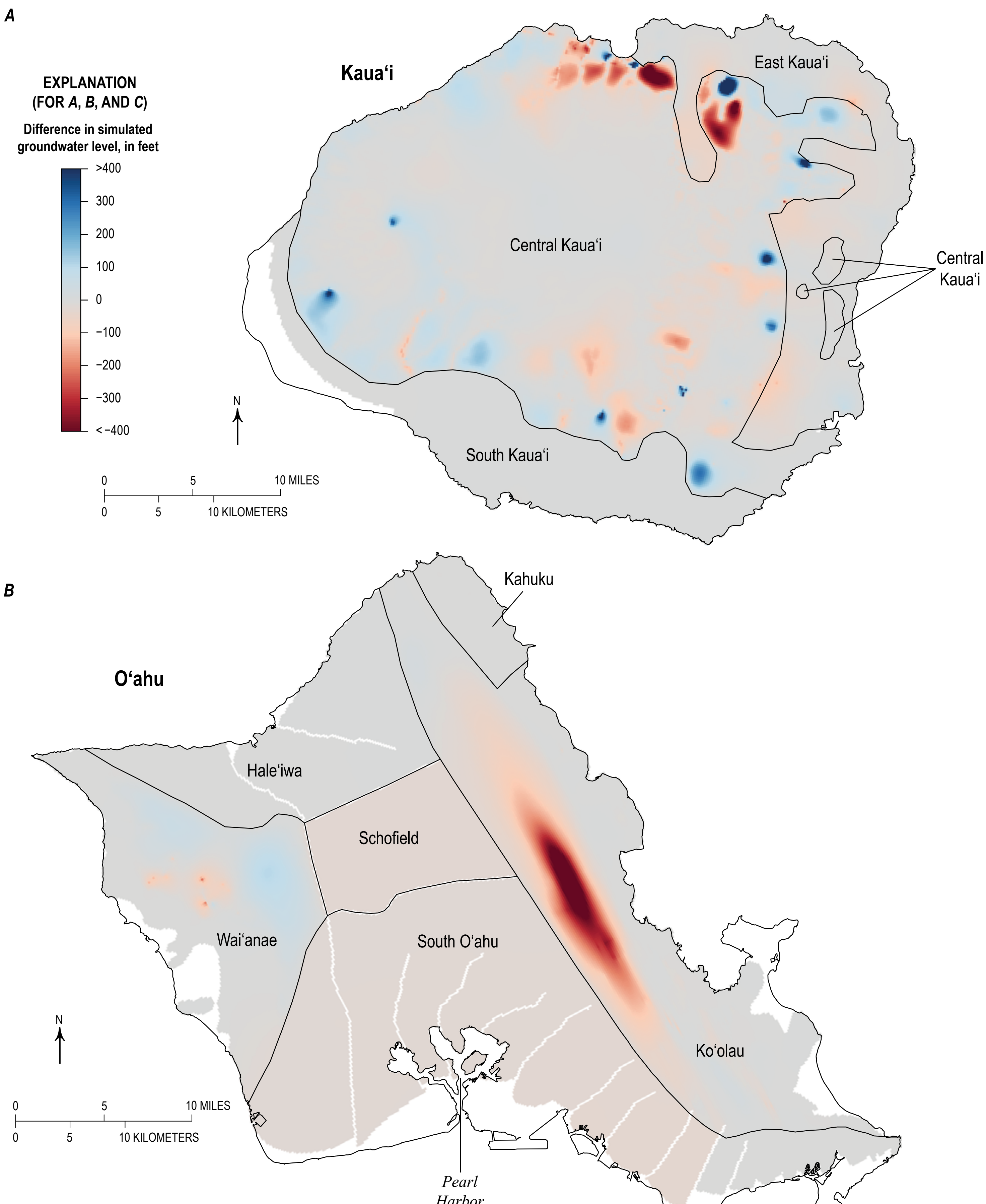
A
Kaua‘i
EXPLANATION
(FOR A, B, AND C)
Difference in simulated groundwater level, in feet
>400
300
200
100
0
−100
−200
−300
< −400
N
0
5
10 MILES
0
5
10 KILOMETERS
East Kaua‘i
Central Kaua‘i
Central Kaua‘i
South Kaua‘i
B
O‘ahu
Kahuku
Hale‘iwa
Schofield
Wai‘anae
South O‘ahu
Ko‘olau
Pearl Harbor
N
0
5
10 MILES
0
5
10 KILOMETERS

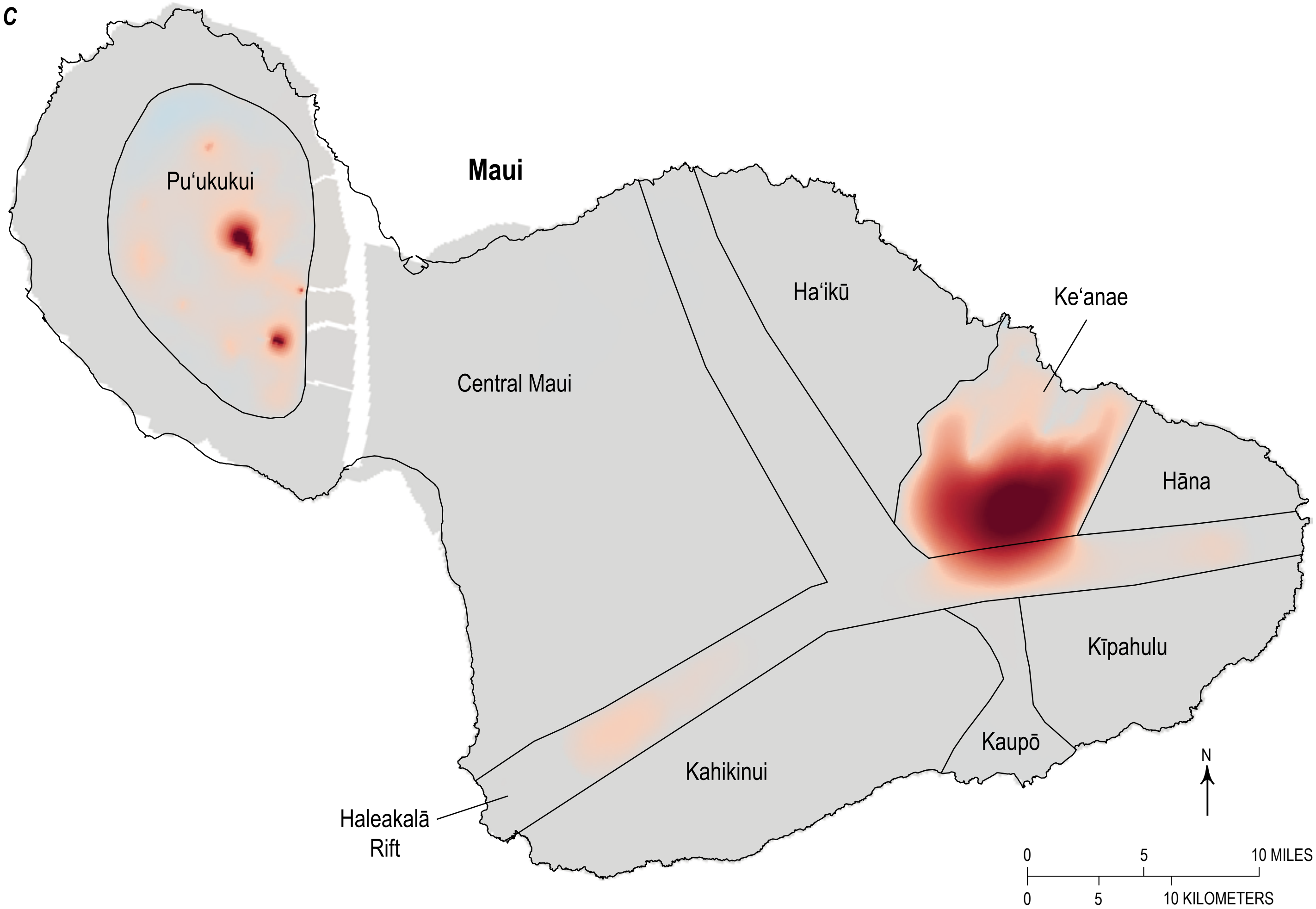

Figure 43. Maps showing differences in groundwater levels from Assessment II, computed by subtracting results of the Predevelopment scenario from those of the Current scenario simulated using models of the volcanic aquifers of (*A*) Kaua‘i, (*B*) O‘ahu, and (*C*) Maui, Hawai‘i. Differences indicate changes caused by increasing groundwater withdrawal and changing recharge from rates represented by the Predevelopment scenario to those represented by the Current scenario. Gray areas represent 0.0 values.

In the South Kaua‘i sector, a substantial increase in recharge (23.2 Mgal/d), combined with an increase in subsurface inflow from the Central Kaua‘i sector that is enhanced by leaks from Current-scenario surface-water reservoirs, partially mitigates the consequences of withdrawals on discharge to the ocean; as a result, reduction of groundwater discharge to the ocean that is indicated in Assessment II (fig. 40*A*) is less than that indicated in Assessment I (fig. 37*A*). Recharge in the Hale‘iwa sector increased by 7.1 Mgal/d, which more than offsets the Current-scenario withdrawal and reduction of inflows from other sectors combined; thus, discharge to the ocean has increased (compare figures 42*B* and 32 *B*). In contrast, recharge in the Kahuku sector increases by only 0.5 Mgal/d, which offsets only a small fraction of the Current-scenario withdrawal from this sector.

Current-scenario recharge is less than Predevelopment-scenario recharge in the freshwater-lens settings of the South O‘ahu, Ha‘ikū (Maui), Hāna (Maui), Kīpahulu (Maui), and Kahikinui (Maui) sectors (table 8, fig. 40). In the South O‘ahu sector, recharge decreases by 10.1 Mgal/d, which is small relative to the large Current-scenario groundwater-withdrawal rate from this sector (fig. 40*B*). Even so, the recharge decrease, combined with the withdrawal from the sector and decreased inflow from the Schofield sector, causes reductions in discharge to streams, springs, and the ocean, as well as in the sum of flows across boundaries with adjacent sectors, and these reductions are greater in Assessment II than they are in Assessment I (compare tables 6 and 8, figures 37*B* and 40*B*). In the Ha‘ikū, Hāna, Kīpahulu, and Kahikinui sectors on Maui, decreases in recharge (44.7, 20.6, 27.0, and 14.2 Mgal/d, respectively) are much larger than Current-scenario withdrawals (table 8, fig. 40*C*). Inflows to these sectors from adjacent sectors are also substantially reduced. Reductions in groundwater discharge to the ocean that result from the combination of recharge reductions

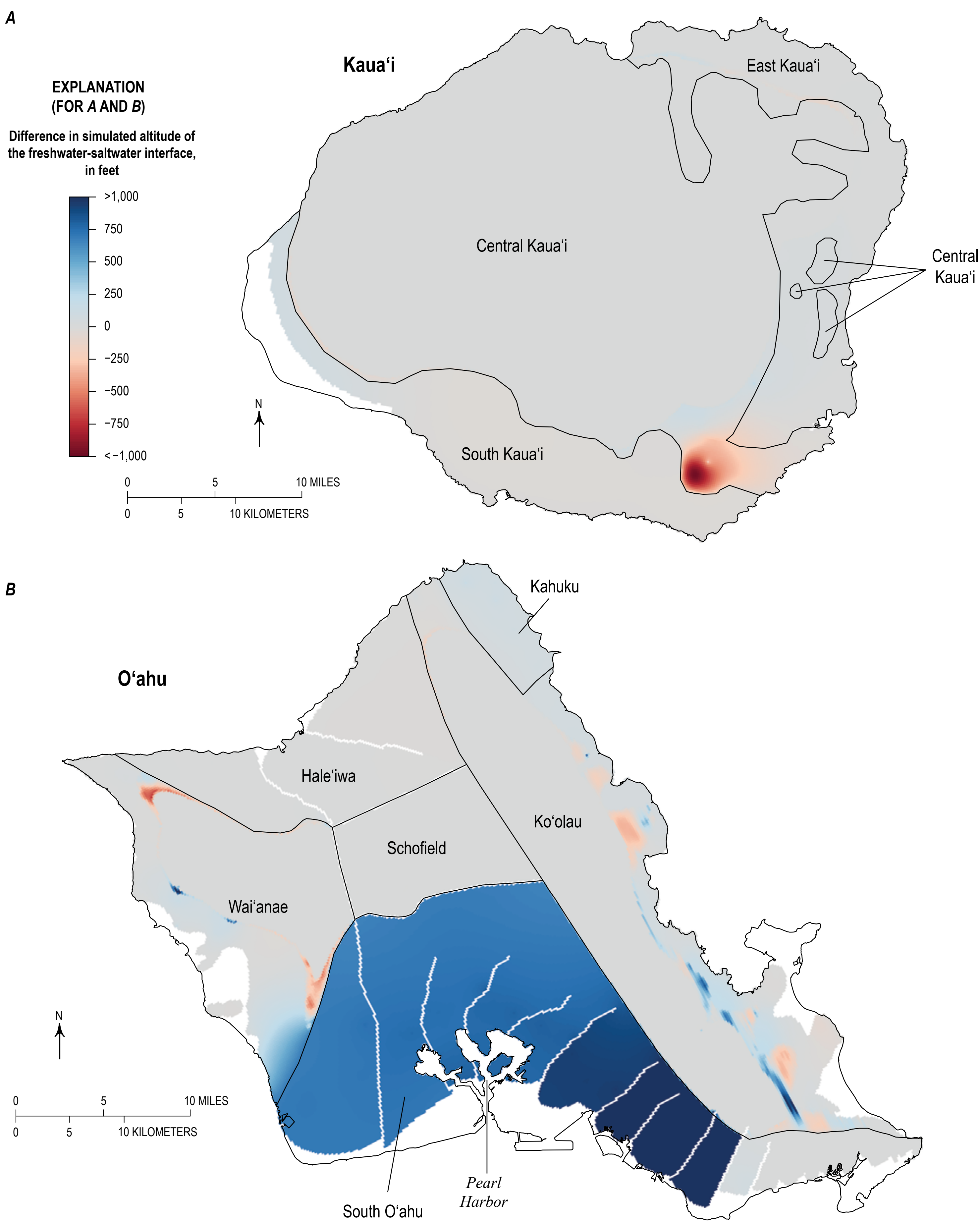
A
Kaua‘i
EXPLANATION
(FOR A AND B)
Difference in simulated altitude of the freshwater-saltwater interface, in feet
>1,000
750
500
250
0
−250
−500
−750
< −1,000
East Kaua‘i
Central Kaua‘i
Central Kaua‘i
South Kaua‘i
N
0 5 10 MILES
0 5 10 KILOMETERS
B
O‘ahu
Kahuku
Hale‘iwa
Ko‘olau
Schofield
Wai‘anae
South O‘ahu
Pearl Harbor
N
0 5 10 MILES
0 5 10 KILOMETERS

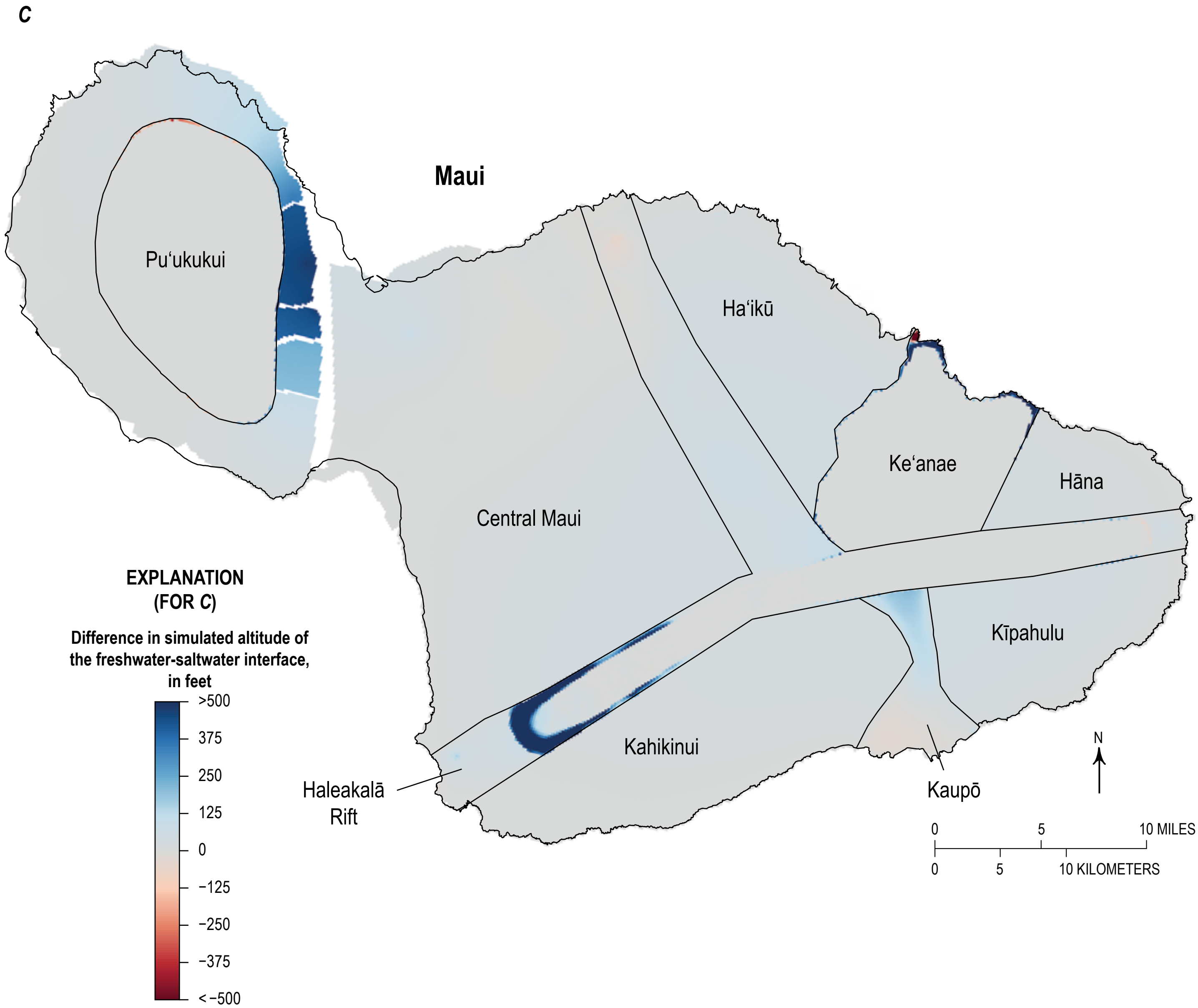

Figure 44. Maps showing differences in altitude of the freshwater-saltwater interface from Assessment II, computed by subtracting results of the Predevelopment scenario from those of the Current scenario simulated using models of the volcanic aquifers of (*A*) Kaua‘i, (*B*) O‘ahu, and (*C*) Maui, Hawai‘i. Differences indicate changes caused by increasing groundwater withdrawal and changing recharge from rates represented by the Predevelopment scenario to those represented by the Current scenario. Gray areas represent 0.0 values.

and withdrawals (indicated by Assessment II) (table 8, fig. 40*C*) are far greater than those of withdrawals alone (indicated by Assessment I) (table 6 and fig. 37*C*).

Model simulations for Assessment II indicate that the combination of differences in recharge and Current-scenario groundwater withdrawals causes changes in simulated water levels, altitude of the freshwater-saltwater interface, and freshwater thickness. In the high-permeability aquifers characteristic of freshwater-lens settings, water-level changes are generally lower in magnitude, less focused, and less easily discerned compared to the higher magnitude, focused changes in sectors encompass dike-impounded-groundwater and thickly saturated settings (fig. 43), but changes in interface altitude (fig. 44) and freshwater thickness (fig. 45) are more readily apparent and can be more easily related to changes in withdrawal and recharge simulated in Assessment II. In the South O‘ahu sector, substantial interface rise (fig. 44*B*) and decreased freshwater thickness (fig. 45*B*) result from the high Current-scenario withdrawal and decreased recharge in this sector (fig. 40*B*). The decreased recharge exacerbates the effects of withdrawal; as a result, interface rise and freshwater

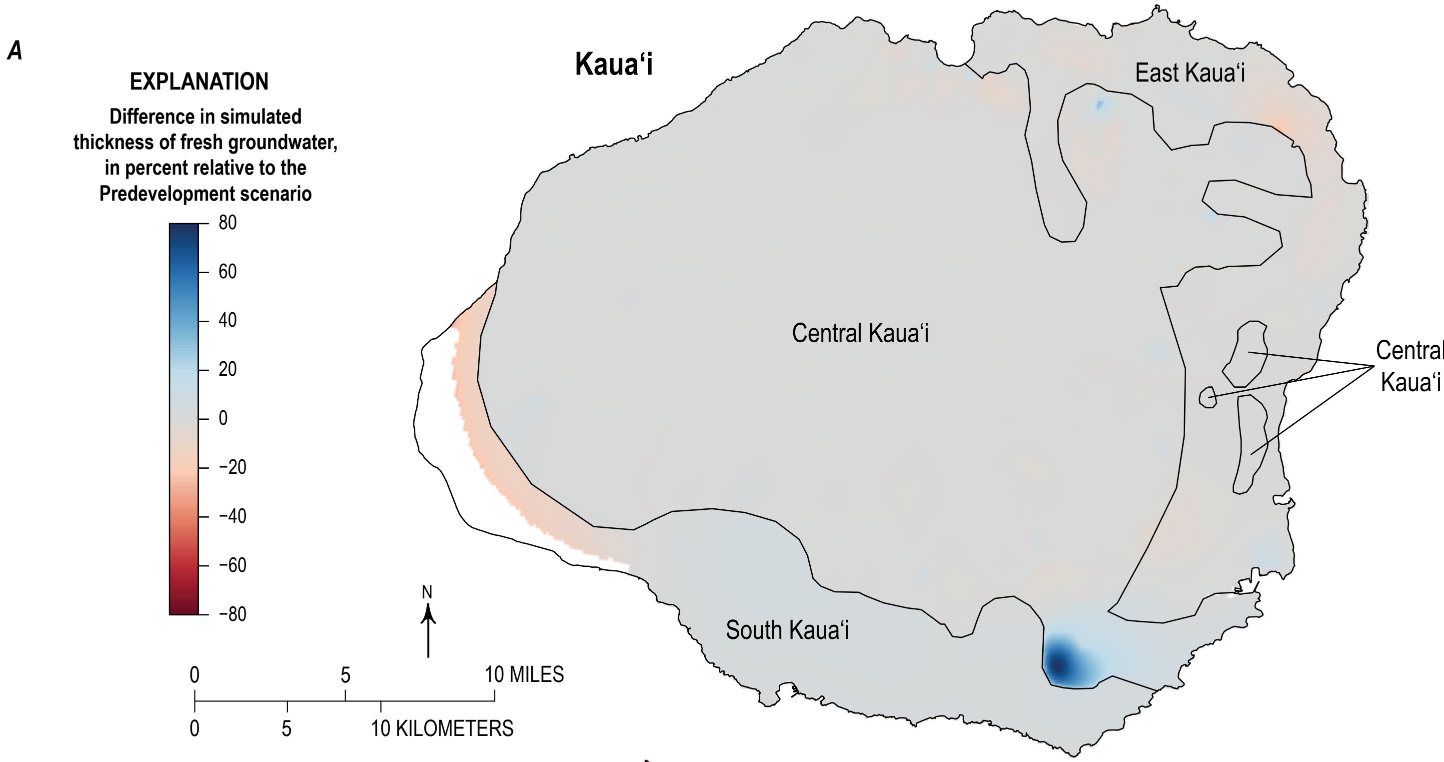
A
EXPLANATION
Difference in simulated thickness of fresh groundwater, in percent relative to the Predevelopment scenario
80
60
40
20
0
−20
−40
−60
−80
Kauaʻi
East Kauaʻi
Central Kauaʻi
Central Kauaʻi
South Kauaʻi
N
0 5 10 MILES
0 5 10 KILOMETERS

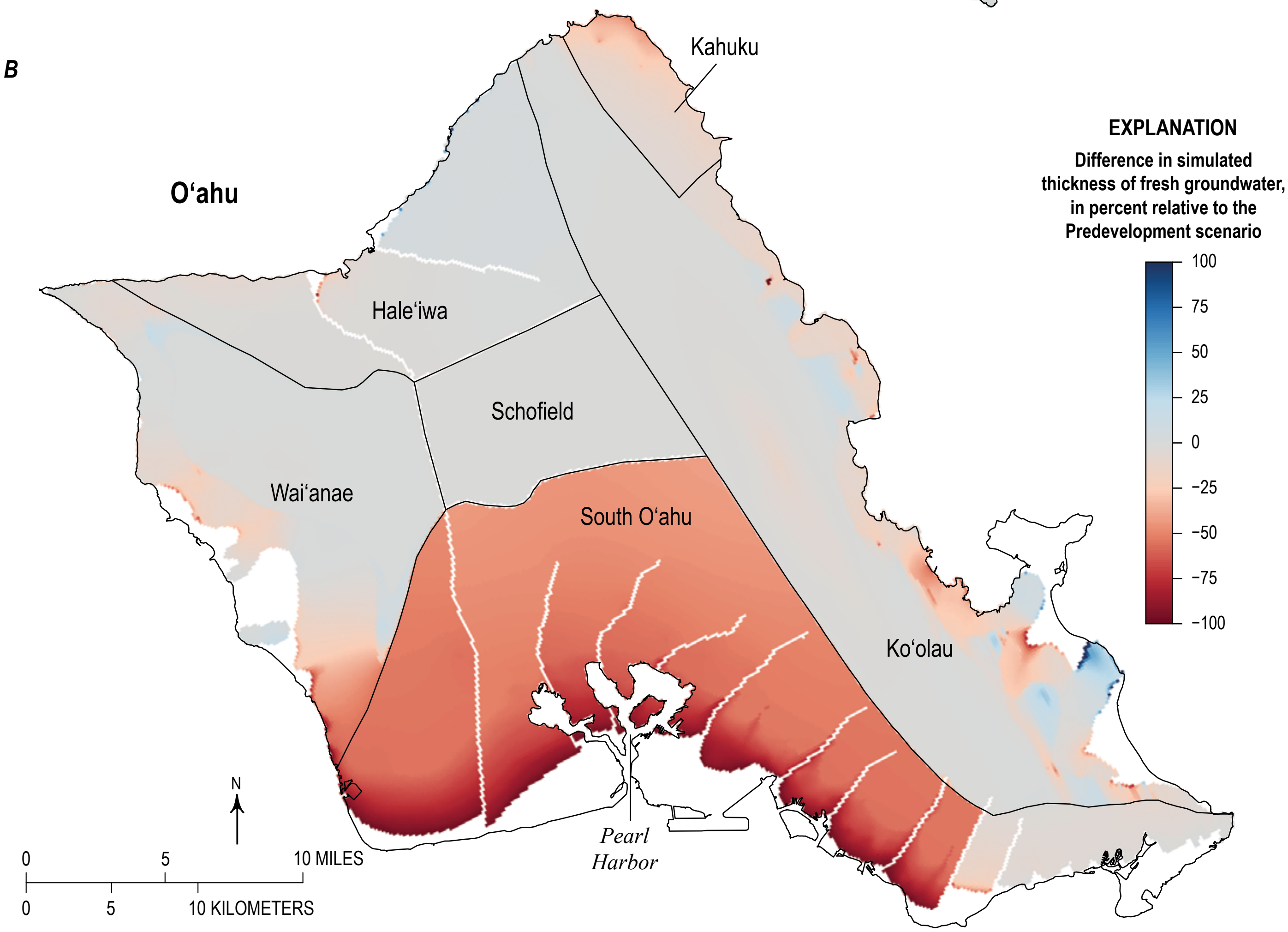
B
Oʻahu
Kahuku
Haleʻiwa
Schofield
Waiʻanae
South Oʻahu
Koʻolau
Pearl Harbor
EXPLANATION
Difference in simulated thickness of fresh groundwater, in percent relative to the Predevelopment scenario
100
75
50
25
0
−25
−50
−75
−100
N
0 5 10 MILES
0 5 10 KILOMETERS

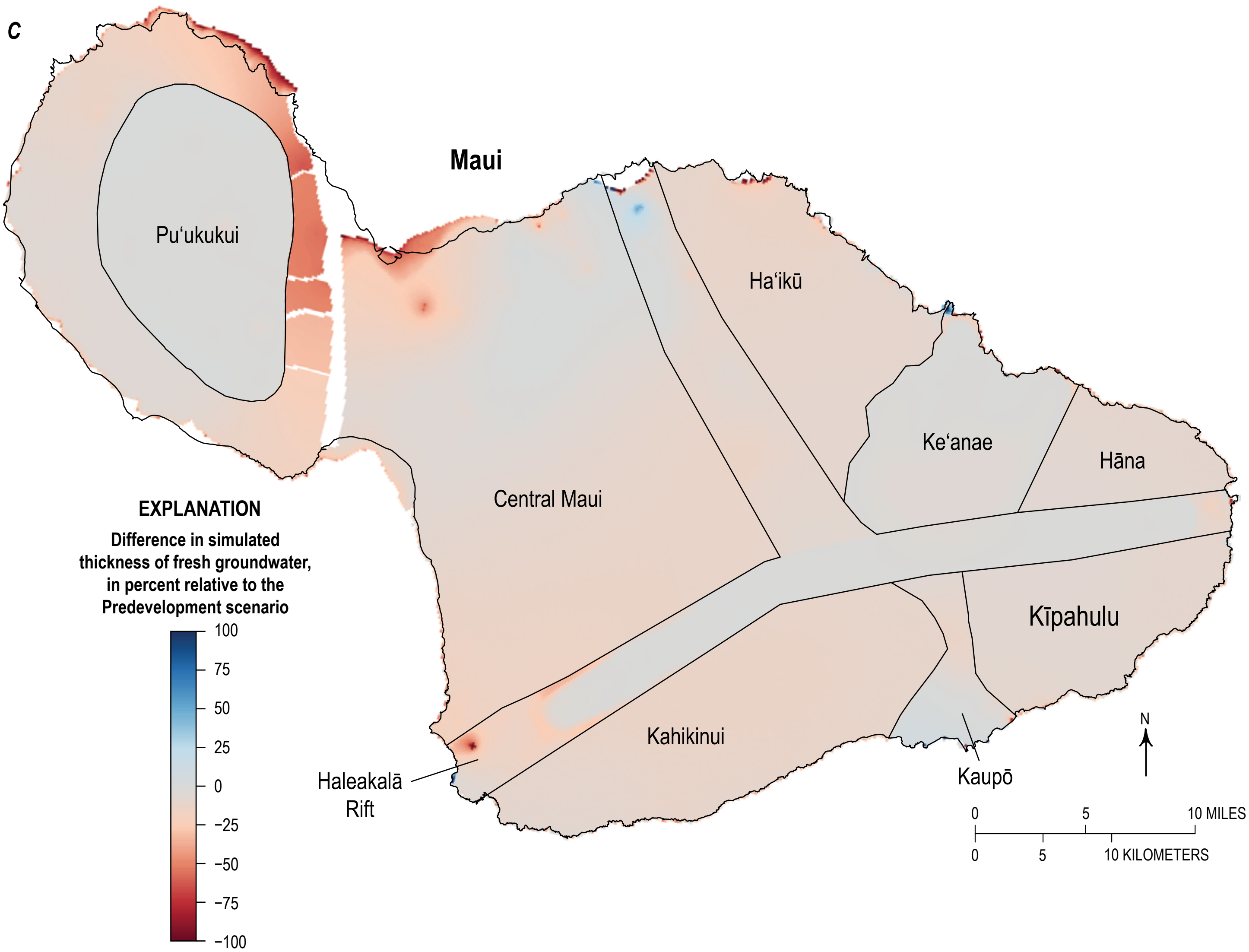

Figure 45. Maps showing percentage differences in thickness of fresh groundwater from Assessment II, computed by subtracting results of the Predevelopment scenario from those of the Current scenario simulated using models of the volcanic aquifers of (*A*) Kaua‘i, (*B*) O‘ahu, and (*C*) Maui, Hawai‘i. Differences indicate changes caused by increasing groundwater withdrawal and changing recharge from rates represented by the Predevelopment scenario to those represented by the Current scenario. Gray areas represent 0.0 values.

thinning are greater in Assessment II than they are in Assessment I (compare figures 34*B* and 44*B*; 35*B* and 45*B*). In the Kahuku sector, interface rise and decreased freshwater thickness result from withdrawals, despite a small increase in recharge to this sector. Interface rise and decreases in freshwater thickness are also indicated in the Ha‘ikū, Hāna, Kīpahulu, and Kahikinui sectors on Maui, and because these changes result almost entirely from decreases in recharge, they are apparent in Assessment II but not in Assessment I (compare figures 34*C* and 44*C*; 35*C* and 45*C*). In the Hale‘iwa sector on O‘ahu, fresh-groundwater thickness is slightly greater in Assessment II than it is in Assessment I because Current-scenario recharge is higher than Predevelopment-scenario recharge (compare figures 35*B* and 45*B*).

Results for the Central Maui and South Kaua‘i sectors illustrate how the location of changes in recharge and groundwater withdrawals within a sector affect changes in the altitude of the freshwater-saltwater interface and freshwater thickness. Interface rise and decreased freshwater thickness are indicated in much of the Central Maui sector, but downward shift of the interface and increased freshwater thickness are indicated in areas where recharge increased (figs. 38*C*, 44*C*, 45*C*). Similarly, downward shift of the interface and an increase in freshwater thickness are indicated in the eastern part of the South Kaua‘i sector where recharge increases in Assessment II offset the effects of withdrawals (figs. 38*A*, 44*A*, 45*A*).

Effects of Future Changes in Groundwater Withdrawal and Rainfall

Because Hawai‘i relies on groundwater for nearly all of its drinking water, withdrawals from Hawai‘i's volcanic aquifers are anticipated to increase as the population increases (State of Hawai‘i, 2019). Consequences of future increases in groundwater withdrawal will be superimposed on changes in recharge that result from future rainfall changes.

In this study, assessments of how future increases in groundwater withdrawals and changes in rainfall may affect the availability of groundwater were made using simulations with the O‘ahu numerical model. Two future scenarios—Increased Withdrawal and Future Rainfall (table 2)—were simulated and their results were compared to those of the Current scenario to assess the effects of (1) increased withdrawals independent from effects of future climate change and (2) projected rainfall amounts that are based on future climate-change projections independent from effects of increased withdrawals (table 3).

Assessment III—Effects of Increased Withdrawals

The objective of Assessment III is to study the potential effects of increasing groundwater withdrawals on O‘ahu above the rates in the Current scenario (table 3). For this assessment, a hypothetical Increased Withdrawal scenario (table 2) was created that is based on rates specified in water-use permits issued by the State of Hawai‘i Commission on Water Resource Management (CWRM) (Lenore Ohye, CWRM, written commun., July 2019). The Increased Withdrawal scenario uses the same recharge distribution used in the Current scenario; therefore, differences between the steady-state results of the two scenarios indicate the effect of increasing withdrawals independent of potential effects from changing recharge.

Increased Withdrawal Scenario

For most wells on O‘ahu, the rates for groundwater withdrawal in permits from CWRM are equal to or higher than the withdrawal rates simulated in the Current scenario (which reflect actual withdrawals; Izuka and others, 2021). For a few wells, however, the permit withdrawal rate is lower than the Current-scenario rate. Also, not all wells on O‘ahu have permit rates in the CWRM data—for example, well permits were not issued for some pumped wells that are outside of areas that CWRM has designated to be “groundwater management” areas (State of Hawai‘i, 2019). Whereas the purpose of Assessment III is to assess the effect of increased withdrawals, withdrawal rates for wells in the Increased Withdrawal scenario are the higher of the permit or the Current-scenario rate.

The permits from CWRM included both single-well permits and multiple-well permits. For single-well permits, the groundwater-withdrawal rate for the Increased Withdrawal scenario is set to the higher of either the permit rate or the Current-scenario rate. For multiple-well permits in which a single permit rate is issued for a group of wells, the permit rate is divided by the number of wells on the permit to determine an average permit rate. If the average permit rate is higher than the Current-scenario rates for all wells covered by the permit, then the average permit rate is used in the Increased Withdrawal scenario. If the Current-scenario rate at one or more wells covered by the permit is higher than the average rate, then the Current-scenario rates are assigned to those wells, and the remainder of the permit rate is distributed equally among the other wells covered by the permit.

Groundwater withdrawals for tunnels simulated as drains are not increased in the Increased Withdrawal scenario because water flow from tunnels is a function of the hydraulic properties of the aquifer and the difference between the head in the aquifer and the altitude of the tunnel (Izuka and others, 2021). Increasing withdrawal from conventional wells can lower the head in the aquifer and cause reductions in tunnel yield; thus, reduction of tunnel yield is one of the possible consequences of increasing the withdrawal rate from conventional wells. In the Increased Withdrawal scenario, tunnel flow was allowed to decrease in response to increasing the withdrawal rate from conventional wells. In Assessment III, decreases in tunnel flow were considered a consequence of increasing withdrawals.

Results

Simulated total groundwater-withdrawal rate from wells on O‘ahu for the Increased Withdrawal scenario is 288.0 Mgal/d, which is 99.9 Mgal/d greater than the total withdrawal rate from wells in the Current scenario (table 9). This difference constitutes an islandwide increase in well withdrawals of 53 percent relative to the Current-scenario rate. The model simulations for Assessment III indicate that the increase will result in substantial declines in groundwater discharge to streams, springs, and the ocean on O‘ahu (fig. 46).

The largest simulated increases in groundwater-withdrawal rates from wells are in the South O‘ahu (51.7 Mgal/d), Schofield (18.0 Mgal/d), and Hale‘iwa (17.8 Mgal/d) sectors (table 10, figs. 47, 48). Relative to the Current-scenario rates (table 6), the largest percentage increases are in the Hale‘iwa (481 percent) and Schofield (200 percent) sectors. In the analysis for Assessment III, subtraction of the simulated results of the Current scenario from those of the Increased Withdrawal scenario results in reductions in groundwater discharge to

Table 9. Comparison of islandwide groundwater budgets for the Increased Withdrawal and Current scenarios (Assessment III) simulated using the numerical groundwater model of the volcanic aquifers of O‘ahu, Hawai‘i.

[Difference between scenarios represents Increased Withdrawal minus Current scenarios; differences between scenarios may not be equal to differences between values in columns, owing to rounding. Mgal/d, million gallons per day]

Scenario	Recharge (Mgal/d)	Withdrawal (Mgal/d)			Groundwater discharge (Mgal/d)	
		Wells	Tunnels	Total	To streams and springs	To ocean
Current	597.6	188.0	33.2	221.2	127.7	248.6
Increased Withdrawal	597.6	288.0	33.0	321.0	88.6	188.3
Difference between scenarios	0.0	99.9	−0.3	99.8	−39.1	−60.3

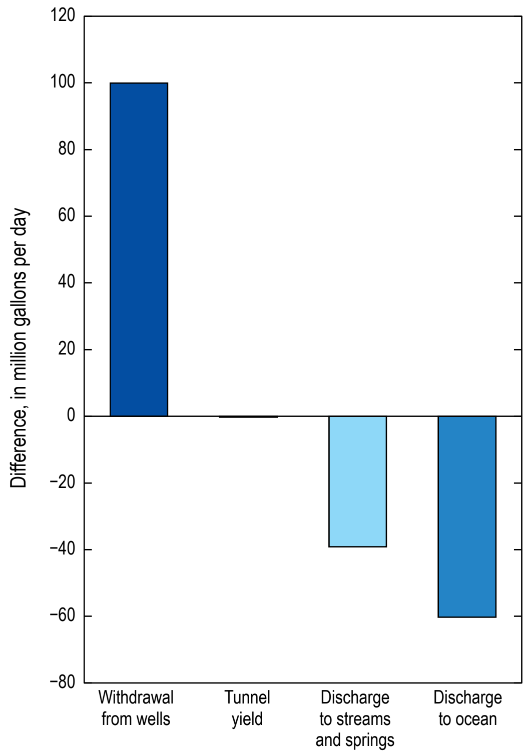

Figure 46. Bar graph showing differences in islandwide groundwater budgets from Assessment III, computed by subtracting results of the Current scenario from those of the Increased Withdrawal scenario simulated using model of the volcanic aquifers of O‘ahu, Hawai‘i. Differences indicate changes caused by increasing groundwater withdrawal from rates represented by the Current scenario to those represented by the Increased Withdrawal scenario.

Table 10. Differences in sector groundwater budgets from Assessment III (Increased Withdrawal scenario minus Current scenario), determined from simulations using the numerical groundwater model of the volcanic aquifers of O‘ahu, Hawai‘i.

[Totals may not be equal to sum of values in columns, owing to rounding. Mgal/d, million gallons per day]

Sector	Principal groundwater setting	Differences (Mgal/d)					
		Recharge	Withdrawal from wells	Tunnel yield	Discharge to streams and springs	Discharge to ocean	Subsurface flow to or from other sectors[1]
South O‘ahu	Freshwater lens	0.0	51.7	0.0	−36.5	−22.9	7.7
Hale‘iwa	Freshwater lens	0.0	17.8	0.0	0.0	−23.9	6.0
Kahuku	Freshwater lens	0.0	4.0	0.0	0.0	−3.9	−0.1
Ko‘olau	Dike-impounded groundwater	0.0	8.1	−0.2	−2.6	−5.3	−0.1
Wai‘anae	Dike-impounded groundwater	0.0	0.3	−0.1	−0.1	−4.3	4.1
Schofield	Enigmatic[2]	0.0	18.0	0.0	0.0	0.0	−17.7
	Total	0.0	99.9	−0.3	−39.1	−60.3	0.0

[1]Positive values indicate increased outflow or decreased inflow; negative values indicate decreased outflow or increased inflow.

[2]Enigmatic groundwater occurrences do not fit into one of the four principal groundwater settings discussed in this report, and their relation to the geologic framework of volcanic aquifers is not fully understood (see Izuka and others, 2018, 2021).

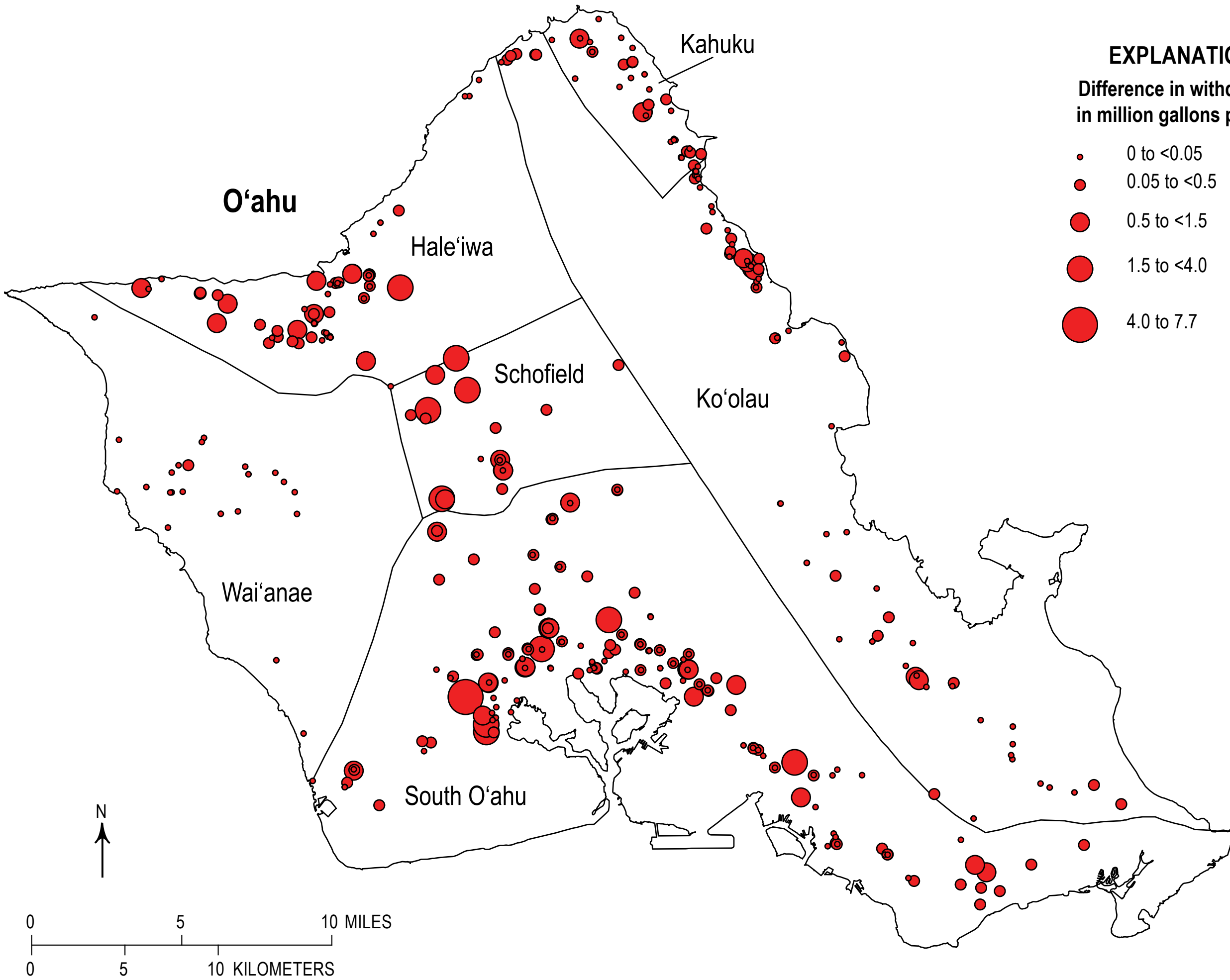

Figure 47. Map showing differences in groundwater-withdrawal rates from Assessment III, computed by subtracting rates of the Current scenario from those of the Increased Withdrawal scenario simulated using model of the volcanic aquifers of O‘ahu, Hawai‘i.

streams and springs (figs. 46, 48, 49), reductions in groundwater discharge to the ocean (figs. 46, 48, 50), declines in groundwater levels (fig. 51), upward movement of the freshwater-saltwater interface (fig. 52), and reductions in the thickness of fresh groundwater (fig. 53).

Sectors that encompass dike-impounded-groundwater settings.—In the results of Assessment III, groundwater-withdrawal rates from wells in the dike-impounded-groundwater settings of the Ko‘olau and Wai‘anae sectors increase by 8.1 and 0.3 Mgal/d, respectively (table 10, fig. 48). Subsurface outflow from the Ko‘olau sector to the Kahuku and Schofield sectors increases, but subsurface outflow to the South O‘ahu and Hale‘iwa sectors decreases by nearly the same amount. Most of the increased groundwater withdrawal from wells in the Ko‘olau sector is compensated by reduced groundwater discharge to streams, springs, and the ocean, but a small fraction is compensated by decreased tunnel yield.

Increase in the rate of groundwater withdrawal from wells in the Wai‘anae sector is small, but the subsurface outflow rate from the sector increases by 4.1 Mgal/d as a result of increased withdrawals from adjacent sectors (table 10, fig. 48). The combination of increased outflow and increased well withdrawal from the Wai‘anae sector is largely compensated by decreased discharge to the ocean, but a small fraction is compensated by reduced groundwater discharge to streams and springs, and another small fraction is compensated by reduced tunnel yield.

Increases in groundwater withdrawal in the Ko‘olau and Wai‘anae sectors cause focused water-level declines (figs. 47, 51). Water-level declines that result from withdrawals from the Schofield sector also spread into the Wai‘anae sector. Localized rise of the freshwater-saltwater interface is evident in areas seaward of the water-level declines (fig. 52), but interface altitudes remain unchanged in most areas of the dike-impounded-groundwater settings because fresh water extends down to the bottom of the model. Water-level decline and interface rise result in a reduction in fresh-groundwater thickness in parts of sectors that encompass dike-impounded-groundwater settings (fig. 53).

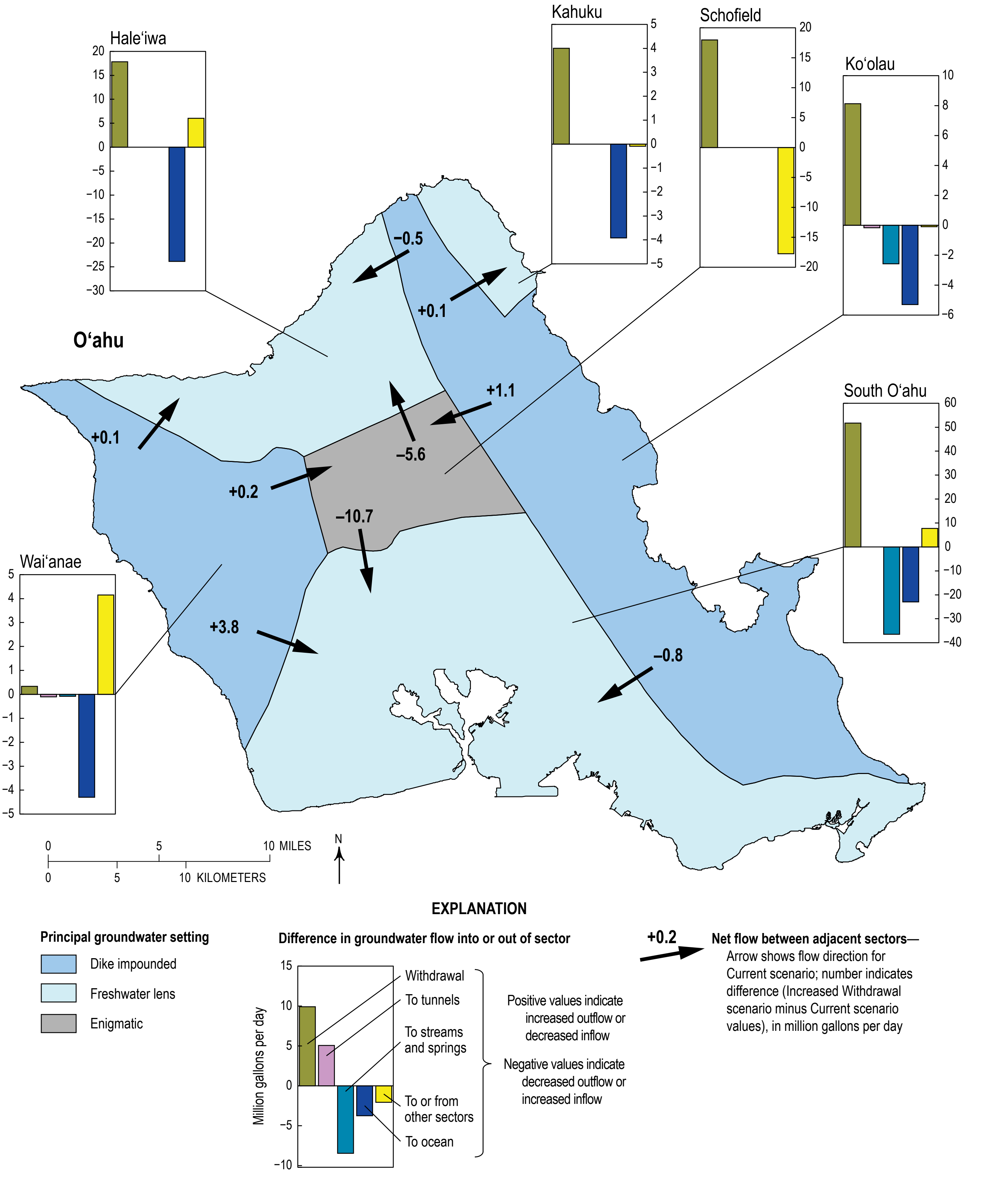

Figure 48. Map and bar graphs showing differences in sector groundwater budgets from Assessment III, computed by subtracting results of the Current scenario from those of the Increased Withdrawal scenario simulated using model of the volcanic aquifers of O‘ahu, Hawai‘i. Differences indicate changes caused by increasing groundwater withdrawal from rates represented by the Current scenario to those represented by the Increased Withdrawal scenario. Note that vertical axes of bar graphs are at different scales to show wide range of values. Values that indicate flow between sectors may not agree exactly with totals shown in table 10, owing to rounding.

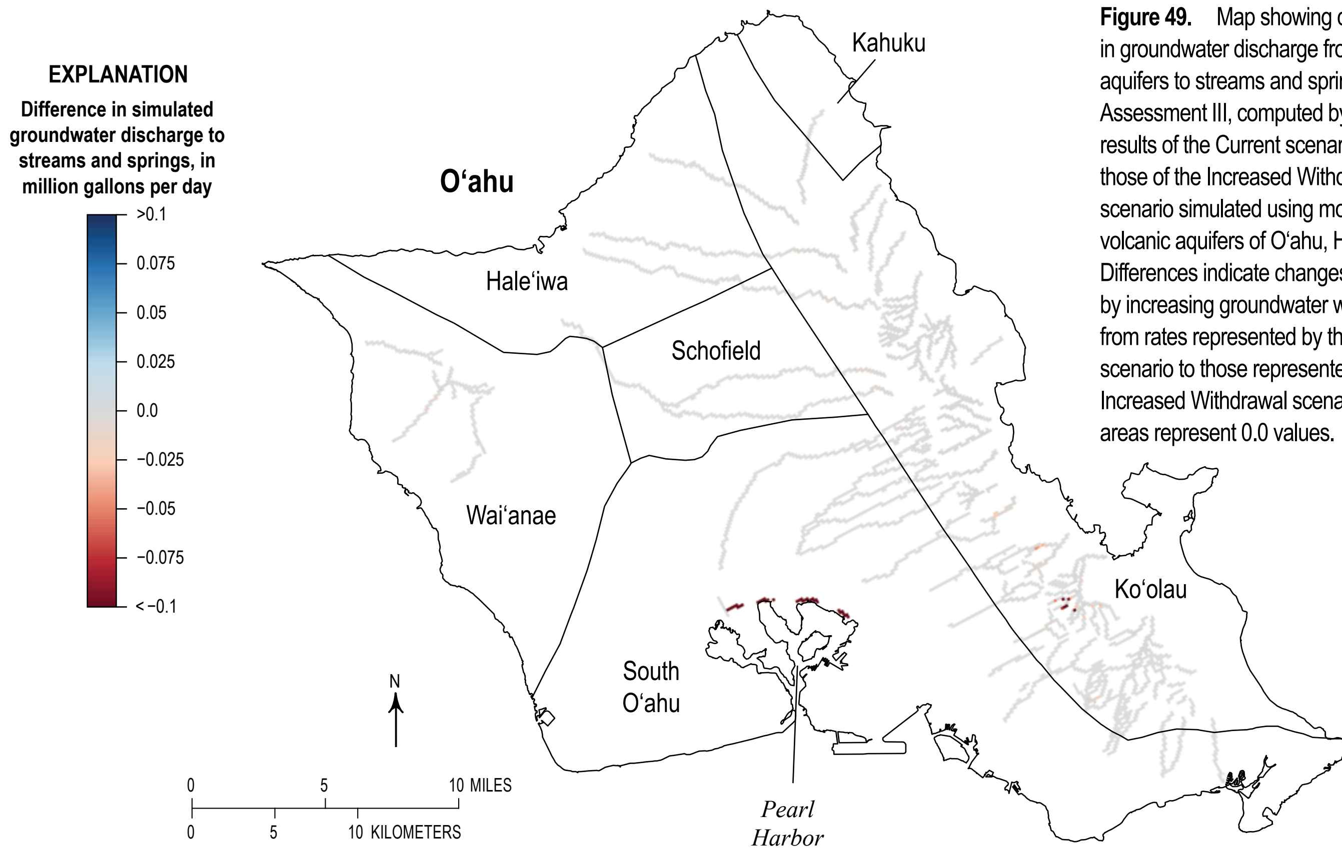

Figure 49. Map showing differences in groundwater discharge from volcanic aquifers to streams and springs from Assessment III, computed by subtracting results of the Current scenario from those of the Increased Withdrawal scenario simulated using model of the volcanic aquifers of Oʻahu, Hawaiʻi. Differences indicate changes caused by increasing groundwater withdrawal from rates represented by the Current scenario to those represented by the Increased Withdrawal scenario. Gray areas represent 0.0 values.

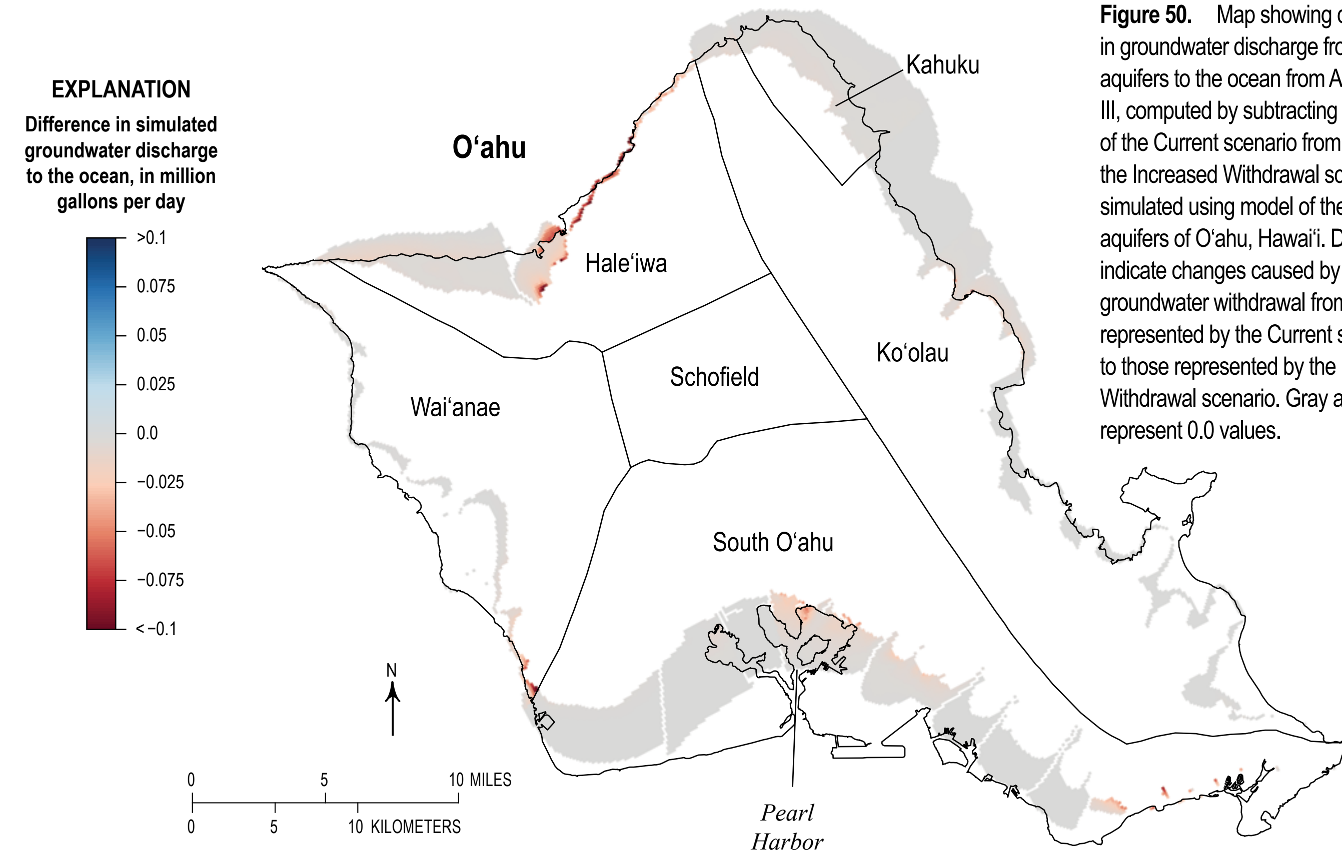

Figure 50. Map showing differences in groundwater discharge from volcanic aquifers to the ocean from Assessment III, computed by subtracting results of the Current scenario from those of the Increased Withdrawal scenario simulated using model of the volcanic aquifers of Oʻahu, Hawaiʻi. Differences indicate changes caused by increasing groundwater withdrawal from rates represented by the Current scenario to those represented by the Increased Withdrawal scenario. Gray areas represent 0.0 values.

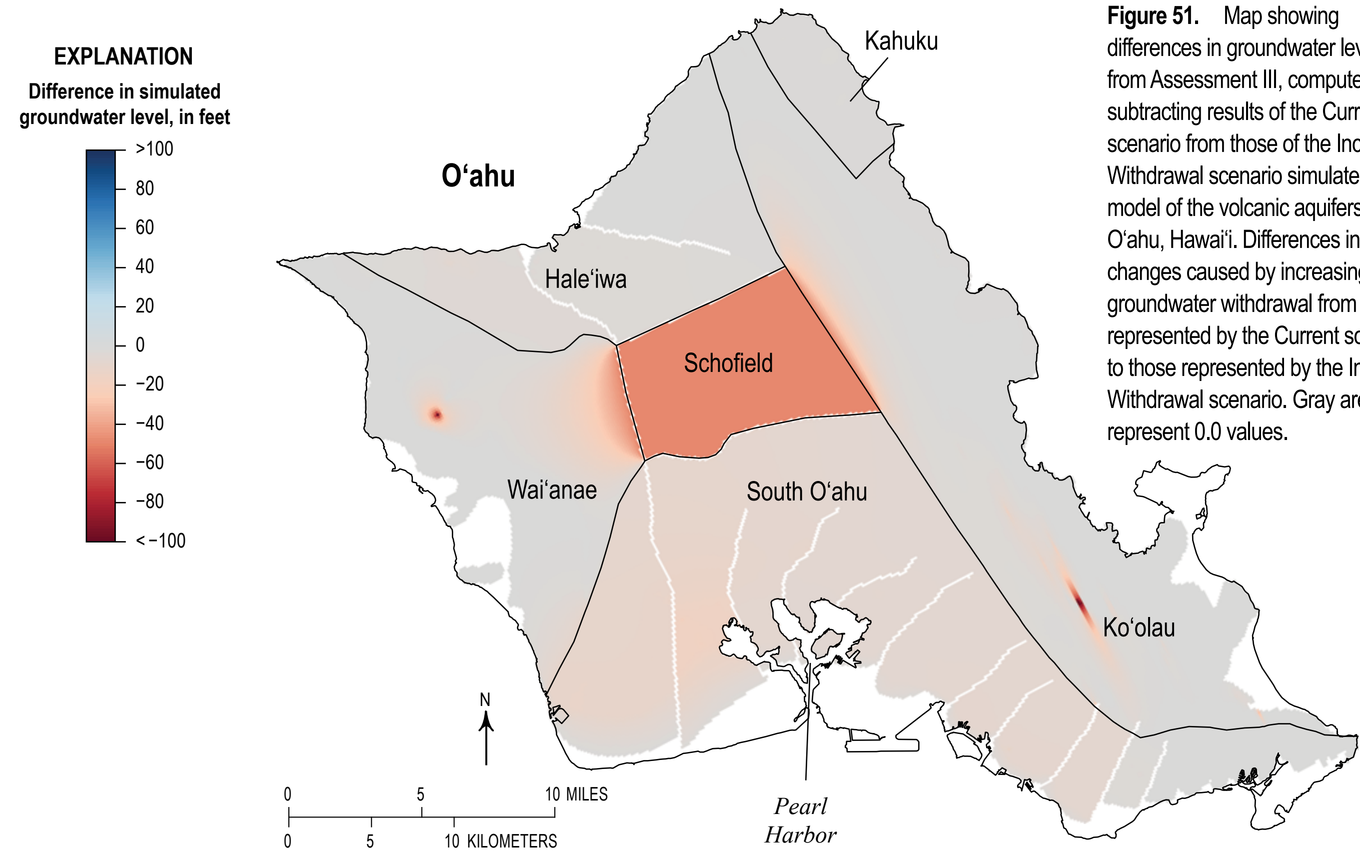

Figure 51. Map showing differences in groundwater levels from Assessment III, computed by subtracting results of the Current scenario from those of the Increased Withdrawal scenario simulated using model of the volcanic aquifers of O‘ahu, Hawai‘i. Differences indicate changes caused by increasing groundwater withdrawal from rates represented by the Current scenario to those represented by the Increased Withdrawal scenario. Gray areas represent 0.0 values.

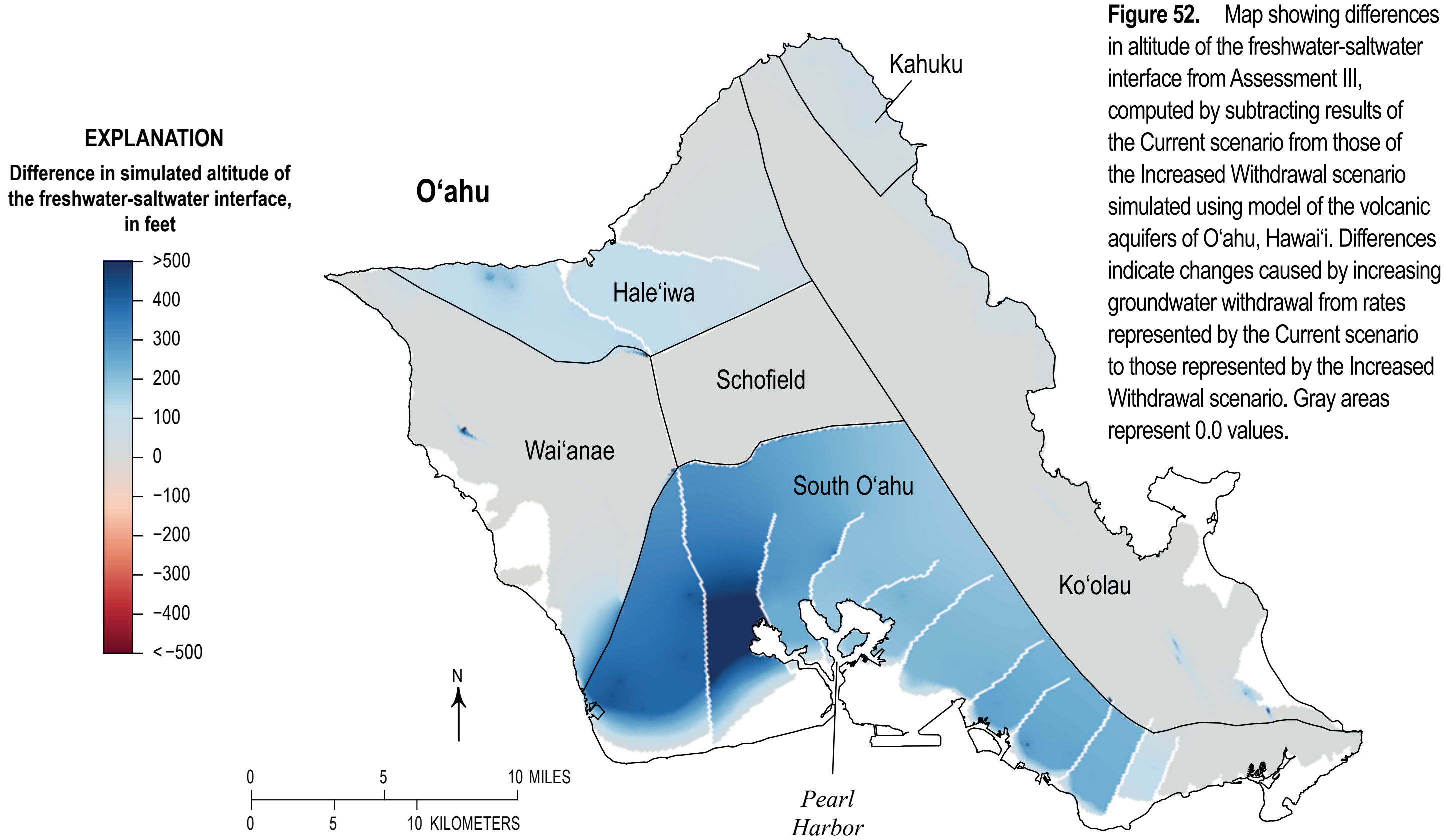

Figure 52. Map showing differences in altitude of the freshwater-saltwater interface from Assessment III, computed by subtracting results of the Current scenario from those of the Increased Withdrawal scenario simulated using model of the volcanic aquifers of O‘ahu, Hawai‘i. Differences indicate changes caused by increasing groundwater withdrawal from rates represented by the Current scenario to those represented by the Increased Withdrawal scenario. Gray areas represent 0.0 values.

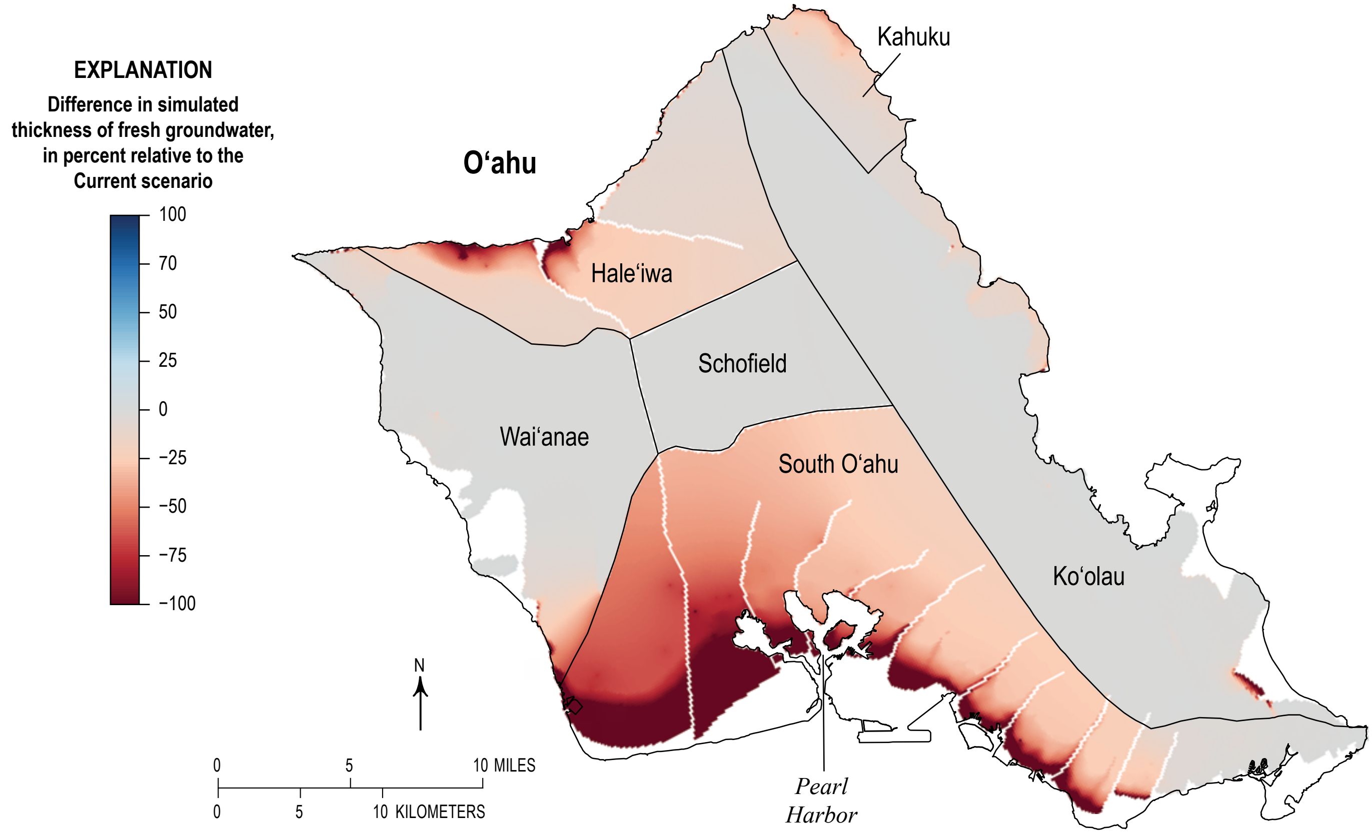

Figure 53. Map showing differences in thickness of fresh groundwater from Assessment III, computed by subtracting results of the Current scenario from those of the Increased Withdrawal scenario simulated using model of the volcanic aquifers of Oʻahu, Hawaiʻi. Differences indicate changes caused by increasing groundwater withdrawal from rates represented by the Current scenario to those represented by the Increased Withdrawal scenario. Gray areas represent 0.0 values.

Schofield sector.—The groundwater-withdrawal rate from wells in the Schofield sector increases by 18.0 Mgal/d in Assessment III (table 10, fig. 48). Because no groundwater in this sector of the model discharges directly to the ocean or streams, increased withdrawals from the sector are compensated only by reduced subsurface outflow to freshwater-lens settings in the South Oʻahu and Haleʻiwa sectors and induced subsurface inflow from the dike-impounded-groundwater settings in the Koʻolau and Waiʻanae sectors.

The large increase in simulated groundwater withdrawal results in substantial and widespread decline in water levels in the Schofield sector (fig. 51). The water-level decline also spreads partway into the adjacent Waiʻanae and Koʻolau sectors. The model-simulated freshwater-saltwater interface in the Schofield sector, however, does not rise in response to increased withdrawals (fig. 52) because fresh groundwater extends down to the bottom of the Oʻahu model. Thinning of the fresh-groundwater body results from lowering of water levels in the sector, but as a percentage of the total thickness of fresh groundwater, the thinning is not substantial (fig. 53).

Sectors that encompass the freshwater-lens setting.—In Assessment III, groundwater withdrawals from wells in the freshwater-lens settings of the South Oʻahu, Haleʻiwa, and Kahuku sectors increase by 51.7, 17.8, and 4.0 Mgal/d, respectively (table 10, fig. 48). Most of the effect of the increased withdrawals from the Kahuku and Haleʻiwa sectors is compensated by a decrease in groundwater discharge to the ocean (figs. 48, 50). Net subsurface inflows to the South Oʻahu and Haleʻiwa sectors decrease, largely as a result of increased withdrawals from the Schofield sector, although subsurface inflows from the Waiʻanae sector to the Haleʻiwa and South Oʻahu sectors increase. The combination of increased withdrawals and decreased subsurface inflow to the Haleʻiwa sector is compensated by decreases in groundwater discharge to the ocean. In the South Oʻahu sector, the combination of increased withdrawals and decreased subsurface inflow is compensated by substantial decreases in groundwater discharge to the ocean and springs near Pearl Harbor (table 10, figs. 48, 49, 50). None of the Oʻahu sectors that encompass freshwater-lens settings have tunnels.

The large increases in groundwater withdrawal result in broadly dispersed declines in water levels in the freshwater-lens settings in the Kahuku, South Oʻahu, and Haleʻiwa sectors (fig. 51). The magnitudes of the declines are less than they are in the Schofield sector, even in the South Oʻahu sector where the withdrawal increase is nearly three times that of the Schofield sector. On the other hand, rise of the freshwater-saltwater interface is more widespread and substantial in the sectors that encompass freshwater-lens settings than it is in sectors that encompass other settings (figs. 48, 52). Interface rise is especially evident in the South O‘ahu sector, which has the highest increase in withdrawal (figs. 47, 48, 52). The combination of water-level decline and interface rise results in substantial reduction in the thickness of the freshwater lenses (fig. 53).

Assessment IV—Effects of Future Changes in Rainfall

The objective of Assessment IV is to evaluate the potential effects of projected future changes in rainfall, independent of the effects from possible future increases in groundwater withdrawal (table 3). For this assessment, the Future Rainfall scenario (table 2) is simulated using the O‘ahu model and compared to the Current scenario. The withdrawal rates specified in the Future Rainfall and Current scenarios are the same, so differences between the scenarios provide information on the effect of rainfall changes, independent of the effects of potential future changes in withdrawal.

Future Rainfall Scenario

The Intergovernmental Panel on Climate Change (IPCC) issues future-climate projections that are based on results of integrated general-circulation-model (GCM) simulations of various scenarios of greenhouse-gas emissions (Intergovernmental Panel on Climate Change [IPCC], 2013). Because the GCM results are too coarse to resolve small-scale, topography-dependent climate patterns such as orographic rainfall in Hawai‘i (Timm and Diaz, 2009), climatologists have used various approaches to downscale the GCM results. For the Future Rainfall scenario in this study, rainfall projections from statistical downscaling (Elison Timm and others, 2015) are used to compute estimated future groundwater recharge for the O‘ahu model. The rainfall projections indicate that for Hawai‘i overall, rainfall will decrease in the future. The lower future rainfall will result in lower future groundwater recharge (Mair and others, 2019).

Recharge for the Future Rainfall scenario is computed using the soil water-balance model that Izuka and others (2018) used to estimate the recharge for the Current scenario. The model uses multiple spatial datasets, which include rainfall, fog interception, irrigation, evapotranspiration, runoff, soil type, and land cover, that relate to groundwater recharge. The spatial datasets are merged, creating subareas that have homogeneous properties, and the model calculates recharge on a daily interval for each subarea. The model of O‘ahu that computed the recharge used in the Current scenario had 387,533 subareas (Izuka and others, 2018).

To compute recharge for the Future Rainfall scenario, this study uses the same water-balance model of O‘ahu created by Izuka and others (2018) that was used to compute the Current-scenario recharge, except that rainfall (and related runoff-to-rainfall ratios) is derived from statistically downscaled projections for midcentury (2041–2070) under representative concentration pathway (RCP) 8.5 by Elison Timm and others (2015). RCP 8.5 has the highest radiative forcing of the RCPs described in the IPCC’s fifth assessment report (IPCC, 2013) and assumes conditions that lead to the highest greenhouse-gas emissions (Riahi and others, 2011). The projections of Elison Timm and others (2015) indicate that on average, RCP 8.5 will lead to a decrease in future rainfall in Hawai‘i. Changes in land area resulting from possible future sea-level rise were assumed to be negligible for the purposes of this study. The Future Rainfall scenario was computed using the same land cover (and parameters related to land cover) and reference evapotranspiration that Izuka and others (2018) used to compute the recharge that was used in the Current scenario of this study.

Elison Timm and others (2015) expressed their rainfall projections as anomalies (differences) relative to mean historical (1978–2007) rainfall from Giambelluca and others (2013). Elison Timm and others (2015) computed wet-season (November through April) and dry-season (May through October) anomalies for hundreds of rain gages in Hawai‘i and used spatial interpolation to generate gridded spatial datasets (maps) of anomalies for each island.

In this study, future monthly rainfall (2041–2070) used in the computation of recharge for the Future Rainfall scenario was computed by applying the anomalies of Elison Timm and others (2015) to the historical monthly rainfall for each subarea:

$$RF_m = RH_m \left(1 + \frac{\overline{A}_{s_m}}{\overline{RS}_{s_m}}\right)\left(\frac{\overline{R1}_m}{\overline{R2}_m}\right) \qquad (1)$$

where

- m = month in a specified range of years;
- s = season that contains month m;
- RF_m = future rainfall for month m during 2041–2070 [in units of length];
- RH_m = historical rainfall for month m during 1978–2007 [in units of length];
- $\overline{A}_{s_m}$ = mean rainfall anomaly for season s that contains month m (from Elison Timm and others, 2015) [in units of length];
- $\overline{RS}_{s_m}$ = mean rainfall for season s that contains month m during 1978–2007 (from Giambelluca and others, 2013) [in units of length];
- $\overline{R1}_m$ = mean rainfall value for month m for the period 1978–2007 (value is from Giambelluca and others, 2013) [in units of length]; and
- $\overline{R2}_m$ = mean rainfall value for month m, computed from individual monthly values for the period 1978–2007 (individual values are from Frazier and others, 2016) [in units of length].

Historical monthly rainfall (RH_m) was determined from datasets for Hawai‘i (computed by Frazier and others [2016] and Giambelluca and others [2013]) using the methods described by Izuka and others (2018). Daily future rainfall, required by the water-balance model to compute daily recharge, was derived from the future monthly rainfall using the method of fragments described by Mair and others (2019).

The water-balance model uses runoff-to-rainfall ratios to determine runoff. Daily runoff for a given subarea is the product of daily rainfall and a seasonal runoff-to-rainfall ratio. In computing recharge for the Future Rainfall scenario in this study, seasonal rainfall-to-runoff ratios that incorporate both the historical 1978–2007 rainfall and the midcentury RCP 8.5 rainfall projection were computed using the methods described in Mair and others (2019). Seasonal ratios were computed for each of the catchment

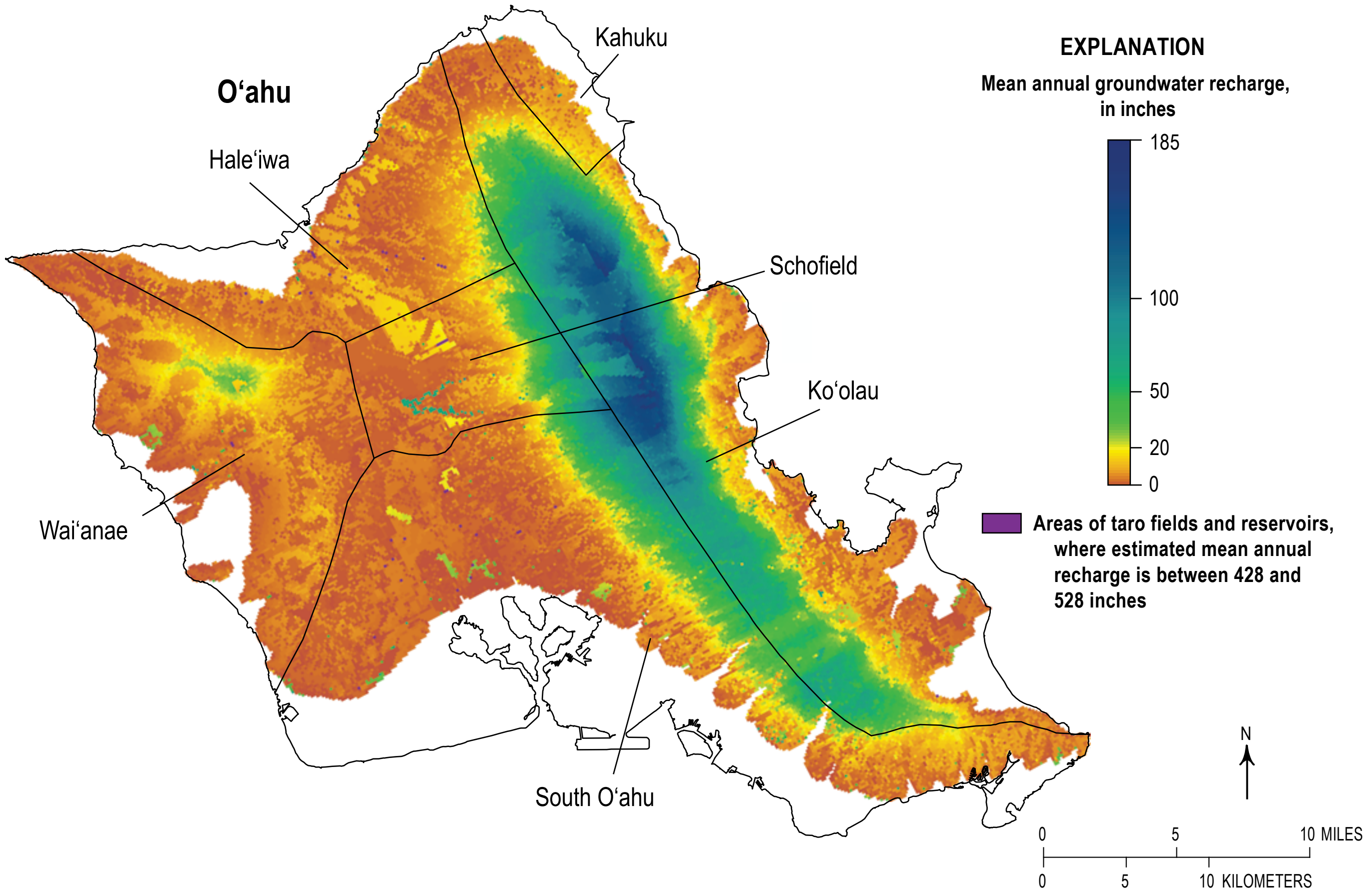

Figure 54. Map showing distribution of groundwater recharge for the Future Rainfall scenario from Assessment IV, simulated using model of the volcanic aquifers of O‘ahu, Hawai‘i.

zones of O‘ahu described by Izuka and others (2018). A geospatial dataset of the future recharge can be accessed online (Rotzoll and Johnson, 2023). As in the calibrated O‘ahu model of Izuka and others (2021), which represents the Current scenario in this study, recharge for the Future Rainfall scenario was applied only to model cells whose tops were above sea level, and no recharge was applied to cells covered by caprock (fig. 54).

Groundwater-withdrawal rates for wells in the Future Rainfall scenario are the same as those in the Current scenario. Discharge to free-flowing tunnels, simulated using drains in the model, was allowed to change if heads in the aquifer changed as a result of differences in recharge between the Future Rainfall and Current scenarios. Change to tunnel flows is one of the consequences being evaluated in Assessment IV.

Results

Recharge simulated in the Future Rainfall scenario is 508.3 Mgal/d (table 11), which is 89.3 Mgal/d less than in the Current scenario. This difference indicates an islandwide decrease in recharge of 15 percent relative to the Current-scenario rate. The decrease is widely distributed across the model (fig. 55). The model simulations for Assessment IV indicate that the decrease will result in substantial reductions in groundwater discharge to streams, springs, and the ocean on O‘ahu (fig. 56). The simulations also indicate that tunnel yields on O‘ahu will decrease by 3.7 Mgal/d, which is 11 percent relative to the tunnel yields in the Current scenario.

The analysis for Assessment IV also indicates substantial reductions in recharge (0.9–38.0 Mgal/d) in each of the sectors

Table 11. Comparison of islandwide groundwater budgets for the Future Rainfall and Current scenarios (Assessment IV) simulated using the numerical groundwater model of the volcanic aquifers of O‘ahu, Hawai‘i.

[Difference between scenarios represents Future Rainfall minus Current scenarios; differences between scenarios may not be equal to difference between values in columns, owing to rounding. Mgal/d, million gallons per day]

Scenario	Recharge (Mgal/d)	Withdrawal (Mgal/d)			Groundwater discharge (Mgal/d)	
		Wells	Tunnels	Total	To streams and springs	To ocean
Current	597.6	188.0	33.2	221.2	127.7	248.6
Future Rainfall	508.3	188.0	29.5	217.5	102.3	188.4
Difference between scenarios	−89.3	0.0	−3.7	−3.7	−25.4	−60.2

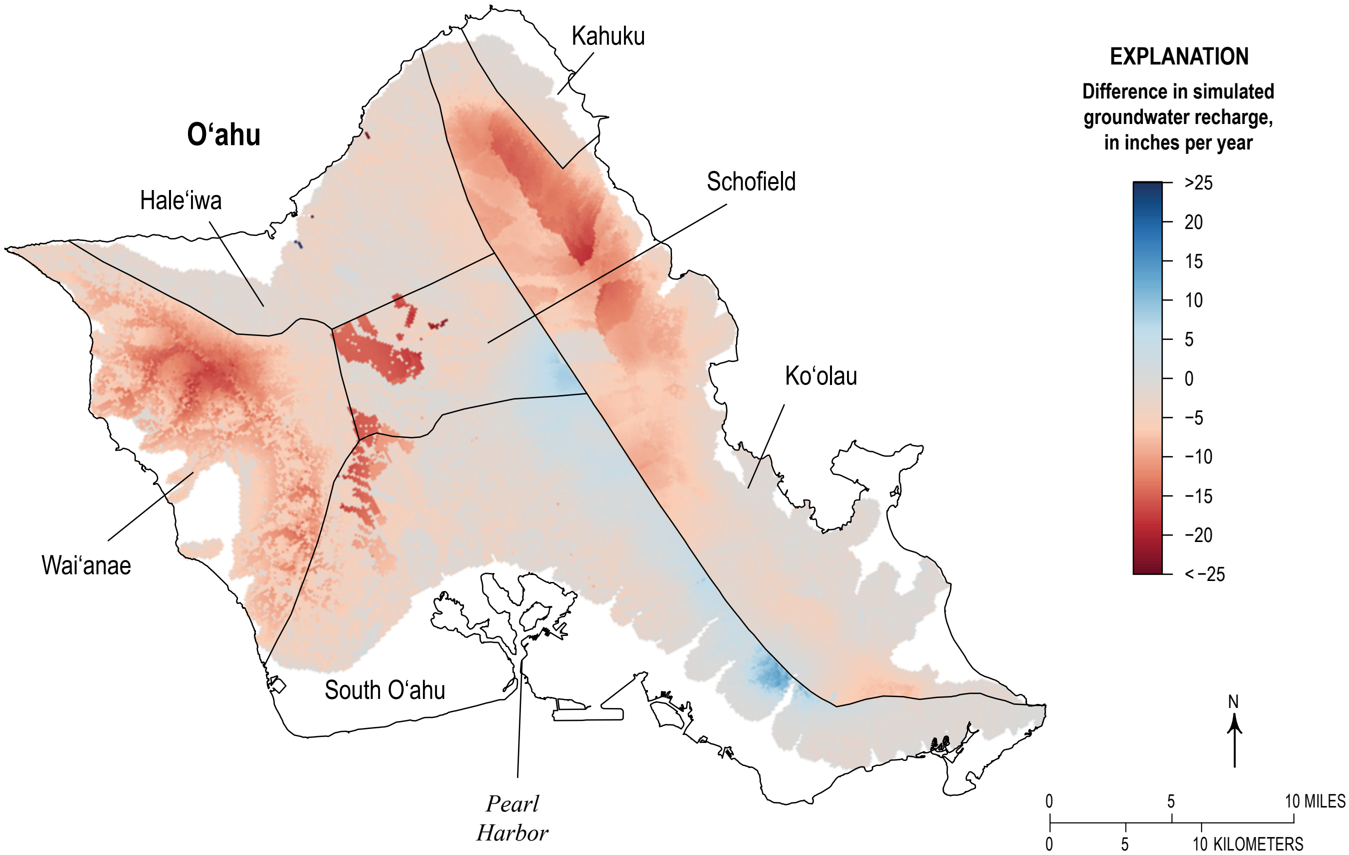

Figure 55. Map showing differences in groundwater recharge from Assessment IV, computed by subtracting rates of the Current scenario from those of the Future Rainfall scenario simulated using model of the volcanic aquifers of O‘ahu, Hawai‘i. Gray areas represent 0.0 values.

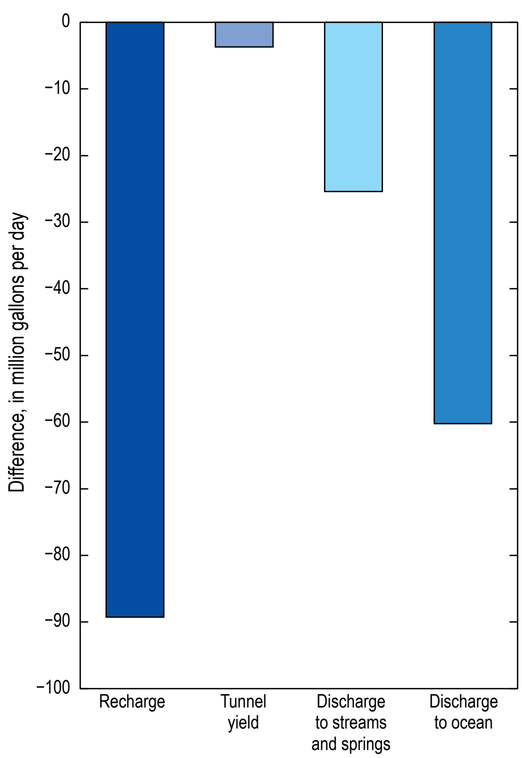

Figure 56. Bar graph showing differences in islandwide groundwater budgets from Assessment IV, computed by subtracting results of the Current scenario from those of the Future Rainfall scenario simulated using model of the volcanic aquifers of O‘ahu, Hawai‘i. Differences indicate changes caused by changing recharge from rates represented by the Current scenario to those represented by the Future Rainfall scenario.

of the O‘ahu model (table 12, fig. 57). Relative to the Current-scenario recharge rates (table 4), the reductions ranged from 9 to 54 percent. The widespread recharge reduction in the O‘ahu model results in substantial reductions in groundwater discharge to streams and springs (figs. 57, 58), reduced groundwater discharge to the ocean (figs. 57, 59), declines in groundwater levels (fig. 60), upward movement of the freshwater-saltwater interface (fig. 61), and reduced thickness of fresh groundwater (fig. 62). The reduced recharge also causes reduced subsurface flow from upgradient to downgradient sectors (fig. 57).

Sectors that encompass dike-impounded-groundwater settings.—In Assessment IV, recharge rates in the dike-impounded-groundwater settings of the Ko‘olau and Wai‘anae sectors decrease by 38.0 and 28.5 Mgal/d, respectively (table 12, fig. 57). Subsurface outflow from these sectors to most downgradient sectors, including the Schofield sector and sectors that encompass freshwater-lens settings, decreases as a result of the reduced recharge. The reduced recharge also results in reduced groundwater discharge to streams and springs (figs. 57, 58), reduced groundwater discharge to the ocean (figs. 57, 59), and reduced tunnel yield. In the Wai‘anae sector, groundwater discharge to the ocean compensates for most of the reduction in recharge, whereas in the Ko‘olau sector, reductions in groundwater discharge to streams and springs, groundwater discharge to the ocean, and subsurface flow to other sectors are similar (fig. 57). Tunnel yield in the Ko‘olau sector declines by 2.5 Mgal/d, which is about 8 percent relative to the yield in the Current scenario (table 4); in the Wai‘anae sector, all of the tunnel yield ceases.

The reduced recharge causes widespread water-level declines in parts of the Ko‘olau and Wai‘anae sectors (fig. 60). Largest water-level declines in these sectors generally correspond with location of largest recharge reduction (fig. 55), although the magnitude of water-level decline also depends on hydraulic properties—declines tend to be greater in parts of these sectors where hydraulic conductivity is exceptionally low (compare figures 23*C* and 60). The area of large water-level decline in the Wai‘anae sector coincides with areas of reduced groundwater recharge (compare figures 55 and 60).

Table 12. Differences in sector groundwater budgets from Assessment IV (Future Rainfall scenario minus Current scenario), determined from simulations using the numerical groundwater model of the volcanic aquifers of O‘ahu, Hawai‘i.

[Totals may not be equal to sum of values in columns, owing to rounding. Mgal/d, million gallons per day]

Sector	Principal groundwater setting	Differences (Mgal/d)					
		Recharge	Withdrawal from wells	Tunnel yield	Discharge to streams and springs	Discharge to ocean	Subsurface flow to or from other sectors[1]
South O‘ahu	Freshwater lens	−8.8	0.0	0.0	−11.5	−8.3	11.0
Hale‘iwa	Freshwater lens	−6.3	0.0	0.0	0.0	−19.0	12.7
Kahuku	Freshwater lens	−0.9	0.0	0.0	0.0	−4.2	3.3
Ko‘olau	Dike-impounded groundwater	−38.0	0.0	−2.5	−12.8	−10.1	−12.6
Wai‘anae	Dike-impounded groundwater	−28.5	0.0	−1.2	−1.1	−18.6	−7.6
Schofield	Enigmatic[2]	−6.7	0.0	0.0	0.0	0.0	−6.7
	Total	−89.3	0.0	−3.7	−25.4	−60.2	0.0

[1]Positive values indicate increased outflow or decreased inflow; negative values indicate decreased outflow or increased inflow.

[2]Enigmatic groundwater occurrences do not fit into one of the four principal groundwater settings discussed in this report, and their relation to the geologic framework of volcanic aquifers is not fully understood (see Izuka and others, 2018, 2021).

Figure 57. Map and bar graphs showing differences in sector groundwater budgets from Assessment IV, computed by subtracting results of the Current scenario from those of the Future Rainfall scenario simulated using model of the volcanic aquifers of O‘ahu, Hawai‘i. Differences indicate changes caused by changing recharge from rates represented by the Current scenario to those represented by the Future Rainfall scenario. Note that vertical axes of bar graphs are at different scales to show wide range of values. Values that indicate flow between sectors may not agree exactly with totals shown in table 12, owing to rounding.

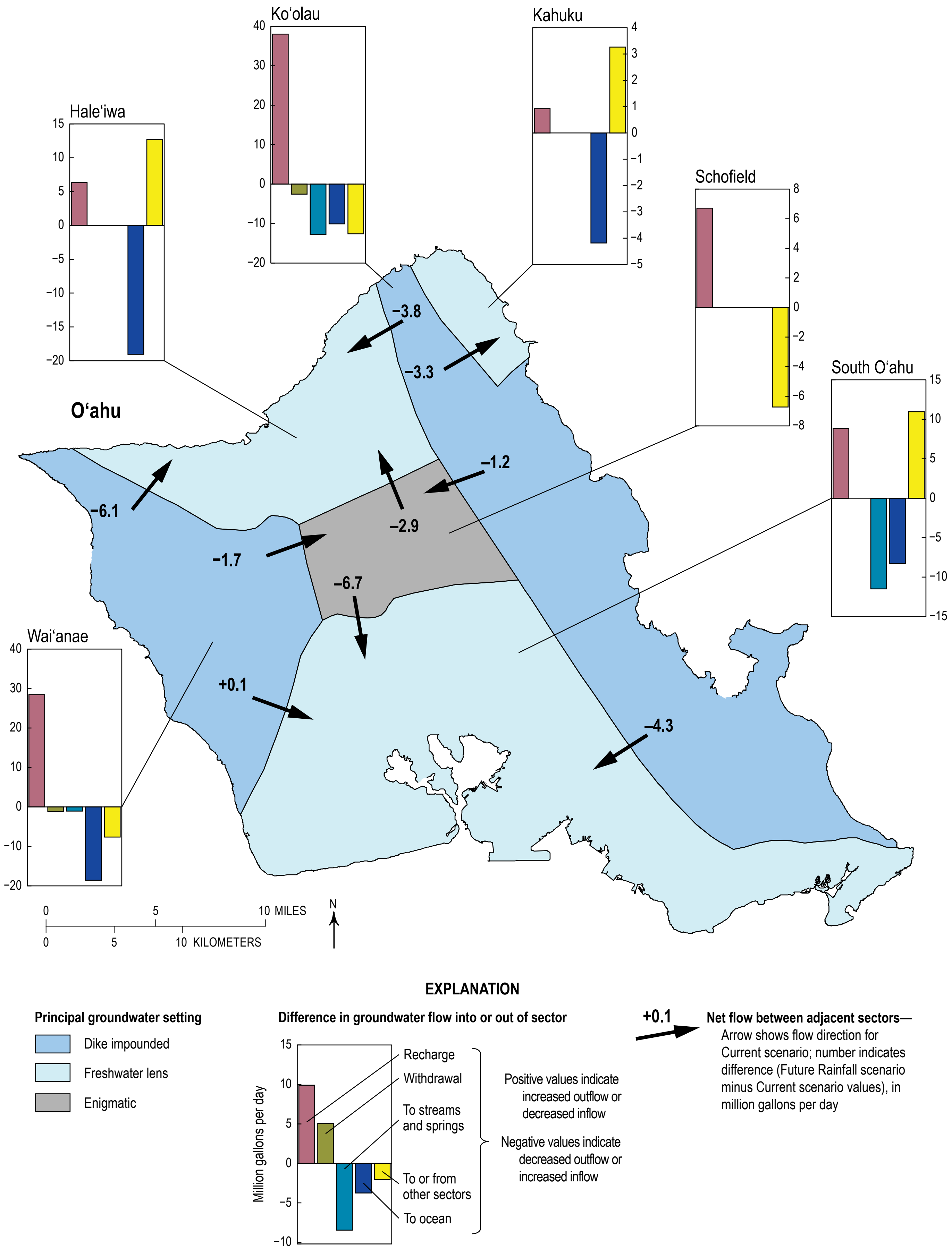
Hale‘iwa
Ko‘olau
Kahuku
Schofield
South O‘ahu
Wai‘anae
O‘ahu
−3.8
−3.3
−1.2
−2.9
−6.1
−1.7
−6.7
+0.1
−4.3
0 5 10 MILES
0 5 10 KILOMETERS
N
EXPLANATION
Principal groundwater setting
Dike impounded
Freshwater lens
Enigmatic
Difference in groundwater flow into or out of sector
Million gallons per day
Recharge
Withdrawal
To streams and springs
To or from other sectors
To ocean
Positive values indicate increased outflow or decreased inflow
Negative values indicate decreased outflow or increased inflow
+0.1
Net flow between adjacent sectors—
Arrow shows flow direction for Current scenario; number indicates difference (Future Rainfall scenario minus Current scenario values), in million gallons per day

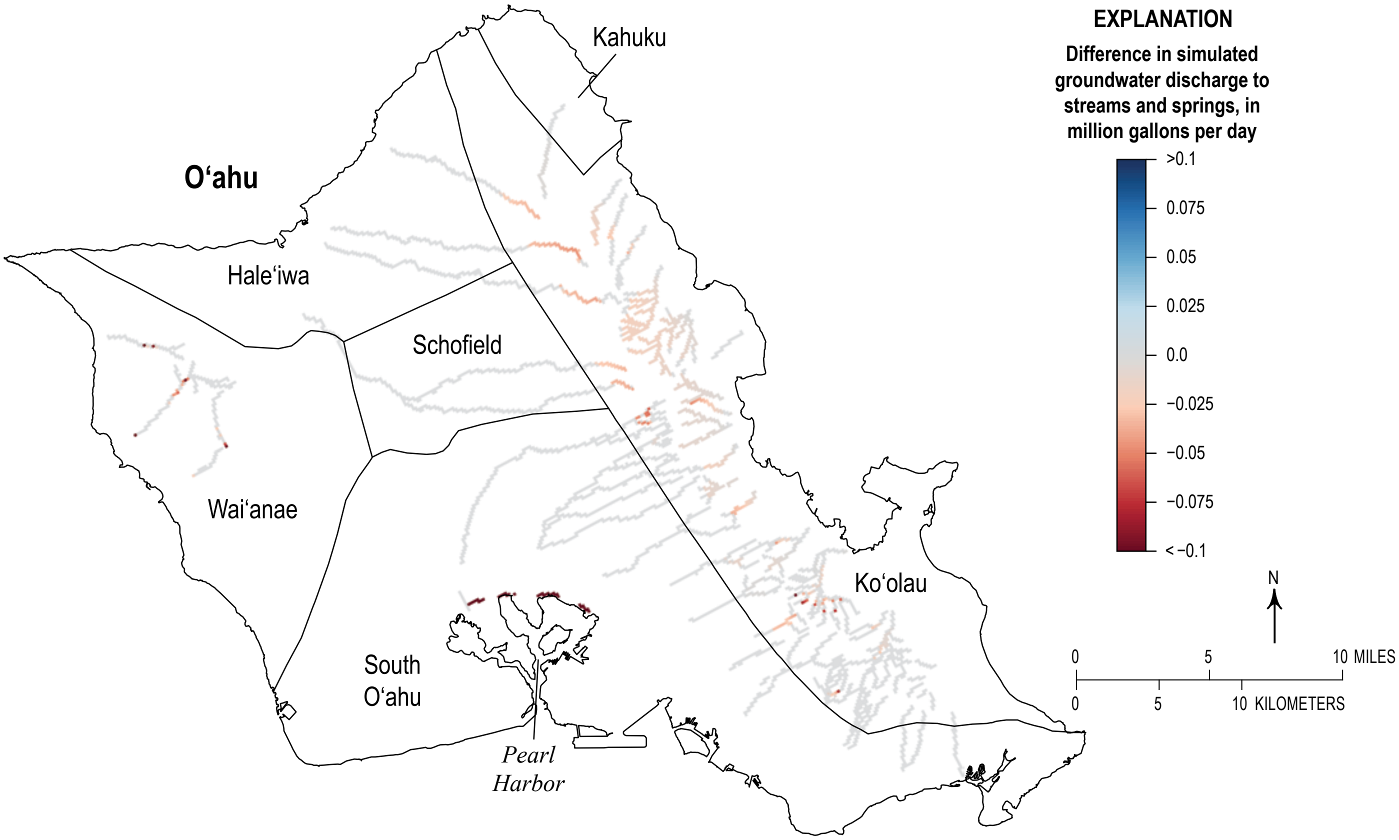

Figure 58. Map showing differences in groundwater discharge from volcanic aquifers to streams and springs from Assessment IV, computed by subtracting results of the Current scenario from those of the Future Rainfall scenario simulated using model of the volcanic aquifers of O‘ahu, Hawai‘i. Differences indicate changes caused by changing recharge from rates represented by the Current scenario to those represented by the Future Rainfall scenario. Gray areas represent 0.0 values.

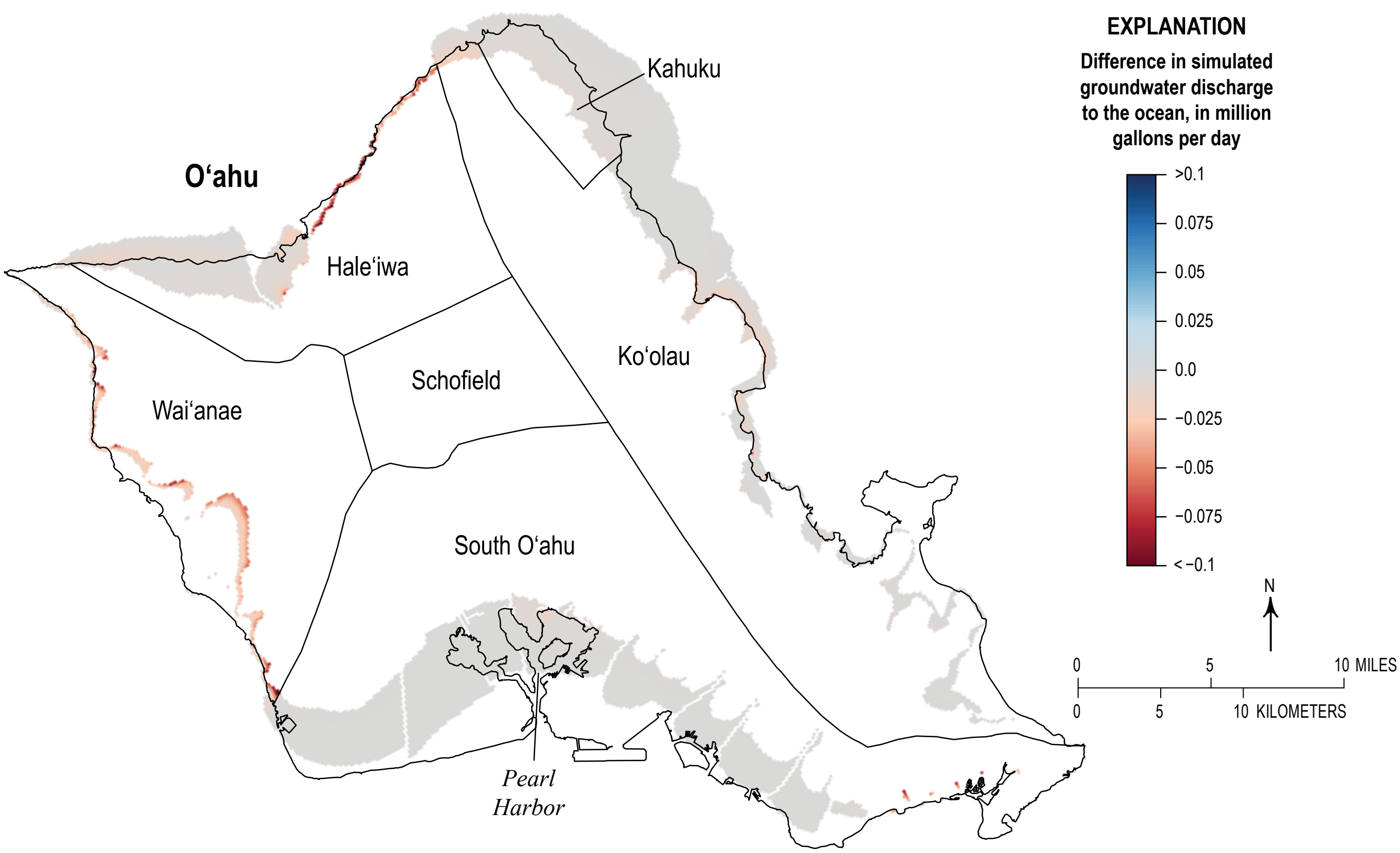

Figure 59. Map showing differences in groundwater discharge from volcanic aquifers to the ocean from Assessment IV, computed by subtracting results of the Current scenario from those of the Future Rainfall scenario simulated using model of the volcanic aquifers of O‘ahu, Hawai‘i. Differences indicate changes caused by changing recharge from rates represented by the Current scenario to those represented by the Future Rainfall scenario. Gray areas represent 0.0 values.

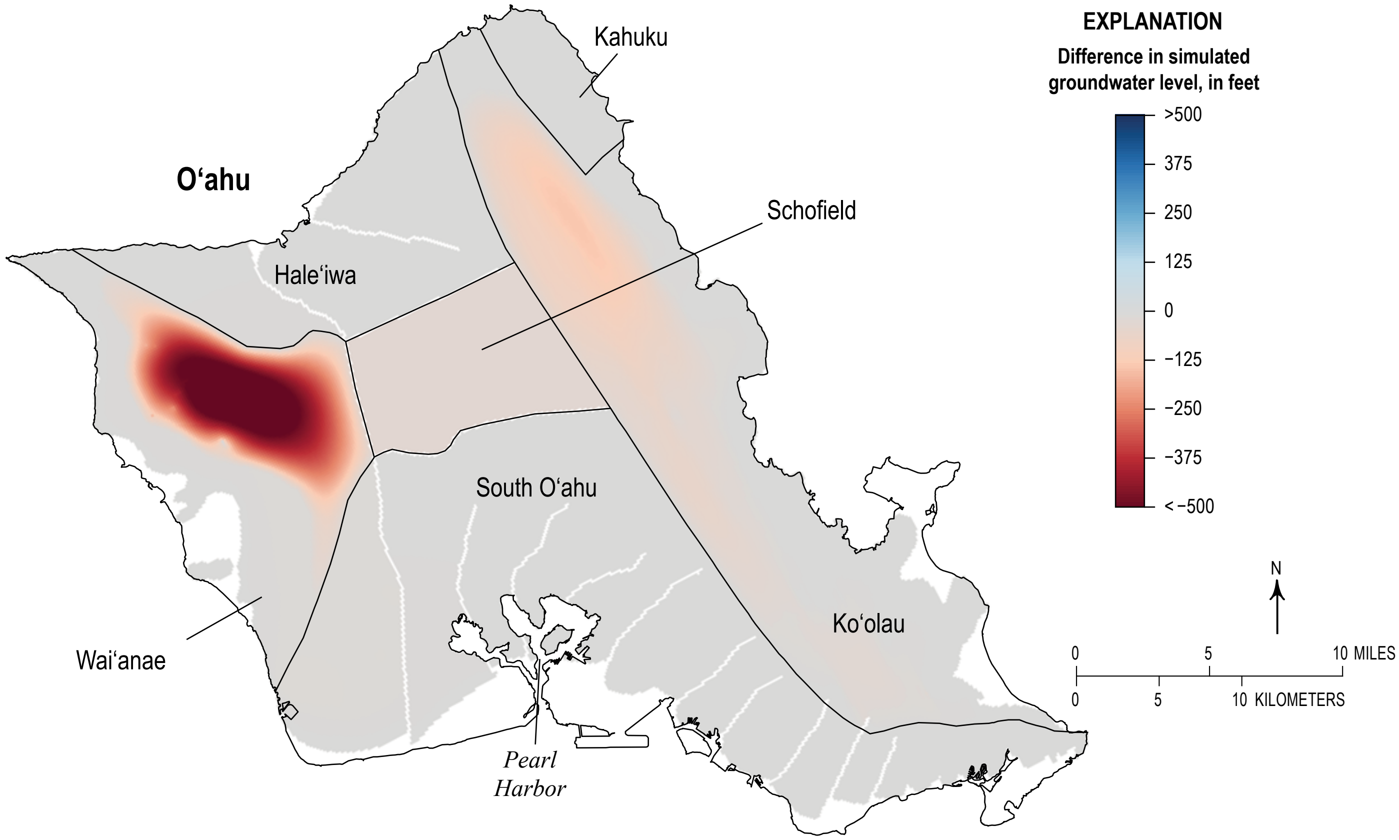

Figure 60. Map showing differences in groundwater levels from Assessment IV, computed by subtracting results of the Current scenario from those of the Future Rainfall scenario simulated using model of the volcanic aquifers of O‘ahu, Hawai‘i. Differences indicate changes caused by changing recharge from rates represented by the Current scenario to those represented by the Future Rainfall scenario. Gray areas represent 0.0 values.

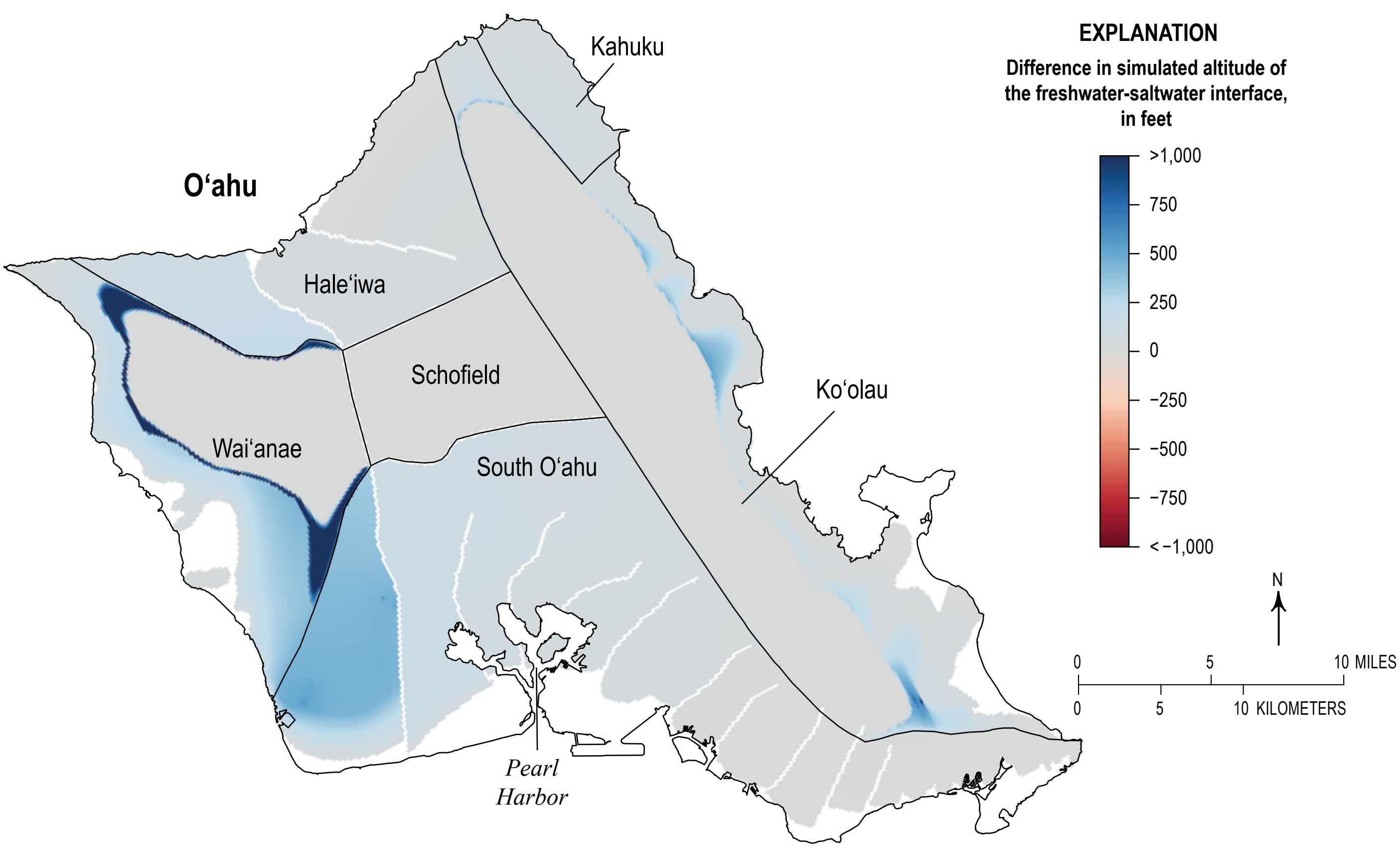

Figure 61. Map showing differences in the altitude of freshwater-saltwater interface from Assessment IV, computed by subtracting results of the Current scenario from those of the Future Rainfall scenario simulated using model of the volcanic aquifers of O‘ahu, Hawai‘i. Differences indicate changes caused by changing recharge from rates represented by the Current scenario to those represented by the Future Rainfall scenario. Gray areas represent 0.0 values.

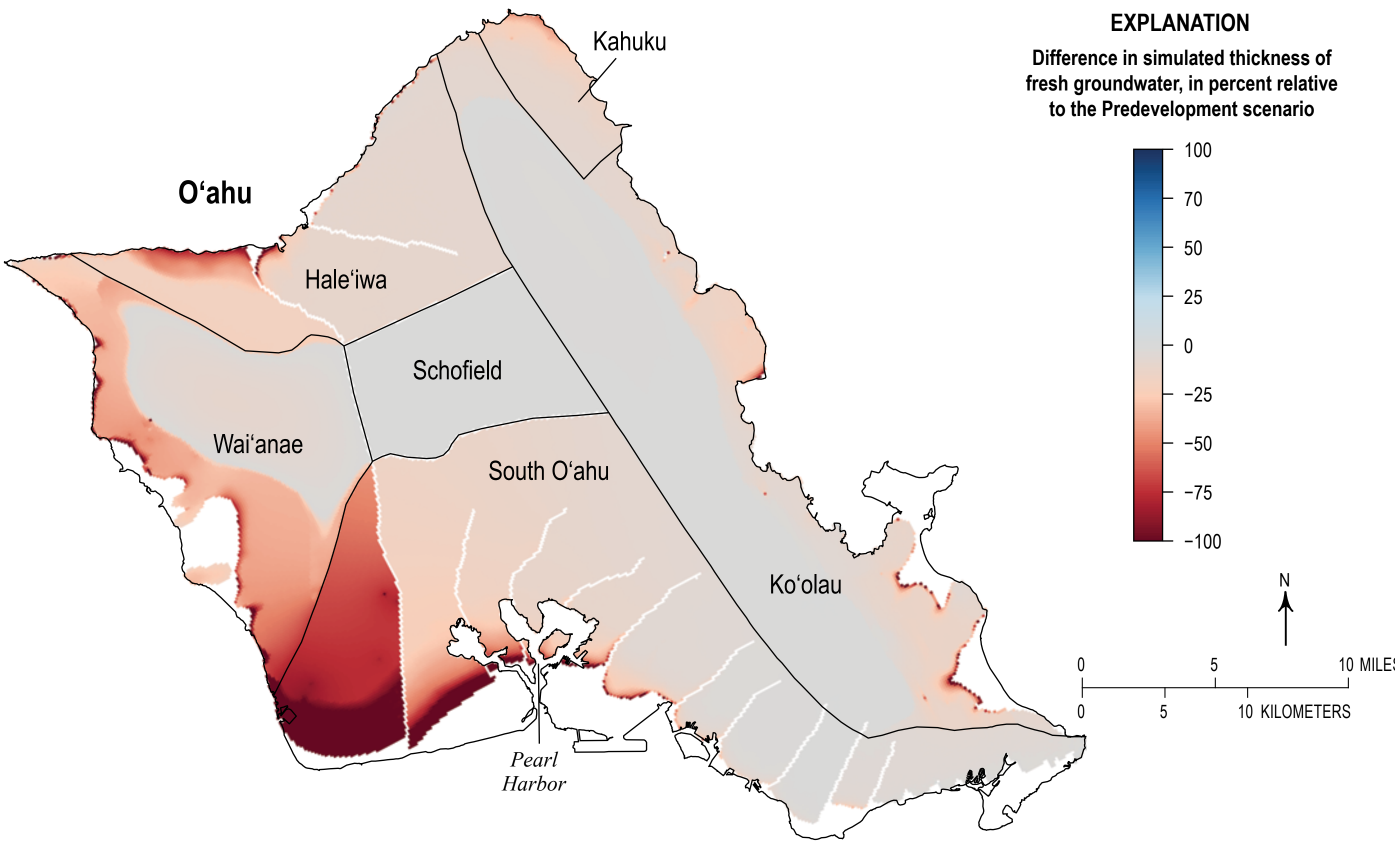

Figure 62. Map showing differences in thickness of fresh groundwater from Assessment IV, computed by subtracting results of the Current scenario from those of the Future Rainfall scenario simulated using model of the volcanic aquifers of O‘ahu, Hawai‘i. Differences indicate changes caused by changing recharge from rates represented by the Current scenario to those represented by the Future Rainfall scenario. Gray areas represent 0.0 values.

The reduced recharge also causes upward and landward movement of the freshwater-saltwater interface in the sectors that encompass the dike-impounded-groundwater setting (figs. 57, 61). Although the interface altitude in inland parts of both the Wai‘anae and Ko‘olau sectors remains deep, substantial interface rise is apparent in seaward areas, especially in the Wai‘anae sector. A substantial rise is evident at the periphery of a low-permeability *K* zone in the Wai‘anae sector, where reduction in recharge causes the interface to encroach landward into areas that in the Current scenario were entirely filled with fresh groundwater. The combination of water-level decline and interface rise results in a reduction in fresh-groundwater thickness (fig. 62).

Schofield sector.—In the Schofield sector, the recharge rate in the Future Rainfall scenario is 6.7 Mgal/d less than it is in the Current scenario (table 12, fig. 57). Subsurface inflows from the dike-impounded-groundwater settings in the Ko‘olau and Wai‘anae sectors are also less in the Future Rainfall scenario than they are in the Current scenario. The reduction in recharge plus the reduced subsurface inflow to the Schofield sector are compensated by an equivalent reduction in net subsurface outflows to the freshwater-lens settings in the South O‘ahu and Hale‘iwa sectors.

Assessment IV indicates that reductions in recharge in the Future Rainfall scenario will result in broad water-level declines in the Schofield sector (fig. 60), but no rise of the freshwater-saltwater interface is indicated (fig. 61). The thickness of fresh groundwater is reduced as a result of water-level declines, but the reduction is small as a percentage of the total thickness of fresh groundwater (fig. 62).

Sectors that encompass freshwater-lens settings.—In Assessment IV, recharge rates in the freshwater-lens settings of the South O‘ahu, Hale‘iwa, and Kahuku sectors decrease by 8.8, 6.3, and 0.9 Mgal/d, respectively (table 12, fig. 57). Simulated subsurface inflows to these sectors from all but one of the adjacent sectors are also reduced. In the Kahuku and Hale‘iwa sectors, the reduced recharge plus the reduced subsurface inflow are compensated by equivalent reductions in simulated groundwater discharge to the ocean (figs. 57, 59). Reduced recharge and subsurface inflow to the South O‘ahu sector are compensated mostly by reductions in groundwater discharge to the springs near Pearl Harbor, although reduction in groundwater discharge to the ocean is substantial (figs. 57, 58, 59).

Decreases in recharge represented by Assessment IV result in low-magnitude decreases in water levels in the freshwater-lens settings in the South O‘ahu, Kahuku, and Hale‘iwa sectors (fig. 60). Rise of the simulated freshwater-saltwater interface, however, is substantial (fig. 61), especially in the western part of the South O‘ahu sector, where reductions in recharge are large (fig. 55), and in the western part of the Hale‘iwa sector, where reductions in subsurface inflow from the Wai‘anae sector are large (fig. 57). Areas of substantial reduction of the freshwater thickness (fig. 62) generally coincide with the areas of substantial rise of the freshwater-saltwater interface.

Implications for Groundwater Availability

The amount of fresh groundwater available for human use from Hawai‘i’s volcanic aquifers is constrained by the consequences of groundwater withdrawal—water-table decline, salt water and transition-zone rise, and reduction of natural groundwater discharge. Results of this study indicate that multiple factors, including spatial distribution and magnitude of recharge and groundwater withdrawals, three-dimensional variation of hydrogeologic properties, and geometry of coasts and streams where groundwater naturally discharge, affect the availability of groundwater from Hawai‘i’s volcanic aquifers. Simulations using the numerical models of the volcanic aquifers of Kaua‘i, O‘ahu, and Maui allow the comprehensive consideration of the multiple factors to quantify the consequences of groundwater withdrawal.

Model simulations in this study indicate that high-volume groundwater withdrawals that have emerged in Hawai‘i since the first well was drilled in the 1870s have caused substantial reductions in groundwater discharge to streams and springs, reductions in groundwater discharge to the ocean, declines in groundwater levels, and upward movement of the freshwater-saltwater interface. Simulations also indicate that if withdrawals are increased in the future, the result will include further reductions in groundwater discharge to streams, springs, and the ocean; declines in groundwater levels; and upward movement of the interface. Limits placed on these consequences can limit the amount of groundwater available for human use. The effects of withdrawal are, and will continue to be, superimposed on the effects of recharge changes resulting from land-cover and climate changes—increases in recharge can ameliorate the effects of withdrawal, whereas decreases in recharge can exacerbate the effects of withdrawal.

Consequences of Groundwater Withdrawal

Assessments I and III evaluated the effects of groundwater withdrawals independently from the effects of changes in recharge. The results of these assessments have implications for groundwater availability. Simulations in this study indicate that historical groundwater withdrawals have had, and future withdrawal increases will have, the following consequences:

1. *Reductions in natural groundwater discharge to streams, springs, and the ocean.*—Specific effects of withdrawals depend on the principal groundwater setting, the magnitude of withdrawals, and the proximity of the withdrawals to sites of natural groundwater discharge, such as streams, springs, and the ocean.
2. *Reduction in subsurface outflows to, or inducement of subsurface inflows from, adjacent sectors.*—The changes in subsurface flows affect the water budgets and groundwater availability in the other sectors. Limits placed on reductions in subsurface flow between adjacent sectors can become limitations to groundwater availability, particularly for sectors—such as those that encompass dike-impounded-groundwater settings (on all islands) and the Schofield sector (on O‘ahu)—that contribute substantial subsurface flow to freshwater-lens settings that are important sources of water for human use in Hawai‘i.
3. *Reductions in groundwater discharge to streams and springs.*—These reductions can be substantial in (a) dike-impounded-groundwater settings such as those of the Ko‘olau (on O‘ahu), Pu‘ukukui (on Maui), and Central Kaua‘i sectors; (b) the caprock-influenced, freshwater-lens setting of the South O‘ahu sector; and (c) the thickly saturated setting of the East Kaua‘i sector. Limits placed on streamflow or springflow reduction (for example, to maintain instream flows or protect fluvial and wetland habitats) can limit groundwater availability in these sectors. In contrast, some sectors, such as the Schofield (on O‘ahu) and Haleakalā Rift (on Maui) sectors and most sectors that encompass freshwater-lens settings (other than the South O‘ahu sector), have little or no connection to streams. Withdrawals from the Schofield sector can, however, indirectly affect springs in the Pearl Harbor area by reducing subsurface flows to the South O‘ahu sector.
4. *Reductions in groundwater discharge to the ocean.*—These reductions can be substantial in freshwater-lens settings, but the reductions can also be substantial in dike-impounded-groundwater and the thickly saturated settings if production wells are near the coast. Limits placed on reductions in groundwater discharge to the ocean (for example, to protect coastal ecosystems that rely on fresh-groundwater discharge) can limit groundwater availability from these settings. Withdrawal from landlocked sectors such as the Pu‘ukukui (on Maui) and Schofield (on O‘ahu) can indirectly affect groundwater discharge to the ocean by reducing subsurface flows to other sectors.
5. *Lowering of groundwater levels.*—In low-permeability aquifers such as those in the dike-impounded-groundwater setting, withdrawals result in focused, high-magnitude water-level declines. In high-permeability aquifers such as those of the freshwater-lens settings and the Schofield sector, withdrawals cause lower magnitude but widespread water-level declines. Limits placed on water-level decline (for example, to protect the productivity of shallow wells) can limit groundwater availability in these settings.
6. *Rise of the freshwater-saltwater interface.*—Interface rise is notable in the freshwater-lens settings, especially in the heavily developed South O‘ahu, Central Maui, and Hale‘iwa (on O‘ahu) sectors. Localized interface rise near high-production wells results from withdrawals in

dike-impounded-groundwater settings such as those of the Koʻolau and Waiʻanae sectors (on Oʻahu) and the Central Kauaʻi sector. Interface rise that results from large withdrawals from one sector can spread into other sectors (for example, effects of withdrawals from the Central Kauaʻi sector spread into the East Kauaʻi sector). Limits placed on interface rise (for example, to prevent wells from producing salty water) can limit groundwater availability in these settings. In contrast, the simulations in this study indicated little or no interface rise in the Schofield (Oʻahu) sector (despite high withdrawal rates) and parts of dike-impounded groundwater settings that are not near coast.

7. *Future increases in withdrawals from wells can reduce the productivity of tunnels.*—In Assessment III, some of the simulated future increases in well withdrawals in the dike-impounded-groundwater settings of the Waiʻanae and Koʻolau sectors on Oʻahu came at the expense of tunnel yield.

Effects of Changing Recharge

Assessment II evaluated the combined effects of changes in groundwater withdrawal and recharge that occurred between the periods represented by the Predevelopment (1870) and Current (2001–2010) scenarios. Assessment II indicates that the following effects occurred when recharge changed:

1. Recharge in some areas of Hawaiʻi increased between the periods represented by the Predevelopment and Current scenarios. Although some of the increase results from differences in the rainfall periods used in the recharge computation, the largest increases correspond with land-cover changes by humans, particularly the conversion of large areas of land for agriculture. Crop irrigation and leaks from surface-water reservoirs created localized areas of enhanced recharge. Notable examples are the large area of enhanced recharge that correspond to sugarcane fields in the Central Maui sector and reservoirs in the Central Kauaʻi sector.

2. Recharge in some areas of Hawaiʻi decreased between the periods represented by the Predevelopment and Current scenarios. The reductions result, in part, from differences in the rainfall periods used in the recharge computations, but reductions also result from land-cover changes such as the replacement of native forest with nonnative forest. Reductions in recharge in the models also are associated with loss of predevelopment taro fields; however, the method used to estimate recharge for the models assumed that in all taro fields, water seeps from the field into the ground (Izuka and others, 2018). In reality, some taro fields were constructed in wetlands where groundwater naturally discharges to the surface (see section entitled “Study Limitations”).

3. Increases in recharge can offset the effects of groundwater withdrawals, thereby lessening the severity of reductions in groundwater discharge to streams, springs, and the ocean; lowering of water levels; and upward movement of the freshwater-saltwater interface. The degree of offset depends on the magnitude of the recharge increases, their locations relative to the production wells and to streams, springs and the coasts, and the principal groundwater setting. In addition, the net effect of crop irrigation on groundwater availability depends on the source of the irrigation water. Irrigation using water diverted from streams that would normally have run off to the ocean can have a positive net effect on groundwater availability (although it comes at the expense of streamflow). Irrigation using groundwater has a negative net effect on groundwater availability.

4. Decreases in recharge can exacerbate the effects of groundwater withdrawals, resulting in greater reduction of groundwater discharge to streams, springs, and the ocean; lowering of water levels; and rise of the freshwater-saltwater interface. The degree of exacerbation depends on the magnitude of the recharge decreases; their location relative to the production wells and to streams, springs, and the coasts; and the principal groundwater setting.

Assessment IV examined how an overall decrease in rainfall projected for midcentury (2041–2070) by statistical downscaling of results for RCP 8.5 (Elison Timm and others, 2015) will affect groundwater recharge and availability on Oʻahu, independent of effects from possible future increases in groundwater withdrawal. Assessment IV indicates that the following will result from the projected decrease in rainfall:

1. The projected decrease in rainfall will result in an islandwide decrease in recharge on Oʻahu of 15 percent relative to the recharge represented in the Current scenario; recharge in individual sectors of Oʻahu would decrease by 9 to 53 percent.

2. Even if withdrawal rates from wells remain unchanged from the Current scenario, the estimated decrease in recharge in the Future Rainfall scenario would result in substantial reductions in groundwater discharge to streams and springs, reductions in groundwater discharge to the ocean, declines in groundwater levels, and upward movement and landward encroachment of the freshwater-saltwater interface. The magnitude of the effects depends on the magnitude of the recharge increases or decreases; their location relative to production wells and to streams, springs, and the coast; and the principal groundwater setting. These effects can constrain the availability of groundwater for human use by exacerbating the effects of groundwater withdrawals.

3. Estimated reductions in recharge to upgradient sectors such as the Schofield sector and the dike-impounded-groundwater settings in the Koʻolau and Waiʻanae sectors would result in reduction of subsurface flows to the freshwater-lens

settings in the South Oʻahu and Haleʻiwa sectors, which are important sources of water for human use.

4. The estimated reductions in recharge would cause tunnel yield on Oʻahu to decrease by 11 percent relative to the yield in the Current scenario. Simulated tunnel yield decreased by 8 percent in the Koʻolau sector and ceased completely in the Waiʻanae sector.

Other Islands in Hawaiʻi

The model simulations in this study demonstrate that each of the principal groundwater settings responds differently to groundwater withdrawals, and the foregoing discussions indicate that some generalizations can be made about the consequences of groundwater withdrawal that limit groundwater availability for a given setting. The simulations that use groundwater models of Kauaʻi, Oʻahu, and Maui in this study thus have implications for analogous settings in the other islands of Hawaiʻi. Groundwater availability in areas where the freshwater-lens setting is predominant is likely to be constrained by limits placed on saltwater rise (for example, to protect existing wells near the coast) and coastal discharge (for example, to protect nearshore ecosystems), whereas groundwater availability in areas where the dike-impounded-groundwater, caprock-influenced freshwater-lens, or thickly saturated settings are predominant are likely to be constrained by limits placed on water-table depression and reductions in groundwater discharge to streams and springs. The implications do not extend, however, to areas where hydrogeology is not accounted for by the principal groundwater settings of this study, such as parts of the Island of Hawaiʻi (Thomas and others, 1996; Oki, 1999; Bauer, 2003; Attias and others, 2020).

Essential Next Step

This study contributes to the determination of groundwater availability by quantifying the consequences of withdrawals for a finite set of circumstances represented by the scenarios simulated using the numerical groundwater models. An essential step in assessing groundwater availability is setting the acceptable limits to the consequences of groundwater withdrawal. Setting limits commonly involves multiple stakeholders and consideration of diverse factors—such as human and environmental health, traditional and customary practices, economic growth, legal rights, and statutes—that are outside the physical hydrogeology of this study. However, once these limits are set, numerical model simulations can be used to quantify the amount of water that can be withdrawn within those limits and thereby inform management decisions that seek to balance the need to limit the consequences of groundwater withdrawals with the need to develop more water for human use.

Study Limitations

Conclusions that can be drawn from the results of the groundwater-flow models in this study are limited by the shortcomings of groundwater-flow models in general and specific developmental aspects of the individual numerical groundwater-flow models used this study. Groundwater-flow models are simplified mathematical representations of complex real-world groundwater systems. Limitations related to construction and calibration of the groundwater-flow models used in this study and limitations of numerical models in general are described by Izuka and others (2021). Limitations relevant to the use of the models for the interpretations drawn in this report are discussed below.

The conclusions in this study are based on simulations of the withdrawal and recharge conditions represented by the five scenarios listed in table 2 and the comparisons made in the four assessments listed in table 3. Scenarios that represent alternative withdrawal and recharge conditions may lead to other conclusions. For example, changing the location of production wells can alter the relative proportion of the effects of withdrawals on streams and the ocean. Effects of withdrawals are small in areas where withdrawals simulated in the scenarios of this study are small; larger effects will result if withdrawals are larger in alternative scenarios (other factors being equal). Only one projection—statistical downscaling of RCP 8.5—is used to study the potential effects of future climate change; other RCPs exist that are based on assumptions about greenhouse-gas concentrations projected for various scenarios of human activity in the future, which may or may not become reality, and other methods besides statistical downscaling have been used to increase the resolution of GCM results for Hawaiʻi.

The model simulations in this study are steady-state simulations. The simulations provide an estimate of the magnitude of changes that would ultimately result if withdrawal and recharge conditions represented by a given scenario remained steady for an infinite time. The models do not indicate the rate at which the consequences of withdrawals or the changes in groundwater flows related to changes in recharge will develop.

Because the models' sharp freshwater-saltwater interface is a simplified representation of a transition zone that has variable thickness, the models can only assess broad movement of the underlying salt water in response to changes in groundwater withdrawals. The models cannot quantify changes in the salinity of water pumped at specific wells.

In reality, groundwater withdrawals from the volcanic aquifers can cause reductions of groundwater discharge to streams that flow over caprock. In the volcanic-aquifer models of this study, the effect of caprock (which is largely nonvolcanic) is simulated using head-dependent boundaries rather than hydrogeologic units. As a result, possible withdrawal-induced reductions of groundwater discharge to streams on the caprock would be simulated in the models as reduction in discharge to the ocean, not streams.

Because the models in this study do not simulate perched groundwater, if a well in reality withdraws water from a perched system whose water would otherwise flow to an underlying nonperched saturated aquifer, the effect will be accounted for in the models as withdrawal from the underlying nonperched saturated aquifer. However, if a well in reality withdraws water from a perched system whose water would otherwise discharge to a stream, the model may not accurately account for the resulting reduction in stream base flow.

Locations of streams simulated in the models used in this study are based on the National Hydrologic Dataset (U.S. Geological Survey, 2012); however, not all reaches indicated by the National Hydrologic Dataset were included in the models. Omitted are some youthful streams that are unlikely to have incised deeply enough to receive groundwater discharge from the saturated zone of the volcanic aquifers. Although this approach is satisfactory for the purposes of this study, it is possible that in reality, some lower reaches of the omitted streams are connected to groundwater and therefore could be affected by groundwater withdrawals from the volcanic aquifers.

The method used to estimate recharge in the models in this study assumed that for flooded taro fields, water seeps into the ground at a fixed rate of 455 in/yr and that all of the water used to irrigate the taro fields was sourced from surface water (Izuka and others, 2018). In reality, however, some taro fields were unirrigated because they were constructed in natural wetlands where groundwater discharges to the surface. Thus, recharge for some areas covered by taro fields, particularly on O‘ahu and Maui, may be overestimated by Izuka and others (2018). Their recharge estimate for Kaua‘i used a slightly different approach by reducing the seepage rate in all areas mapped as taro by 50 percent (that is, 227.5 in/yr) on the basis of an estimate that one-half of the taro fields on Kaua‘i were not irrigated. Although this approach improved the islandwide estimate of enhanced recharge in taro fields, recharge for taro fields is overestimated in some areas and underestimated in other areas of the island. Better spatial data on the distribution of taro irrigation practices is needed to assess recharge in taro fields more accurately.

All numerical models are limited by spatial discretization. Each cell in the models used in this study represents a volume that has horizontal dimensions of 500 by 500 ft. The vertical dimension of each cell depends on whether a model has one or two layers and varies with topography and bathymetry: most active model cells are hundreds to thousands of feet thick. This level of horizontal and vertical discretization limits the models' ability to resolve small geologic features such as individual dikes and narrow stream reaches. Single-layer models are unable to simulate variations of hydraulic properties with depth or groundwater flow in three dimensions; in two-layer models, this ability is limited. Also, *K* zones used in the models are a simplification of the diverse hydraulic properties that may exist in nature. These aspects affect the precision with which the models can simulate groundwater flow and the distribution of the effects of withdrawals. Although the models have adequate resolution for the island-scale assessment of groundwater availability in this study, greater resolution may be needed to study local effects of groundwater development (for example, the variable effects along the course of an individual stream) or to assess the fine-scale flow of groundwater (for example, for studies of contaminant transport).

The calibrated models used in this study are generally consistent with conceptual models that are based on current understanding of the hydrogeology of the volcanic aquifers of Kaua‘i, O‘ahu, and Maui and are considered to be the most plausible representation on the basis of available data. However, hydrogeologic uncertainties still exist, such as the hydrogeology related to the enigmatic Schofield high-level groundwater. Alternative model parameter values may result in calibrations that are equally satisfactory as the calibration of the models used in this study. Simulations using the alternative parameter values may indicate groundwater-withdrawal effects that differ from those in this study.

Summary

The amount of fresh groundwater available for human use from Hawai‘i's volcanic aquifers is constrained by the consequences of groundwater withdrawal. Since the first modern well was drilled in Hawai‘i in 1879, total groundwater withdrawals on Kaua‘i, O‘ahu, and Maui have risen to nearly 400 million gallons per day (Mgal/d). Model simulations indicate that these withdrawals have caused (1) reductions in groundwater discharge to streams and springs, particularly in dike-impounded-groundwater settings, caprock-influenced freshwater-lens settings, and thickly saturated settings, (2) reductions in groundwater discharge to the ocean, particularly in freshwater-lens settings and anywhere production wells are near the coast, (3) changes in subsurface flows between sectors within an island, (4) lowering of groundwater levels, particularly in low-permeability aquifers such as those in the dike-impounded-groundwater setting or where withdrawals are high, and (5) rise of the freshwater-saltwater interface, especially in heavily developed freshwater-lens settings. Model simulations also indicate that future increases in groundwater withdrawals will increase the severity of the consequences and that increased withdrawals from wells can reduce the amount of water that is produced by tunnels. If communities place limits on any of these consequences, these limits will, in turn, limit how much water can be taken from the aquifer for human use. For example, restrictions to protect stream or coastal ecosystems and traditional and customary practices that rely on groundwater discharge, limitations on reduction of subsurface flows to protect productivity of critical groundwater areas, and limitations on water-level decline and interface rise to protect the productivity of existing wells can limit groundwater availability from Hawai‘i's volcanic aquifers.

Model simulations in this study show that changes in recharge can alter the effect of withdrawals. Increases in recharge can offset the consequences of groundwater withdrawals by lessening the severity of (1) reductions in groundwater discharge to streams, springs, and the ocean, (2) lowering of water levels, and (3) upward movement of salt water. Historically, substantial increases in recharge in Hawai‘i correspond with land-cover changes by humans, particularly

activities related to agriculture, such as crop irrigation and construction of reservoirs. On the other hand, decreases in recharge can exacerbate the effects of withdrawals by increasing the severity of (1) reduction of groundwater discharge to streams, springs, and the ocean, (2) reduction of tunnel yields, (3) lowering of water levels, and (4) rise of the freshwater-saltwater interface. Historically, substantial decreases in recharge result from land-cover changes such as the loss of predevelopment taro fields and replacement of native forest by nonnative forest. Substantial decreases in recharge for the future on O‘ahu are also indicated by analysis of rainfall projections from statistical downscaling of results for midcentury (2041–2070) under representative concentration pathway (RCP) 8.5.

Results from the model simulations in this study show that multiple factors affect the consequences of groundwater withdrawals, which, in turn, affect the availability of groundwater from Hawai‘i's volcanic aquifers. Each of the principal groundwater settings responds differently to groundwater withdrawals; thus, the consequences that limit groundwater availability differ among the settings. The consequences of withdrawals also depend on the magnitude and location of withdrawals relative to sites of groundwater discharge such as streams, springs, and the ocean. The degree to which recharge changes alter the consequences of withdrawal depends on hydrogeology and the magnitude and location of the recharge changes. Simulations using the numerical models of Hawai‘i's volcanic aquifers allow the comprehensive consideration of the multiple factors to quantify the consequences of groundwater withdrawal.

The results of simulations using groundwater models of the islands of Kaua‘i, O‘ahu, and Maui in this study have implications for other islands in Hawai‘i. Groundwater availability in areas where the freshwater-lens setting is predominant is likely to be constrained by limits placed on saltwater rise and coastal discharge, whereas groundwater availability in areas where the dike-impounded-groundwater, caprock-influenced freshwater-lens, or thickly saturated settings is predominant are likely to be constrained by limits placed on water-table depression and reductions in groundwater discharge to streams and springs. The implications do not extend to areas where hydrogeology is not accounted for by the principal groundwater settings discussed in this study.

A critical part of assessing groundwater availability is the process of determining and establishing acceptable limits to the consequences of groundwater withdrawal. This process commonly involves multiple stakeholders and consideration of diverse factors that are outside the physical hydrogeologic science of this study. This study contributes to the determination of groundwater availability by quantifying the expected consequences of withdrawals for a finite set of circumstances. The models in this study also can be used, within limitations, to test other circumstances to inform management decisions that seek to balance the need to limit the consequences of groundwater withdrawals with the need to develop water for human use.

References Cited

Attias, E., Thomas, D., Sherman, D., Ismail, K., and Constable, S., 2020, Marine electrical imaging reveals novel freshwater transport mechanism in Hawai‘i: Science Advances, v. 6, 8 p., accessed March 30, 2021, at https://advances.sciencemag.org/content/advances/6/48/eabd4866.full.pdf.

Bakker, M., Schaars, F., Hughes, J.D., Langevin, C.D., and Dausman, A.M., 2013, Documentation of the Seawater Intrusion (SWI2) Package for MODFLOW: U.S. Geological Survey Techniques and Methods, book 6, chap. A46, 47 p., https://pubs.usgs.gov/tm/6a46/.

Bassiouni, M., and Oki, D.S., 2013, Trends and shifts in streamflow in Hawai‘i, 1913–2008: Hydrological Processes, v. 27, no. 10, p. 1484–1500, accessed May 24, 2012, at https://onlinelibrary.wiley.com/doi/10.1002/hyp.9298/full.

Bauer, G.R., 2003, A study of the ground-water conditions in North and South Kona and South Kohala districts, Island of Hawaii, 1991–2002: State of Hawaii Department of Land and Natural Resources, Commission on Water Resource Management, PR-2003-01, 92 p.

Chu, P.-S., Chen, Y.R., and Schroeder, T.A., 2010, Changes in precipitation extremes in the Hawaiian Islands in a warming climate: Journal of Climate, v. 23, no. 18, p. 4881–4900, https://doi.org/10.1175/2010JCLI3484.1.

Clague, D.A., and Dalrymple, G.B., 1987, The Hawaiian-Emperor volcanic chain—Part 1. Geologic evolution, chap. 1 *of* Decker, R.W., Wright, T.L., and Stauffer, P.H., eds., Volcanism in Hawaii—Volume 1: U.S. Geological Survey Professional Paper 1350, p. 5–54, https://pubs.usgs.gov/pp/1987/1350/.

Clague, D.A., and Sherrod, D.R., 2014, Growth and degradation of Hawaiian volcanoes, *in* Poland, M.P., Takahashi, J.T., and Landowski, C.M., eds., Characteristics of Hawaiian volcanoes: U.S. Geological Survey Professional Paper 1801, p. 97–146, https://pubs.usgs.gov/pp/1801/.

Cooper, H.H., Jr., 1964, A hypothesis concerning the dynamic balance of fresh water and salt water in a coastal aquifer, *in* Cooper, H.H., Jr., Kohout, F.A., Henry, H.R., and Glover, R.E., eds., Sea water in coastal aquifers— Relation of salt water to fresh ground water: U.S. Geological Survey Water Supply Paper 1613–C, p. C1–C12.

Cuddihy, L.W., and Stone, C.P., 1990, Alteration of Native Hawaiian vegetation—Effects of humans, their activities and introductions: University of Hawaii, Manoa, Cooperative National Park Resources Studies Unit, 138 p.

Davis, D.A., 1963, Hawaii, *in* McGuinness, C.L., The role of ground water in the national water situation—With state summaries based on reports by District Offices of Ground Water Branch: U.S. Geological Survey Water-Supply Paper 1800, p. 271–293.

Elison Timm, O., Giambelluca, T.W., and Diaz, H.F., 2015, Statistical downscaling of rainfall changes in Hawai‘i based on the CMIP5 global model projections: Journal of Geophysical Research - Atmospheres, v. 120, no. 1, p. 92–112, https://doi.org/10.1002/2014JD022059.

Frazier, A.G., Giambelluca, T.W., Diaz, H.F., and Needham, H.L., 2016, Comparison of geostatistical approaches to spatially interpolate month-year rainfall for the Hawaiian Islands: International Journal of Climatology, v. 36, no. 3, p. 1459–1470, https://doi.org/10.1002/joc.4437.

Giambelluca, T.W., Chen, Q., Frazier, A.G., Price, J.P., Chen, Y.-L., Chu, P.-S., Eischeid, J.K., and Delparte, D.M., 2013, Online rainfall atlas of Hawai‘i: Bulletin of the American Meteorological Society, v. 94, no. 3, p. 313–316, https://doi.org/10.1175/BAMS-D-11-00228.1.

Giambelluca, T.W., Nullet, M.A., and Schroeder, T.A., 1986, Rainfall atlas of Hawai‘i: State of Hawai‘i Department of Land and Natural Resources, Division of Water and Land Development, Report R76, 267 p.

Giambelluca, T.W., and Schroeder, T.A., 1998, Climate, *in* Juvik, S.P., and Juvik, J.O., eds., Atlas of Hawai‘i (3d ed.): Honolulu, Hawai‘i, University of Hawai‘i Press, 333 p.

Gingerich, S.B., 1999a, Ground water and surface water in the Haiku area, east Maui, Hawaii: U.S. Geological Survey Water-Resources Investigations Report 98–4142, 38 p., https://doi.org/10.3133/wri984142.

Gingerich, S.B., 1999b, Ground-water occurrence and contribution to streamflow, northeast Maui, Hawaii: U.S. Geological Survey Water-Resources Investigations Report 99–4090, 69 p., 1 plate.

Harbaugh, A.W., 2005, MODFLOW-2005, The U.S. Geological Survey modular ground-water model—The ground-water flow process: U.S. Geological Survey Techniques and Methods, book 6, chap. A16, [variously paged], https://doi.org/10.3133/tm6A16.

Hirashima, G.T., 1962, Effect of the Haiku Tunnel on Kahaluu Stream, Oahu, Hawaii, *in* Geological Survey research 1962—Short papers in geology and hydrology, articles 60–119: U.S. Geological Survey Professional Paper 450–C, p. C118–C120.

Hunt, C.D., Jr., 1996, Geohydrology of the island of Oahu, Hawaii: U.S. Geological Survey Professional Paper 1412–B, 54 p., https://doi.org/10.3133/pp1412B.

Intergovernmental Panel on Climate Change [IPCC], 2013, Summary for policymakers, *in* Stocker, T.F., Qin, D., Plattner, G.-K., Tignor, M., Allen, S.K., Boschung, J., Nauels, A., Xia, Y., Bex, V., and Midgley, P.M., eds., Climate Change 2013—The Physical Science Basis, Contribution of Working Group I to the Fifth Assessment Report of the Intergovernmental Panel on Climate Change: Cambridge, United Kingdom, and New York, N.Y., Cambridge University Press, 29 p., https://www.ipcc.ch/pdf/assessment-report/ar5/wg1/WG1AR5_SPM_FINAL.pdf.

Izuka, S.K., Engott, J.A., Rotzoll, K., Bassiouni, M., Johnson, A.G., Miller, L.D., Rotzoll, Kolja, and Mair, A., 2018, Volcanic aquifers of Hawai‘i—Hydrogeology, water budgets, and conceptual models (ver. 2.0, March 2018): U.S. Geological Survey Scientific Investigations Report 2015–5164, 158 p., https://doi.org/10.3133/sir20155164.

Izuka, S.K., and Gingerich, S.B., 1998, Ground water in the southern Lihue Basin, Kauai, Hawaii: U.S. Geological Survey Water-Resources Investigations Report 98–4031, 71 p., https://doi.org/10.3133/wri984031.

Izuka, S.K., and Gingerich, S.B., 2003, A thick lens of fresh groundwater in the southern Lihue Basin, Kauai, Hawaii, USA: Hydrogeology Journal, v. 11, no. 2, p. 240–248, https://doi.org/10.1007/s10040-002-0233-5.

Izuka, S.K., Rotzoll, K., and Nishikawa, T., 2021, Volcanic aquifers of Hawai‘i—Construction and calibration of numerical models for assessing groundwater availability on Kaua‘i, O‘ahu, and Maui: U.S. Geological Survey Scientific Investigations Report 2020–5126, 63 p., https://doi.org/10.3133/sir20205126.

Juvik, J.O., and Nullet, D., 1995, Relationships between rainfall, cloud-water interception, and canopy throughfall in a Hawaiian montane forest, chap. 11 *of* Hamilton, L.S., Juvik, J.O., and Scatena, F.N., eds., Tropical montane cloud forests: New York, Springer-Verlag, p. 165–182.

Kauahikaua, J., 1993, Geophysical characteristics of the hydrothermal systems of Kilauea volcano, Hawai‘i: Geothermics, v. 22, no. 4, p. 271–299, https://doi.org/10.1016/0375-6505(93)90004-7.

Kirch, P.V., 1982, The impact of the prehistoric Polynesians on the Hawaiian ecosystem: Pacific Science, v. 36, no. 1, p. 1–14.

Kirch, P.V., 1998, Archaeology, *in* Juvik, S.P., and Juvik, J.O., eds., Atlas of Hawai‘i (3d ed.): Honolulu, Hawai‘i, University of Hawai‘i Press, p. 161–168.

Kirch, P.V., 2000, On the road of the winds—An archaeological history of the Pacific islands before European contact: Berkeley, Calif., University of California Press, 424 p.

Kruk, M.C., and Levinson, D.H., 2008, Evaluating the impacts of climate change on rainfall extremes for Hawaii and coastal Alaska: Proceedings, 24th Conference on Severe Local Storms, American Meteorological Society, October 27–31, 2008, Savannah, Georgia, accessed January 6, 2015, at https://ams.confex.com/ams/pdfpapers/142172.pdf.

Langenheim, V.A.M., and Clague, D.A., 1987, The Hawaiian-Emperor volcanic chain—Part II. Stratigraphic framework of volcanic rocks of the Hawaiian Islands, chap. 1 *of* Decker, R.W., Wright, T.L., and Stauffer, P.H., eds., Volcanism in Hawaii—Volume 1: U.S. Geological Survey Professional Paper 1350, p. 55–84, https://pubs.usgs.gov/pp/1987/1350/.

Lau, L.S., and Mink, J.F., 2006, Hydrology of the Hawaiian Islands: Honolulu, Hawai‘i, University of Hawai‘i Press, 274 p.

Macdonald, G.A., Abbott, A.T., and Peterson, F.L, 1983, Volcanoes in the sea—The geology of Hawaii (2d ed.): Honolulu, Hawaiʻi, University of Hawaii Press, 517 p.

Macdonald, G.A., and Katsura, T., 1964, Chemical composition of Hawaiian lavas: Journal of Petrology, v. 5, no. 1, p. 82–133, https://doi.org/10.1093/petrology/5.1.82.

Mair, A., Johnson, A.G., Rotzoll, K., and Oki, D.S., 2019, Estimated groundwater recharge from a water-budget model incorporating selected climate projections, Island of Maui, Hawaiʻi: U.S. Geological Survey Scientific Investigations Report 2019–5064, 46 p., https://doi.org/10.3133/sir20195064.

Meinzer, O.E., 1923, The occurrence of ground water in the United States, with a discussion of principles: U.S. Geological Survey Water-Supply Paper 489, 321 p., https://doi.org/10.3133/wsp489.

Meyer, W., 2000, A reevaluation of the occurrence of ground water in the Nahiku area, east Maui, Hawaii: U.S. Geological Survey Professional Paper 1618, 81 p., https://doi.org/10.3133/pp1618.

Mink, J.F., and Lau, L.S., 1980, Hawaiian groundwater geology and hydrology, and early mathematical models: Honolulu University of Hawaii at Manoa, Water Resources Research Center Technical Memorandum Report 62, 74 p.

Moore, J.G., 1987, Subsidence of the Hawaiian Ridge, chap. 2 *of* Decker, R.W., Wright, T.L., and Stauffer, P.H., eds., Volcanism in Hawaii—Volume 1: U.S. Geological Survey Professional Paper 1350, p. 85–100, https://pubs.usgs.gov/pp/1987/1350/.

Moore, R.B., and Trusdell, F.A., 1993, Geology of Kilauea volcano: Geothermics, v. 22, no. 4, p. 243–254, https://doi.org/10.1016/0375-6505(93)90002-5.

Newman, T.S., 1972, Man in the prehistoric Hawaiian ecosystem, *in* Kay, E.A., ed., Natural history of the Hawaiian Islands—Selected readings: Honolulu, Hawaiʻi, University of Hawaiʻi Press, p. 559–603.

Nichols, W.D., Shade, P.J., and Hunt, C.D., Jr., 1996, Summary of the Oahu, Hawaii, Regional Aquifer-System Analysis: U.S. Geological Survey Professional Paper 1412–A, 61 p., https://doi.org/10.3133/pp1412A.

Oki, D.S., 1998, Geohydrology of the central Oahu, Hawaii, ground-water flow system and numerical simulation of the effects of additional pumping: U.S. Geological Survey Water-Resources Investigations Report 97–4276, 132 p., https://doi.org/10.3133/wri974276.

Oki, D.S., 1999, Geohydrology and numerical simulation of the ground-water flow system of Kona, Island of Hawaii: U.S. Geological Survey Water-Resources Investigations Report 99–4073, 70 p., https://doi.org/10.3133/wri994073.

Oki, D.S., 2004, Trends in streamflow characteristics at long-term gaging stations, Hawaii: U.S. Geological Survey Scientific Investigations Report 2004–5080, 116 p., https://doi.org/10.3133/sir20045080.

Oki, D.S., 2005, Numerical simulation of the effects of low-permeability valley-fill barriers and the redistribution of ground-water withdrawals in the Pearl Harbor area, Oahu, Hawaii: U.S. Geological Survey Scientific Investigations Report 2005–5253, 111 p., https://doi.org/10.3133/sir20055253.

Palmer, H.S., 1927, The geology of the Honolulu artesian system: Supplement to the Report of the Honolulu Sewer and Water Commission, 68 p.

Palmer, H.S., 1946, The geology of the Honolulu ground water supply: Honolulu, Hawaiʻi, Board of Water Supply, City and County of Honolulu, 55 p.

Reilly, T.E., Dennehy, K.F., Alley, W.M., and Cunningham, W.L., 2008, Ground-water availability in the United States: U.S. Geological Survey Circular 1323, 70 p., https://pubs.usgs.gov/circ/1323/.

Riahi, K., Rao, S., Krey, V., Cho, C., Chirkov, V., Fischer, G., Kindermann, G., Nakicenovic, N., and Rafaj, P., 2011, RCP 8.5—A scenario of comparatively high greenhouse gas emissions: Climatic Change, v. 109, p. 33–57, https://doi.org/10.1007/s10584-011-0149-y.

Rotzoll, K., and El-Kadi, A.I., 2008, Estimating hydraulic conductivity from specific capacity for Hawaii aquifers, USA: Hydrogeology Journal, v. 16, p. 969–979, https://doi.org/10.1007/s10040-007-0271-0.

Rotzoll, K., and Izuka, S.K., 2023, MODFLOW–2005 and SWI2 models for assessing groundwater availability scenarios in volcanic aquifers on Kauai, Oahu, and Maui, Hawaii: U.S. Geological Survey data release, https://doi.org/10.5066/P97CPK5C.

Rotzoll, K., and Johnson, A.G., 2023, Mean annual water-budget components for Oahu, Hawaii, for future-climate conditions, CMIP5 RCP8.5 2041–70 scenario rainfall and 2010 land cover: U.S. Geological Survey data release, https://doi.org/10.5066/P9L4N2ZI.

Schmitt, R.C., 1998, Population, *in* Juvik, S.P., and Juvik, J.O., eds., Atlas of Hawaiʻi (3d ed.): Honolulu, Hawaiʻi, University of Hawaiʻi Press, p. 183–197.

Scholl, M.A., Gingerich, S.B., and Tribble, G.W., 2002, The influence of microclimates and fog on stable isotope signatures used in interpretation of regional hydrology—East Maui, Hawaii: Journal of Hydrology, v. 264, nos. 1–4, p. 170–184, https://doi.org/10.1016/S0022-1694(02)00073-2.

Sherrod, D.R., Sinton, J.M., Watkins, S.E., and Brunt, K.M., 2021, Geologic map of the State of Hawaiʻi: U.S. Geological Survey Scientific Investigations Map 3143, 72 p., 5 sheets, scales 1:100,000 and 1:250,000, https://doi.org/10.3133/sim3143.

Soroos, R.L., 1973, Determination of hydraulic conductivity of some Oahu aquifers with step-drawdown test data: Honolulu, University of Hawaii, M.S. thesis, 239 p.

Souza, W.R., and Voss, C.I., 1987, Analysis of an anisotropic coastal aquifer system using variable-density flow and solute transport simulation: Journal of Hydrology, v. 92, p. 17–41, https://doi.org/10.1016/0022-1694(87)90087-4.

State of Hawai‘i, 2019, Hawai‘i Water Plan—Water resource protection plan 2019 update: State of Hawai‘i, Commission on Water Resource Management, accessed July 22, 2019, at https://files.hawaii.gov/dlnr/cwrm/planning/wrpp2019update/WRPP_201907.pdf.

State of Hawai‘i Department of Business, Economic Development & Tourism, 2021, Census—Hawaii redistricting data: State of Hawai‘i, Department of Business, Economic Development & Tourism website, accessed October 7, 2021, at https://census.hawaii.gov/census_2020/data/redistricting/.

Stearns, H.T., 1940, Supplement to the geology and ground-water resources of the island of Oahu, Hawaii: Hawaii Division of Hydrography Bulletin 5, 164 p.

Stearns, H.T., 1946, Geology of the Hawaiian Islands: Hawaii Division of Hydrography Bulletin 8, 106 p.

Stearns, H.T., 1966, Geology of the State of Hawaii: Palo Alto, Calif., Pacific Books, 266 p.

Stearns, H.T., and Vaksvik, K.N., 1935, Geology and ground-water resources of the Island of Oahu, Hawaii: Hawaii Division of Hydrography Bulletin 1, 479 p.

Takasaki, K.J., 1978, Summary appraisals of the Nation’s ground-water resources—Hawaii region: U.S. Geological Survey Professional Paper 813–M, 29 p., https://doi.org/10.3133/pp813M.

Takasaki, K.J., and Mink, J.F., 1985, Evaluation of major dike-impounded ground-water reservoirs, Island of Oahu: U.S. Geological Survey Water-Supply Paper 2217, 77 p., https://doi.org/10.3133/wsp2217.

Theis, C.V., 1940, The source of water derived from wells—Essential factors controlling the response of an aquifer to development: Civil Engineering, v. 10, p. 277–280.

Thomas, D.M., Paillet, F.L., and Conrad, M.E., 1996, Hydrogeology of the Hawaii Scientific drilling project borehole KP-1—2. Groundwater geochemistry and regional flow patterns: Journal of Geophysical Research—Solid Earth, v. 101, no. B5, p. 11,683–11,694.

Timm, O., and Diaz, H.F., 2009, Synoptic-statistical approach to regional downscaling of IPCC twenty-first-century climate projections—Seasonal rainfall over the Hawaiian Islands: Journal of Climate, v 22, p. 4261–4280. https://doi.org/10.1175/2009JCLI2833.1.

U.S. Census Bureau, 2021, 2020 Census apportionment results: U.S. Census Bureau website, accessed April 30, 2021, at https://www.census.gov/data/tables/2020/dec/2020-apportionment-data.html.

U.S. Geological Survey, 2012, The National Map—National hydrography dataset: U.S. Geological Survey website, accessed February 12, 2013, at https://nhd.usgs.gov/data.html.

Walker, G.P.L., 1987, The dike complex of Koolau Volcano, Oahu—Internal structure of a Hawaiian rift zone, chap. 41 *of* Decker, R.W., Wright, T.L., and Stauffer, P.H., eds., Volcanism in Hawaii—Volume 2: U.S. Geological Survey Professional Paper 1350, p. 961–993, https://pubs.usgs.gov/pp/1987/1350/.

Wentworth, C.K., 1928, Principles of stream erosion in Hawaii: Journal of Geology, v. 36, no. 5, p. 385–410, https://doi.org/10.1086/623529.

Wolfe, E.W., and Morris, J., 1996, Geologic map of the Island of Hawaii: U.S. Geological Survey Miscellaneous Investigations Series Map I–2524–A, scale 1:100,000, https://doi.org/10.3133/i2524A.

Woodcock, D., 2003, To restore the watersheds—Early twentieth-century tree planting in Hawai‘i: Annals of the Association of American Geographers, v. 93, no. 3, p. 624–635, https://doi.org/10.1111/1467-8306.9303006.

Zhang, C., Wang, Y., Hamilton, K., and Lauer, A., 2016, Dynamical downscaling of the climate for the Hawaiian Islands. Part II—Projection for the late twenty-first century: Journal of Climate, v. 29, p. 8333–8354, https://doi.org/10.1175/JCLI-D-16-0038.1.

Ziegler, A.C., 2002, Hawaiian natural history, ecology, and evolution: Honolulu, Hawai‘i, University of Hawai‘i Press, 477 p.

Moffett Field Publishing Service Center
Manuscript approved October 21, 2022
Edited by Taryn A. Lindquist
Illustration support by JoJo Mangano
Layout by Cory Hurd

Izuka and Rotzoll—**Volcanic Aquifers of Hawai‘i—Contributions to Assessing Groundwater Availability on Kaua‘i, O‘ahu, and Maui**—Professional Paper 1876, ver. 1.1

ISSN 2330-7102 (online)
https://doi.org/10.3133/pp1876